SOUND SPEED VARIATIONS IN THE ARABIAN GULF AND THEIR EFFECT ON MULTIBEAM ECHO SOUNDING

F. ALAMRI

March 1998

TECHNICAL REPORT NO. 189

PREFACE

In order to make our extensive series of technical reports more readily available, we have scanned the old master copies and produced electronic versions in Portable Document Format. The quality of the images varies depending on the quality of the originals. The images have not been converted to searchable text.

SOUND SPEED VARIATIONS IN THE ARABIAN GULF AND THEIR EFFECT ON MULTIBEAM ECHO SOUNDING

Fahad Alamri

Department of Geodesy and Geomatics Engineering
University of New Brunswick
P.O. Box 4400
Fredericton, N.B.
Canada
E3B 5A3

March 1998

PREFACE

This technical report is a reproduction of a report submitted in partial fulfillment of the requirements for the degree of Master of Engineering in the Department of Geodesy and Geomatics Engineering, March 1996. This work was made possible by Saudi Aramco, which provided both financial support and the data upon which this work was based. The research was supervised by Dr. David Wells, and additional support was provided by the Natural Sciences and Engineering Research Council of Canada.

As with any copyrighted material, permission to reprint or quote extensively from this report must be received from the author. The citation to this work should appear as follows:

Alamri, F. (1998). *Sound Speed Variations in the Arabian Gulf, and Their Effect on Multibeam Echo Sounding*. M.Eng. report, Department of Geodesy and Geomatics Engineering Technical Report No. 189, University of New Brunswick, Fredericton, New Brunswick, Canada, 209 pp.

ABSTRACT

The objective of this project is to study the effect of sound speed variations on multibeam echosounders using real field data from the anomalous operating environment of the Arabian Gulf. The data were collected on the Saudi Aramco concession area between 1991 and 1995. Algorithms for the speed of sound in seawater are compared. The updated version of the Chen and Millero formula is recommended for use in areas with salinities of up to 65‰ and temperatures up to 40°C. Variability of the salinity, temperature, and sound speed within the Gulf is assessed and described. The temporal and spatial variations of sound speed in the water column are studied and recommendations for certain sampling procedures to be followed are given. Those recommendations include the continuation of usage of the current CTD probe to measure sound speed profiles (SSPs) thrice a day, the usage of a pressure sensor to measure the transducer depth accurately, and the creation of a database for the SSPs with a coordinated position of each cast.

TABLE OF CONTENTS

LIST OF TABLES

LIST OF FIGURES

ACKNOWLEDGMENT

The author would like to extend his sincere thanks to many individuals who helped him complete this report. First I thank Almighty Allah for my existence and well-being. Then I would like to thank the following: Mr. Claus Christensen, supervisor of the hydrographic survey unit, for giving me this opportunity to fulfill a long awaited dream of obtaining this degree plus providing the data that was necessary for this report. Then my gratitude for my supervisor, Dr. David Wells, for his guidance through this period and patience in answering my many questions. Many thanks also goes to Dr. John Hughes Clarke for his generosity in allowing me to use his SSP software tools and showing lots of patience in answering my many questions especially regarding refraction issues. Another person that was also helpful during my stay at UNB is Dr. Larry Mayer, so I would like to thank him very much. Last but not least my family for their support, encouragement, patience, and understanding.

Chapter 1

BACKGROUND AND REPORT OUTLINE

1.1 INTRODUCTION

The objective of this project is to study the effect of sound speed variations on multibeam echosounders using real field data from the anomalous operating environment of the Arabian Gulf. This study concentrate on the concession area of Saudi Aramco. Saudi Aramco is the largest oil company in the world. As a result, the Hydrographic Survey Unit (HSU) was established in the beginning of the 1980s to carry out the responsibility of supporting the exploration and production of offshore oil activities which centered around the Saudi Arabian concession area of the Arabian Gulf. The HSU also maintains a complete record of the navigational charts of the Gulf for ship routes in and out of the Gulf.

Recently, Saudi Aramco bought a new survey vessel that was built in Bergen, Norway, particularly to meet Aramco surveying demands. A Simrad EM1000 Multibeam Echo Sounder System was bought as part of the many new improvements that were added to enhance the hydrographic surveying operations carried out by HSU. This system provides both the seafloor bathymetry and sonar imagery. It is designed for hull-mounted operation mapping the seafloor utilizing several beams making a fan-shaped geometry. This attains the maximum allowable coverage of 7.4 times the water depth or 150° swath angle or roughly 75° to each side of the ship track. This coverage capability of the system was the main reason behind Aramco's investment. This was especially true due to the added responsibility of mapping the Red Sea.

Now that Saudi Aramco has a multibeam system, its hydrographic surveyors are faced with new problems in multibeam swath bathymetry that they are not familiar with or have little knowledge about. These problems are common now to all surveyors around the world, who are working with multibeam systems, but familiar only with the conventional single vertical beam echo sounder. This author, being a member of HSU, will only explore one problem (refraction) that is common to situations similar to that of the Arabian Gulf.

This topic stimulated the interest of the author because of the important effects of refraction phenomena on the quality of swath bathymetry, producing what are known as refraction artifacts due to unmonitored or uncorrected for sound speed variations in the water column and the fact that the unique environment that exists in the Gulf might be particularly prone to such problems. The Arabian Gulf environment is discussed in more detail in section 1.2. The Gulf's unique characteristics are that it is shallow in depth, with a very high salinity and is almost surrounded by land with only a narrow passage to the Indian Ocean.

Description of the refraction phenomena and the method proposed to tackle this problem is given in section 1.3.

The author's expectations of this master of engineering report are given in section 1.4. To maintain his research within the time limit, a timetable of milestone dates are also given (see Table 1-1 at the end of this chapter).

1.2 ENVIRONMENT

The Arabian Gulf is an extremely shallow marginal sea with an average depth of 35 m. Its length is over 1000 km and the width is 200-300 km, covering an area of approximately 226,000 km^2. The maximum depth is about 100 m near the narrow Strait of Hormuz.

The Gulf is almost surrounded by land. Its only entrance to the Indian Ocean is the 60 km wide Strait of Hormuz. The Gulf can be thought of as a restricted arm for the Indian Ocean [Nawab et al., 1981].

1.2.1 Climate

The Arabian Gulf lies between latitudes 24°N and 30.30° N. It has an extreme contrast in climate, from the hot summer months to the occasional freezing temperatures experienced in the two to three months of winter. The Gulf climate resembles that of the Eastern Province of Saudi Arabia, since it is almost surrounded by land with just a single narrow passage to the Indian Ocean. The climate is considered as arid, sub-tropical with very high variability corresponding to the changes of seasons.

The climate can be divided into four seasons. Summer starts in May and extends to September. Air-temperature rises to 40° to 50°C in the hot times especially in June to August. 'Shamals', the Arabic word for northerly winds, are predominantly NW directional winds blowing usually for two to three days at a speed of 25-30 miles per hour. Shamals are the main cause for wind-driven currents and waves directed mainly toward southeast. Shamals increase during June and July. August is the hottest, but the calmest, month.

From October to November, fall is characterized by decreasing temperatures and rising humidity. Beginning usually in November, winds become south to southeast created by the leading boundary of the fronts of the first winter storms coming from the Mediterranean to hit the Arabian Gulf.

Winter usually starts in December and extends to February. It is characterized by stormy periods with strong winds and some rain, thunderstorms, and blowing dust, with intermittent calm weather. Some freezing temperatures have been experienced in the Eastern Province of Saudi Arabia and the Gulf.

By March, the first month of spring, the wind starts to diminish and a gradual rise in temperatures begins. Thunderstorms may still occur in the spring, but with no uniform pattern from year to year [Nawab et al., 1981].

1.2.2 Factors Affecting Salinity and Temperature of the Gulf

The following are the most important factors that contribute to the Gulf temperature and salinity distributions:

- *Air Temperature*: The temperature in the summer in the Gulf ranges from 40°C to 50°C but the air temperature may decrease to near the freezing mark in the winter. The effect of constant winds, high temperature, and low precipitation lead to excessive evaporation of the Gulf water with an annual rate of 124 cm/year as reported by Purser [1973], causing high salinity especially in coastal areas. This loss does not cause a lowering trends in the sea level because of the influx of seawater flowing through Hormuz from the Indian Ocean.

- *Annual Rainfall*: The average annual rainfall in the eastern coast of Saudi Arabia is less than 5 cm [Purser, 1973]. The Iranian coast receives 20 to 50 cm, injecting more fresh water into the Gulf. The Saudi coast lacks water influx into the Gulf, except for rare flooding of the desert wadis caused by local storms. Therefore, the salinity is higher on the Saudi coast that on the Iranian coast [Purser, 1973].
- *Regional Currents:* There is believed to be a slow circulatory surface current that flows into the Gulf moving anti-clockwise along the Iranian coast as a direct result of the high loss of water due to the imbalance between high evaporation and precipitation and river inflow. The evaporation lowers sea level, which causes inflow from the Indian Ocean, and this flow is deflected by the Coriolis effect to create a counter-clockwise current. This surface current is created by the process of bringing in new ocean water from the Indian Ocean and has a strong relation to the temperature and salinity distribution within the Gulf water. Due to the combined effect of water cooling and evaporation the highly saline water sinks to the bottom lowering the temperature and raising salinity for these deeper waters [Purser, 1973].
- *Fluvial Influx:* There is a considerable amount of water influx into the Gulf from Shatt al Arab as a result of the large rainfall of the Zagros and Taurus mountains which supply the Eupherate and Karun rivers that combine at Shatt al Arab. There is no significant fluvial influx to mention from the Saudi coast [Purser, 1973].

Strong Wind: Wind is an important driving force for the Gulf oceanographic environment. Even though it does not affect the temperature and salinity directly it has an impact on waves and current generation. Shamal blows mainly from the NW in the northern part of the Gulf but tends to veer to the North as one approaches the United Arab Emirates (UAE) coast in the SE. In some parts of the Gulf, winds of 7 to 10 on the Beaufort scale occur. This strong wind is the main generator of strong waves and currents [Seibold, 1970].

1.2.3 Salinity

There is a limited water interchange of Gulf water with the Indian Ocean. Surface salinities in the central part of the gulf average 37 to 40‰, while shallow parts of the UAE coast have shown salinities of 40 to 50‰, rising to 60 to 70‰ in remote lagoons and coastal embayments such as the Gulf of Salwa[Purser, 1973]. Salinity of the surface water increases from 36.6‰ near the entrance to 40.6‰ near the northwest end of the basin. Figure 1-1 is a map showing the majority salinity trends within the Gulf. This also identifies the general area of interest in this study. Figure 1-2 shows a 2-4‰ change of salinity with increased depth along the central axial of the Gulf.

1.2.4 Temperature

As was previously seen in the salinity trends, lagoons away from the main body of water have high temperature. Temperatures attained during the summer for surface waters are typically 36° C in the central part of the Gulf. Winter temperatures may fall below 20° C with higher temperatures usually in the coastal areas[Purser, 1973]. Temperatures measurements suggests a poorly defined thermocline which rises from 40 m near the Strait of Hormuz to 20 m near the northwest end of the Gulf (see Figure 1-3).

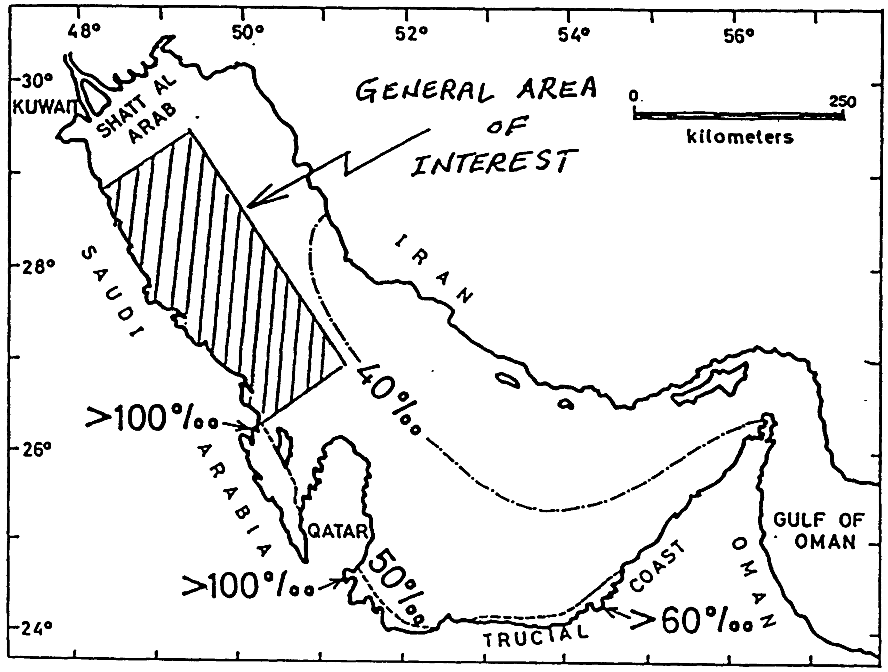

Figure 1-1 Major salinity trends in the Arabian Gulf (from Emery [1956]).

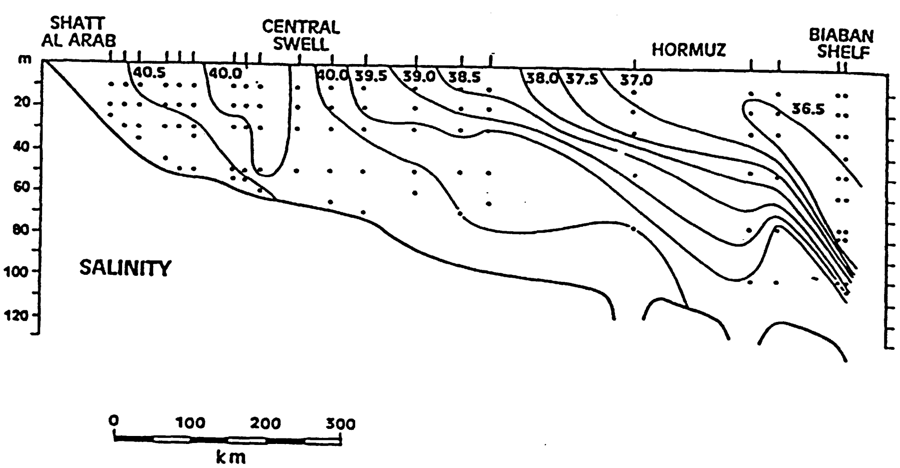

Figure 1-2 Vertical distribution of salinity profile along the axis of the Arabian Gulf

(From Seibold [1970]).

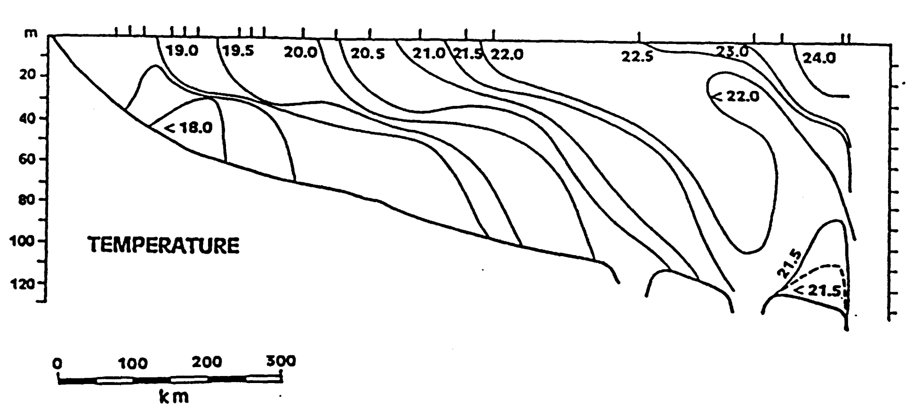

Figure 1-3 Vertical distribution of temperature profile along the axis of the Gulf (From Seibold [1970]).

1.2.5 Sound Speed Profiles in the Arabian Gulf

In coastal regions and on the continental shelves, sound speed profiles (SSPs) become irregular and unpredictable because of the great influence of water surface heating and cooling, salinity changes, and currents [Urick, 1975]. The Gulf is no exception to this. Fresh water sources complicate the SSP, causing the salinity changes and thus temporally and spatially unstable layers. The effect of this is minimal, since the only fresh input is the small river influx that is far from the area of interest to Saudi Aramco operations at the Shatt al Arab connection with the Gulf.

Many measured SSPs are available for the work proposed here. These profiles generally indicate that the sound speed does not change from water surface to bottom by very much except in the Marjan (area on the northern Arabian coast). One goal of this report is to characterize this variability in more detail.

1.3 REFRACTION

Refraction is the most important phenomenon that interferes with simple divergence and straight line propagation. A sound ray traveling obliquely in the ocean will change direction as it enters layers of different sound speed. The sound ray is refracted or bent toward the region of lower sound speed.

Sound speed in seawater is influenced by variations in three factors: temperature, salinity, and pressure. Salinity variation is of most importance near the mouths of large rivers where fresh water runs into the sea or in the areas of large ocean currents such the Gulf Stream. Pressure influence is quite regular with about 0.017 m/s increase in sound speed per metre increase in depth. Temperature variation is the most influential near the surface and our lack of knowledge of the actual temperature-driven sound speed variation makes prediction of the exact path of a sound beam quite difficult.

The path of a ray of sound through a medium in which the velocity changes with depth can be calculated by the application of Snell's Law [Kinsler and Frey, 1962].

1.3.1 Ray Path Theory

Propagation of sound in any medium can be described mathematically by solution of the wave equation using the appropriate boundary and medium conditions.

Solution of the wave equation can be done by two theoretical approaches normal-mode theory and ray theory. In normal-mode theory, the propagation is described in terms of characteristic functions called normal-modes each of which is a solution of the wave equation. This theory is suited for a shallow water sound propagation of less than 100 m.

Ray theory solves for the position of wave fronts along which the phase or time function of the solution is constant and the existence of rays that describe where in space the sound emanating from a source is being sent.

1.3.2 Snell's Law

Snell's Law which describes the refraction of sound rays in a medium of variable velocity, is a direct result of the ray theory mentioned above. Snell's Law states that in a medium consisting of constant velocity, grazing angles θ_1, θ_2, θ_3,.... of a ray at the layer boundaries are related to the sound velocity c_1, c_2, c_3,..... of the layers by

$$\frac{\cos\theta_1}{c_1} = \frac{\cos\theta_2}{c_2} = \frac{\cos\theta_3}{c_3} = \frac{1}{c_0}$$

where $1/c_0$ is the ray constant which the reciprocal of the sound velocity c_0 in the layer in which the ray become horizontal [Urick, 1975].

1.3.3 Isovelocity

Snell's Law is the basis for ray computation for most software applications which enable the 'tracing' of a particular ray through different layers. One approach to model the actual profile is to divide the SSP into layers of constant velocity or isovelocity layers (see Figure 1-4). The accuracy of this approach will depend on the number of layers used as compared to the actual variations. In a medium having isovelocity layers, the rays consist of a series of straight-line segments joined together, by Snell's law. In this approach as well as the next approach (isogradient), an assumption has to be made: the ocean is assumed to be horizontally stratified, with no horizontal gradient. This assumption has two consequences

- a) Local: within the ray path (horizontal distance is nearly equal to the water depth)
- b) Regional: the assumption that SSP is the same at both ends of a harbor.

If (a) is not valid we can't assume vertical gradient only because then there is an azimuthal dependence of the refraction solution. The regional (b) effect is a question of applicability of an SSP within a survey area for a duration of time or a spatial region. This will be reflected in the SSP sampling spacing factor; and thus will influence when and where we take another SSP.

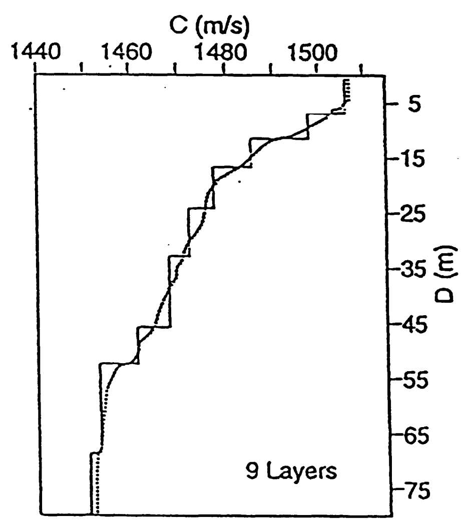

Figure 1-4 Isovelocity layers (From Hughes Clarke et al. [1995])

1.3.4 Isogradient

This is the second approach that can be used (see Figure 1-5). For a medium in which the speed changes linearly with depth, the sound rays can be shown to be arcs of circles. Under the isogradient model (assumption) SSP can be divided into layers of constant gradient (isogradient layers) [Kinsler and Frey, 1962].

This model is supposedly more accurate representation of the actual SSP, but if the isovelocity model was chosen to be incremented in very tiny segments, it will practically yield the same representation of the actual SSP.

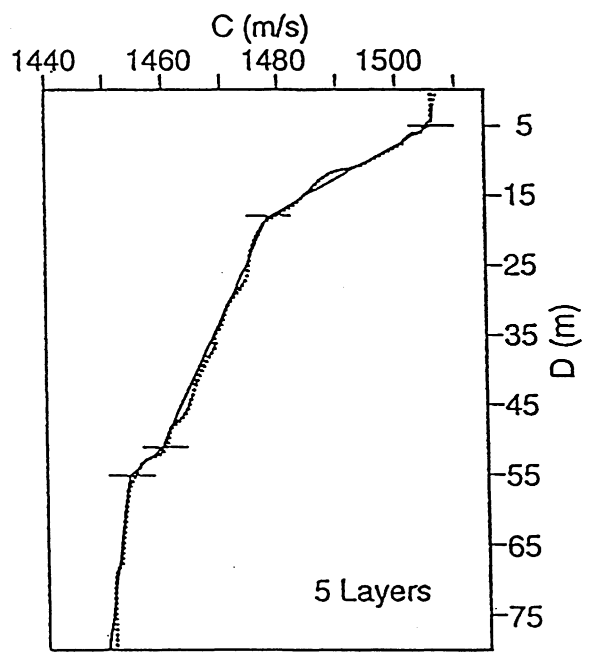

Figure 1-5 Isogradient layers (From Hughes Clarke et. al. [1995])

1.4 AVAILABLE DATA

There are two types of data available for this research study. i.e. Sea-Bird Electronics Inc. SEACAT profiler Conductivity-Temperature - Depth probe (CTD) data, and Navitronics SVP-1 sound speed direct-measurement data. The latter measures the sound speed directly, not the individual parameters as we have from the SEACAT profiler. According to Christensen [1995], HSU Supervisor, SVP-1 data are questionable as far as their accuracy is concerned and should be used with caution. From his experience, SVP-1 data are only good within 5 m/s accuracy. Consequently, this data will not be used in this proposed work.

The SSP data available are for ten different locations, but only six of them have enough data to actually be able to find the temporal effect. The other four locations have very few records. Each location is actually an oil field. The ten locations are Safaniya, Zuluf, Marjan, Lawhah, Berri, Juaymah, Abu Safa, Ras Tanura, Tanajib, and Khafji. Some of the data records are available in analogue form, and some are in digital form. Appendix I gives the available data listings for the six locations broken down to the number of records in each month for each location. Very few multiple data records were available for a single day since the SSP measurements are usually taken once in the morning of each survey operational day.

1.5 PROPOSED WORK

Variations in sound speed through the entire water column must be taken into account to correctly interpret swath bathymetry measurements. Knowledge of the complete sound speed profile is necessary to account for refraction effects on oblique acoustic rays. The lack of knowledge of the actual SSPs will limit the maximum obtainable swath angular sector. Not compensating for refraction effects will yield errors in determination of angle of arrival and the ray path. Those discrepancies give rise to errors in both travel time and cross-track distance computation which increases as the incidence angle increases. This study includes five different investigations:

- *Sound speed measurement procedures and calculations.* What formula should be used to extract the SSP from CTD measurement? METOCEAN plc [Pike and Beiboer, 1994] compared the different algorithms for the speed of sound. In this work, we extend their comparison study to include the high temperature and salinity of the Gulf. There is no ground truthing available for these calculations, because the best way to check these is by directly measuring sound speed with a well-calibrated, highly accurate velocimeter, in an area of high salinity, and at the same time, in the same spot, taking CTD measurements and perform sound speed calculations using the different formulae. Such data were not available for this study. This should be done if an accurate conclusion is to be drawn to the best formula to be used - something worth looking into in the future. What will be done in this report is a comparison study of the different algorithms, using the Chen and Millero formula [1977] as a standard since it is the most widely accepted formula in the oceanographic world. Furthermore, since no formula has been validated over a salinity of 40‰, an inter-comparison study of the different algorithms will also be performed to suggest which formulae solutions are close to each other and which are not.

- *Variability of salinity, temperature and SSP in the area of interest in the Gulf*. Based on the data available, these parameters and the SSP will be assessed and described.
- *Effect of ray bending on the outer beams*. This is the main problem addressed. A ray tracing program shall be created starting with routines of Hughes Clarke [1995] with the addition of an isogradient-solution routine (by the author). Using measured sound speed profiles, a look-up table (LUT) of refraction solutions will be created. The axes of this LUT are launch inclination angles and travel (propagation) time. The ray trace solution for discrete ray angles ranging from vertical to the lowest launch inclination angle that is expected will be prepared. Rays should be traced out to the maximum possible travel time. For each time/angle pair, there is one depth and one cross-track unique solution contained in the LUT.
- *A sensitivity study of temporal and spatial variations on the refraction solution for actual depths*. This study will use actual SSPs available from the SEACAT profiler CTD/SV probe for those areas of the Arabian Gulf in which Saudi Aramco operates. Calculation of sound speed in the available SSPs were made using the Chen and Millero formula. These profile will be recalculated if other formula should be suggested by the first investigation (sound speed measurement procedures and calculations).

- *An isogradient solution will be attempted in the proposed LUT program that will be used in the sensitivity studies for different water masses temporally and spatially.* These sensitivity studies should show the effect on the soundings of near transducer changes in SSP, as well as the shape of the SSP.
- *Investigation of practical methods for refraction errors*. The feasibility of installing an accurate velocimeter near the transducer will be investigated , in order to help define multibeam sonar results within the accuracy specified in IHO S . 44 [1987]. Current operational practices of other hydrographic agencies for correcting of refraction errors will be considered, (such as like the Royal Danish Navy towed velocimeter system) in order to identify what procedure to implement under the unique conditions in the Gulf (high salinities and temperatures).

1.6 REPORT CONTENT

This is a description of the content of the rest of this report. In Chapter 2, the different sound speed algorithms will be compared. Temperature, salinity and sound speed variations in the Gulf will be described in Chapter 3. Chapter 4 will discuss the spatial and temporal effect of the observed SSP from the Gulf on multibeam echo sounding bathymetry. Chapter 5 will give conclusions and recommendations.

1.7 EXPECTATIONS

Lack of knowledge of actual refraction of sound in seawater is a very important source of error in swath bathymetry. The effect of changes in the SSP from day-to-day temporal changes of 10 different locations in the area of interest will be assessed and described. So, this study hopefully will result in recommendations on the following:

1. What formula to use to calculate the SSP in the unique situation in the Gulf.
2. Procedures to follow for SSP sampling, including frequency, categorized by the area and month or season.
3. Practical methods for correcting refraction errors on multibeam echosounder bathymetric systems based on literature search on current practices of other agencies.

Table 1-1 Milestone-Dates timetable.

Event	Milestone Completion Date
1. Isogradient Ray Tracing Program.	1 September 1995
2. Extension of algorithm comparisons for calculating the best sound speed equation.	1 November 1995
3. Variability of salinity, temperature, and SSP within the ten locations.	1 December 1995
4. Sensitivity study of temporal and spatial variations on the refraction solution for actual depth.	15 January 1996
5. Delivery of first draft of MEng report.	6 March 1996
6. Presentation and Delivery of final draft of MEng report.	25 March 1996

Chapter 2

SOUND SPEED ALGORITHMS COMPARISON FOR OPTIMAL EQUATION IN THE SAUDI ARAMCO CONCESSION AREA IN THE ARABIAN GULF

2.1 INTRODUCTION

The purpose of this chapter is to provide guidelines for the speed of sound measurement techniques for use with multi beam echo sounders operating in the Saudi Aramco concession area of the Arabian Gulf. This is an extension to the comparison study conducted by METOCEAN plc [Pike and Beiboer, 1994]. The extension is performed to suggest a single formula or formulae to include a wider range of temperatures and salinities since the Gulf experiences an unusual wide range of both of these oceanographic parameters. Also, an update correction to one formula was introduced by Millero and Li [1994] since the Pike and Beiboer study resulting in a slight change in findings of this study as compared to theirs.

2.1.1 Outline

The measurement techniques will be explained in section 2.1.2. and reasons for the comparison study is given in section 2.1.3.

Methodology will be discussed in section 2.2 which includes the selection of algorithms, pressure to depth conversion, and the study approach. Section 2.3 will discuss the results and give recommendations to be followed.

2.1.2 Measurement Techniques

Sound speed measurement in seawater can be accomplished in two ways. One is the direct method where a velocimeter is deployed into the sea from a ship. A velocimeter is an acoustic device to measure the travel time of short pulses between a projector and a receiver. It operates on the so-called "sing-around" or "bowler" principle in which the arrival of a pulse at the receiver initiates the succeeding pulse transmission from the projector.

The other method is called the indirect method. This employs a Conductivity-Temperature - Depth probe (CTD). Conductivity is the quantity from which salinity can be obtained. Measurements of these three oceanographic quantities or parameters (temperature, salinity, and pressure which can be converted into depth) can be used with an algorithm relating these parameters to sound speed in seawater. There are many equations calculate the sound speed from these oceanographic parameters. Some of them use depth term instead of pressure. Some of these equations are listed in section 2.2.1.

2.1.3 Reasons for the Study

Determining the correct sound speed profile is very critical in correcting for acoustic refraction in multibeam echo sounder data, particularly for the outer beams. In the extreme case of an outer beam which is 75° off the vertical axis, the sound speed at the transducer and the mean sound speed between the transducer depth and the bottom depth, must each be known to about ±1 m/s in order to provide a sounding accuracy of

±1 % of depth [Dodds, 1994]. The ±1 m/s is used as criterion to decide if a certain difference from a benchmark value is negligible or not.

There are five well-known algorithms that are used in this study. These algorithms are applied outside their validity ranges to investigate the possibility of using CTD measurement of the high temperature and salinity of the Arabian Gulf. CTD generally gives more reliable data than the velocimeter. For example, the SVP-16 is accurate to 0.2 m/s [Applied Microsystems Ltd., 1990] while the value determined by de Moustier [Hughes Clarke et al., 1995] for CTD accuracy using the Mackenzie formula was 0.051 m/s. Usage of other formulae would give a comparable results. Velocimeters are susceptible to frequent breakdowns and requires constant calibration [de Moustier, 1995]. Biological fouling and small dimension changes seriously affect the accuracy. Calibration of a velocimeter is needed in cases of a path length change which could be caused by accidental bumping the sound chamber reflector plate or spacing rods. Calibration is a laboratory intensive operation that requires access to reference instruments of sufficient accuracy to ensure accurate calibration for the velocimeter, if these instruments are not available then shipment of the velocimeter to the factory for recalibration is necessary.

2.2 METHODOLOGY

2.2.1 Selection of Algorithms

Five algorithms were selected for this study for four reasons:

First: The METOCEAN plc [Pike and Beiboer, 1994] study recommended four of five equations be used in certain conditions. Those recommendations are:

I. Chen & Millero [1977] used for water depths less than 1000 m.

II. Del Grosso [1974] used for water depths greater than 1000 m.

III. Mackenzie [1981] used for quick computation up to 8000 m water depth.

IV. Medwin [1975] for quick computation up to 1000 m water depth.

For comprehensive description and original scientific measurement, the original papers by the respective author(s)of each equation should be consulted. The list of references at the end of this report, lists a number of good reviews and fruitful discussion of the above mentioned equations as well as some other ones.

The actual algorithm of all the five equations are given as Mathcad outputs of two computational examples, in Appendix II. The range of validity of all equations used was taken from Pike and Beiboer [1994] and is as follow:

Chen & Millero [1977] temperature range is 0° C to 40° C, salinity range is 30‰ to 40‰, and pressure is 0 bar to 1000 bar.

Del Grosso [1974] validity range is indicated in Table 2-1 below in which the maximum valid pressure is indicated for each temperature and salinity:

Table 2-1 The range of validity of the Del Grosso formula.

	Temperature in °C			
Salinity ‰	0	5	10	15
33	1034	1034	275	69
34	1034	1034	207	207
35	1034	1034	414	207
36	1034	1034	275	69
38	69	69	414	414

Mackenzie [1981] is stated to be valid for naturally occurring seawater in the intervals indicated in Table 2-2 below:

Table 2-2 The range of validity of the Mackenzie formula.

Pressure in kg/cm^2	Temperature in °C	Salinity ‰
0	0-30	30-40
50	0-20	32-40
100	0-14	32-34
	0-16	35-38
	10-16	39-40
200	0-12	32-36
	0-16	37
	8-16	38-39
500	0-5	33-36
	12-14	38-39
800	0-5	34-35

Medwin [1975] validity range is indicated in Table 2-3 below in which the maximum valid pressure (bar) is indicated for each temperature and salinity:

Table 2-3 The range of validity of the Medwin formula.

	Temperature in °C			
Salinity ‰	0	5	10	15
33	100	100	100	69
34	100	100	100	100
35	100	100	100	100
36	100	100	100	69
38	69	69	100	100

Wilson [1960] temperature range is-4° C - 30° C, salinity range is 0‰ - 37‰ and pressure in kg/cm^2.

Second: The Wilson formula [1960] has been the standard for sound speed calculation in seawater by hydrographic surveyor for many years, because of its simplicity for rapid computation, which lends itself to hand-held calculators. Therefore, we have included it in the comparison as the fifth equation. Actually the simplified version of this equation with depth term is the version that has been used by the surveyors, and it is that version of Wilson's formula that was used in this comparative study.

Even though, questions about inconsistent values from this equation arose as early as a decade ago, surveyors have kept using it to correct for depth measurement in single vertical beam echosounder, evidently because of its simplicity. It is used to convert time registered by the echosounder to depth. Now that oblique propagation of acoustic signals is possible (as the case in multi beam echosounder), ray bending makes a small error in the calculated sound speed result in rather significant errors in both position and depth.

Third: Two things that are in mind when the study was conducted. One is to find the most accurate formula for the sound speed computation. The other is to find the simplest algorithm which maintains adequate accuracy. A tradeoff between computation speed and accuracy is required. Reliable velocimeter data would be required to validate the chosen equations.

Fourth: A slight correction has been added to the Chen and Millero equation [1977] that appeared in a recent paper by Millero and Li [1994]. This correction followed previous research that suggested that Del Grosso equation [1974] was more accurate. That is why in this study the corrected Chen and Millero equation [1994] was used as the benchmark for the appraisal of the other four algorithms. However, no extension of the standard ranges of temperature (0° C - 40° C) and salinity (30‰ - 40‰) was made by Millero and Li (1994). This formulae has been accepted as standard formula in the oceanic community [Pike and Beiboer, 1994].

2.2.2 Pressure to Depth Conversion Discussion

Depth to pressure conversion and vice versa must be taken into account when assessing sound speed algorithms in deep oceans. The UNESCO algorithm has been accepted since its introduction as the standard pressure to depth relationship [Pike and Beiboer, 1994]. However, because we are dealing with a very shallow area of less than 60 metres (the average depth of the Gulf is 35m), a simple version of the UNESCO formula[Pike and Beiboer, 1994] was used. Using this simple version of the full UNESCO formula means ignoring the geopotential term (Δd) which leads to an error of calculated speed of sound at 100m of ± 0.04 m/s which is negligible (an error of ± 0.1 m/s at 250m depth was shown on [Pike and Beiboer, 1994]). So, we used the simple UNESCO algorithm and calculate the depth based on the pressure for a common latitude of 28° C - two examples of the depth / pressure conversion and the comparison for these different sound speed formulae is given in Appendix II.

2.2.3 Study Approach

The sound speed was calculated for different ranges of temperatures and salinities for two depths of 10 m and 60 m using each of the five formulae. The two depths were used to illustrate the comparative change between near surface and deep water. These equations were used first in comparison to each other in different scenarios of varying salinities and temperatures. Then differences to the benchmark equation (Chen and Millero[1994]) was shown.

In the comparison, calculations of sound speed by the five equations were performed in two scenarios:

First: Varying temperature from 15° C to 40° C in an increment of 5° C and keeping salinity constant at 35‰ at a depth of 10 m and 60 m and 65‰ at the same two depths.

Second: Varying salinity from 35‰ to 65‰ in an increment of 5‰ and keeping temperature constant at 15° C at a depth of 10 m and 60 m and 35° C at the same two depths (see Tables 2-1 to 2-8 and Figures 2-1 to 2-8 gathered together in Appendix III).

Then showing the amount by which the corresponding speed of sound using the other four equations exceeded Chen and Millero. The divergence of each from the benchmark equation were determined analogous to the previous comparisons, that is according to:

First: Varying temperature from 15° C to 40° C in an increment of 5° C and keeping salinity constant at 35‰ at a depth of 10 m and 60 m and 65‰ at the same two depths.

Second: Varying salinity from 35‰ to 65‰ in an increment of 5‰ and keeping temperature constant at 15° C at a depth of 10 m and 60 m and 35° C at the same two depths. (see Tables 2-9 to 2-16 and Figures 2-9 to 2-16 gathered together in Appendix III)

2.3 RESULTS AND RECOMMENDATIONS

Much of the calculation carried out in this report was based upon a master file on Math Soft MathCad 5.0 encompassing all five speed of sound equations in seawater and the simple UNESCO pressure to depth conversion formula. The two examples presented in Appendix II are printout of this file for two different situations (one example is for temperature value of 35° C, salinity range of 35‰ to 65‰ and depth of 10 metres the other example is for salinity value of 35‰, temperature range of 15° C to 40° C and depth of 10 metres).

As shown, this file creates a number of ASCII files. These ASCII files were then imported into a Microsoft Excel spreadsheet and manipulated to produce the various figures and tables shown in Appendix III.

2.3.1 Comparison of Formulae

Tables 2-1 to 2-16 and Figures 2-1 to 2-16 (found in Appendix III) clearly demonstrate that the Wilson equation is unsuitable, as it diverges significantly from the other formulae. The Wilson equation seems to stand alone by itself from the rest. This supports the finding of Pike and Beiboer [1994] that this equation should not be used for precise computation. The difference to Chen and Millero equation ranged from a minimum of 1.918 m/s occurring at 15° C, 35‰ and 10 m of depth to a maximum of 14.292 m/s occurring at 40° C, 35‰ and 60 m of depth. This is interesting, since the maximum difference didn't occur at any extreme of the range of parameters namely at 40° C, 65‰ and 60 m of depth where it is only 12.913 m/s. This suggests the correlation between these equations is not really linear.

The other four equations show close agreement with each other (from Tables 2-1 to 2-8 and Figures 2-1 to 2-8 found in Appendix III). The differences of the other four equations as compared to Chen and Millero equation have also suggested a similar conclusion (from Tables 2-9 to 2-16 and Figures 2-9 to 2-16 found in Appendix III) with agreement to Del Grosso's being the closest almost throughout the tested ranges. The difference between the two equations is almost negligible (a maximum of 0.728 m/s at 40° C, 65‰ and 60 m of depth).

The other two simple equations (Medwin and Mackenzie) have shown some potential to be used in certain situations (when rapid computation and use of hand-held calculator is necessary). The Medwin equation shows closer agreement to Chen and Millero at high temperatures, while at low temperatures the Mackenzie equation is closer. The Medwin equation is closer than the Mackenzie equation to the two precise equations when varying salinity at high temperature (maximum of 1.114 m/s was found at 40° C, 65‰, at 10 m depth). This is in a way expected since the Medwin equation is a simplified version of the Del Grosso equation. The Mackenzie equation has differences greater than ±1 m/s to the Chen and Millero equation (maximum of 2.24 m/s was found at 40° C, 65‰, at 10 m depth)

2.3.2 Recommendations

The following are some recommendations to be followed regarding sound speed calculation in the abnormal situation in the Saudi Aramco concession area in the Arabian Gulf:

- The Wilson equation should not be used at all because it is clear that it does not fit well with the other formulae. This fact was recognized a long time ago, but because of its simplicity, it is still in use.

- For the time being, the updated version of Chen and Millero formula should be employed. This should be done for the sake of completeness since the difference between the corrected and uncorrected version of the formula is negligible (a maximum of ±0.016 m/s was obtained).

- For rapid computation, or when depth is known but not pressure, and when working with hand-held calculators, and only when it is necessary, the Medwin equation should be employed.

- Perform direct observations of sound speed versus depth using a well-calibrated velocimeter of known accuracy such as the SVP-16 (accurate to 0.2 m/s) in certain coastal locations of high salinity and variable temperature. Sufficient care should be taken in taking these direct measurements. Then compare those values to the sound speed values using the four equations, excluding Wilson, derived from oceanographic parameters for the same spots and at the same water depths . This comparison should be run for at least a year to show the corresponding temporal changes and the performance of these algorithms under different situations. This is the long-term approach, but should be done as soon as possible. Recommendation of one formula that gives a calculated sound speed in seawater in the Arabian Gulf accurate to ±1 m/s would then be possible and should be expected.

Chapter 3

TEMPERATURE, SALINITY AND SOUND SPEED VARIATION DESCRIPTION

3.1 SCOPE

This chapter gives a description of the temperature and salinity variations in the following locations of the study area: Abu Safa, Berri, Ras Tanura, Safaniyah, and Zuluf. Sound speed variation descriptions will also be given for each of the five locations as well as for Marjan. See Figure 3-1 on next page for the approximate position of each location in the Arabian Gulf.

A general overview of the factors affecting temperature and salinity (the two main factors responsible for sound speed variation in seawater) was given in Chapter 1. Also since a general description of the variation of those two oceanic parameters in the Gulf was also given in Chapter 1, the assessment and characterization of these two oceanic parameters and their resultant sound speed are described here based on the available data in specific locations for specific times of the year. Therefore, any conclusion drawn from these data records will be for those times and locations only.

The original profiles were stacked together to yield a slide show of profiles as time of the year progresses where variations can be monitored dynamically. A common scale for all profiles of each type (temperature, salinity, or sound speed) was selected and the slide shows were created using Microsoft PowerPoint. Disks contain these PowerPoint files can be obtained from the author. It was decided that no printouts of

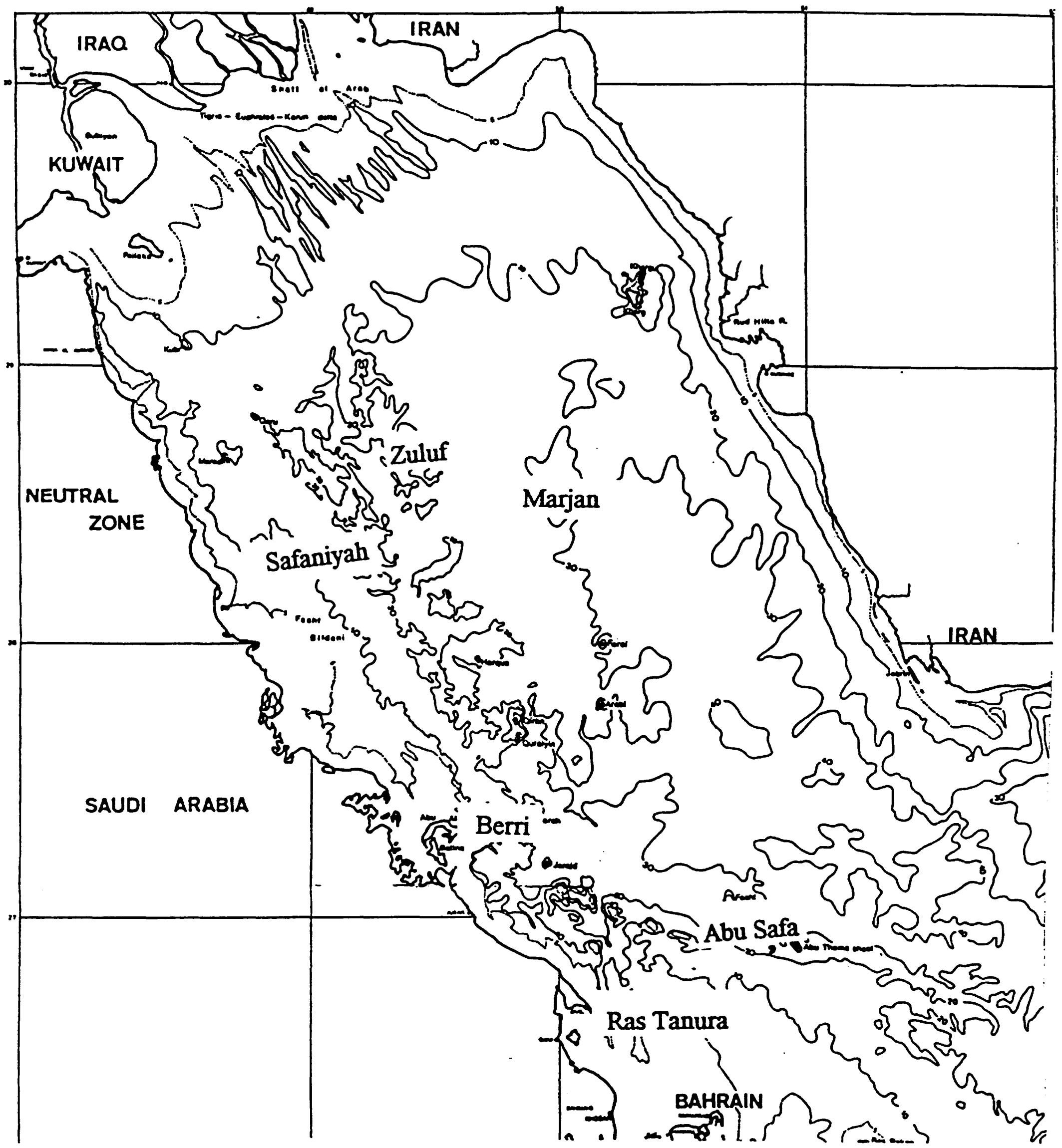

Figure 3-1 Map of the Arabian Gulf showing the approximate position of each of the six locations (from Purser[1973])

these files would be given in this report to save some trees. Instead a three-dimensional line graph is given for each location showing the variation for selected depths depending on the available depth attained during the observation.

3.2 ABU SAFA

3.2.1 Temperature Variation

The available data here were for ten days. The selected depths were 2.5 m, 5.0 m, 10.0 m, and 15.0 m for this area. Figure 3-2, shown on Appendix IV, a representation of the temperature profile in Abu Safa, is a selection of the original data created to present the general picture of the variation for the available three months.

The temperature for 2.5 m of water starts to decline from December 2, 1994, where it is about 25°C, to about 23°C on December 14, 1994. Then it stabilized at that value to December 18, 1994. January 11 showed a reading of 21°C. February showed readings of 17.5°C for the days 20, 22 ,and 23, 1992. There is an abnormal low temperature of 3.5°C on February 21, 1992 that shows up as a dip in the graph below (Figure 3-2 shown on Appendix IV).

All the profiles except the one for February 21 seem to be almost straight lines which means homogeneous water temperatures along the profiles. The profile for February 21, 1992 is either an interesting situation or there could have been an instrument reading error. There is a layer of increased temperature with depth up to 15 m then a constant temperature of 17.2°C the rest of the profile. So from 15 m down it looks like the other profiles for February. One possible reason is that the instrument was put in the water before it was allowed to heat up for two minutes as suggested by the manufacturer. There is a suspicion of the presence of such cold water, however, we have to remember this is February the coldest month in the Gulf area. Therefore, a careful monitoring of such profile should be maintain in the future and another sound speed dip should be done to confirm if the first dip is correct.

3.2.2 Salinity Variation

Figure 3-3, shown on Appendix IV, is based on salinity data for the same ten days. It gives a general picture of the salinity profile in Abu Safa for the same three months at water depths of 2.5 m, 5 m, 10 m, and 15 m.

Salinity was about 38.3‰ in 2.5 m of water for December 2, 1994. Then it decreases to 38‰ on December 14, 1994. It stabilized at that a value of 37.5‰ from December 16, 1994 to January 11, 1995. February showed salinity readings of 40.3‰ for days 20, 22 ,and 23, 1992. There is an abnormally high salinity of 60‰ for February 21, 1992 that shows up as a spike in the graph. February 21, 1992 is the same day that had the cold temperature revealed in section 3.2.1.

All the profiles except the one for February 21, 1992 seem to be almost straight lines which means homogeneous water salinity along the profiles. Again the profile for February 21, 1992 has a decrease in salinity with depth until about 15 m where the salinity becomes constant the rest of the way. Similar reasoning to the one given in section 3.2.1 is suggested, and the same recommendation and procedure for sound speed profile observations should be maintained.

3.2.3 Sound Speed Variation

Figure 3-4, shown on Appendix IV, shows the sound speed variation calculated from the corresponding temperatures and salinities. There are 13 days of sound speed data profiled in this figure. We had more sound speed profiles than temperature and salinity because we had some data that were only in sound speed values with no corresponding temperatures and salinities. So the picture that can be drawn from the sound speed profiles data are for a wider length of the year. It spans from September 24 to February 23, a period of about five months.

Sound speed ranged from about 1557 m/s in 2.5 m of water for September 24, 1994 to 1500 m/s in February 21, 1992. There is certainly a decreasing trend in sound speed as time progresses from September to February. Most of the profiles seem to represent a quite homogeneous water environment except for the data of February 21, 1992. This goes well with our observations that we made in sections 3.2.1 and 3.2.2. September 24, 1994 is another interesting profile. There seems to be a constant decrease in sound speed with depth. It started at a depth of 30 m of about 1554 m/s and ended up at 42 m of 1547 m/s. This profile will be chosen as one of those used in the upcoming investigation of spatial and temporal effect of sound speed variation on the refraction solution.

3.3 BERRI

3.3.1 Temperature Variation

The available data here are for twelve days. Figure 3-5, shown on Appendix IV, a representation of temperature profile in Berri, is a selection of the original data created to present a general picture of the variation for the available data from October 29 to February 18. The selected depths were 2.5 m, 5 m, 10 m, and 15 m for this area.

The temperature for 2.5 m of water started at 27.7°C on October 29, 1992 and increased slightly to 29.1°C on November 2 and 3, 1994. Then it started to decrease toward the end of the month as it fell to 25°C on the 29th. The temperature decreased even further to 18.9°C on January 3, 1993 and to 17.5°C in February 4, 1992. The last temperature readings for the rest of February changed only few tenths of a degree, ranging from 18.7°C to 18.2°C.

All the profiles seems to be almost straight lines which means homogeneous water temperature along the profiles. No abnormal profiles here.

3.3.2 Salinity Variation

Figure 3-6, shown on Appendix IV, is based on salinity data for the same twelve days. It gives a general picture of the salinity profile in Berri for the same period at water depths of 2.5 m, 5 m, 10 m, and 15 m.

Salinity was about 40.06‰ in 2.5 m of water for October 29, 1992 and then decreased and stabilized to 38‰ on November 2 and 3, 1994. It decreased to 37.8‰ on

November 29, 1994. Then it experience a noticeable increase to 40.33‰, 40.36‰, and 41.21‰ on January 3, 1993 February 4, and 8, 1992 respectively. It shows a slight decrease to 40.96‰ on February 9, 1992 and an even sharper decrease on February 9, 1992 to 31.568‰. This last salinity number seem to be abnormal as it comes between two days of much higher salinity in the same general area as salinity increase to 40.64‰ on February 15, 1992 in the same year. February 16 and 18, 1992 show values of 40.69‰ and 40.52‰. This means that in the same area on February 10, 1992 fresh water was present at that site and this record seems more believable than did the abnormal situation that was experienced in Abu Safa (sections 3.2.1 and 3.2.2) where it was an obvious matter of the instrument not taking time to adjust or warm up. In this case it was seen only in the salinity not in both salinity and temperature records.

Profiles seems to be almost straight lines which means homogeneous water salinity along the profiles with profiles for two days where a gradual increase with depth in salinity occurred between about 15 m to 20 m of water on November 2 and 3, 1994. There is the interesting profile that we mentioned of it having an abnormal low value for 2.5 m in the previous paragraph. This profile showed a fresh water up to about 5.5 m then it stabilized at the normal saline water of 40.66‰ the rest of the water depths. A possible reason for this could be local rainstorm or a wadi mouth.

3.3.3 Sound Speed Variation

Because the temperature profile shows a homogeneous water temperature, the shapes of sound speed profile will generally resemble those of the salinity. The same twelve days of data were selected to give us the general picture of the sound speed variation for the top 15 m of water for the same time as the previous two sections. The graph in Figure 3-7, shown on Appendix IV, shows sound speed variations calculated from the corresponding temperatures and salinities.

Sound speed ranged from about 1547 m/s in 2.5 m of water for October 29, 1992 to a low of 1514 m/s on February 10, 1995. There is certainly a decreasing trend in sound speed as time progresses from October to February. Most of the profiles represent quite homogeneous sound speed water environments except for February 10, 1995. There exists a shift in sound speed between 5 m and 10 m from 1515 m/s to 1524 m/s with shallower water than 5 m having the lower value and deeper water than 10 m having the higher value. This shift is represented by a dip in the 3-D line graph of Figure 3-7 shown on Appendix IV. This goes well with our observation that we made in section 3.3.2 about this particular profile.

3.4 RAS TANURA

3.4.1 Temperature Variation

The available data here are for 41 days. From those 41 days we selected nine widespread days of data presented in Figure 3-8, shown on Appendix IV. This is a representation of temperature profile in Ras Tanura created to present the general picture of the variation for the available data from February 20 to November 3. The selected depths were 2.5 m, 5 m, and 10 m for this area.

The temperature in 2.5 m of water ranged from a minimum of 15.8°C on February 20, 1992 to a maximum 32.5°C on August 24, 1992. It starts at its minimum then it starts increasing slightly to reach 16.2°C and 17.7°C on March 6 and 14, 1992 consecutively. The next available reading is on July 5, 1993 when it reaches to 29.46°C and then there is a slight decrease to 28.77°C then it reaches its maximum before starts to decline. The temperature shows a reading of 31.89°C, 27.54°C and 27.06°C on September 25, 1992, October 17, 1992, and November 3, 1992 respectively.

The nine profiles that were selected here seems to be almost straight lines which means there is a homogeneous water temperature along the profiles. There are about three profiles, however, that demonstrate some heterogeneity in the water masses. A very interesting profile is that of July 11, 1993. On that day, it looks like a straight line up to about 30 m depth then there seemed to be a shift of quite abrupt change of temperature of about 5°C between 30 m to 40 m before it assumed the new colder temperature of 23°C at 40 m thereon. The two other abnormal profiles were those of March 8 and 14, 1992, which demonstrated a warmer layer of about 5°C from the water surface to about 10 m down.

3.4.2 Salinity Variation

Figure 3-9, shown on Appendix IV, is based on salinity data for the same selected nine days. This figure gives a general picture of the salinity profile in Ras Tanura for the same period at 2.5 m, 5 m, and 10 m depths.

Salinity profiles here are marked by an up and down reading of about 2‰ in the selected nine days of data. Salinity increased from about 40.70‰ in 2.5 m of water on February 20, 1992 to 40.87‰ on March 6, 1992 then decreased to 39.28‰ on March 14, 1992. It increases again to 40.19‰ on July 5, 1992. Then it decreased to 39.76‰ on July 11, 1993 then increased again to 40.38‰ on August 24, 1992. Then it experienced an unnoticeable decrease to 40.29‰ on September 25, 1992 before it increased on the last two days to reach 40.56‰ and 40.87‰ on October 17, 1992 and November 3, 1992.

The same three days that had rather unusual temperature profiles also had unusual salinity profiles. The salinity profile for July 11, 1993 showed some low salinity in the top two metres before stabilized around 40‰. Therefore, the CTD probe not settling down could be the case or the real existence of heterogeneous water masses could be the case. As we have said earlier, no definite answer could be given and it is worth taking another observation when something like this happens in the future. Other profiles seem to be almost straight lines which means homogeneous water salinity along the profiles.

3.4.3 Sound Speed Variation

The same nine days of data were selected to give us the general picture of the sound speed variation for the top 10 m of water for the same time as in sections 3.4.1 and 3.4.2. The 3-D line graph in Figure 3-10, shown on Appendix IV, shows the sound speed variation from February 20 to November 3 calculated from the corresponding temperatures and salinities. In Figure 3-10, shown on Appendix IV, the shape of the sound speed variation resembles that in Figure 3-8 for temperature variation for the same site.

Sound speed ranged from a minimum of about 1517 m/s in 2.5 m of water for February 20, 1992 to a maximum of 1556.47 m/s on August 24, 1992. There is an increasing trend in sound speed as time progressed from February to August then it started to decrease again. The two profiles mentioned above in sections 3.4.1 and 3.4.2 as abnormal profiles in March give a quite expected result of sound speed profile shapes. These resemble the corresponding temperature profiles since temperature is the most influential factor behind sound speed in seawater. The third interesting profile we mentioned in section 3.4.2, of July 11, 1993, was again followed the same profile shape of temperature in the most part except for the top two metres which was influenced by the low salinity on that day.

3.5 SAFANIYAH

3.5.1 Temperature Variation

The available data here are for fourteen days. From those we selected nine widespread days of data for presentation in Figure 3-11, shown on Appendix IV. This is a representation of the temperature profile in Safaniyah created to present the general picture of the variation for the available data from October 27 to February 4. The selected depths were 2.5 m, 5 m, and 10 m for this area. This was done because most of the data were taken in shallow areas and those three depths were common to the available data.

The temperature for 2.5 m of water ranged from a maximum of 26.74°C on October 27, 1992 to a minimum of 13.22°C on January 29, 1992. It started at its maximum then it decreased slightly to reach 26.47°C on October 28, 1992 and dipped even further to 24.41°C on January 13, 1992. The slide continued for the temperature in January as we have 16.64°C and 14.77°C on January 19 and 25. It reached its minimum then it started increasing again slowly to end with 16.23°C on February 4, 1995. We have two readings for February 2, one in 1992 and the other in 1995, and because it was not possible to be taken exactly in the same place but rather where the survey took place within that oil field, there is a difference of about 0.65°C which could be attributed to temporal and regional differences.

Almost nothing is abnormal about the profiles that are available here since they seem to be almost straight lines. This means homogeneous water temperatures along the profiles, except there is the shift of about 1°C between 8.6 m depth and 11 m depth in the profile of February 2, 1992. This makes this profile consist mainly of two layers with the colder layer below. This area also represents one of the coldest among the different locations included in this study.

3.5.2 Salinity Variation

Figure 3-12, shown on Appendix IV, is based on salinity data for the same selected nine days. It gives a general picture of the salinity profile in Safaniyah for the same period at 2.5 m, 5 m, and 10 m depths.

Salinity profiles for the period of three months and seven days are marked by oscillations of about 5‰ to 6‰ in the selected nine days data. This can be explained by noticing that the lower salinity was recorded in those profiles for 1995 whereas the high salinity was for of 1992. Therefore, it is clear that the area surveyed in 1995 are definitely much different and probably not in the same vicinity of that for 1992. The changes in salinity here are thus due to a change of sampling site.

All profiles seem to be almost straight lines. This means homogeneous water salinity along the profiles if we do not consider the top two metres which usually have either higher or lower salinity than the rest of the profile. The exception is for one profile on January 13, 1992, which has two readings in about 32.6 m and 32.8 m depth which are lower by about 5‰.

Those changes in salinity and temperature at the top few metres resulting in sound speed changes are more important than the ones happening in the deep water very far from the multi beam transducer. This is because changes near the transducer, or the transducer pitching up and down in two different layers, as we will see later, have much more effect on the refraction solution.

3.5.3 Sound Speed Variation

The same nine days of data were selected to give us a general picture of the sound speed variations for the top 10 m of water for the same time as that used in sections 3.5.1 and 3.5.2. The 3-D line graph in Figure 3-13, shown on Appendix IV, shows the sound speed variation from October 27 to February 4 calculated from the corresponding temperatures and salinities.

Sound speed ranges from a maximum of about 1544.8 m/s in 2.5 m of water for October 27, 1992 to a minimum of 1508 m/s on January 25, 1995. There was a decrease in sound speed as time progressed from October to January as temperature drops to a low mark. This makes the shape of the 3-D line graph resemble that of the temperature in Figure 3-11. The sound speed started to increase slightly to 1509.73 m/s on January 29, 1992. Then we have the two readings for February 2, one in 1992 and the other in 1995. Because it is not possible to be taken exactly in the same place, but rather where the survey took place within that oil field, there is a difference of about 5 m/s which could be attributed to temporal from year to year and regional differences.

The effect of salinity on sound speed can be evident in the same profile mentioned above in section 3.5.2 for 13 January 1992. Low salinity at 32.6 m and 32.8 m depth have resulted in lower sound speed at those two depths in that profile than the rest of the profile.

There is not much difference in the sound speed profile from top to bottom which an indicative of a homogeneous water mass. However, there is the result of that shift in temperature profile mentioned in section 3.5.1 in the profile of February 2, 1992. This yielded a similar shift of about 2.42 m/s between 8.6 m depth and 11 m depth.

3.6 ZULUF

3.6.1 Temperature Variation

The available data here are for thirty days. From those we selected eleven widespread days data to give Figure 3-14, shown on Appendix IV. This is a representation of the temperature variations in Zuluf area created to present a general picture for the period of the year from August 13 to April 1. The selected depths were 2.5 m, 5 m, 10 m, 15 m, and 20 m for this area.

The temperature for 2.5 m of water ranged from a maximum of 30.19°C on August 13, 1991 to a minimum of 17.31°C on February 20, 1995. The temperature started at its maximum then decreased slightly to reach 30.15°C and 29.12°C on September 17 and 30, 1991 respectively. In October, it reached 28.64°C and 28.27°C on October 7 and 19, 1991. It showed even lower temperatures in November as it dipped to 24.41°C on November 26, 1991. December showed a further decline to reach 20.89°C on December 20, 1991 and likewise for January and February, the coldest two months of the year, it reached 18.33°C on January 8, 1992 before it hit its minimum on February 20, 1995. In March and April, it started to increase again or warm up as it recorded 18.73°C and 19.06°C on March 19, 1995 and April 1, 1995.

Some of the profiles that were available for this area show some interesting changes in temperature from top to bottom of the profile. One of them is the profile of August 13, 1991. Here, the profile looks like a constant temperature of 30°C up to a depth of 10 m, from there it has a constant gradient until it reached about 27°C at a depth of 16 m. It then assumed this value for the rest of the profile. Another profile is that of September 19, 1991. Here the temperature gradient is not as steep as it does not assume the 27°C until a depth of about 35 m for the rest of the profile starting at the top with about 30°C temperature. A third one is the profile of November 20,1991. This profile has almost a constant temperature of about 24.4°C in the first 15 m of water, then it has a positive temperature gradient that indicate a temperature increase with depth for the rest of the profile. There is 27.7°C in the last recorded temperature in the deepest point in the profile of 38.98 m. The rest of the profiles are either straight lines or close to straight lines with a maximum of 1°C change from top to bottom.

3.6.2 Salinity Variation

Figure 3-15, shown on the next page, is based on salinity data for the same selected eleven days to give the general picture of the salinity variation in Zuluf for the same period in the year (i.e. from August 13 to April 1). The selected depths are 2.5 m, 5m, 10m, 15m and 20m.

The salinity profile seem to be hopping around 40‰ for most of the 2.5 m readings. It varied from a minimum of 38.7‰ on March 19, 1995, to a maximum of 40.7‰ on January 8, 1992.

The salinity profiles look homogeneous from top to bottom as one can see in Figure 3-15. There is a maximum of 0.9‰ difference from one depth point to the next in the same profile (on December 20,1991 at 2.5 m and 5 m depth).

3.6.3 Sound Speed Variation

The same selected eleven days of sound speed profiles were calculated from the corresponding temperatures and salinities. Figure 3-16, shown on Appendix IV, gives us the idea about the temporal variation of sound speed in Zuluf at 2.5 m, 5 m, 10 m, 15 m and 20 m.

Sound speed at 2.5 m ranged from a minimum of 1519 m/s on February 20, 1995 to a maximum of 1551 m/s on August 13, 1991. The sound speed profiles look to be homogenous in this area with not much change from top to bottom of the profiles. There is no apparent gradient to mention in this section.

We said in section 1.3 that temperature has more influence on the calculated sound speed. We see a very evident demonstration of that statement here. There is a resemblance of the shape of the sound speed variation graph to the temperature graph. This demonstrates the dominance of temperature on the other two factors (salinity and pressure) on the outcome of the sound speed especially in shallow areas.

3.7 MARJAN

3.7.1 Sound Speed Variation

Marjan was the only area for which we had sound speed profile data but no temperature or salinity data available. We have 40 sound speed profiles for 40 days over a period from January to September. From those, we chose seven days, from February 13, 1992 to September 22, 1992, to show the temporal variability of sound speed.

Figures 3-17, 3-18, and 3-19 were created. Each figure is a 3-D line graph showing the temporal variation of sound speed for three depth points. Figure 3-17, shown on Appendix IV, shows the variation for 2.5 m, 5 m and 10 m. Figure 3-18, shown on Appendix IV, shows the variation for 15 m, 20 m, and 25 m while Figure 3-19, shown on Appendix IV, shows the variation for 30 m, 35 m, and 40 m of water.

The sound speed at 2.5 m for this area ranged from a minimum of 1517 m/s on February 13, 1992, to a maximum of 1550 m/s on September 9, 1992. The profiles seem to be nearly homogeneous in the top 10 m of water. This is good news for multibeam echosounding surveys as we will see in the Chapter 4 because it minimizes the effect of refraction phenomena on the outer beams. In fact, most of the profiles seem to be relatively homogeneous from top to bottom with the exception of three profiles for two days in September and one in May. There is an apparent gradient in the profiles in September as the difference between the sound speed at 20 m and 25 m is about 7 m/s. The other profile that has another gradient but is not as steep is that of May 8, 1992, where the difference between the two depth points of 2.5 m and 40 m is 11 m/s varying slowly and spreading over the 37.5 m of water.

As we will see in Chapter 4 the gradient in the profile is more important if it was near the transducer. This is because its effect diminishes on the refraction solution as it moves away from the transducer and deeper in the profile.

Chapter 4

SOUND SPEED PROFILE VARIATION EFFECT ON MULTIBEAM ECHOSOUNDING

4.1 SCOPE

This chapter will describe the effect of sound speed profile (SSP) variation in the water column on multibeam echosounding in the following six locations of the study area: Abu Safa, Berri, Marjan, Ras Tanura, Safaniya, and Zuluf. Those are the locations for which we have data. The look-up tables strategy for refraction solution will be introduced. Then the approach that was taken will be summarized and the logic behind it will be given supported by the many figures to follow in Appendix V for the different scenarios. This will determine at least a general picture of those effects at each location and within the whole study area. Results of those scenarios will be discussed. Finally, comments on most interesting points that came out of these results will be given.

4.2 THE LOOK-UP TABLE STRATEGY FOR REFRACTION SOLUTIONS

Ray tracing computation is a computer intensive process. Therefore, a pre-calculated look-up tables of depth and across-track solutions for different transit times and angles are usually prepared. For the purpose of finding both the spatial and temporal effect a C-program, that uses the gradient model described in Chapter 1, was developed to achieve this purpose. This program was developed as an option in Hughes Clarke's [1995] sound speed software tools. It consists of subroutines written in the Cprogramming language added to the original ray tracing program. The program takes a measured SSP and returns two look-up tables (LUT) of refraction solutions . One of the LUTs is for depth and the other is for across-track. The axis of the LUT is the launch inclination angle and the other is the transit time. The program produces a ray trace solution for discrete ray angles ranging from zero or vertical to 75° off vertical.

The mathematical model that was used in this program can be found in Hughes Clarke et al. [1995]. These lecture notes give even deeper treatment to the refraction phenomena.

4.3 STUDY APPROACH OF THE SSP VARIATION EFFECT

To find out the regional spatial and temporal effect of the sound speed profile variations the following six scenarios were used for a common depth of 30 m.

1. The effect on the refraction solution of using one SSP for the summer instead of one SSP for the winter. The two SSPs were taken from an extensive study of repeated measurements of temperature and salinity profiles that were taken in the general area between Berri and Karan Island [Basson et al., 1978]. Then using the temperature and the salinity at each depth point from 0 m to 30 m at 5 m interval, the corresponding sound speed at each depth point was calculated using the previously recommended Chen and Millero equation (corrected version), as recommended in Chapter 2. This was done to find the maximum error in depth and across-track (vertical and horizontal) and to give us a feel for the change from season to season in the study area since this region between Berri and Karan Island is situated almost central to our six locations. The effect on the

refraction solution was calculated for transducer depths of 2.5 m as well as 4.3 m (this is the transducer depth of the multibeam system of Saudi Aramco's survey vessel (Karan-8)). The reason we used two different transducer depths was to illustrate the effect of the up and down motion of the survey vessel in the water column. The deeper the transducer is the less it is prone to the refraction effect. See Figure 4-1a for the across-track error, Figure 4-1b for depth error for 2.5 m transducer depth case and 4-2 for both across-track and depth errors for 4.3 m transducer depth case (located in Appendix V).

2. The effect on the refraction solution of using one SSP for the summer at each location (highest sound speed values of the available data for that location) instead of SSP for the winter in the same location (lowest sound speed values of the available data for that location). This produced six situations supplying us with the error in depth and across-track from season to season in each location. This was also done for two transducer depths 2.5m and 4.3m and for the same reason as in (1). See Figures 4-3a to 4-8a for the across-track error, 4-3b to 4-8b for depth error for the 2.5 m transducer depth case and 4-9 to 4-14 for both across-track and depth errors for the 4.3 m transducer depth case (all figures for this chapter are shown in Appendix V).

3. The effect of using one SSP for the summer at each location, instead of one SSP for the summer in the general area. This produced six situations supplying us with the error in depth and across-track from the same season but for different areas comparing each location to that of the general area. Here we used only a 4.3 m transducer depth and for

the rest of the scenarios as well. See Figures 4-15, 16, 17, 18, 19, 20 (shown in Appendix V) for both across-track and depth errors for the 4.3m transducer depth case.

4. The effect of using one SSP for the winter at each location instead of one SSP for the winter for the general area. This produced six situations supplying us with the error in depth and across-track from the same season but for different areas comparing each location to that of the general area. See Figures 4-21, 22, 23, 24, 25, 26 (shown in Appendix V) for both across-track and depth errors for the 4.3 m transducer depth case.

5. This step involved different combinations depending on data availability in each location, but generally the effect of using one of two SSPs for two consecutive days instead of the other was computed. If one abnormal SSP was found then the comparison to that was also done. Comparisons were made for one month apart in the same year or in a different year, two days apart, same day morning and afternoon, and afternoon of the next day or the previous day.

Let us look at what was done at each site in alphabetical order starting with Abu Safa. Here, six scenarios were performed

1. Figure 4-27, shown in Appendix V, shows the effect of using one SSP over another of the next day, both of which are considered normal (i.e. the difference from top to bottom of the SSP is within 2 m/s). Both SSPs are for days in February 1992.

2. Figure 4-28, shown in Appendix V, shows the effect of using one SSP over another of the next day. One of them is considered abnormal (i.e. SSP has a speed gradient for the first 15 m of water with a maximum difference of 25 m/s at the top of the SSP) and the other is a normal SSP that was used in (1). Both SSPs are for days in February 1992.

3. Figure 4-29, shown in Appendix V, shows the effect of using one SSP over another of the next day. Both SSPs have a gentle speed gradient for 2.5 m/s at different depths of the profile. Both SSPs are for days in September 1994.

4. Figure 4-30, shown in Appendix V, shows the effect of using one SSP over another that is three days apart, both of which are considered normal. Both SSPs are for days in February 1992.

5. Figure 4-31, shown in Appendix V, shows the effect of using one SSP over another that is two days apart, both of which are considered normal, but one has a shift of 1.5 m/s at about the depth of 12m. Both SSPs are for days in October 1994.

6. Figure 4-32, shown in Appendix V, shows the effect of using one SSP over another that is one month apart, both of which are considered normal. One SSP is in October 1992 and the other is in November 1994, two years later.

In Berri, five scenarios were performed:

1. Figure 4-33, shown in Appendix V, shows the effect of using one SSP over another of the next day, both of which are considered normal. Both SSPs are for days in February 1995.

2. Figure 4-34, shown in Appendix V, shows the effect of using one SSP over another of the next day, both of which are considered normal. Both SSPs are for days in February 1995.

3. Figure 4-35, shown in Appendix V, shows the effect of using one SSP over another of the next day. One of them is considered abnormal (i.e. SSP has a speed gradient for the first 5 m of water with a maximum difference of 40 m/s at the top of the SSP) and the other is a normal SSP. Both SSPs are for days in February 1995.

4. Figure 4-36, shown in Appendix V, the effect of using one SSP over another that are four days apart, both of which are considered normal. Both SSPs are for days in February 1992 and 1995, three years apart .

5. Figure 4-37, shown in Appendix V, shows the effect of using one SSP over another that is one month apart, both of which are considered normal. One SSP is in October 1992 and the other is in November 1994, two years later.

In Marjan, six scenarios were performed:

1. Figure 4-38, shown in Appendix V, shows the effect of using one SSP over another of the next day, both of which are considered normal because their shapes look very similar even though the difference from top to bottom of the profile is about 3 m/s. Both SSPs are for days in March 1993.

2. Figure 4-39, shown in Appendix V, shows the effect of using one SSP over another of the next day, both of which are considered abnormal even though their shapes look very similar but the difference from top to bottom of the profile is about 13 m/s. Both SSPs are for days in May 1992.

3. Figure 4-40, shown in Appendix V, shows the effect of using one SSP over another of the same day. One SSP was collected in the morning and the other in the afternoon, both of which are considered abnormal, but note the shapes of the two SSPs as the negative speed gradient situated in the last 10 m of the profiles. Both SSPs are for days in September 1992.

4. Figure 4-41, shown in Appendix V, the effect of using one SSP over another of the next day. One SSP is the same morning as in (3) and the other is for the next day morning. Both SSPs are considered abnormal, but note the shapes of the two SSPs as the negative speed gradient situated in the last 10 m of the profiles. Both SSPs are for days in September.

5. Figure 4-42, shown in Appendix V, shows the effect of using one SSP over another of the next day. One SSP is the same afternoon as in (3) and the other is for the next day morning. Both SSPs are considered abnormal, but note the shapes of the two SSPs as the negative speed gradient situated in the last 10 m of the profiles. Both SSP are for days in September 1992.

6. Figure 4-43, shown in Appendix V, shows the effect of using one SSP over another that is one month apart. One SSP is considered abnormal because the difference from top to bottom is 5 m/s while the other is normal as it resembles a straight line. One SSP is in April 1992 and the other is in March 1993, one year later.

In Ras Tanura, seven scenarios were performed:

1. Figure 4-44, shown in Appendix V, shows the effect of using one SSP over another of the next day, both of which are considered normal. Both SSPs are for days in March 1992.

2. Figure 4-45, shown in Appendix V, shows the effect of using one SSP over another of the next day. One of them is considered abnormal (i.e. SSP has a speed gradient for the first 12 m of water with a maximum difference of 25 m/s at the top of the SSP) and the other is a normal SSP that was used in (1). Both SSPs are for days in March 1992.

3. Figure 4-46, shown in Appendix V, shows the effect of using one SSP over another of the same day. One SSP was collected in the morning and the other in the afternoon, both of which are considered normal. Both SSPs are for days in August 1992.

4. Figure 4-47, shown in Appendix V, shows the effect of using one SSP over another of the previous day. One SSP is the same morning cast in 3 and the other is for the previous day morning one year later since there was no SSP in the same year one day before or after. One SSP of the previous day is considered abnormal because there is change in sound speed near the transducer of about 1.3 m/s and a gradual shift or step from 20 m to 24 m depth of about 7 m/s. Both SSPs are for days in August 1992 and 1993.

5. Figure 4-48, shown in Appendix V, shows the effect of using one SSP over another of the next day. One SSP is the same afternoon in (3) and the other is for

the previous day morning abnormal cast used in (4). Both SSPs are for days in August 1992 and 1993.

6. Figure 4-49, shown in Appendix V, shows the effect of using one SSP over another that is one month apart. One SSP is considered abnormal because of the a positive speed gradient of 2m/s from the depth of 15 m to 20 m while the other is normal as it resembles a straight line. One SSP is in August 1992 and the other is in September 1992 of the same year.

7. Figure 4-50, shown in Appendix V, shows the effect of using one SSP in the beginning of the month over another that at the end of the month a year later. Both SSPs are in September 1992 and 1993 and considered normal but one has an apparent bad reading near the 24 m depth mark.

In Safaniyah, four scenarios were performed:

1. Figure 4-51, shown in Appendix V, shows the effect of using one SSP over another of the next day, both of which are considered normal. Both SSPs are for days in December 1993.

2. Figure 4-52, shown in Appendix V, shows the effect of using one SSP over another of the next day, both of which are considered abnormal even though their shapes look very similar but the difference from top to bottom of the profile is

about 4 m/s and the profile has a negative slope before becoming straight vertical line after the 20 m depth mark. Both SSPs are for days in June 1994.

3. Figure 4-53, shown in Appendix V, shows the effect of using one SSP over another of the same day but three years apart. One SSP is considered normal while the other has a shift 2.5 m/s making a slope from the 8m to 12m water depth connecting what looks like two straight vertical line segments. Both SSPs were collected in the same day in February 1992 and 1995.

4. Figure 4-54, shown in Appendix V, shows the effect of using one SSP in the beginning of the month over another that at the end of the month on the same year. Both SSPs are in December 1993 and considered normal.

In Zuluf, four scenarios were performed:

1. Figure 4-55, shown in Appendix V, shows the effect of using one SSP over another of the next day, both of which are considered normal. One SSP is in last day of March 1995 and the other in the fist day of April 1995.

2. Figure 4-56, shown in Appendix V, shows the effect of using one SSP over another of the next day, both of which are considered abnormal but the shapes of the SSPs look similar with the difference from top to bottom in one SSP is 4 m/s and in the other is 2 m/s. One SSP is on the last day of March 1993, and the other

on the fist day of April 1993. Note that these two SSPs were collected two years earlier than the ones in (1).

3. Figure 4-57, shown in Appendix V, shows the effect of using one SSP over another of the same day but two years later. One SSP is considered normal while the other has a difference of 4 m/s from top to bottom (abnormal). SSPs were collected on the first of April 1995 and 1993, and were used in (1) and (2).

4. Figure 4-58, shown in Appendix V, shows the effect of using one SSP over another of the next day, both of which are considered abnormal even though their shapes look very similar but the difference from top to bottom of the profile is about 10 m/s. Both SSP are for days in May 1992.

5. Figure 4-59, shown in Appendix V, shows the effect of using one SSP over another that is one month apart. Both SSPs could be considered abnormal because of difference from top to bottom of the profile is about 10 m/s in one while the other has a maximum 4 m/s in a zigzag shape profile. One SSP is in April 1993, and the other is in May 1992.

6. This step involved comparing scenarios of different days within the same month but for different location. There was only one month (February) for which we had SSP data

for all six locations. Six scenarios were created from this month to give the feel for winter variation within all the study area. Those six are as follows:

1. Figure 4-60, shown in Appendix V, shows the effect of using one SSP of Abu Safa over SSP of Berri. The two are four days and three years apart. One SSP was collected in February 1995 and the other was collected in February 1992. Both SSPs could be considered normal.

2. Figure 4-61, shown in Appendix V, shows the effect of using one SSP of Berri over SSP of Ras Tanura. The two are 13 days and three years apart. One SSP was collected in February 1995 and the other was collected in February 1992. Both SSPs could be considered normal.

3. Figure 4-62, shown in Appendix V, shows the effect of using one SSP of Berri over SSP of Safaniyah. The two are 12 days apart and in the same year. Both SSPs were collected in February 1995. Both SSPs could be considered normal.

4. Figure 4-63, shown in Appendix V, shows the effect of using one SSP of Abu Safa over SSP of Marjan. The two are one day apart and in the same year. Both SSPs were collected in February 1992. Both SSPs could be considered normal.

5. Figure 4-64, shown in Appendix V, shows the effect of using one SSP of Marjan over SSP of Zuluf. The two are one day and three years apart. One SSP

was collected in February 1992, and the other was collected in February 1995. Both SSPs could be considered normal.

6. Figure 4-65, shown in Appendix V, shows the effect of using one SSP of Safaniyah over SSP of Zuluf. The two are 16 days apart and in the same year. Both SSPs were collected in February 1995. Both SSPs could be considered normal.

There was another month (September) for which we had SSP data for five of the six locations. So five scenarios were created from this month to give the feel for summer variation within the study area. Those five are as follows:

1. Figure 4-66, shown in Appendix V, shows the effect of using one SSP of Abu Safa over SSP of Marjan. The two are two days and two years apart. One SSP was collected in September 1994, and the other was collected in September 1992. One SSP could be considered normal while the other is abnormal which has a difference of 10 m/s from top to bottom of the profile.

2. Figure 4-67, shown in Appendix V, shows the effect of using one SSP of Abu Safa over SSP of Ras Tanura. The two are 7 days and one year apart. One SSP was collected in September 1994, and the other was collected in September 1993. Both SSPs could be considered normal.

3. Figure 4-68, shown in Appendix V, shows the effect of using one SSP of Marjan over SSP of Safaniyah. The two are 10 days and two years apart. One SSP was collected in September 1992, and the other was collected in September 1994. Both SSPs could be considered abnormal. One SSP has a shift in the top 2m of 4 m/s while the other has a difference of 10 m/s from top to bottom of the profile.

4. Figure 4-69, shown in Appendix V, shows the effect of using one SSP of Marjan over SSP of Zuluf. The two are 5 days and one year apart. One SSP was collected in September 1992, and the other was collected in September 1991. One SSP could be considered normal while the other is abnormal which has a difference of 10 m/s from top to bottom of the profile.

5. Figure 4-70, shown in Appendix V, shows the effect of using one SSP of Safaniyah over SSP of Zuluf. The two are 5 days and three years apart. One SSP was collected in September 1994, and the other was collected in September 1991. One SSP could be considered normal while the other is abnormal because it has a shift in the top 2m of 4 m/s.

4.4 DESCRIPTION OF PROCEDURE IN ASSESSING THE SSP VARIATION EFFECT

There are two main types of figures in this chapter. Figures 4-1a,b and Figures 4-3a,b to 4-8a,b which describe the effect of SSP variation for the 2.5 m transducer depth case, while Figure 4-2 and Figures 4-9 to 4-70 describe the effect for a 4.3 m transducer depth case. The reasons for having two different types is that in the first type the whole process or procedure is shown which will be explained later in this section while in the other type only final results are shown. However, the same procedure was followed in preparing all the figures. Let us look at how we achieved the results of each scenario for both types of errors.

1. The two SSPs that makes the scenario were plotted using the Microsoft Excel spreadsheet. A conversion to a TIF file was necessary before importing into CorelDraw as the first element in the figure.

2. The isogradient ray tracing program was run using the two SSPs to find the across-track and depth LUTs for each profile.

3. The Differ program [Hughes Clarke, 1995] was run twice. Once to find the difference in the across-track LUTs and the other to find the difference in the depth LUTs. These two differences give us the corresponding errors in term of formed beam angle and transit time.

4. The Switch program [Hughes Clarke, 1995] was run twice to express the equivalent across-track and depth errors in term of range and depth.

5. A stenciled graph was used showing that the error is within or outside the 1% of depth criterion (in our scenarios this is 30 cm). This is the maximum allowable IHO standard error for producing nautical charts [IHO S 44, 1987]. Of course, this is for depth error only and assumes everything else is perfect (i.e. perfect positioning system, well known draft reading, well-compensated for attitudes, etc.). There is no specific criterion for across-track, so we used the 30 cm as an indicator. This is not totally true, because it depends on the types of bottom detection the multibeam system uses for each beam. For example, the Simrad EM-1000 manual [1994] states that the error in the amplitude detection for small angles is within 1-2 pulse lengths, and ±0.05° bearing estimation in the phase detection on a reasonably flat bottom. This means 15 cm and 78 cm for 75° off vertical.

4.4.1 Description Of Figures Of The SSP Variation Effect

Each figure of the first type shows the whole process. It is a figure in landscape mode containing (as we start from the top left of the page) the two SSPs with a title explaining the specific scenario with each profile is labeled of its Julian day and date or just the name that was given to it. e.g. summer. Then as we move across the page the two across-track or depth LUTs corresponding to the two SSPs and a gray scale that goes from 0 m (dark) to the maximum range of 111.962 m (light) for the across-track LUTs (this is the tangent of 75° times 30m) and to 30 m (light) for the depth LUTs. From the bottom left corner, we find the difference (error) of the two across-track or depth LUTs and their two axes being the formed beam angle and transit time. Then in the center there is a gray scale that goes from 0 m (dark) to the maximum error (across-track or depth) (light). Next to it, there is a graph of the error expressed in term of range and depth. Below that, is the last graph in the page, and (probably the most useful) with a stenciled area that shows the error either within or outside the criterion of 30 cm.

4.5 RESULTS OF THE SSP VARIATION EFFECT

We will look at the transducer position effect within the water column, the season to season variation, the month to month variation, normal day-to-day variation, abnormal day-to-day variation, within day variation, and finally within one month from location to location.

Transducer Position Effect. To show the effect of the transducer moving up or down in the water column, Table 4-1 was created to summarize the difference in errors of the different scenarios for the two drafts (2.5 m and 4.3 m) (see also Figures 4-1a,b and Figures 4-3a,b to 4-8a,b and Figures 4-9 to 4-14, shown in Appendix V). The name of the scenario consists of a letter(s) and or number(s). The letters stand for the following:

A Abu Safa,

B Berri,

F February,

M Marjan,

R Ras Tanura,

S Safaniyah,

Se September,

Su Summer,

W Winter,

Z Zuluf

The numbers represents the Julian days (1 means January 1, and 365 means December 31)

Table 4-1 The effect of transducer vertical motion for the two drafts 2.5m, and 4.3m.

Scenario Name	Across-track Error (m) (2.5m Draft)	Across-track Error (m) (4.3m Draft)	Diff. (m)	Depth Error (m) (2.5m Draft)	Depth Error (m) (4.3m Draft)	Diff. (m)
Su_W	0.814	0.805	0.009	1.003	0.734	0.269
A_51_267	2.173	2.074	0.099	0.891	0.706	0.185
B_35_306	1.881	1.762	0.119	0.478	0.448	0.030
M_44_255	1.859	1.772	0.087	1.053	0.866	0.187
R_60_237	2.531	2.36	0.171	0.677	0.633	0.044
S_20_255	2.808	2.627	0.181	0.824	0.764	0.060
Z_51_225	1.736	1.624	0.112	1.105	0.997	0.108

It is clear from this table that the vertical motion of the transducer in the water column will produce an error which, by itself, could exceed the IHO specification. However, this is compounded by any presence of a speed gradient in the SSP near the transducer which will make the refraction solution impossible to predict. Simrad EM-1000 tries to tackle this problem by monitoring any temperature change near the transducer, but this is half of the problem. What if the change is in salinity rather than temperature (remembering that the Gulf this changes from 35‰ to 65‰ in some areas). This is something to watch for in the future for surveyors on board Karan-8, but temperature monitoring could be useful (although not necessarily sufficient) information used in spotting a change in salinity.

Season-to-Season Variation Effect. Table 4-1 also shows the effect of the seasonal (summer to winter) variation in the SSP in the study area made up of the six locations. Here are two interesting points that can be extracted:

- The across-track errors are greater than the depth errors. This is because the difference in each pair of SSPs is generally a mere shift in sound speed with no strong speed gradient in any SSP.
- As we will see later when we discuss the abnormality or the presence of strong speed gradient in the top few metres of the SSP, depth errors, in specific, in those situations would be much greater than using an SSP from another season. This is another indication of the extreme sensitivity of the transducer vertical position in the presence of strong speed gradient. Therefore, if the transducer was pitching up and down in water mass that has a strong gradient in its SSP then the error can not be accounted for and the only way that this can be recognize in real time is through installing a velocimeter near the transducer. Dodds [1994] recommended this approach. Another practical approach was that of the Royal Danish Administration of Navigation and Hydrography undulating towed vehicle but the disadvantages of high cost, slower speed and risk of possible loss of device makes it unpreferable [Dodds, 1994]. No report of the success of their endeavor is available. These practical methods would not be necessary in our study area, as we have demonstrated that, if two things were done properly:

1. The SSP was measured accurately and correctly as presented previously and even small errors in measured SSP would not be important if all we have is a shift in the whole profile especially for depth errors. That is why we have to know the shape of the profile.

2. The depth of the transducer in real time has to be measured very accurately, because that might eliminate the need for velocimeter installation near the transducer. This can be secured through the use of pressure sensor assuming no wave displacement of profile.

In an attempt to find the effect of making one summer or one winter SSP for the whole area, Table 4-2 was created. This illustrates the error incurred in each location for making the general area SSPs as a model for the area.

Table 4-2 The effect of using one SSP of the General Area for the whole season in each location

Scenario Name	Across-track Error (m) (4.3m Draft)	Depth Error (m) (4.3m Draft)
Su_A_267	0.103	0.061
W_A_51	1.197	0.300
Su_B_306	0.222	0.597
W_B_35	1.164	0.290
Su_M_255	0.390	0.279
W_M_44	1.401	0.359
Su_R_237	0.266	0.274
W_R_60	1.303	0.334
Su_S_255	0.221	0.261
W_S_20	1.621	0.424
Su_Z_225	0.362	0.125
W_Z_51	1.227	0.316

Here, we notice that in some locations summer SSP could be used if no other records are available in the specific location at same time of previous years. Winter SSP should not be used. It is not representative of the area and a better way is to just find the nearest area and closest date in the same year or even in previous years. These suggestions applies in situations when real-time or near real-time SSP were not taken. This should be the exception and real-time SSP should always be taken at the start, mid-day and end of every survey day. When moving to a new location the same procedure should be attempted.

Month-to-Month Variation Effect. Table 4-3 suggests that Marjan and Zuluf temporal variations are more drastic than for the other locations and Safaniyah has the fewest changes. This is also a function of the position of the two SSPs in comparison within each location (lateral change). For convenience we assumed that the lateral change in SSP within each location is nonexistent (in the absence of any data to the contrary). An even more important point to make here is that it does matter where we take SSP within the survey area implying limited spatial variations. Also even after one month in some locations it is still possible to use SSPs for determining the refraction solution.

Table 4-3 The effect of month-to-month variation within each location.

Scenario Name	Across-track Error (m) (4.3m Draft)	Depth Error (m) (4.3m Draft)
A_306_275	0.180	0.070
B_333_303	0.539	0.057
M_103_71	0.403	0.932
R_237_267	0.038	0.170

S_365_336	0.079	0.021
Z_129_98	0.326	0.879

Abnormal Day-to-Day Variation Effect. This is the most important variation because it gives a feel to what to expect when either an abnormal water column environment is visited or an incorrect SSP is used. It is clear from Table 4-4 that the error and especially the vertical error could be larger than using an SSP from one season later. This presents the need for the careful interpretation of the collected SSPs and verification of the inconsistencies especially those irregularities in the top 10 m layer (near transducer). A possible reason for these inconsistencies is that the measuring device was not warmed up or it was not allowed to equilibrate after taking it from room temperature on the ship and deploying it into either much colder or hotter seawater. Making a judgment about what is a real abnormal environment and what is merely bad instrument readings is the key to eliminating most of the refraction artifacts in multibeam echosounding (in the Gulf).

In Table 4-4, Abu Safa, Berri, and Ras Tanura examples seem to suggest only bad readings while true change or different water mass environment could be the reason for the errors in the rest of those examples (Marjan, Safaniyah, and Zuluf).

Table 4-4 The effect of abnormal day-to-day variation within each location.

Scenario Name	Across-track Error (m) (4.3m Draft)	Depth Error (m) (4.3m Draft)
A_53_52	0.623	3.737
B_41_40	0.390	1.812
M_122_123	0.089	0.183
R_68_67	0.741	3.112
S_167_166	0.100	0.210
Z_91_90	0.021	0.165

Normal Day-to-Day Variation Effect. Most of the changes from day to day in the data we had suggest some errors comparable to those presented in Table 4-5. Therefore, it is safe to say that the drastic changes we called abnormal discussed in section 4.5.4 is only the exception to this more general trend. Table 4-5 displays an error within 1 decimetre in all the examples chosen to represent this general case. However, this should in no way give us a reason to suggest that a day to day variation should be ignored or the procedure of taking morning, noon, and late afternoon casts should be abandoned because we never know where exactly an area or month or season is more variable. This study could only be a start to a further long term project of collection and creation of databases with even coordinated position for each cast that is collected to make this more scientific. As far as I know, the data that were used in this study were part of the beginning of such a database. As time progresses and surveyors become aware of the reason for quality assurance of SSP data, such a database will serve to reduce cost and time and attain a good quality hydrographic survey product.

Table 4-5 The effect of normal day-to-day variation within each location.

Scenario Name	Across-track Error (m) (4.3m Draft)	Depth Error (m) (4.3m Draft)
A_54_53	0.022	0.038
B_40_39	0.015	0.057
M_62_61	0.019	0.068
R_67_66	0.010	0.063
S_365_364	0.020	0.010
Z_91_90	0.013	0.014

Within Day Variation Effect. There were only those two occasions where it was possible to investigate the variation within a day, and in those the error was still within the criterion of 30 cm for the 30 m depth as shown in Table 4-6. The reason this is (in my opinion) the most important is that the usual practice is to take one morning cast for the whole day. This might not account for the afternoon sun heating the upper surface of the water and this could be a big source of errors in the summer where a morning cast might indicate an erroneous SSP as cool night weather makes the upper layer cold. As the survey progresses and time passes in the day the upper layer becomes hotter from the direct sizzling July and August sun and you could see a similar scenario in February as well. Lack of data makes drawing any conclusion impossible here, but let us retain our procedure of taking three SSPs in the day. Such procedure will serve as a basis for future study of such variations.

Table 4-6 The effect of normal day-to-day variation within each location.

Scenario Name	Across-track Error (m) (4.3m Draft)	Depth Error (m) (4.3m Draft)
M_255AM_255PM	0.088	0.093
R_221AM_221PM	0.042	0.027

Spatial Variation Effect Within One Month. Table 4-7 gives the spatial variation effect within a month. Two months were taken as examples. One is February and the other is September of years from 1991 to 1995, to show both winter and summer months. All six locations had data in February while no Berri data were available in September. One thing that can seen here is that even though Zuluf is between Marjan and Safaniyah the difference in both months is higher between Zuluf and Safaniyah than Zuluf and Marjan. This is somewhat expected since Safaniyah is on the coast and Zuluf and Marjan are in the deep open sea. See Figure 4-60 to 4-70 for suspected reasons for such difference (located at the end of the chapter).

Table 4-7 The effect of normal spatial variation within one month.

Scenario Name	Across-track Error (m) (4.3m Draft)	Depth Error (m) (4.3m Draft)
A_51_B_47_F	0.200	0.065
B_47_R_60_F	0.307	0.080
B_47_S_35_F	0.673	0.210
A_51_M_50_F	0.177	0.081
M_50_Z_51_F	0.148	0.039
S_35_Z_51_F	0.443	0.155
A_267_M_266_Se	0.529	0.313
A_267_R_260_Se	0.030	0.259
M_266_S_255_Se	0.653	0.254
M_266_Z_260_Se	0.185	0.266
S_255_Z_260_Se	0.468	0.110

In this chapter, we gave the temporal and spatial effect of SSP variation on multibeam echosounding, provided explanation of the different scenarios and described the effect of near transducer SSP variations. Next chapter we will summarize the procedure and provide a conclusion and end up with a list of recommendation.

Chapter 5

CONCLUSION AND RECOMMENDATIONS

In this chapter we will reiterate points made in the previous chapters and give recommendations to be followed and the procedure to be implemented in measuring sound speed profiles.

5.1 SSP PROCEDURE

To measure the SSP, the following steps and points should be followed:

1. The updated version of the Chen and Millero equation should be employed using sound speed probes (CTD) which measure the three variables in the equation.
2. Three daily SSP casts should be taken with CTD, one in the morning, one at noon and one in the late afternoon, to allow for variations within one day to be accounted for.
3. Each SSP should be geographically coordinated in order to be used in the proposed database.
4. Careful verification of each measured SSP should be made to detect the presence of any irregularities based on database of SSPs. If any irregularities are found, two SSPs should be taken in the two extreme ends (shallowest or nearest to coast and deepest or farthest away from the coast). Use of this ray tracing program described in section 4.2, which takes 2 minutes to run, would give a clear idea of how big the error was (across-track and depth) in using either one of those SSPs.

5.2 CONCLUSION

Complete knowledge of the sound speed profile is a must in order to eliminate the refraction artifacts that manifest themselves as across-track, nadir symmetric, swath distortions ("smiles" or "frowns") in the multibeam swath system product. Variation in SSP near the transducer is the most serious and important type of error. Therefore, if the transducer was pitching up and down in water mass that has a strong gradient in its SSP then the error can not be accounted for and the only way that can be known in real time is through installing a velocimeter near the transducer. Another practical approach was that of the Royal Danish Administration of Navigation and Hydrography undulating towed vehicle perhaps, however, the disadvantages of high cost and risk of possible loss of device makes it unreliable. In our study area, these practical methods would not be necessary if two things were done properly:

1. The SSP was measured accurately and correctly. We have to know the shape of the profile.

2. The depth of the transducer in real time has to be measured very accurately. This can be secured through the use of pressure sensor if we assumed there is no wave displacement. Otherwise, possibly, temperature sensor information would indicate real-time change in sound speed.

5.3 RECOMMENDATIONS

The following recommendations were mentioned through out this report and we state them here for importance:

1. To measure the SSP, the current CTD probe should continue to be used with accordance to the procedure presented in 5.1 and the use of the updated version of Chen and Millero equation.

2. To make sure the vertical position of the transducer in the water column, a pressure sensor to measure depth accurately. Watch for effect on the pressure sensor from the forward motion of the survey vessel.

3. Create a database for the SSPs with a coordinated position of each cast. This will help reduce the ship time taken in the future to measure SSP and/or correct for missing SSP.

4. Obtain more information on the success of CHS or other agencies (in sea technologies) on the installment of the velocimeter near the transducer.

REFERENCES

Applied Microsystems LTD. (1990). "Model SVP-16 Sound Velocity Profiler User's Manual." Sidney, B.C., Canada, 66 pp.

Basson, P. W., J.E. Burchard Jr., J. T. Hardy and A. R. G. Price (1978). *Biotopes of the Western Arabian Gulf Marine Life and Environments of Saudi Arabia*. Aramco Department of Loss Prevention and Environmental Affairs, Dhahran, Saudi Arabia.

Chen, C.T., and F. Millero (1977). "Speed of Sound in Seawater at High Pressure." *Journal of Acoustical Society of America*, Vol. 62(5), pp. 1129-1135.

Christensen, C. (1995). Personal Communication. Supervisor, Hydrographic Survey Unit, Saudi Aramco, Ras Tanura, Saudi Arabia, May.

de Moustier, C. (1995). Personal Communication. Research Engineer, Marine Physical Laboratory of the Scripps Institution of Oceanography, San Diego, California, U.S.A., June.

Del Grosso, V.A.(1974). "New Equation for the Speed of Sound in Natural Waters (with Comparison to Other Equations)." *Journal of Acoustical Society of America*, Vol. 56(4), pp. 1084-1091.

Dodds, D.J.(1994). "Methods for Correction of Refraction Errors in Multi Beam Echo Sounders." Final Report on Contract FP962-4-3015/01-HAL, Aurora, Ontario, Canada, December 23, 20 pp.

Emery, K. O. (1956). "Sediments and Water of the Persian Gulf.", *Bull. Am. Assoc. Petrol. Geologists*, Vol. 40, pp. 2354-2383.

Hughes Clarke, J.H., D. Wells and L. Mayer (1995). "Coastal Multibeam Hydrographic Surveys." Course Notes. St. Andrew, New Brunswick, Canada, 18-29 June.

Hughes Clarke, J.H (1995). Personal Communication. Research Associate, Ocean Mapping Group, University of New Brunswick, Fredericton, New Brunswick, Canada, June.

IHO S 44 (1987). *IHO Standards For Hydrographic Surveys, Classification For Deep Sea Soundings And Procedures For Elimination Of Doubtful Data*. The International Hydrographic Organization Special Publication No. 44. 3rd Ed., International Hydrographic Bureau, Monaco, France.

Kinsler, L.E. and A.R. Frey (1962). *Fundamentals of Acoustics.* Second Edition, Wiley, Toronto.

Mackenzie, K.V.(1981). "Nine-term Equation for Sound Speed in the Oceans." *Journal of Acoustical Society of America,* September, Vol. 70(3), pp. 807-812.

Medwin, H.(1975). "Speed of Sound in Water: A Simple Equation for Realistic Parameters." *Journal of Acoustical Society of America,* Vol. 58, pp. 1318-1319.

Millero, F.J., and X. Li (1994). "Comments on 'On equations for speed of sound in seawater'[J. Acoust. Soc. Am. 93. 255-275 (1993)]." *Journal of Acoustical Society of America,* Vol. 95, pp. 2757-2759.

Nawab, Ismail I., Peter C. Speers, and Paul F. Hoye (eds.) (1981). *Aramco and Its World Arabia and the Middle East.* Van Boekhoven-Bosch B. V. and Boom-Ruygrok B. V. of the Elsevier-NDU Graphic Division B.V., Netherlands, Second Printing.

Pike, J.M. and F.L. Beiboer(1994). *A Comparison Between Algorithms For The Speed of Sound in Seawater.* The Hydrographic Society Special Publication No. 34. Report prepared by METOCEAN plc.

Purser, B.H. (ed.) (1973). *The Persian Gulf Holocene Carbonate Sedimentation and Diagenesis in a Shallow Epicontinental Sea.* Springer-Verlag, Berlin, Germany.

Seibold, E. (1970). *Biogenic Sedimentation of the Persian Gulf.* In: The Biology of the Indian Ocean. Symposium Kiel, First Edition.

Simrad Subsea A/S (1994). "SIMRAD EM 1000 Maintenance Manual." Horten, Norway, 265 pp.

Urick, R.J. (1975) *Principles of Underwater Sound.* McGraw-Hill, Toronto.

Wilson, W.D. (1960). "Equation for the Speed of Sound in Sea Water." *Journal of Acoustical Society of America,* Vol. 32(10), pp. 1357.

Appendix I

Listing of the available usable data records

The Available Usable Sound Speed Profile For the Study

	Jan	Feb	Mar	Apr	May	Jun	Jul	Aug	Sep	Oct	Nov	Dec	Total
Abu Safa	1	4							3	9	8	6	31
Berri	2	11			1					1	3		18
Marjan	1	4	8	9	7				10			1	40
RT		2	8	11	8	3	4	10	10	15	1		72
Saf	8	5			3	3		10	6	6		17	58
Zuluf	7	4	12	8	5	1	4	5	2	6	6	4	64
													283

Appendix II

Mathcad output of two computational examples

UNESCO pressure/depth relationship

Hydrostatic pressure in bars

$P := 1.0067$

$\phi := 28 \cdot \frac{\pi}{180}$ Latitude

$g(\phi) := 9.780318\left(1.0 + 5.2788 \cdot 10^{-3} \cdot \sin(\phi)^2 + 2.36 \cdot 10^{-5} \cdot \sin(\phi)^4\right)$

$gg := 2.184 \cdot 10^{-5}$ $\quad C3 := 2.279 \cdot 10^{-10}$

$C1 := 9.72659$ $\quad C4 := -1.82 \cdot 10^{-15}$

$C2 := -2.2512 \cdot 10^{-5}$

Hydrostatic pressure in kg/cm^2

$\Delta d := 0$

$P_k(\phi) := \frac{P \cdot 10}{g(\phi)}$ $\quad P_k(\phi) = 1.028$

$$D(\phi) := \frac{C1 \cdot (P \cdot 10) + C2 \cdot (P \cdot 10)^2 + C3 \cdot (P \cdot 10)^3 + C4 \cdot (P \cdot 10)^4}{\left(g(\phi) + \frac{1}{2} \cdot gg \cdot P\right)} + \frac{\Delta d}{9.8}$$

Salinity between 35 and 65 ppt

$S := 35, 40 .. 65$

S
35
40
45
50
55
60
65

Depth is 10 metres

$D(\phi) = 10$

Temperature is 35 degrees

$T := 35$

Wilson's formula [Pike and Beiboer, 1994]

$a(T) := 1449.14 + 4.5721T - 4.4532 \cdot 10^{-2} \cdot T^2 + 2.6045 \cdot 10^{-4} \cdot T^3$

$C(\phi) := a(T) + \left(1.39799 - 1.1244 \cdot 10^{-2} \cdot T\right) \cdot (S - 35) + 1.643 \cdot 10^{-2} \cdot D(\phi)$

Mackenzie's formula [Pike and Beiboer, 1994]

$a(\phi) := 1448.96 + 4.591T - \left(5.304 \cdot 10^{-2} \cdot T^2\right) + 2.374 \cdot 10^{-4} \cdot T^3 + 1.340(S - 35) + 1.630 \cdot 10^{-2} \cdot D(\phi)$

$C1(\phi) := a(\phi) + 1.675 \cdot 10^{-7} \cdot D(\phi)^2 - 1.025 \cdot 10^{-2} \cdot T \cdot (S - 35) - 7.139 \cdot 10^{-13} \cdot T \cdot D(\phi)^3$

Medwin's formula [Pike and Beiboer, 1994]

$$C2(\phi) := 1449.2 + 4.6T - \left(0.055T^2\right) + 0.00029T^3 + (1.34 - 0.010T)\cdot(S - 35) + 0.016D(\phi)$$

Chen-Millero-Li's equation[Millero and Li, 1994]

$$a1(T) := 1402.388 + 5.03711T - 5.80852\cdot10^{-2}\cdot T^2 + 3.3420\cdot10^{-4}\cdot T^3 - 1.47800\cdot10^{-6}\cdot T^4 + 3.1464\cdot10^{-9}\cdot T^5$$

$$a2(T,P) := \left(0.153563 + 6.8982\cdot10^{-4}\cdot T - 8.1788\cdot10^{-6}\cdot T^2 + 1.3621\cdot10^{-7}\cdot T^3 - 6.1185\cdot10^{-10}\cdot T^4\right)\cdot P$$

$$a3(T,P) := \left(3.1260\cdot10^{-5} - 1.7107\cdot10^{-6}\cdot T + 2.5974\cdot10^{-8}\cdot T^2 - 2.5335\cdot10^{-10}\cdot T^3 + 1.0405\cdot10^{-12}\cdot T^4\right)\cdot P^2$$

$$a4(T,P) := \left(-9.7729\cdot10^{-9} + 3.8504\cdot10^{-10}\cdot T - 2.3643\cdot10^{-12}\cdot T^2\right)\cdot P^3$$

$$C_w(T,P) := a1(T) + a2(T,P) + a3(T,P) + a4(T,P)$$

$$a5(T,P) := \left(0.0029 - 2.19\cdot10^{-4}\cdot T + 1.4\cdot10^{-5}\cdot T^2\right)\cdot P$$

$$a6(T,P) := \left(-4.76\cdot10^{-6} + 3.47\cdot10^{-7}\cdot T - 2.59\cdot10^{-8}\cdot T^2\right)\cdot P^2$$

$$C_c(T,P) := a5(T,P) + a6(T,P) + 2.68\cdot10^{-9}\cdot P^3$$

$$a7(T) := 1.389 - 1.262\cdot10^{-2}\cdot T + 7.164\cdot10^{-5}\cdot T^2 + 2.006\cdot10^{-6}\cdot T^3 - 3.21\cdot10^{-8}\cdot T^4$$

$$a8(T,P) := \left(9.4742\cdot10^{-5} - 1.2580\cdot10^{-5}\cdot T - 6.4885\cdot10^{-8}\cdot T^2 + 1.0507\cdot10^{-8}\cdot T^3 - 2.0122\cdot10^{-10}\cdot T^4\right)\cdot$$

$$a9(T,P) := \left(-3.9064\cdot10^{-7} + 9.1041\cdot10^{-9}\cdot T - 1.6002\cdot10^{-10}\cdot T^2 + 7.988\cdot10^{-12}\cdot T^3\right)\cdot P^2$$

$$a10(T,P) := \left(1.100\cdot10^{-10} + 6.649\cdot10^{-12}\cdot T - 3.389\cdot10^{-13}\cdot T^2\right)\cdot P^3$$

$$A(T,P) := a7(T) + a8(T,P) + a9(T,P) + a10(T,P)$$

$$B(T,P) := -1.922\cdot10^{-2} - 4.42\cdot10^{-5}\cdot T + \left(7.3637\cdot10^{-5} + 1.7945\cdot10^{-7}\cdot T\right)\cdot P$$

$$D(P) := 1.727\cdot10^{-3} - 7.9836\cdot10^{-6}\cdot P$$

$$C_{corr}(\phi) := C_w(T,P) - C_c(T,P) + A(T,P)\cdot S + B(T,P)\cdot S^{\frac{3}{2}} + D(P)\cdot S^2$$

Chen-Millero's equation before correction[Pike and Beiboer, 1994]

$$C_{uncorr}(\phi) := C_w(T,P) + A(T,P)\cdot S + B(T,P)\cdot S^{\frac{3}{2}} + D(P)\cdot S^2$$

$C_{uncorr}(\phi)$
1555.346
1560.404
1565.486
1570.597
1575.738
1580.913
1586.124

Del Grosso's equation[Pike and Beiboer, 1994]

$$DC1(T) := 0.501109398873\cdot 10\cdot T - 0.550946843172\cdot 10^{-1}\cdot T^2 + 0.221535969240\cdot 10^{-3}\cdot T^3$$

$$DC2(S) := 0.132952290781\cdot 10\cdot S + 0.128955756844\cdot 10^{-3}\cdot S^2$$

$$DC3(P_k) := 0.15605925704 P_k + 0.244998688441\cdot 10^{-4}\cdot P_k^{\,2} - 0.883392332513\cdot 10^{-8}\cdot P_k^{\,3}$$

$$B1(S,T,P_k) := -0.127562783426\cdot 10^{-1}\cdot T\cdot S + 0.635191613389\cdot 10^{-2}\cdot T\cdot P_k$$

$$B2(S,T,P_k) := 0.265484716608\cdot 10^{-7}\cdot T^2\cdot P_k^{\,2} - 0.159349479045\cdot 10^{-5}\cdot T\cdot P_k^{\,2}$$

$$B3(S,T,P_k) := 0.522116437235\cdot 10^{-9}\cdot T\cdot P_k^{\,3} - 0.438031096213\cdot 10^{-6}\cdot T^3\cdot P_k$$

$$B4(S,T,P_k) := -0.161674495909\cdot 10^{-8}\cdot S^2\cdot P_k^{\,2} + 0.968403156410\cdot 10^{-4}\cdot T^2\cdot S$$

$$B5(S,T,P_k) := 0.485639620015\cdot 10^{-5}\cdot T\cdot S^2\cdot P_k - 0.340597039004\cdot 10^{-3}\cdot T\cdot S\cdot P_k$$

$$DC4(S,T,P_k) := B1(S,T,P_k) + B2(S,T,P_k) + B3(S,T,P_k) + B4(S,T,P_k) + B5(S,T,P_k)$$

$$V(\phi) := 1402.392 + DC1(T) + DC2(S) + DC3(P_k(\phi)) + DC4(S,T,P_k(\phi))$$

Wilson's formula	Mackenzie's formula	Medwin's formula	Chen-Millero-Li's formula	Del Grosso's formula
$C(\phi)$	$C1(\phi)$	$C2(\phi)$	$C_{corr}(\phi)$	$V(\phi)$
1565.943	1555.013	1555.419	1555.334	1555.159
1570.965	1559.919	1560.369	1560.392	1560.22
1575.987	1564.825	1565.319	1565.474	1565.297
1581.01	1569.731	1570.269	1570.584	1570.388
1586.032	1574.638	1575.219	1575.726	1575.495
1591.054	1579.544	1580.169	1580.901	1580.616
1596.076	1584.45	1585.119	1586.112	1585.753

Difference between Chen-Millero-Li and

Wilson's formula	Medwin's formula	Mackenzie's formula	Del Grosso's formula
$\Delta 1(\phi)$	$\Delta 3(\phi)$	$\Delta 2(\phi)$	$\Delta 4(\phi)$
- 10.609	- 0.085	0.321	0.175
- 10.573	0.023	0.473	0.171
- 10.513	0.155	0.649	0.177
- 10.425	0.316	0.853	0.197
- 10.306	0.507	1.088	0.231
- 10.153	0.732	1.357	0.285
- 9.964	0.993	1.662	0.359

UNESCO pressure/depth relationship

Hydrostatic pressure in bars

$\phi := 28\frac{\pi}{180}$ Latitude

$P := 1.0067$

$g(\phi) := 9.780318\left(1.0 + 5.278810^{-3}\cdot\sin(\phi)^2 + 2.3610^{-5}\cdot\sin(\phi)^4\right)$

$gg := 2.18410^{-5}$

$C3 := 2.27910^{-10}$

Salinity 35

$C1 := 9.72659$

$C4 := -1.8210^{-15}$

$S := 35$

$C2 := -2.251210^{-5}$

Hydrostatic pressure in kg/cm^2

$S = 35$

$\Delta d := 0$

$P_k(\phi) := \frac{P\cdot 10}{g(\phi)}$ $\quad P_k(\phi) = 1.028$

$$D(\phi) := \frac{C1\cdot(P\cdot 10) + C2\cdot(P\cdot 10)^2 + C3\cdot(P\cdot 10)^3 + C4\cdot(P\cdot 10)^4}{\left(g(\phi) + \frac{1}{2}\cdot gg\cdot P\right)} + \frac{\Delta d}{9.8}$$

Depth is 10 metres

Temperature is 15 to 35 degrees

$D(\phi) = 10$

$T := 15, 20..40$

T
15
20
25
30
35
40

Wilson's formula [Pike and Beiboer, 1994]

$a(T) := 1449.14 + 4.5721T - 4.453210^{-2}\cdot T^2 + 2.604510^{-4}\cdot T^3$

$C(\phi) := a(T) + \left(1.39799 - 1.124410^{-2}\cdot T\right)\cdot(S - 35) + 1.64310^{-2}\cdot D(\phi)$

Mackenzie's formula [Pike and Beiboer, 1994]

$a(\phi) := 1448.96 + 4.591T - \left(5.30410^{-2}\cdot T^2\right) + 2.37410^{-4}\cdot T^3 + 1.340(S - 35) + 1.63010^{-2}\cdot D(\phi)$

$C1(\phi) := a(\phi) + 1.67510^{-7}\cdot D(\phi)^2 - 1.02510^{-2}\cdot T\cdot(S - 35) - 7.13910^{-13}\cdot T\cdot D(\phi)^3$

Medwin's formula [Pike and Beiboer, 1994]

$$C2(\phi) := 1449.2 + 4.6\,T - \left(0.055\,T^2\right) + 0.00029\,T^3 + (1.34 - 0.010\,T)\cdot(S - 35) + 0.016\,D(\phi)$$

Chen-Millero-Li's equation[Millero and Li, 1994]

$$a1(T) := 1402.388 + 5.03711\,T - 5.80852\,10^{-2}\cdot T^2 + 3.3420\,10^{-4}\cdot T^3 - 1.47800\,10^{-6}\cdot T^4 + 3.1464\,10^{-9}\cdot T^5$$

$$a2(T,P) := \left(0.153563 + 6.8982\,10^{-4}\cdot T - 8.1788\,10^{-6}\cdot T^2 + 1.3621\,10^{-7}\cdot T^3 - 6.1185\,10^{-10}\cdot T^4\right)\cdot P$$

$$a3(T,P) := \left(3.1260\,10^{-5} - 1.7107\,10^{-6}\cdot T + 2.5974\,10^{-8}\cdot T^2 - 2.5335\,10^{-10}\cdot T^3 + 1.0405\,10^{-12}\cdot T^4\right)\cdot P^2$$

$$a4(T,P) := \left(-9.7729\,10^{-9} + 3.8504\,10^{-10}\cdot T - 2.3643\,10^{-12}\cdot T^2\right)\cdot P^3$$

$$C_w(T,P) := a1(T) + a2(T,P) + a3(T,P) + a4(T,P)$$

$$a5(T,P) := \left(0.0029 - 2.19\,10^{-4}\cdot T + 1.4\,10^{-5}\cdot T^2\right)\cdot P$$

$$a6(T,P) := \left(-4.76\,10^{-6} + 3.47\,10^{-7}\cdot T - 2.59\,10^{-8}\cdot T^2\right)\cdot P^2$$

$$C_c(T,P) := a5(T,P) + a6(T,P) + 2.68\,10^{-9}\cdot P^3$$

$$a7(T) := 1.389 - 1.262\,10^{-2}\cdot T + 7.164\,10^{-5}\cdot T^2 + 2.006\,10^{-6}\cdot T^3 - 3.21\,10^{-8}\cdot T^4$$

$$a8(T,P) := \left(9.4742\,10^{-5} - 1.2580\,10^{-5}\cdot T - 6.4885\,10^{-8}\cdot T^2 + 1.0507\,10^{-8}\cdot T^3 - 2.0122\,10^{-10}\cdot T^4\right)\cdot$$

$$a9(T,P) := \left(-3.9064\,10^{-7} + 9.1041\,10^{-9}\cdot T - 1.6002\,10^{-10}\cdot T^2 + 7.988\,10^{-12}\cdot T^3\right)\cdot P^2$$

$$a10(T,P) := \left(1.100\,10^{-10} + 6.649\,10^{-12}\cdot T - 3.389\,10^{-13}\cdot T^2\right)\cdot P^3$$

$$A(T,P) := a7(T) + a8(T,P) + a9(T,P) + a10(T,P)$$

$$B(T,P) := -1.922\,10^{-2} - 4.42\,10^{-5}\cdot T + \left(7.3637\,10^{-5} + 1.7945\,10^{-7}\cdot T\right)\cdot P$$

$$D(P) := 1.727\,10^{-3} - 7.9836\,10^{-6}\cdot P$$

$$C_{corr}(\phi) := C_w(T,P) - C_c(T,P) + A(T,P)\cdot S + B(T,P)\cdot S^{\frac{3}{2}} + D(P)\cdot S^2$$

Chen-Millero before correction [Pike and Beiboer, 1994]

$$C_{uncorr}(\phi) := C_w(T,P) + A(T,P)\cdot S + B(T,P)\cdot S^{\frac{3}{2}} + D(P)\cdot S^2$$

$C_{uncorr}(\phi)$
1506.83
1521.63
1534.562
1545.765
1555.346
1563.38

Del Grosso's equation [Pike and Beiboer, 1994]

$$DC1(T) := 0.501109398873\cdot T - 0.550946843172\cdot 10^{-1}\cdot T^2 + 0.221535969240\cdot 10^{-3}\cdot T^3$$

$$DC2(S) := 0.132952290781\cdot 10\cdot S + 0.128955756844\cdot 10^{-3}\cdot S^2$$

$$DC3(P_k) := 0.15605925704 P_k + 0.244998688441\cdot 10^{-4}\cdot P_k{}^2 - 0.883392332513\cdot 10^{-8}\cdot P_k{}^3$$

$$B1(S,T,P_k) := -0.127562783426\cdot 10^{-1}\cdot T\cdot S + 0.635191613389\cdot 10^{-2}\cdot T\cdot P_k$$

$$B2(S,T,P_k) := 0.265484716608\cdot 10^{-7}\cdot T^2\cdot P_k{}^2 - 0.159349479045\cdot 10^{-5}\cdot T\cdot P_k{}^2$$

$$B3(S,T,P_k) := 0.522116437235\cdot 10^{-9}\cdot T\cdot P_k{}^3 - 0.438031096213\cdot 10^{-6}\cdot T^3\cdot P_k$$

$$B4(S,T,P_k) := -0.161674495909\cdot 10^{-8}\cdot S^2\cdot P_k{}^2 + 0.968403156410\cdot 10^{-4}\cdot T^2\cdot S$$

$$B5(S,T,P_k) := 0.485639620015\cdot 10^{-5}\cdot T\cdot S^2\cdot P_k - 0.340597039004\cdot 10^{-3}\cdot T\cdot S\cdot P_k$$

$$DC4(S,T,P_k) := B1(S,T,P_k) + B2(S,T,P_k) + B3(S,T,P_k) + B4(S,T,P_k) + B5(S,T,P_k)$$

$$V(\phi) := 1402.392 + DC1(T) + DC2(S) + DC3(P_k(\phi)) + DC4(S,T,P_k(\phi))$$

Wilson's formula	Mackenzie's formula	Medwin's formula	Chen-Millero-Li's formula	Del Grosso's formula
$C(\phi)$	$C1(\phi)$	$C2(\phi)$	$C_{corr}(\phi)$	$V(\phi)$
1508.745	1506.855	1506.964	1506.827	1506.831
1525.017	1521.626	1521.68	1521.626	1521.631
1539.844	1534.457	1534.516	1534.555	1534.508
1553.421	1545.527	1545.69	1545.756	1545.629
1565.943	1555.013	1555.419	1555.334	1555.159
1577.606	1563.093	1563.92	1563.364	1563.265

Difference between Chen-Millero-Li and

Wilson's formula	Medwin's formula	Mackenzie's formula	Del Grosso's formula
$\Delta 1(\phi)$	$\Delta 3(\phi)$	$\Delta 2(\phi)$	$\Delta 4(\phi)$
- 1.918	- 0.137	- 0.028	- 0.004
- 3.391	- 0.054	- 0.001	- 0.005
- 5.288	0.039	0.098	0.048
- 7.665	0.066	0.229	0.127
- 10.609	- 0.085	0.321	0.175
- 14.242	- 0.556	0.271	0.098

Appendix III

Tables and Figures for Chapter 2

			Table 2-4		
	Speed of Sound calculated at 35 ppt and 10 metres depth				
Temperature	Wilson	Mackenzie	Medwin	Del Grosso	Chen-Millero-Li
15	1508.745	1506.855	1506.964	1506.831	1506.827
20	1525.017	1521.626	1521.68	1521.631	1521.626
25	1539.844	1534.457	1534.516	1534.508	1534.555
30	1553.421	1545.527	1545.69	1545.629	1545.756
35	1565.943	1555.013	1555.419	1555.159	1555.334
40	1577.606	1563.093	1563.92	1563.265	1563.364

			Table 2-5		
	Speed of Sound calculated at 65 ppt and 10 metres depth				
Temperature	Wilson	Mackenzie	Medwin	Del Grosso	Chen-Millero-Li
15	1545.625	1542.443	1542.664	1542.084	1542.332
20	1560.21	1555.676	1555.88	1555.501	1555.716
25	1573.351	1566.97	1567.216	1567.141	1567.402
30	1585.241	1576.502	1576.89	1577.17	1577.51
35	1596.076	1584.45	1585.119	1585.753	1586.112
40	1606.053	1590.993	1592.12	1593.058	1593.234

			Table 2-6		
	Speed of Sound calculated at 35 ppt and 60 metres depth				
Temperature	Wilson	Mackenzie	Medwin	Del Grosso	Chen-Millero-Li
15	1509.567	1507.671	1507.764	1507.656	1507.647
20	1525.839	1522.442	1522.48	1522.454	1522.444
25	1540.665	1535.273	1535.316	1535.324	1535.37
30	1554.242	1546.342	1546.49	1546.429	1546.562
35	1566.764	1555.828	1556.219	1555.934	1556.127
40	1578.427	1563.908	1564.72	1564.002	1564.136

			Table 2-7		
	Speed of Sound calculated at 65 ppt and 60 metres depth				
Temperature	Wilson	Mackenzie	Medwin	Del Grosso	Chen-Millero-Li
15	1546.447	1543.258	1543.464	1543.244	1543.141
20	1561.032	1556.492	1556.68	1556.772	1556.517
25	1574.172	1567.785	1568.016	1568.516	1568.193
30	1586.062	1577.317	1577.69	1578.641	1578.288
35	1596.898	1585.266	1585.919	1587.31	1586.87
40	1606.874	1591.808	1592.92	1594.689	1593.961

			Table 2-8		
	Speed of Sound calculated at 15 degrees and 10 metres depth				
Salinity	Wilson	Mackenzie	Medwin	Del Grosso	Chen-Millero-Li
35	1508.745	1506.855	1506.964	1506.831	1506.827
40	1514.892	1512.786	1512.914	1512.681	1512.667
45	1521.038	1518.718	1518.864	1518.542	1518.533
50	1527.185	1524.649	1524.814	1524.412	1524.431
55	1533.332	1530.58	1530.764	1530.293	1530.361
60	1539.478	1536.511	1536.714	1536.183	1536.328
65	1545.625	1542.443	1542.664	1542.084	1542.332

			Table 2-9		
	Speed of Sound calculated at 35 degrees and 10 metres depth				
Salinity	Wilson	Mackenzie	Medwin	Del Grosso	Chen-Millero-Li
35	1565.943	1555.013	1555.419	1555.159	1555.334
40	1570.965	1559.919	1560.369	1560.22	1560.392
45	1575.987	1564.825	1565.319	1565.297	1565.474
50	1581.01	1569.731	1570.269	1570.388	1570.584
55	1586.032	1574.638	1575.219	1575.495	1575.726
60	1591.054	1579.544	1580.169	1580.616	1580.901
65	1596.076	1584.45	1585.119	1585.753	1586.112

			Table 2-10		
	Speed of Sound calculated at 15 degrees and 60 metres depth				
Salinity	Wilson	Mackenzie	Medwin	Del Grosso	Chen-Millero-Li
35	1509.567	1507.671	1507.764	1507.656	1507.647
40	1515.713	1513.602	1513.714	1513.515	1513.487
45	1521.86	1519.533	1519.664	1519.403	1519.353
50	1528.007	1525.465	1525.614	1525.32	1525.249
55	1534.153	1531.396	1531.564	1531.266	1531.178
60	1540.3	1537.327	1537.514	1537.24	1537.141
65	1546.447	1543.258	1543.464	1543.244	1543.141

			Table 2-11		
	Speed of Sound calculated at 35 degrees and 60 metres depth				
Salinity	Wilson	Mackenzie	Medwin	Del Grosso	Chen-Millero-Li
35	1566.764	1555.828	1556.219	1555.934	1556.127
40	1571.787	1560.734	1561.169	1561.016	1561.181
45	1576.809	1565.641	1566.119	1566.157	1566.259
50	1581.831	1570.547	1571.069	1571.357	1571.364
55	1586.853	1575.453	1576.019	1576.616	1576.499
60	1591.876	1580.359	1580.969	1581.934	1581.667
65	1596.898	1585.266	1585.919	1587.31	1586.87

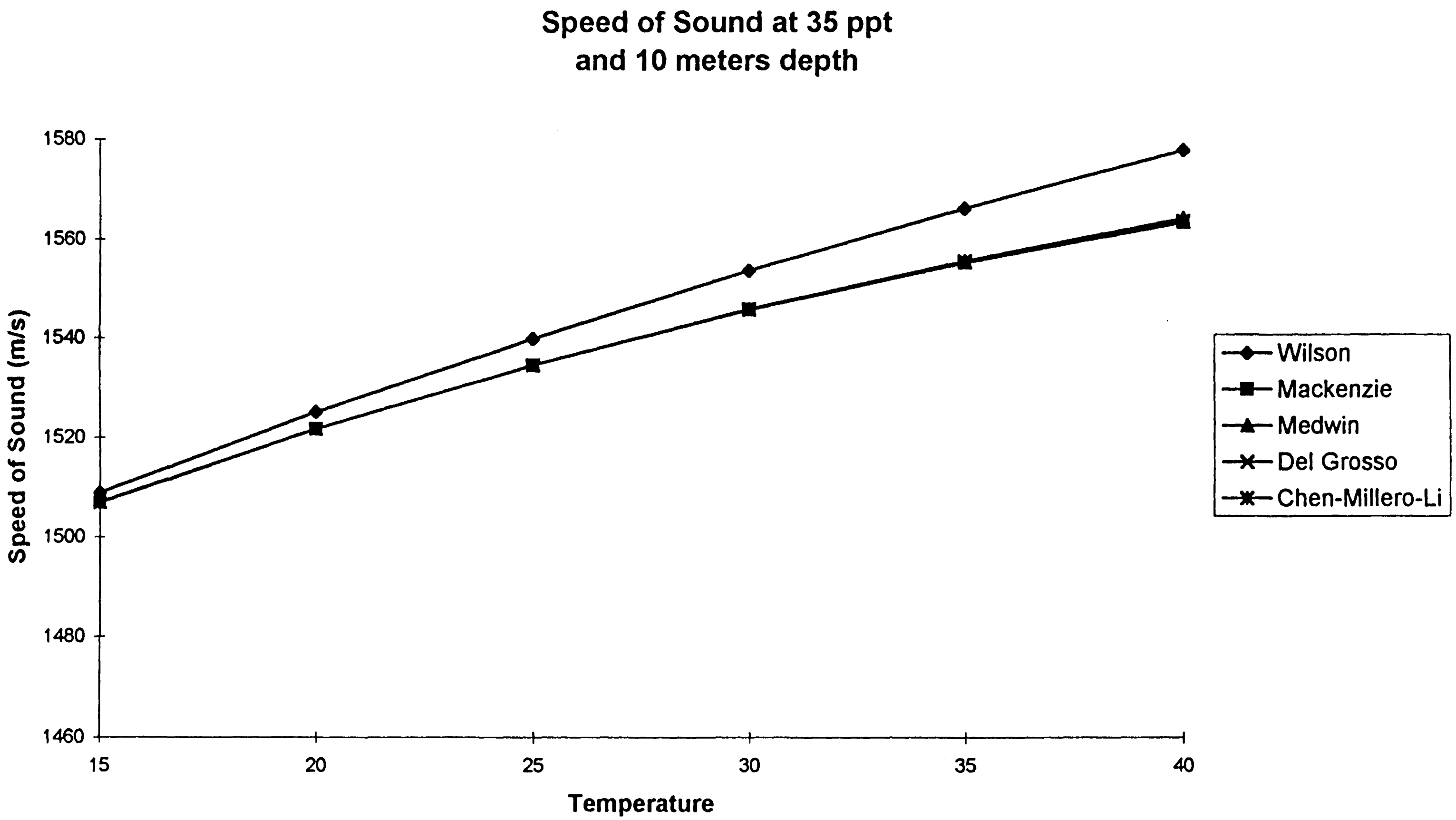

Figure 2-1

Speed of Sound vs. Temperature at 35 ppt salinity and 10 m depth

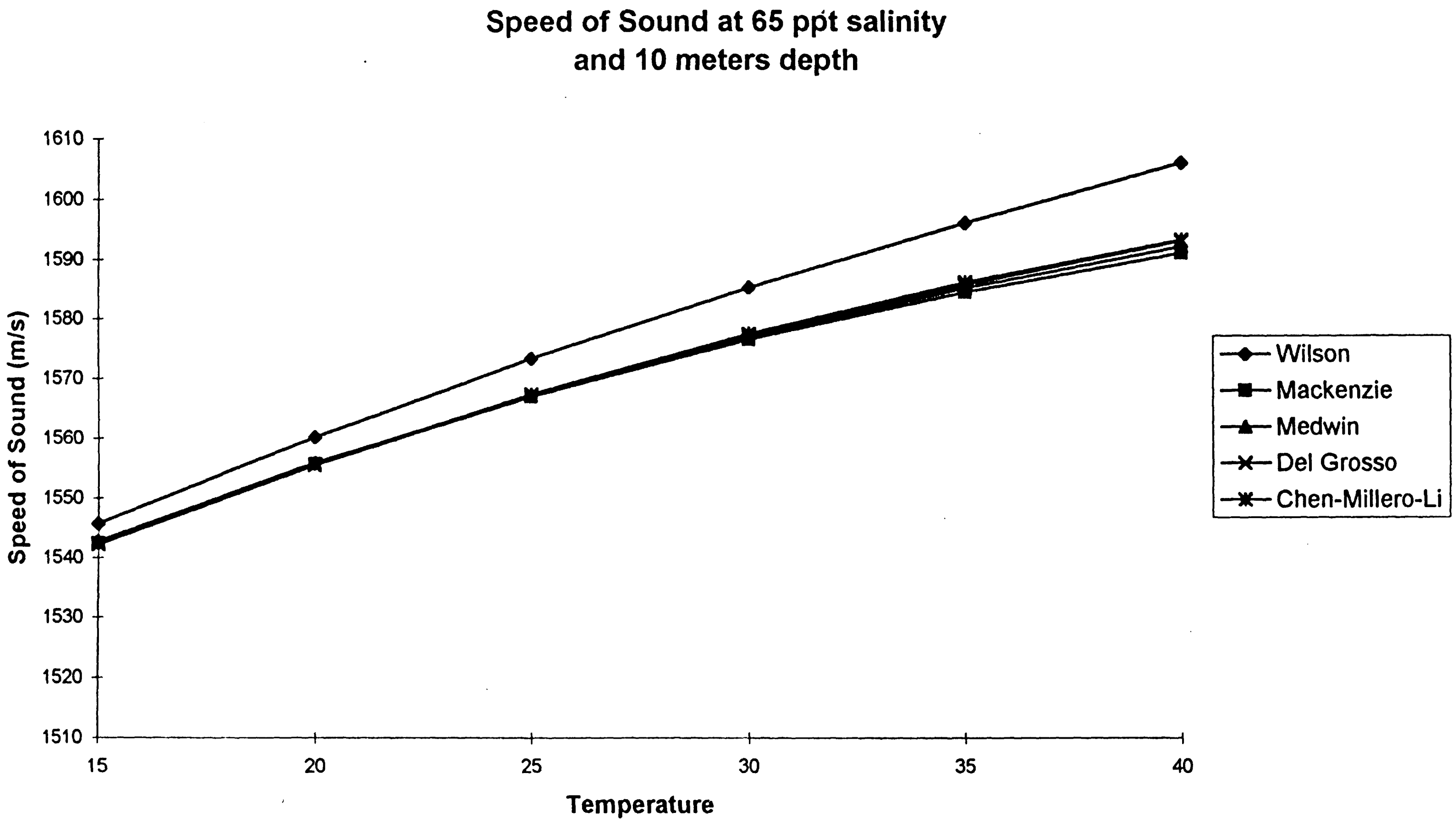

Figure 2-2

Speed of Sound vs. Temperature at 65 ppt salinity and 10 m depth

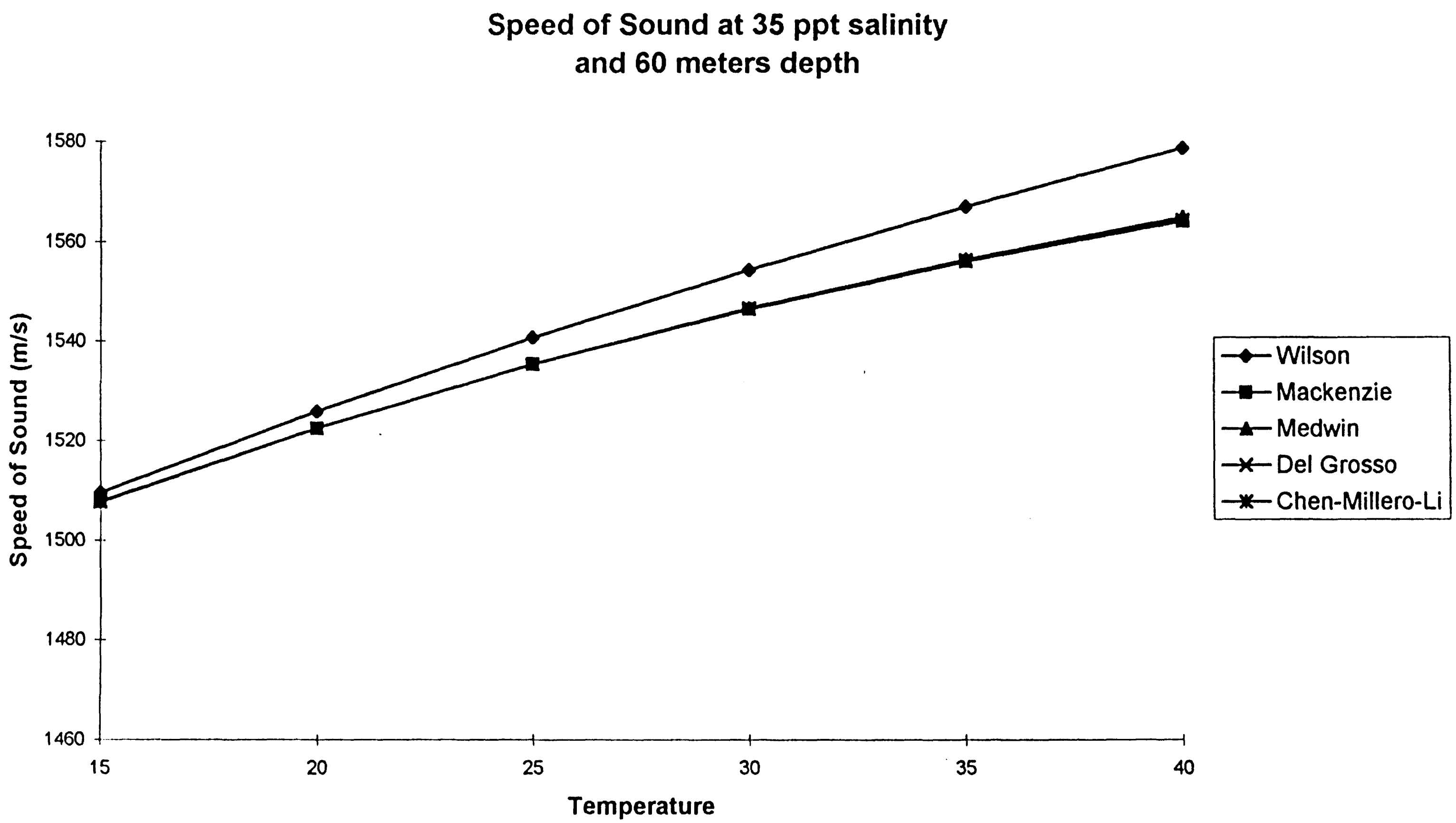

Figure 2-3

Speed of Sound vs. Temperature at 35 ppt salinity and 60 m depth

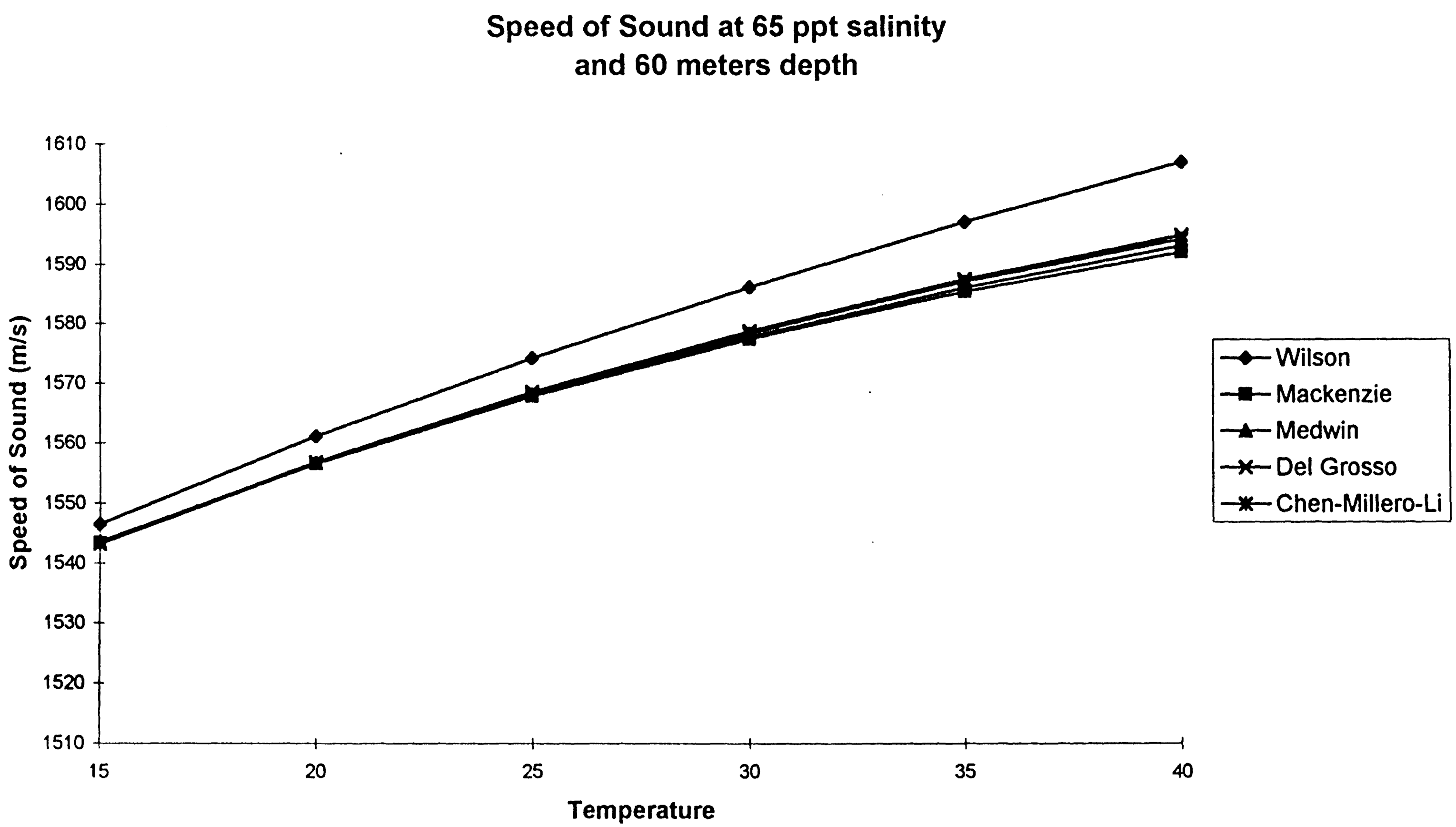

Figure 2-4

Speed of Sound vs. Temperature at 65 ppt salinity and 60 m depth

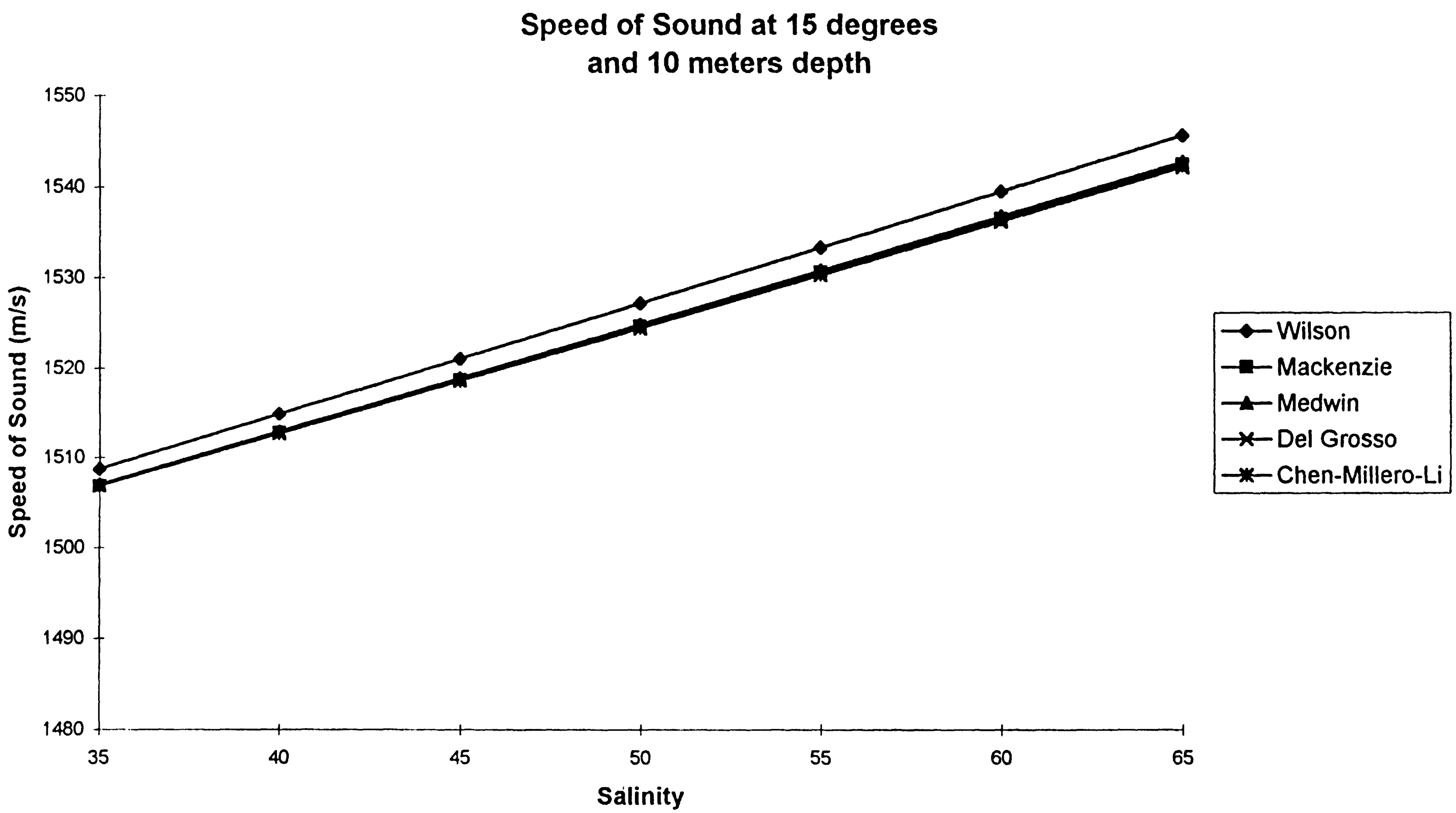

Figure 2-5

Speed of Sound vs. Salinity at 15 degrees and 10 m depth

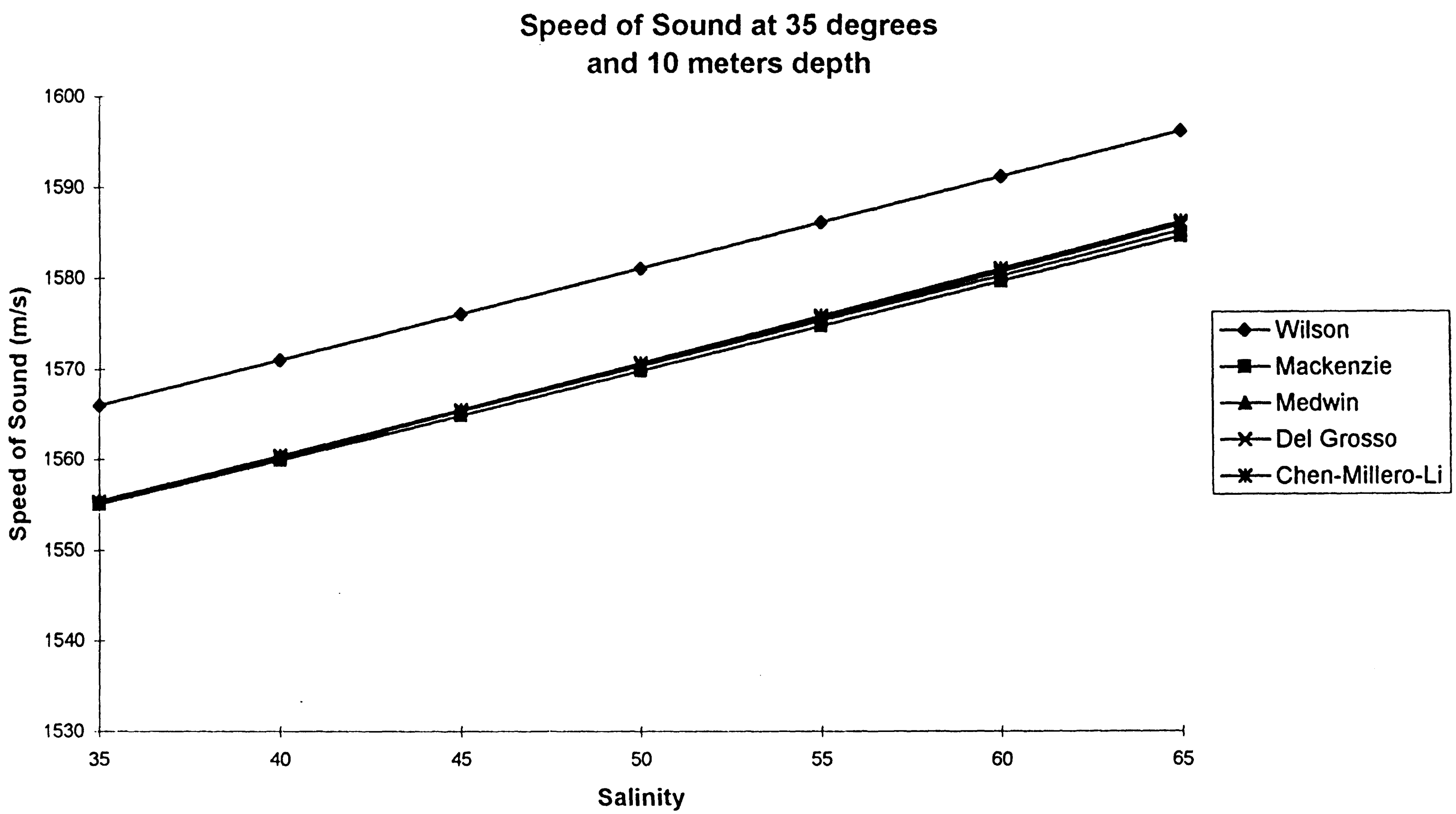

Figure 2-6

Speed of Sound vs. Salinity at 35 degrees and 10 m depth

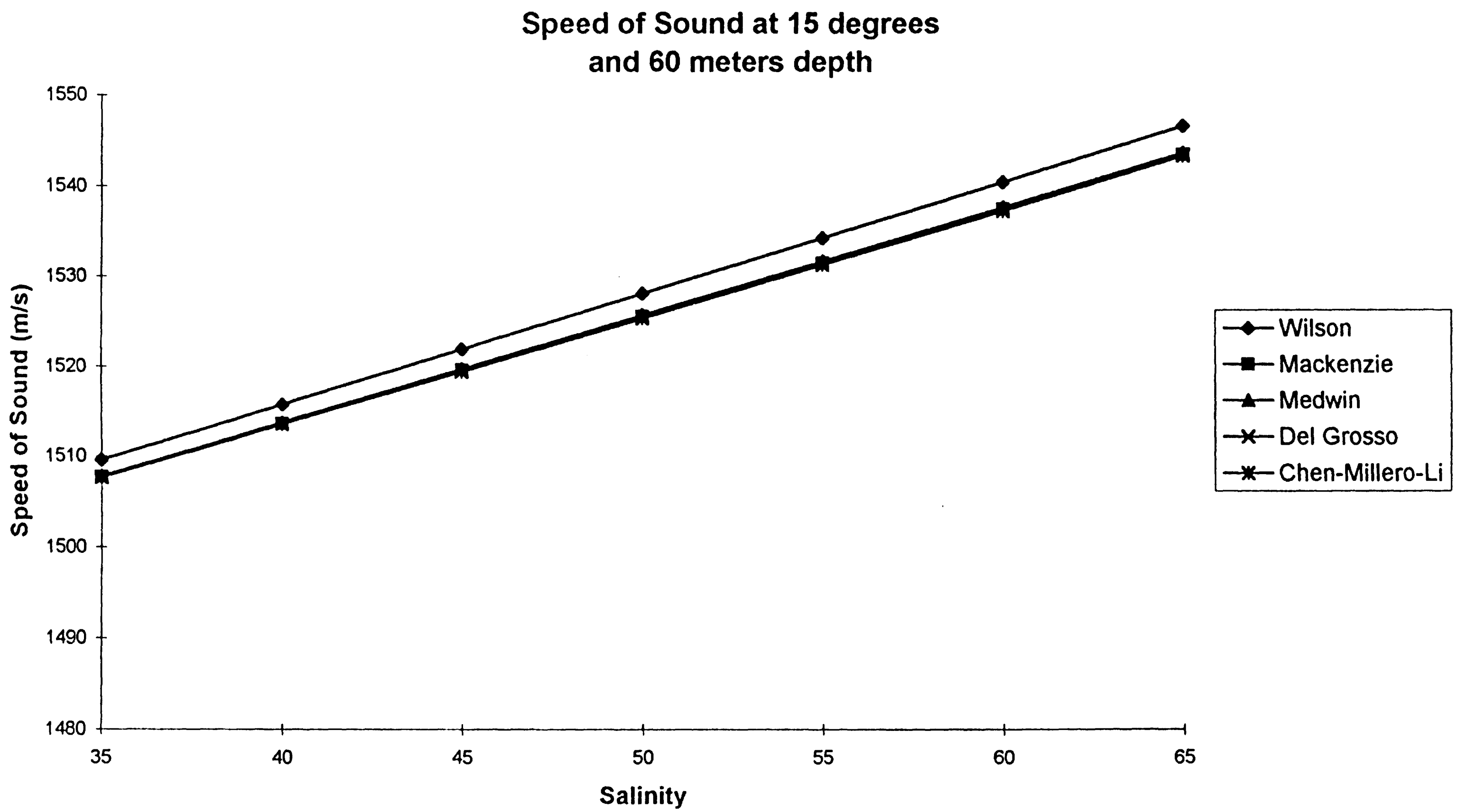

Figure 2-7

Speed of Sound vs. Salinity at 15 degrees and 60 m depth

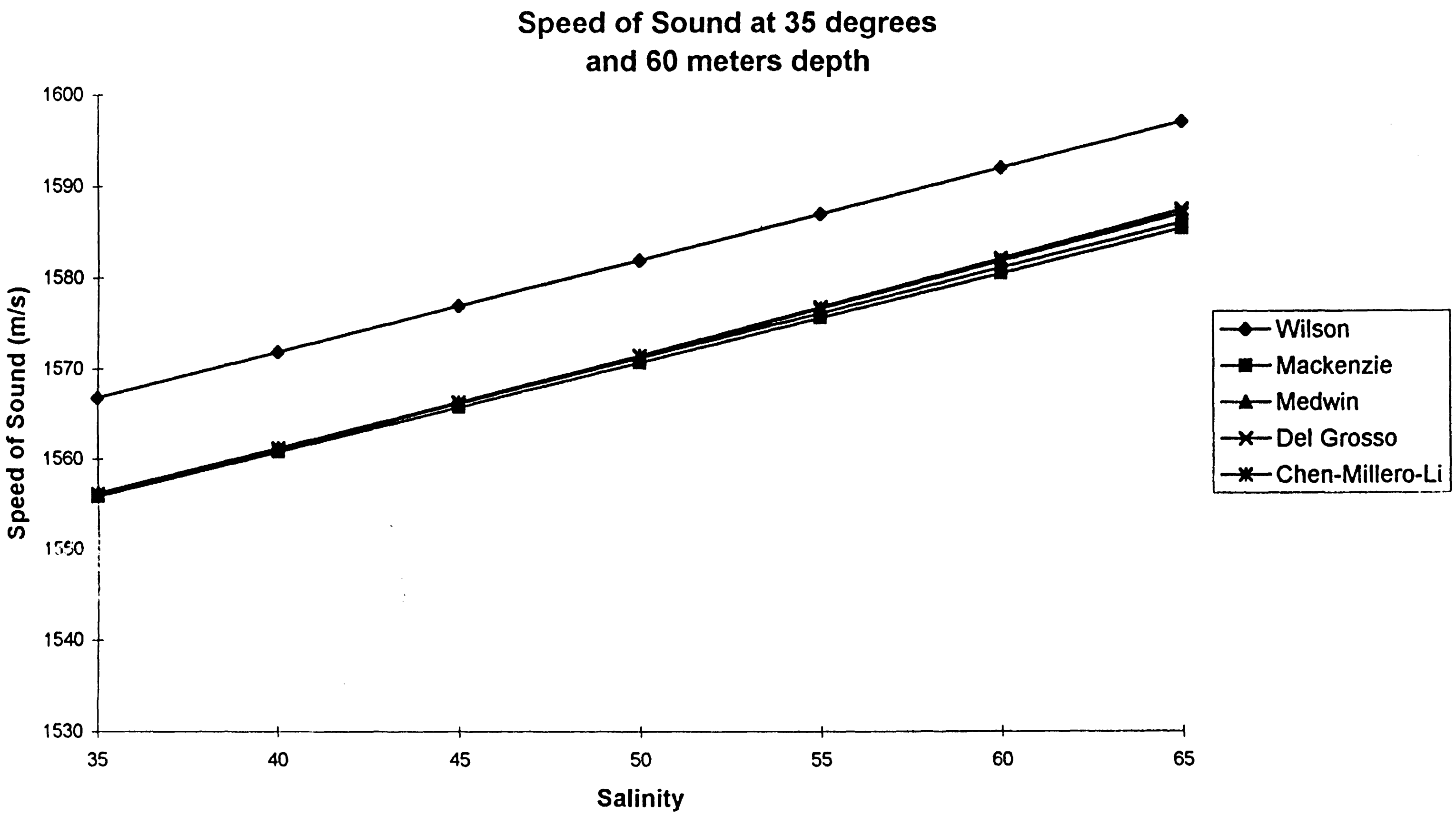

Figure 2-8

Speed of Sound vs. Salinity at 35 degrees and 60 m depth

		Table 2-12		
Amount by which Speed of Sound calculated at 35 ppt salinity and 10 metres depth for different equations exceeded Chen & Millero equation				
Temperature	Wilson	Mackenzie	Medwin	Del Grosso
15	-1.91791	-0.02803	-0.13654	-0.00422
20	-3.39144	-0.00056	-0.05434	-0.00494
25	-5.28847	0.097966	0.039107	0.047593
30	-7.66469	0.229146	0.065963	0.127225
35	-10.609	0.321356	-0.08485	0.174563
40	-14.2424	0.270908	-0.55647	0.098157

		Table 2-13		
Amount by which Speed of Sound calculated at 65 ppt salinity and 10 metres depth for different equations exceeded Chen & Millero equation				
Temperature	Wilson	Mackenzie	Medwin	Del Grosso
15	-3.29276	-0.11048	-0.33149	0.247833
20	-4.49478	0.039408	-0.16438	0.214686
25	-5.94895	0.431694	0.185336	0.260884
30	-7.73098	1.007952	0.619769	0.340235
35	-9.96437	1.661978	0.99327	0.35877
40	-12.8192	2.240974	1.11359	0.175927

		Table 2-14		
Amount by which Speed of Sound calculated at 35 ppt salinity and 60 metres depth for different equations exceeded Chen & Millero equation				
Temperature	Wilson	Mackenzie	Medwin	Del Grosso
15	-1.91936	-0.02357	-0.11649	-0.00842
20	-3.39419	0.002606	-0.03559	-0.00968
25	-5.29566	0.096698	0.053422	0.045898
30	-7.68013	0.219626	0.072024	0.133147
35	-10.6378	0.298489	-0.09214	0.193094
40	-14.2915	0.22775	-0.58405	0.134127

		Table 2-15		
Amount by which Speed of Sound calculated at 65 ppt salinity and 60 metres depth for different equations exceeded Chen & Millero equation				
Temperature	Wilson	Mackenzie	Medwin	Del Grosso
15	-3.30583	-0.11764	-0.32306	-0.1034
20	-4.51487	0.025233	-0.16297	-0.25465
25	-5.97858	0.407981	0.177206	-0.32238
30	-7.77422	0.970627	0.598026	-0.35263
35	-10.0279	1.604384	0.951257	-0.44027
40	-12.9133	2.152837	1.041034	-0.72778

		Table 2-16		
Amount by which Speed of Sound calculated at 35 degrees and 10 metres depth for different equations exceeded Chen & Millero equation				
Salinity	Wilson	Mackenzie	Medwin	Del Grosso
35	-10.609	0.321356	-0.08485	0.174563
40	-10.5735	0.472892	0.022934	0.171327
45	-10.5134	0.648989	0.15528	0.177465
50	-10.4252	0.853168	0.315709	0.196501
55	-10.3059	1.088407	0.507198	0.231412
60	-10.1531	1.357266	0.732308	0.284758
65	-9.96437	1.661978	0.99327	0.35877

		Table 2-17		
Amount by which Speed of Sound calculated at 15 degrees and 10 metres depth for different equations exceeded Chen & Millero equation				
Salinity	Wilson	Mackenzie	Medwin	Del Grosso
35	-1.91791	-0.02803	-0.13654	-0.00422
40	-2.22504	-0.11976	-0.24702	-0.01472
45	-2.50499	-0.18431	-0.33032	-0.00823
50	-2.7544	-0.21832	-0.38308	0.018605
55	-2.97041	-0.21893	-0.40244	0.068647
60	-3.15057	-0.1837	-0.38596	0.144344
65	-3.29276	-0.11048	-0.33149	0.247833

		Table 2-18		
Amount by which Speed of Sound calculated at 15 degrees and 60 metres depth for different equations exceeded Chen & Millero equation				
Salinity	Wilson	Mackenzie	Medwin	Del Grosso
35	-1.91936	-0.02357	-0.11649	-0.00842
40	-2.22606	-0.11486	-0.22654	-0.02758
45	-2.50645	-0.17985	-0.31028	-0.04935
50	-2.75723	-0.21524	-0.36441	-0.07042
55	-2.97561	-0.21821	-0.38614	-0.088
60	-3.15917	-0.18638	-0.37305	-0.09969
65	-3.30583	-0.11764	-0.32306	-0.1034

		Table 2-19		
Amount by which Speed of Sound calculated at 35 degrees and 60 metres depth for different equations exceeded Chen & Millero equation				
Salinity	Wilson	Mackenzie	Medwin	Del Grosso
35	-10.6378	0.298489	-0.09214	0.193094
40	-10.6058	0.446481	0.012103	0.165072
45	-10.5501	0.618217	0.14009	0.101916
50	-10.4671	0.817152	0.295275	0.007081
55	-10.3541	1.046205	0.480578	-0.11652
60	-10.2084	1.307886	0.698509	-0.26636
65	-10.0279	1.604384	0.951257	-0.44027

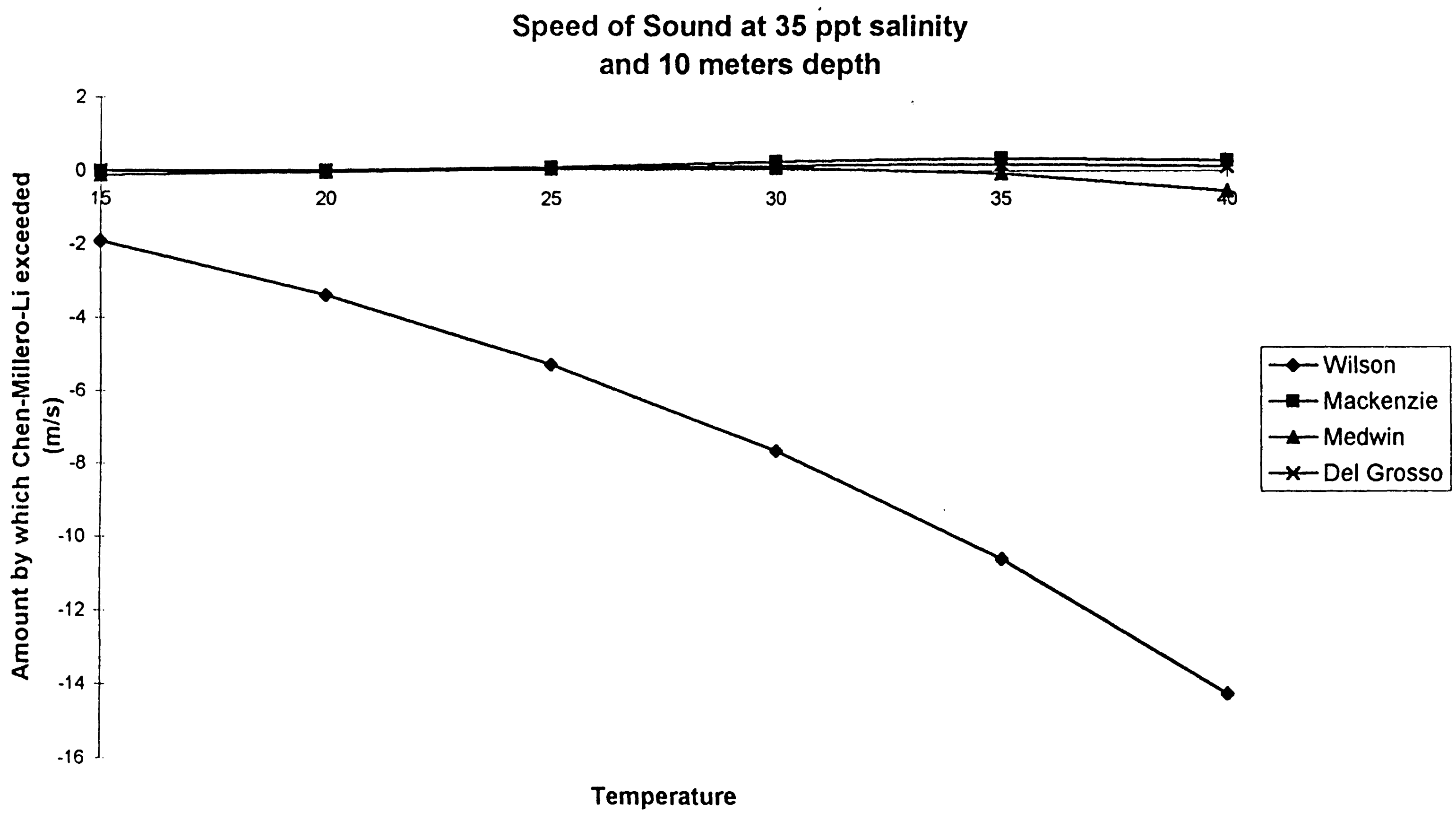

Figure 2-9

Difference of Speed of Sound vs. Temperature at 35 ppt salinity and 10 m depth

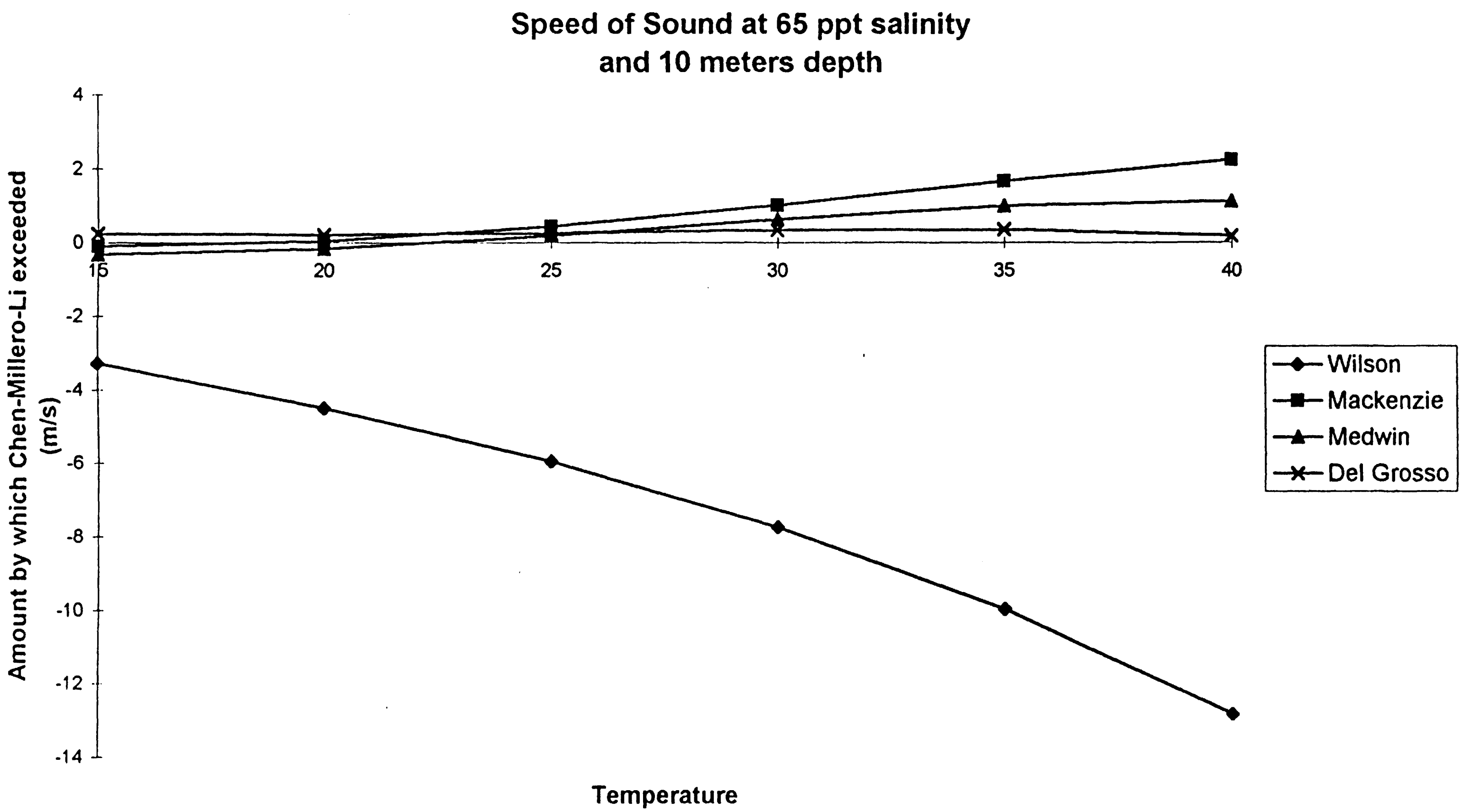

Figure 2-10

Difference of Speed of Sound vs. Temperature at 65 ppt salinity and 10 m depth

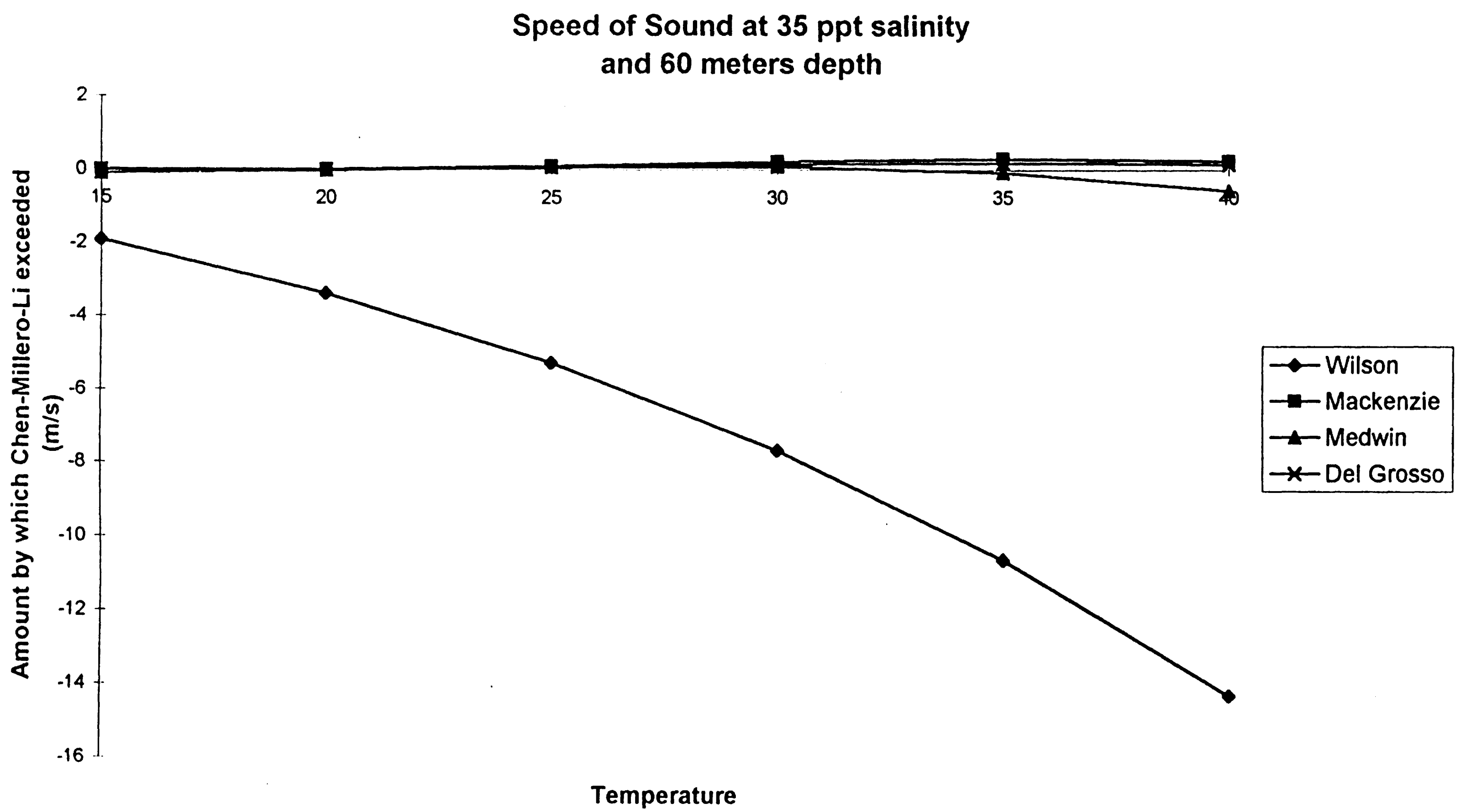

Figure 2-11

Difference of Speed of Sound vs. Temperature at 35 ppt salinity and 60 m depth

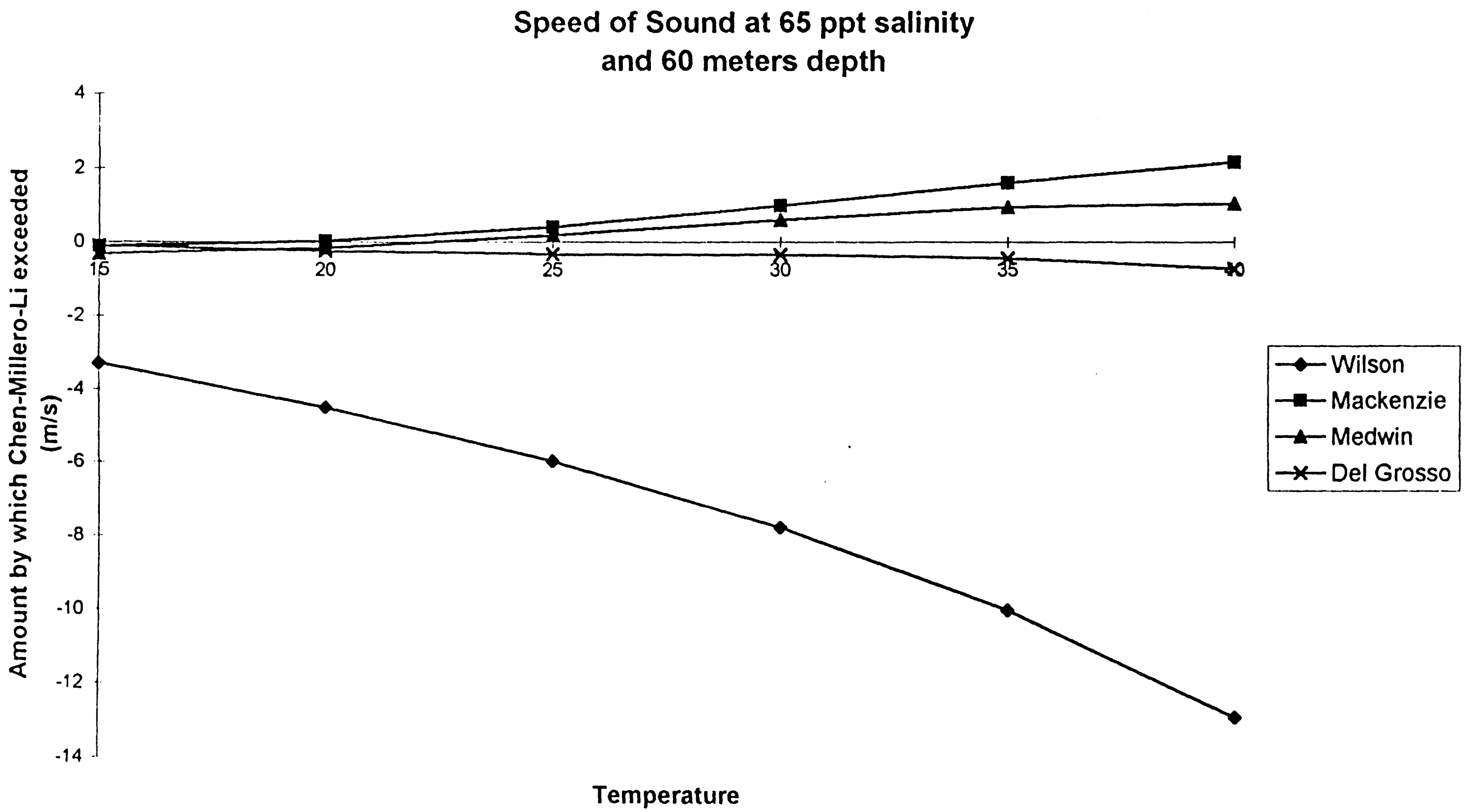

Figure 2-12

Difference of Speed of Sound vs. Temperature at 65 ppt salinity and 60 m depth

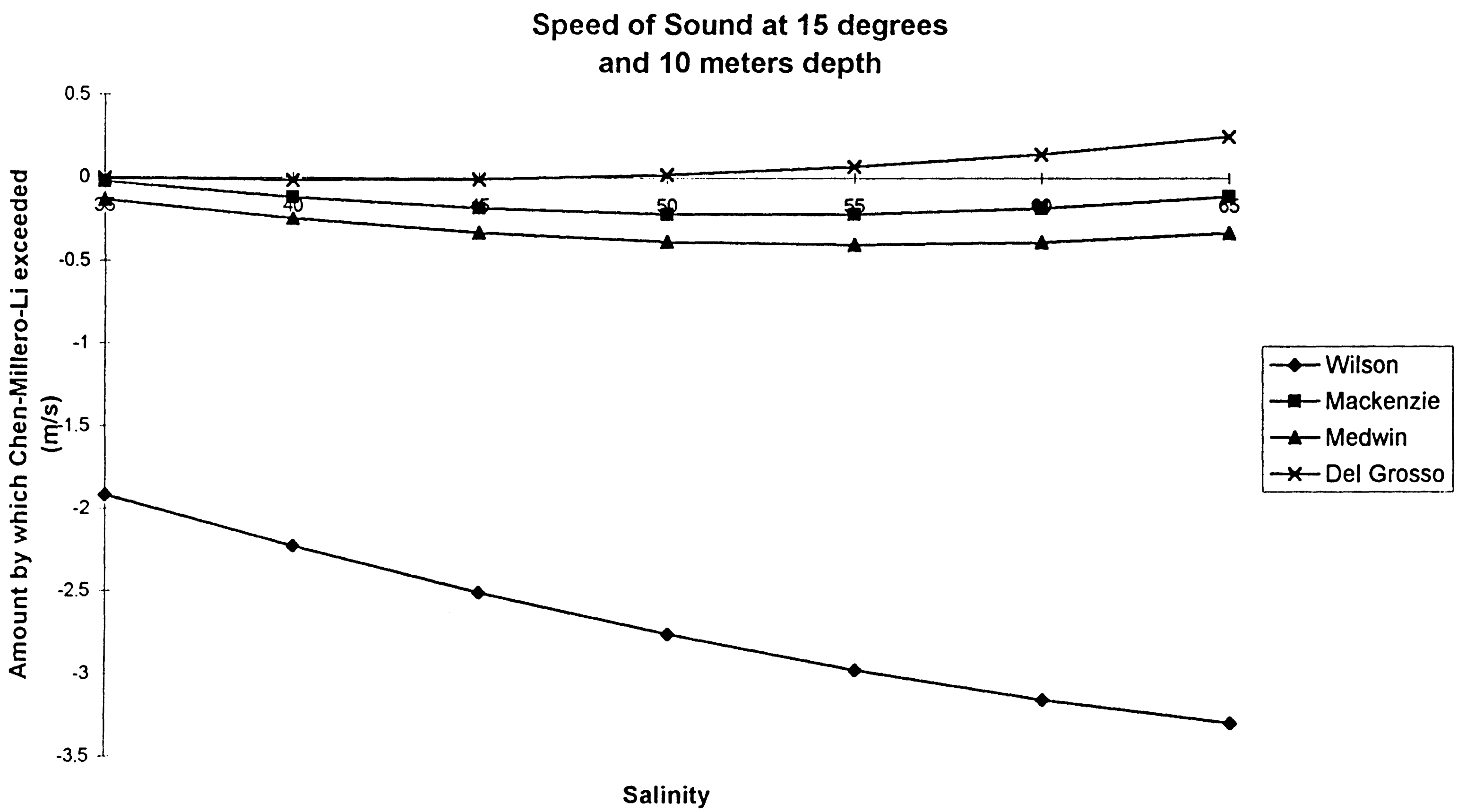

Figure 2-13

Difference of Speed of Sound vs. Salinity at 15 degrees and 10 m depth

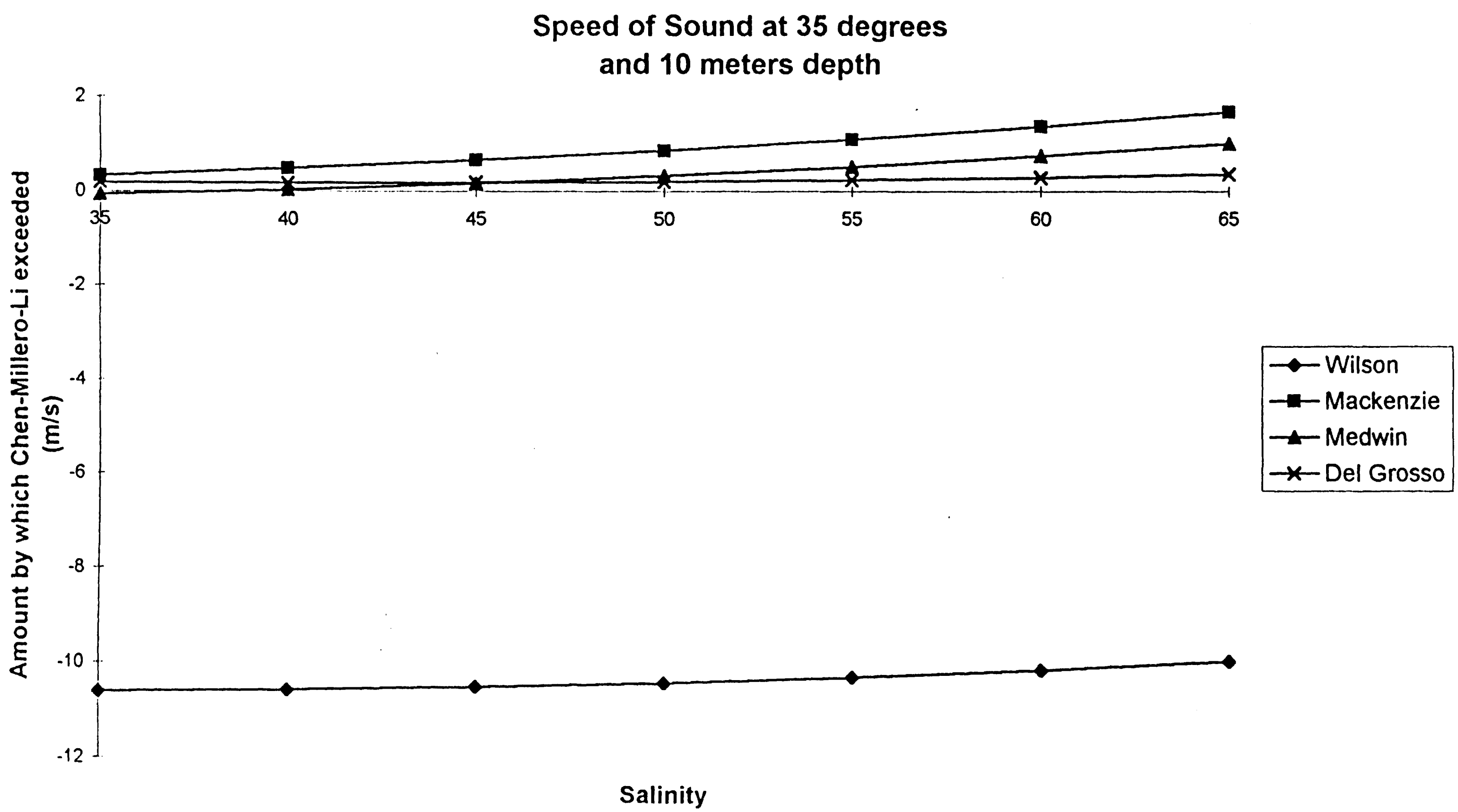

Figure 2-14

Difference of Speed of Sound vs. Salinity at 35 degrees and 10 m depth

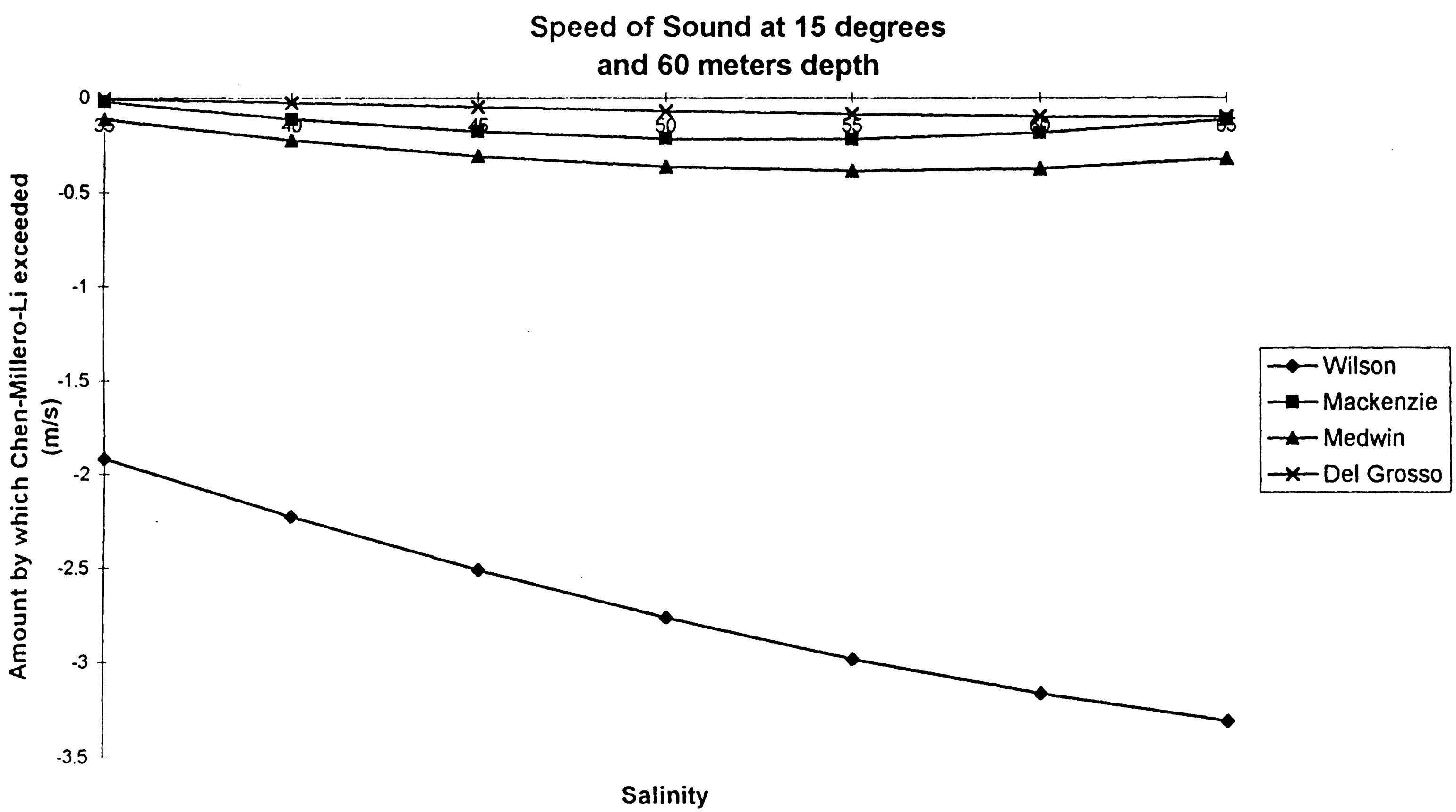

Figure 2-15

Difference of Speed of Sound vs. Salinity at 15 degrees and 60 m depth

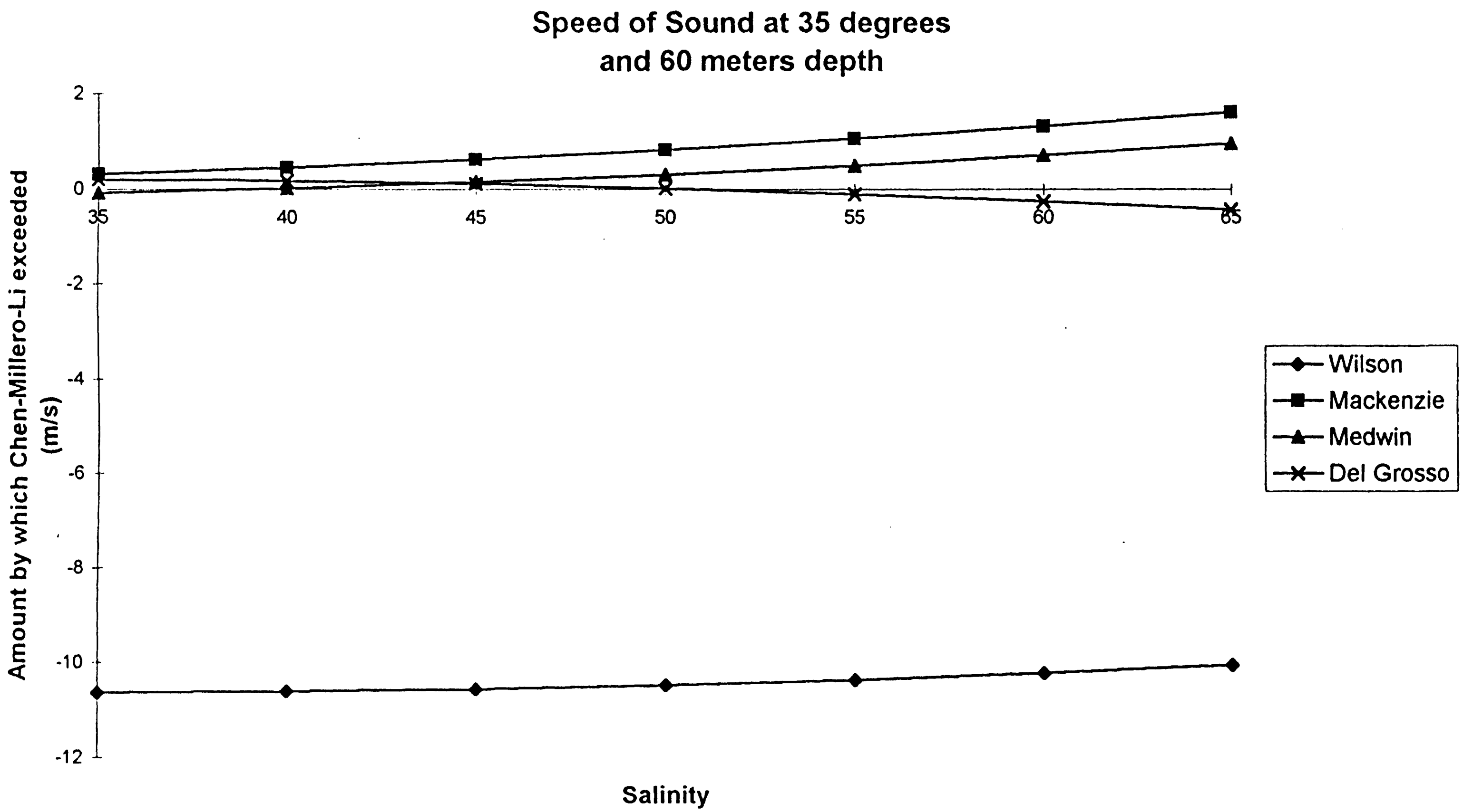

Figure 2-16

Difference of Speed of Sound vs. Salinity at 35 degrees and 60 m depth

Appendix IV

Figures for Chapter 3

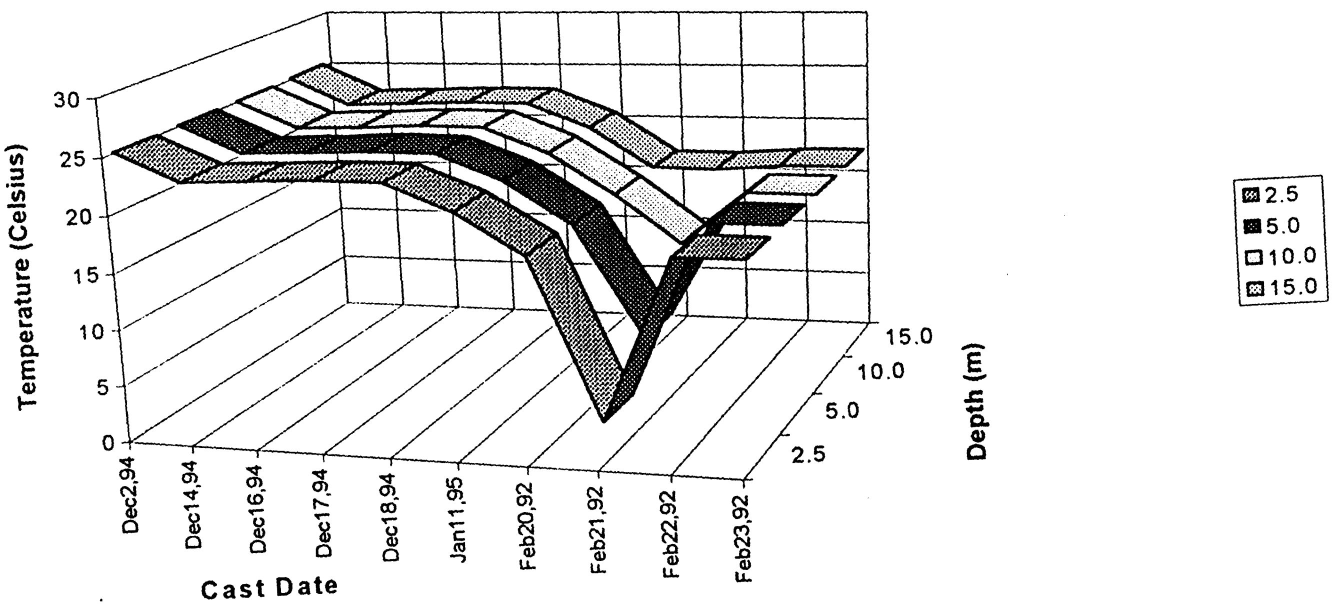

Figure 3-2

Temperature variations in Abu Safa in 2.5, 5.0, 10.0, and 15.0 metres of water.

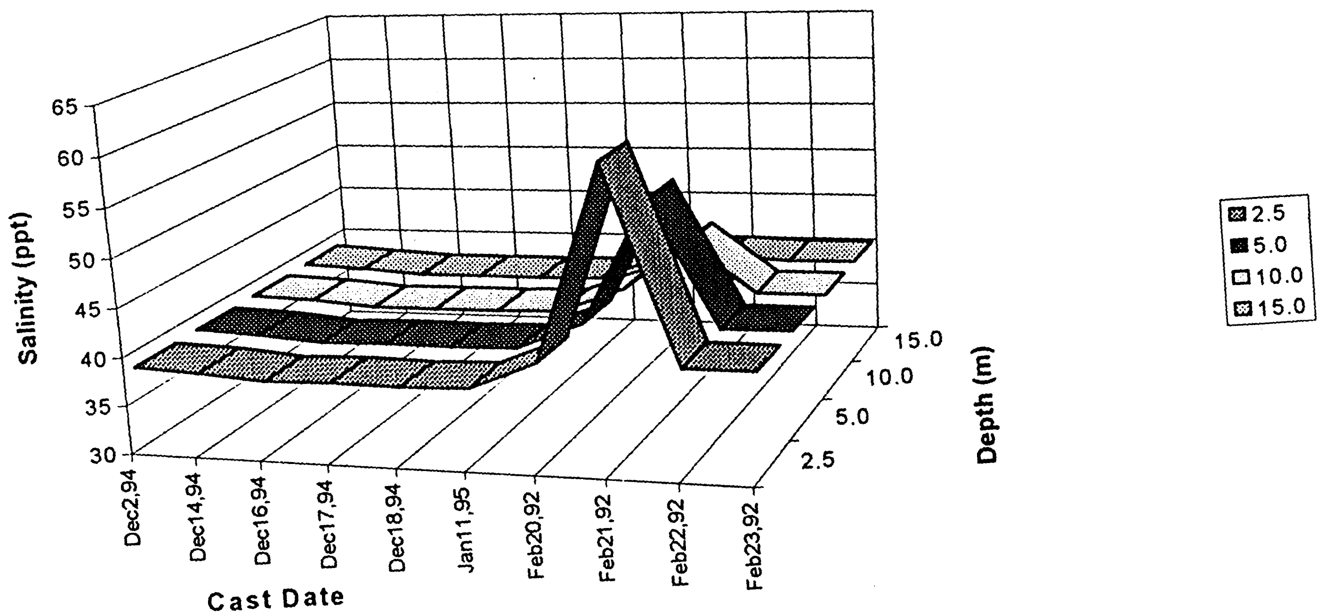

Figure 3-3

Salinity variations in Abu Safa in 2.5, 5.0, 10.0, and 15.0 metres of water.

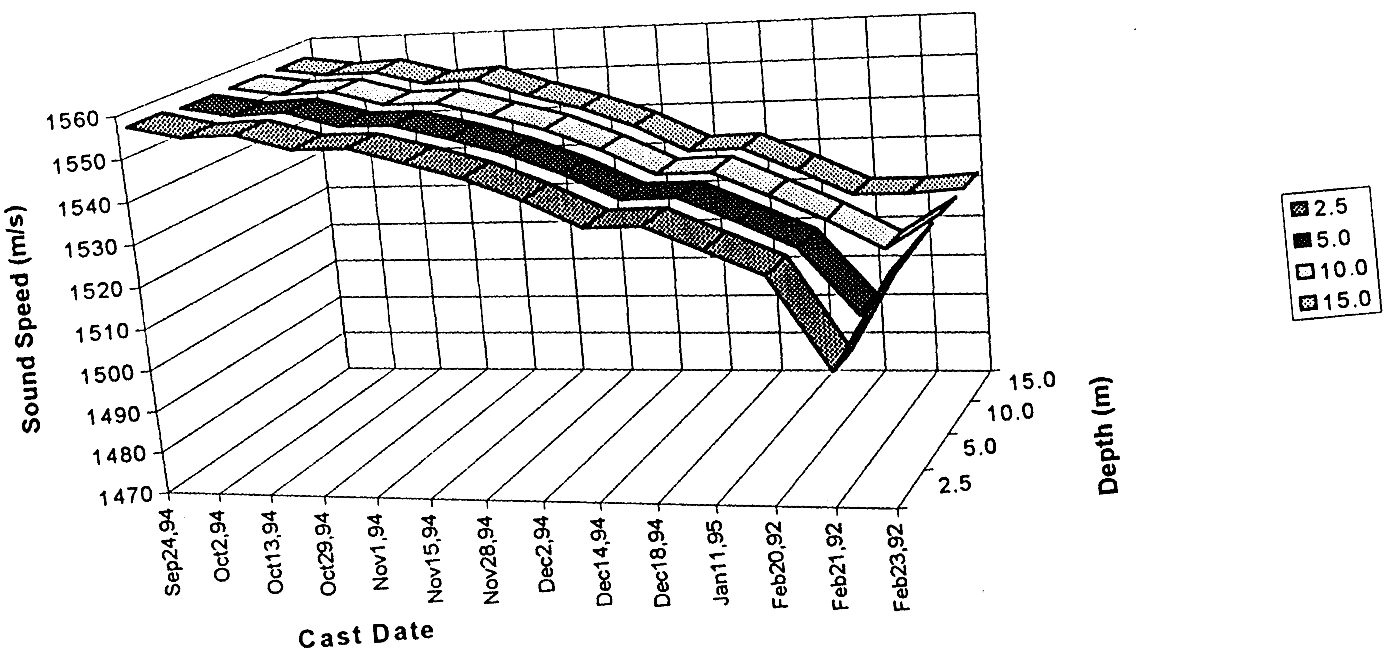

Figure 3-4

Sound speed variations in Abu Safa in 2.5, 5.0, 10.0, and 15.0 metres of water.

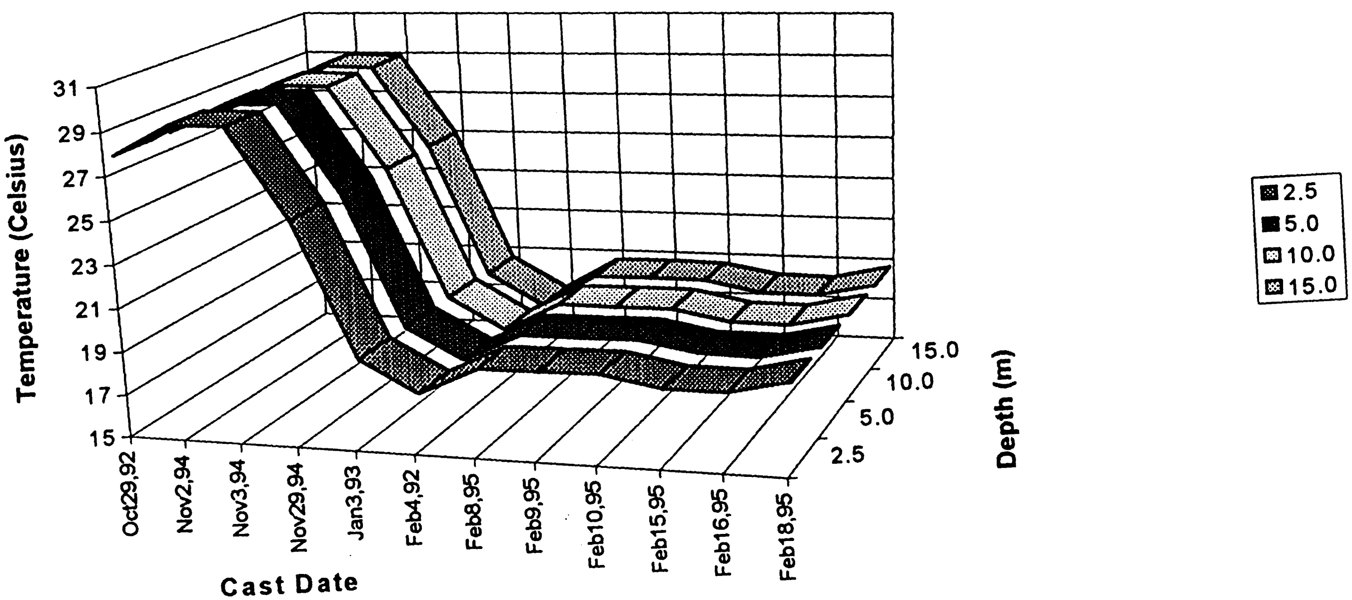

Figure 3-5

Temperature variations in Berri in 2.5, 5.0, 10.0, and 15.0 metres of water.

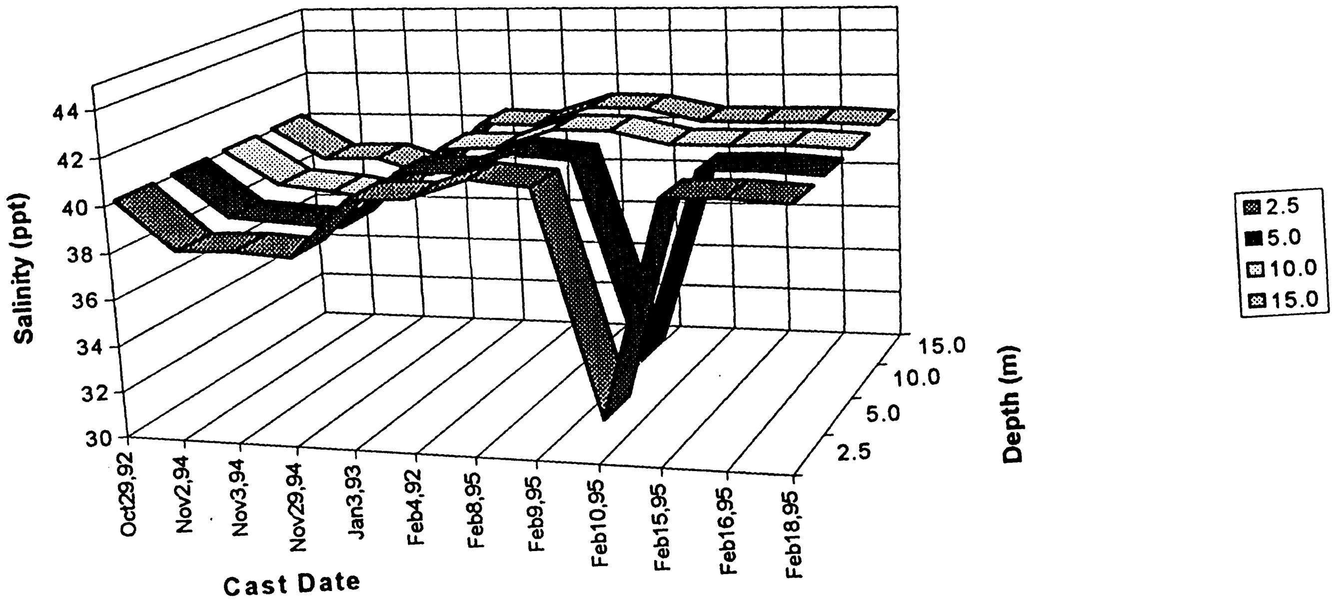

Figure 3-6

Salinity variations in Berri in 2.5, 5.0, 10.0, and 15.0 metres of water.

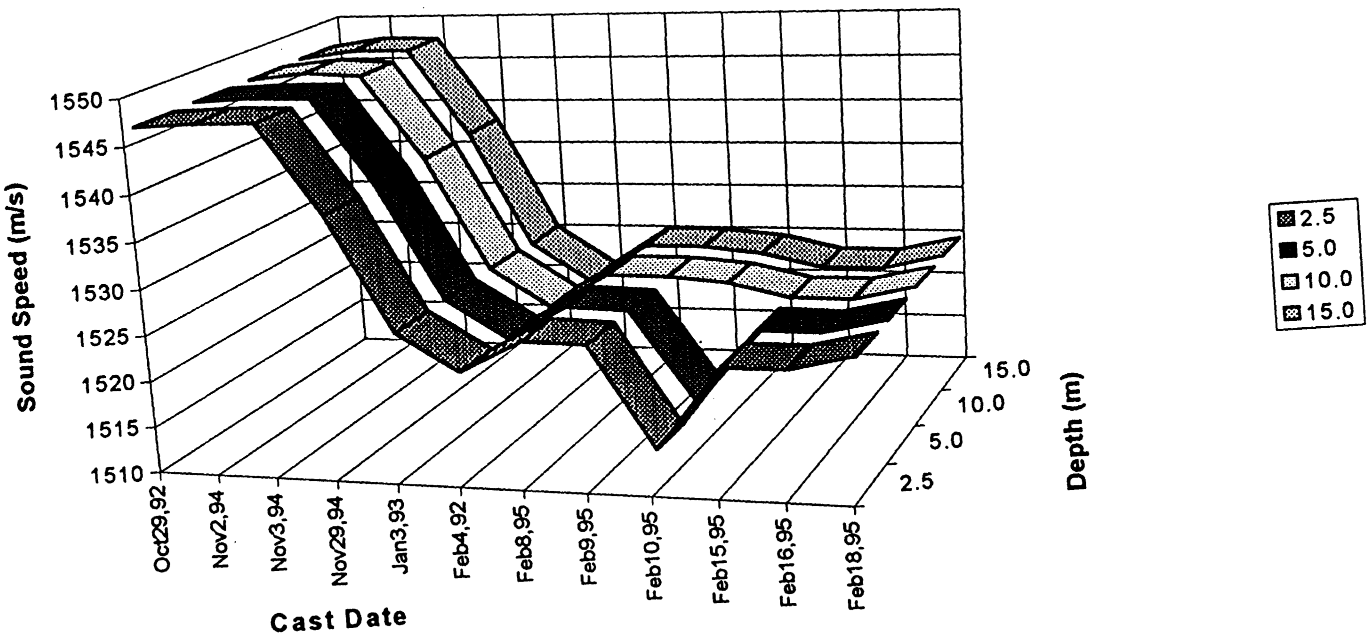

Figure 3-7

Sound speed variations in Berri in 2.5, 5.0, 10.0, and 15.0 metres of water.

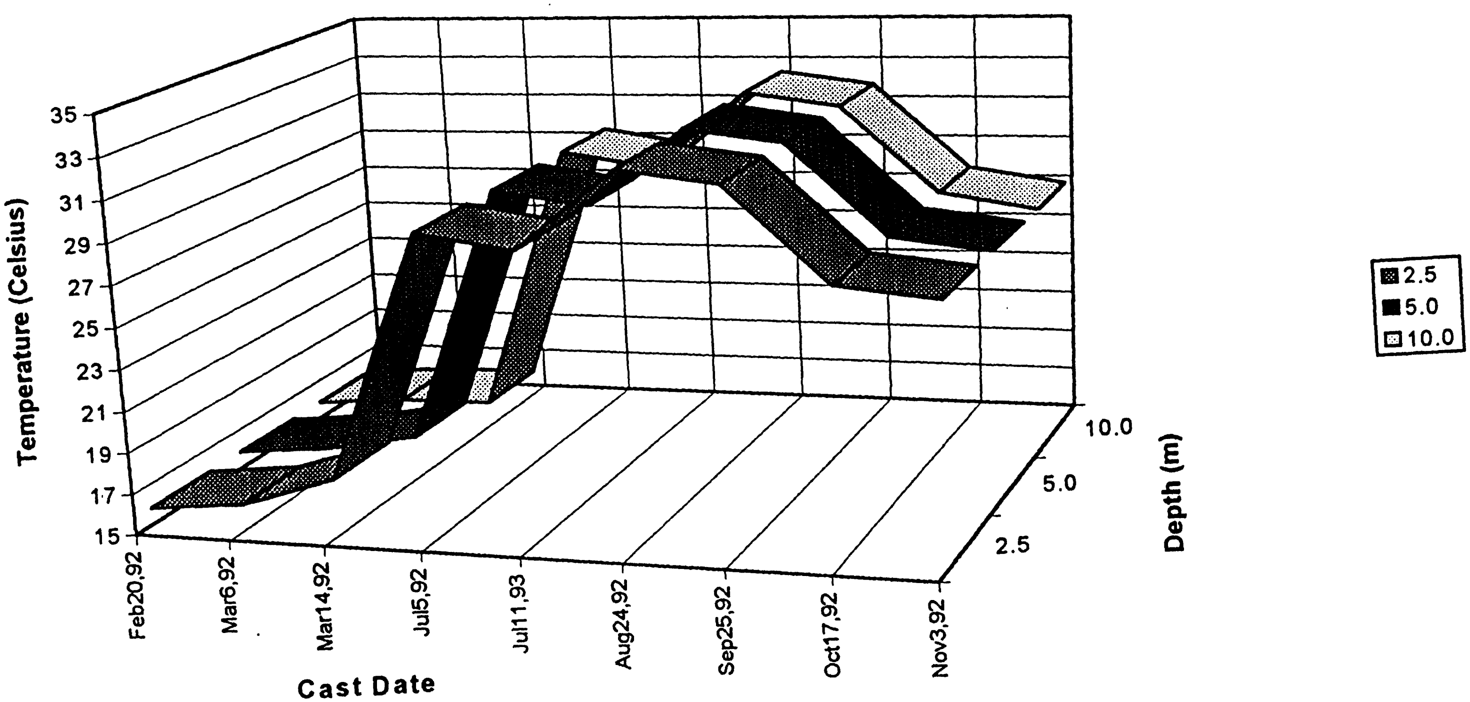

Figure 3-8

Temperature variations in Ras Tanura in 2.5, 5.0, and 10.0 metres of water.

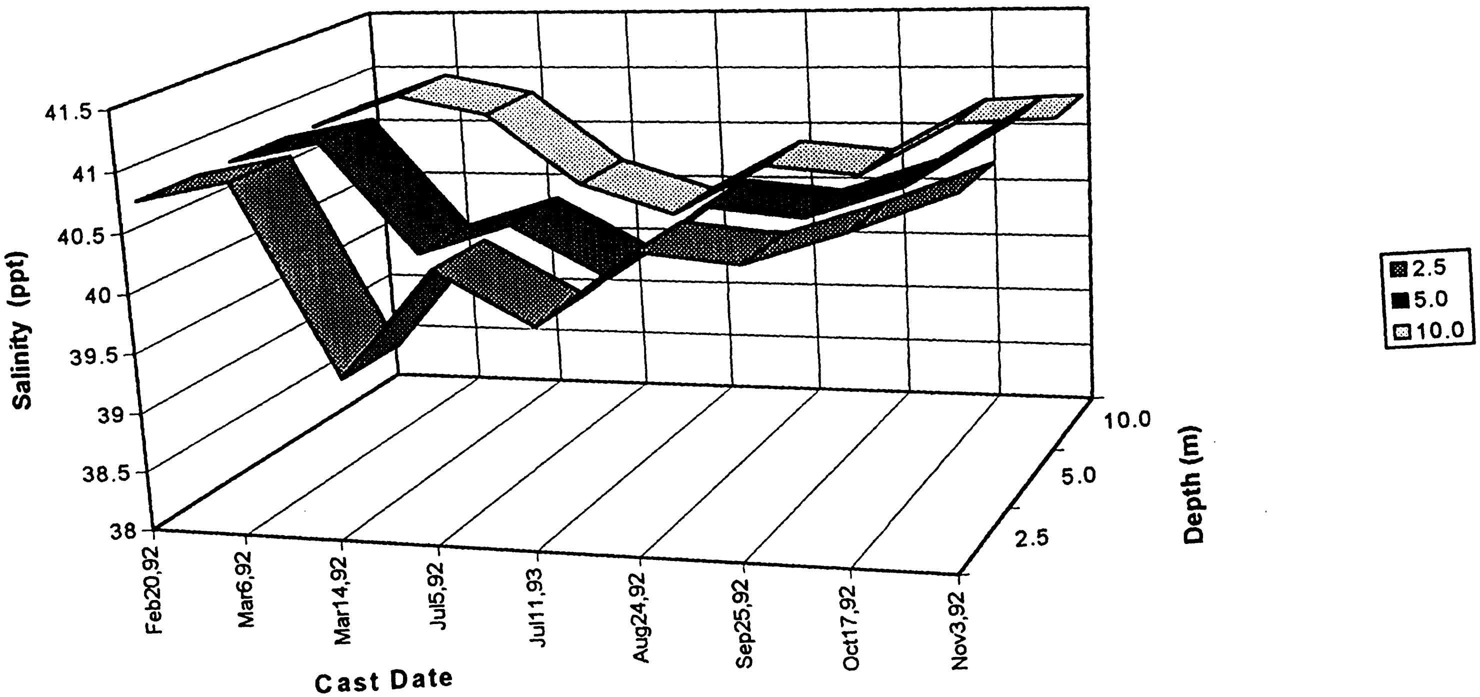

Figure 3-9

Salinity variations in Ras Tanura in 2.5, 5.0, and 10.0 metres of water.

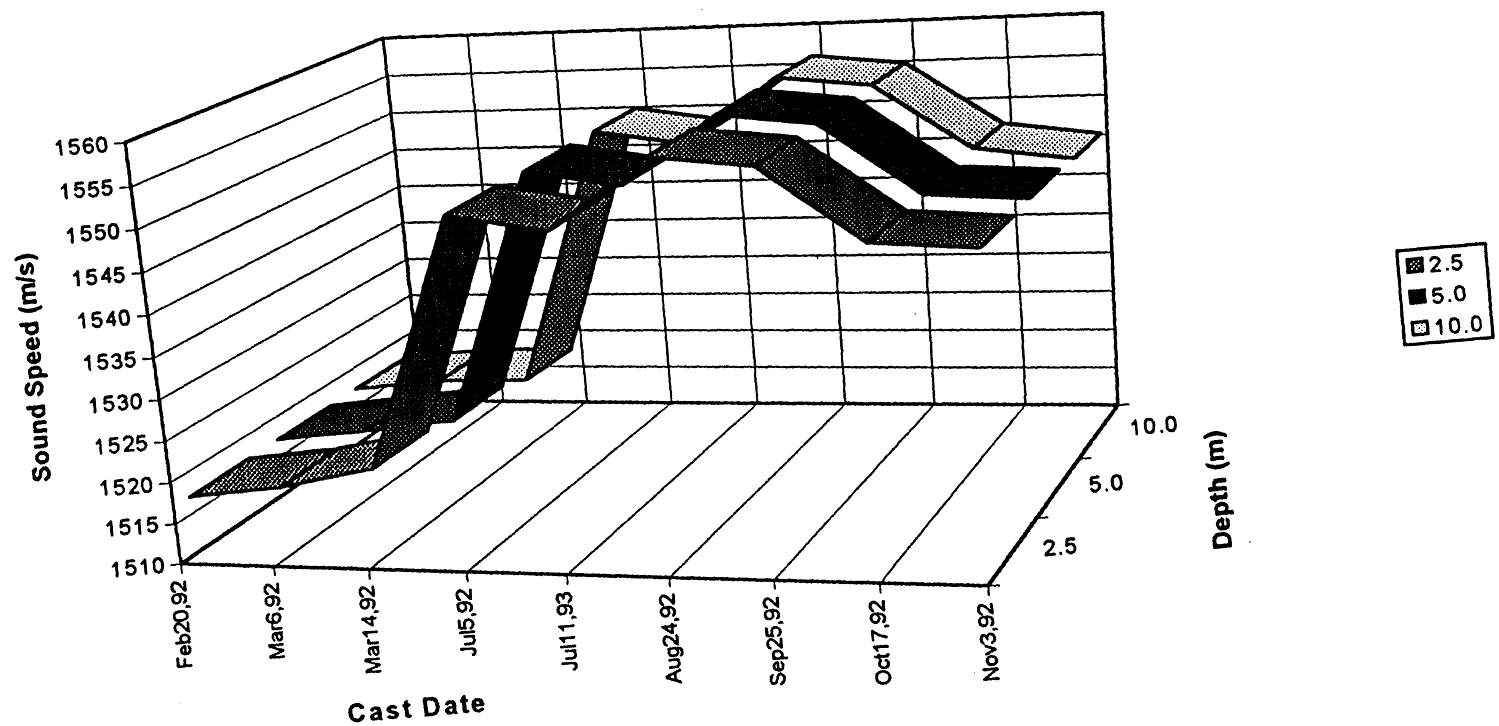

Figure 3-10

Sound speed variations in Ras Tanura in 2.5, 5.0, and 10.0 metres of water.

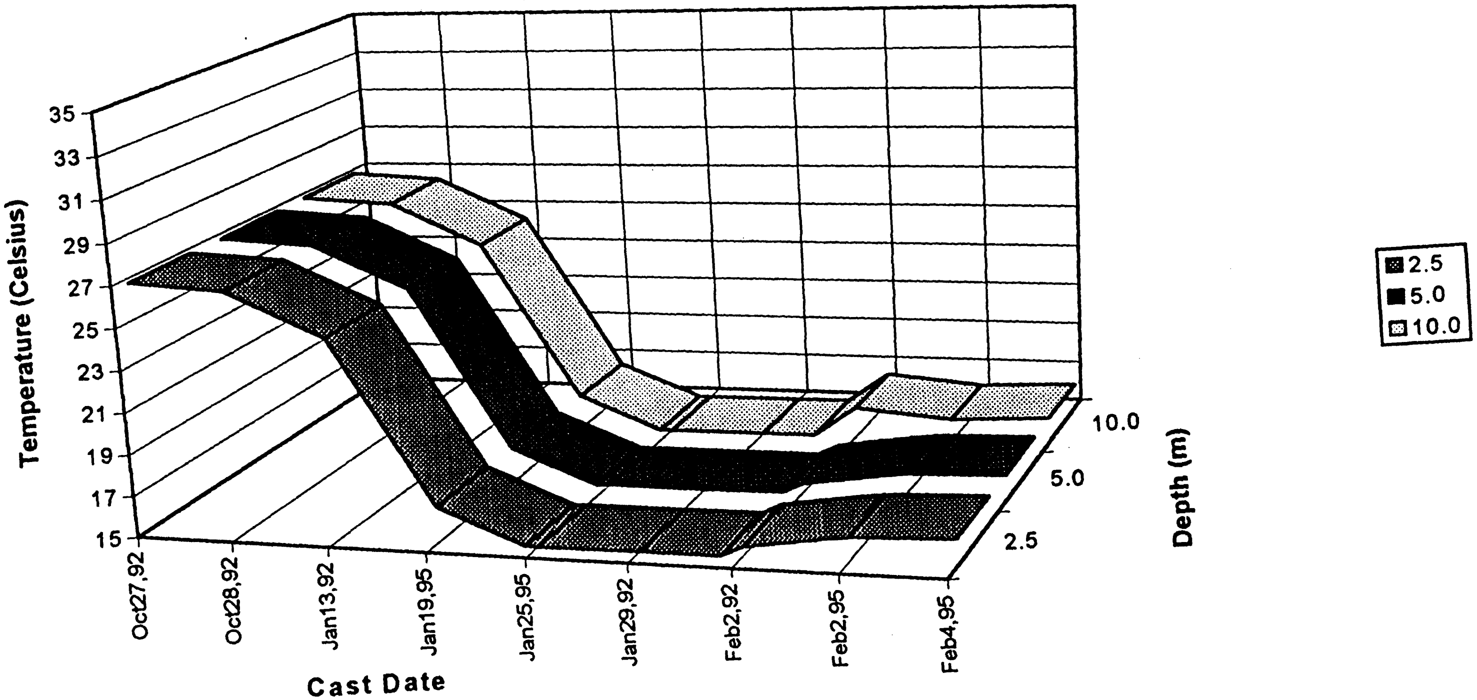

Figure 3-11

Temperature variations in Safaniyah in 2.5, 5.0, and 10.0 metres of water.

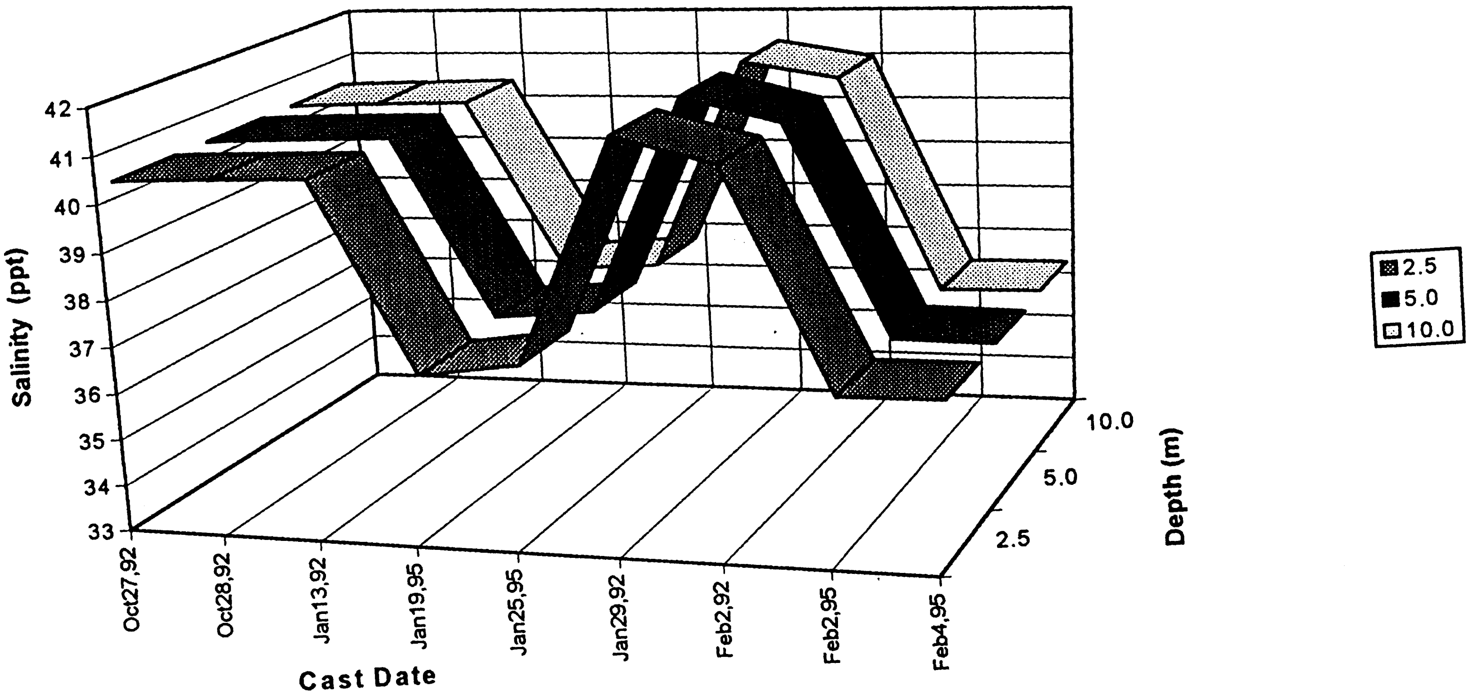

Figure 3-12

Salinity variations in Safaniyah in 2.5, 5.0, and 10.0 metres of water.

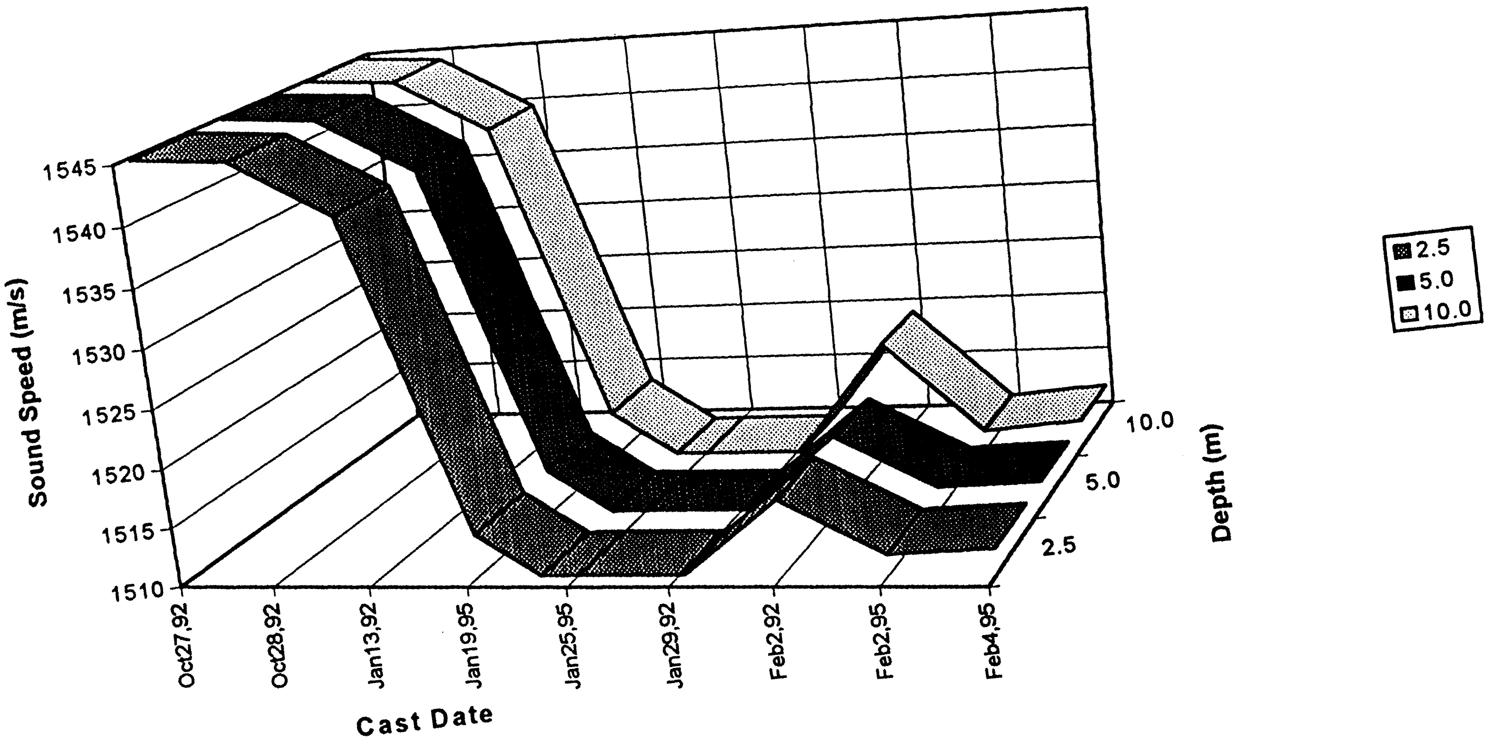

Figure 3-13

Sound speed variations in Safaniyah in 2.5, 5.0, and 10.0 metres of water.

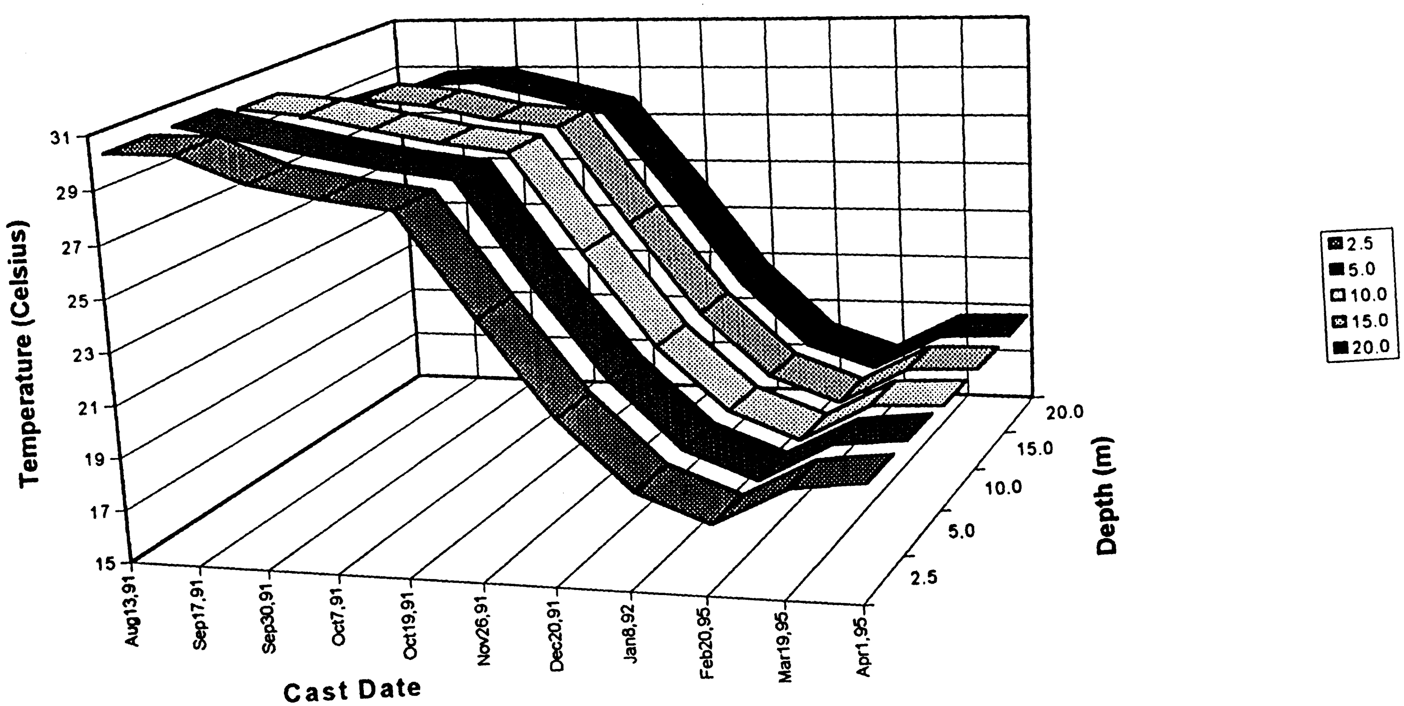

Figure 3-14

Temperature variations in Zuluf in 2.5, 5.0, 10.0, 15.0, and 20.0 metres of water.

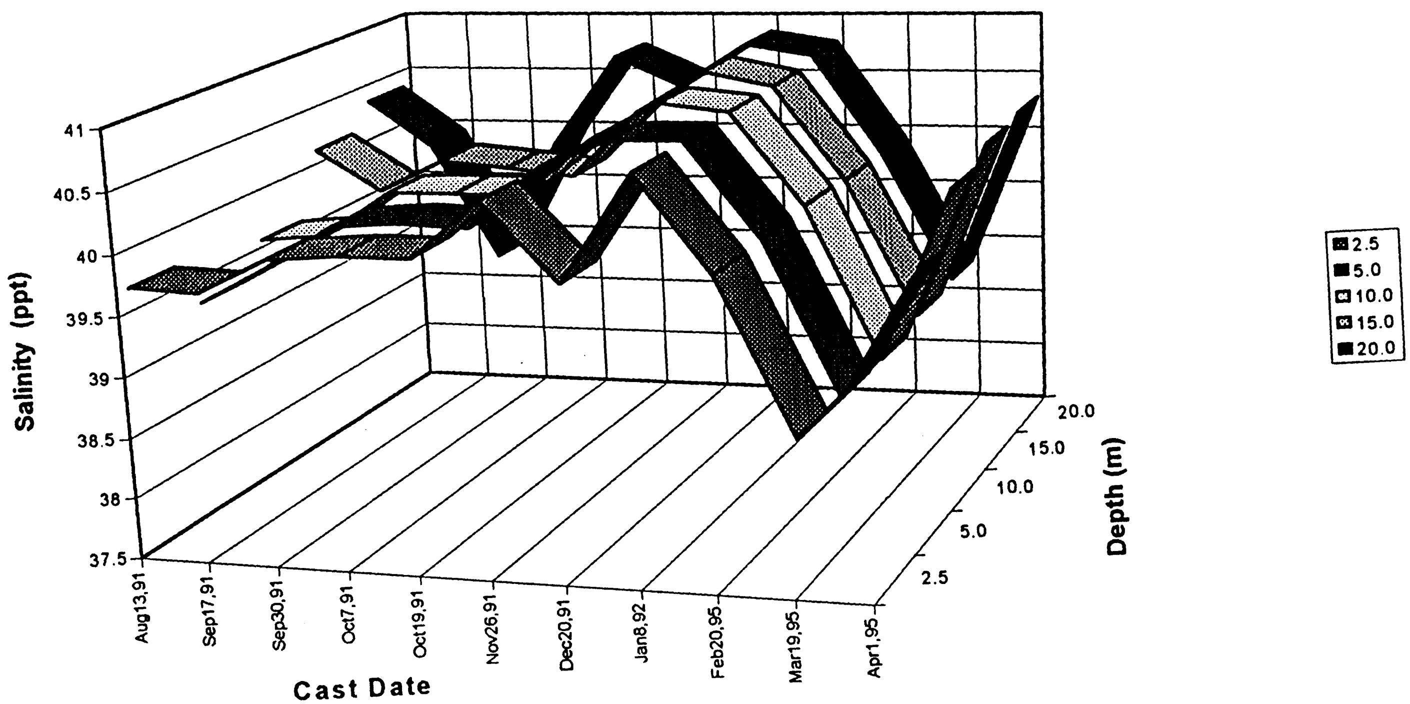

Figure 3-15

Salinity variations in Zuluf in 2.5, 5.0, 10.0, 15.0, and 20.0 metres of water.

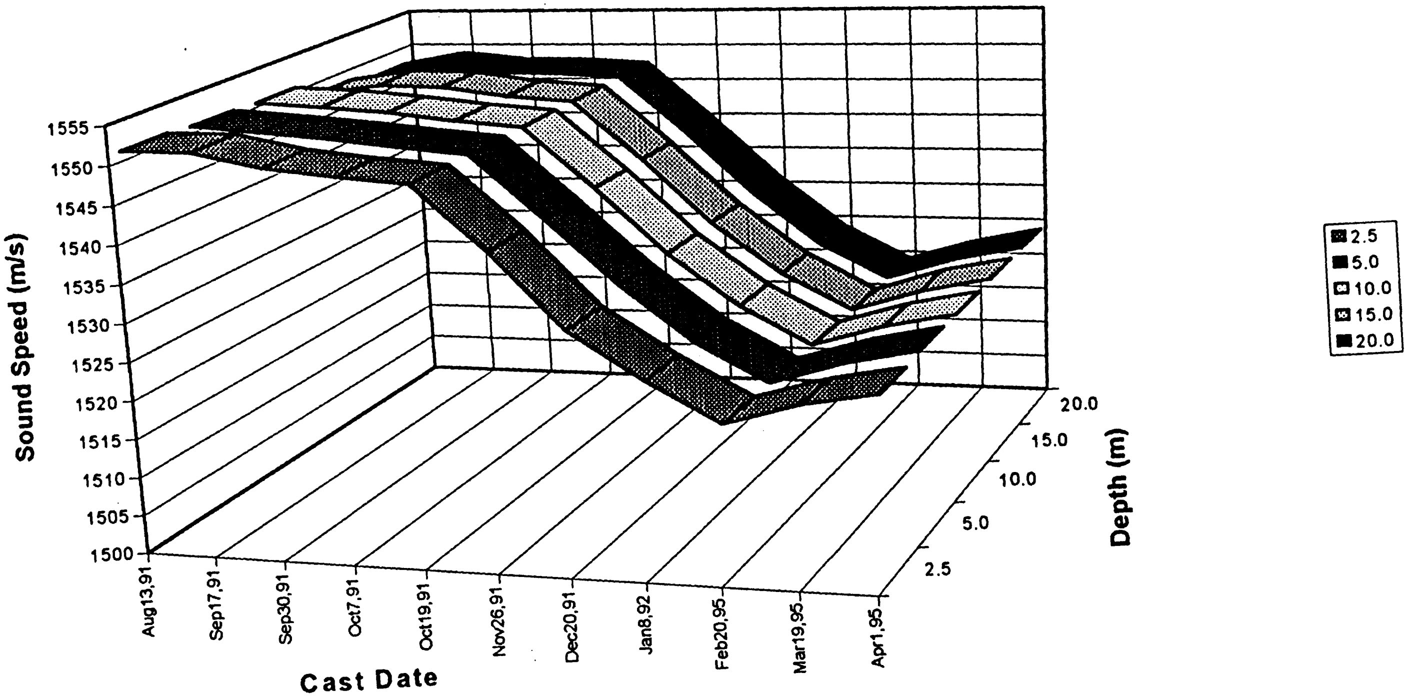

Figure 3-16

Sound speed variations in Zuluf in 2.5, 5.0, 10.0, 15.0, and 20.0 metres of water.

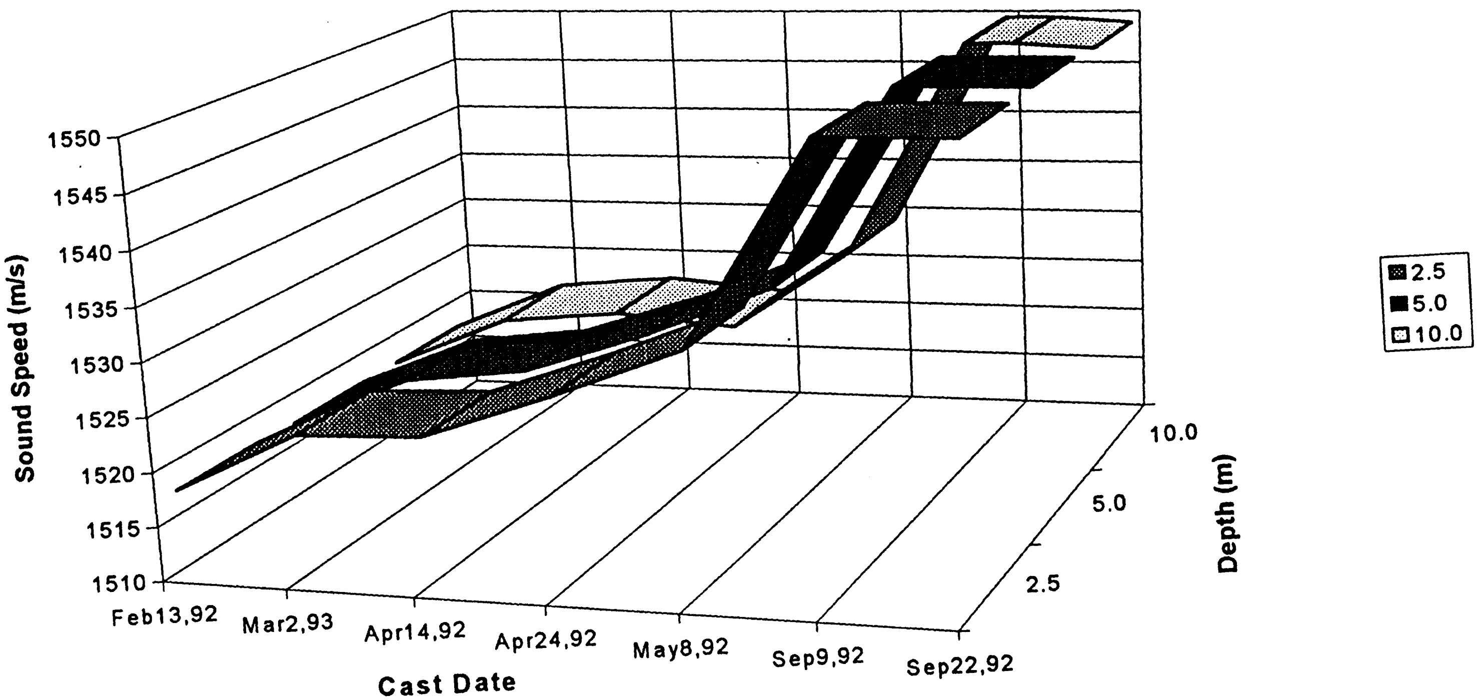

Figure 3-17

Sound speed variations in Marjan in 2.5, 5.0, 10.0, and 15.0 metres of water.

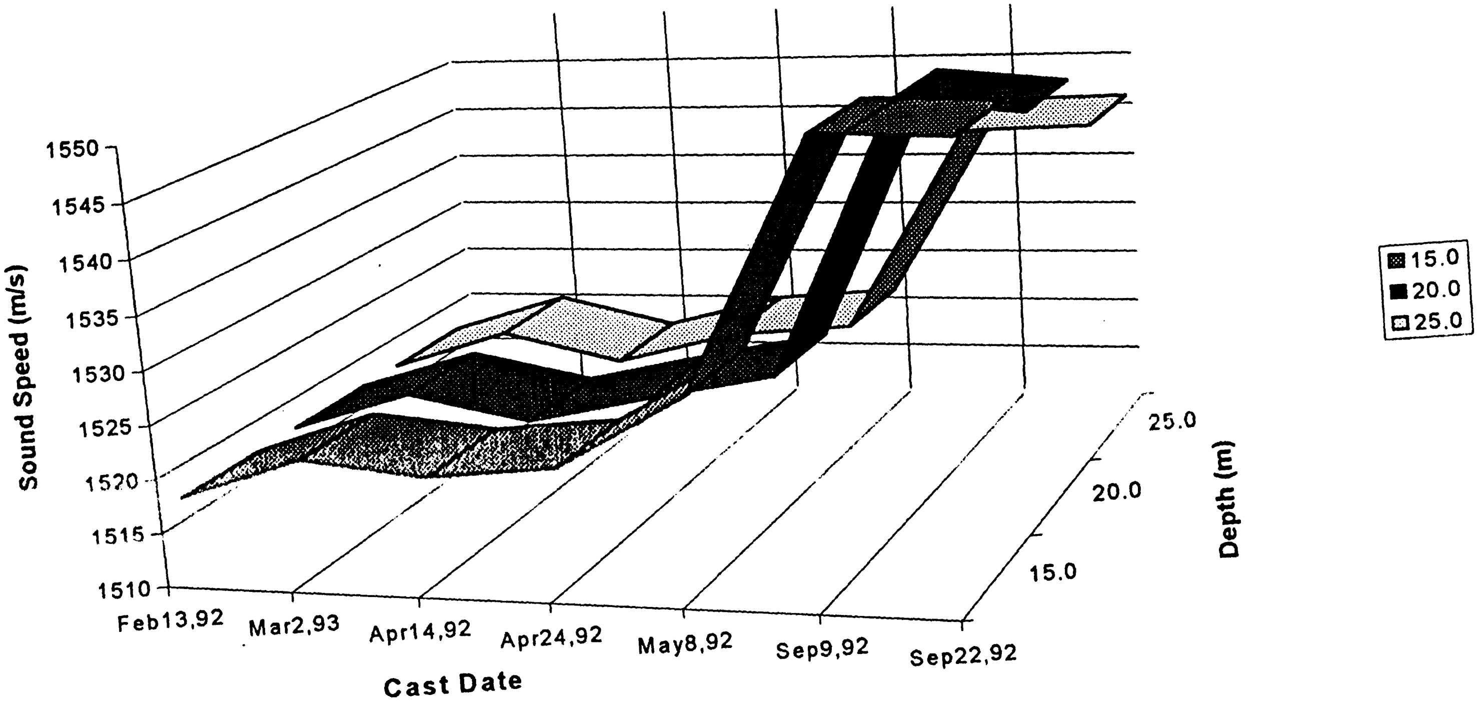

Figure 3-18

Sound speed variations in Marjan in 15.0, 20.0, and 25.0 metres of water.

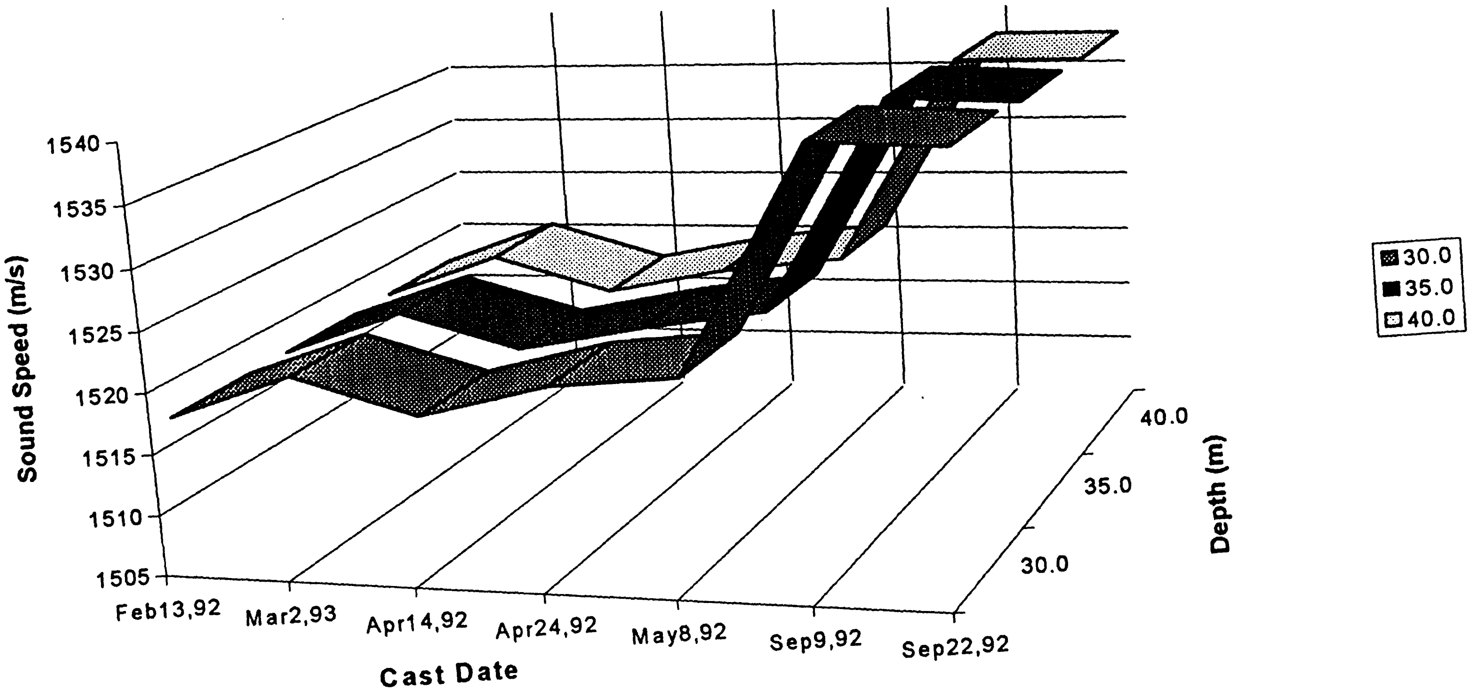

Figure 3-19

Sound speed variations in Marjan in 30.0, 35.0, and 40.0 metres of water.

Appendix V

Figures for Chapter 4

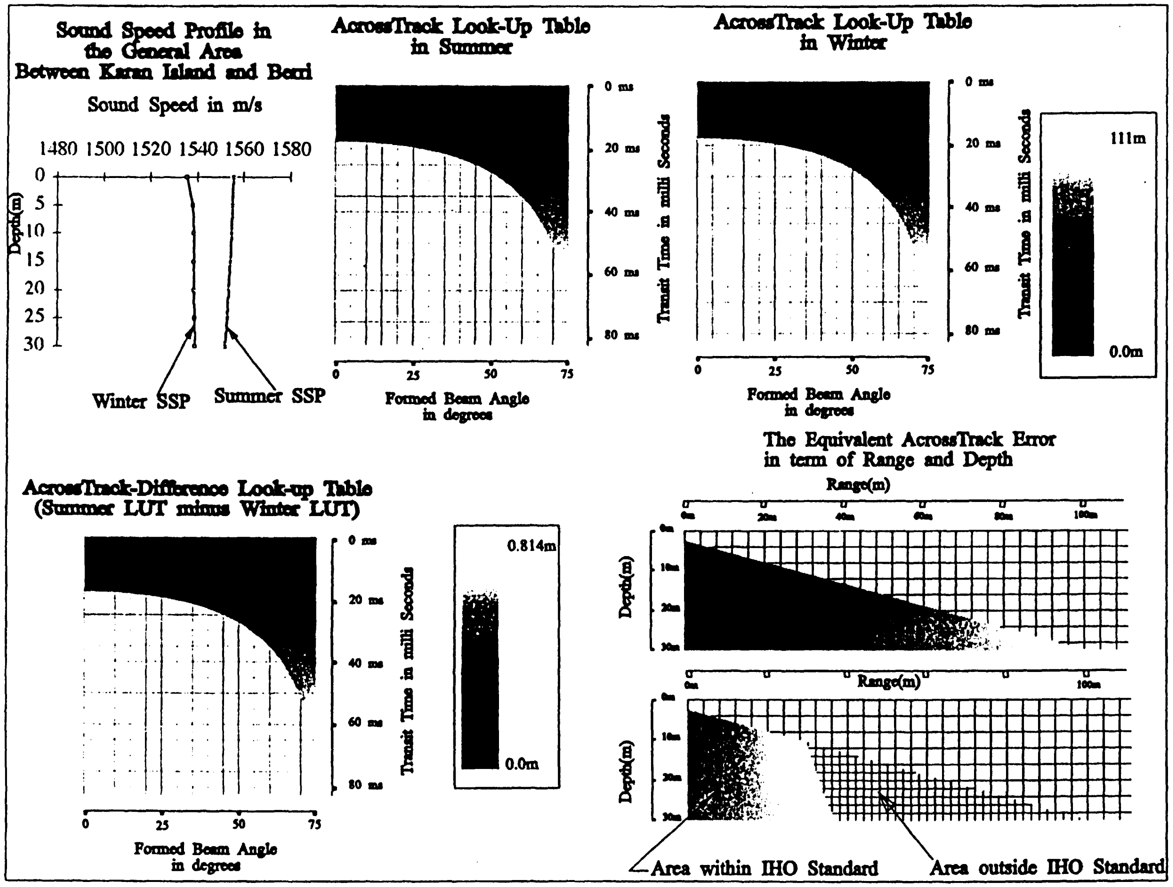

Figure 4-1a

The across-track effect of applying one SSP in summer over another in winter, both SSPs of the general area between Karan Island and Berri for 2.5 m draft case.

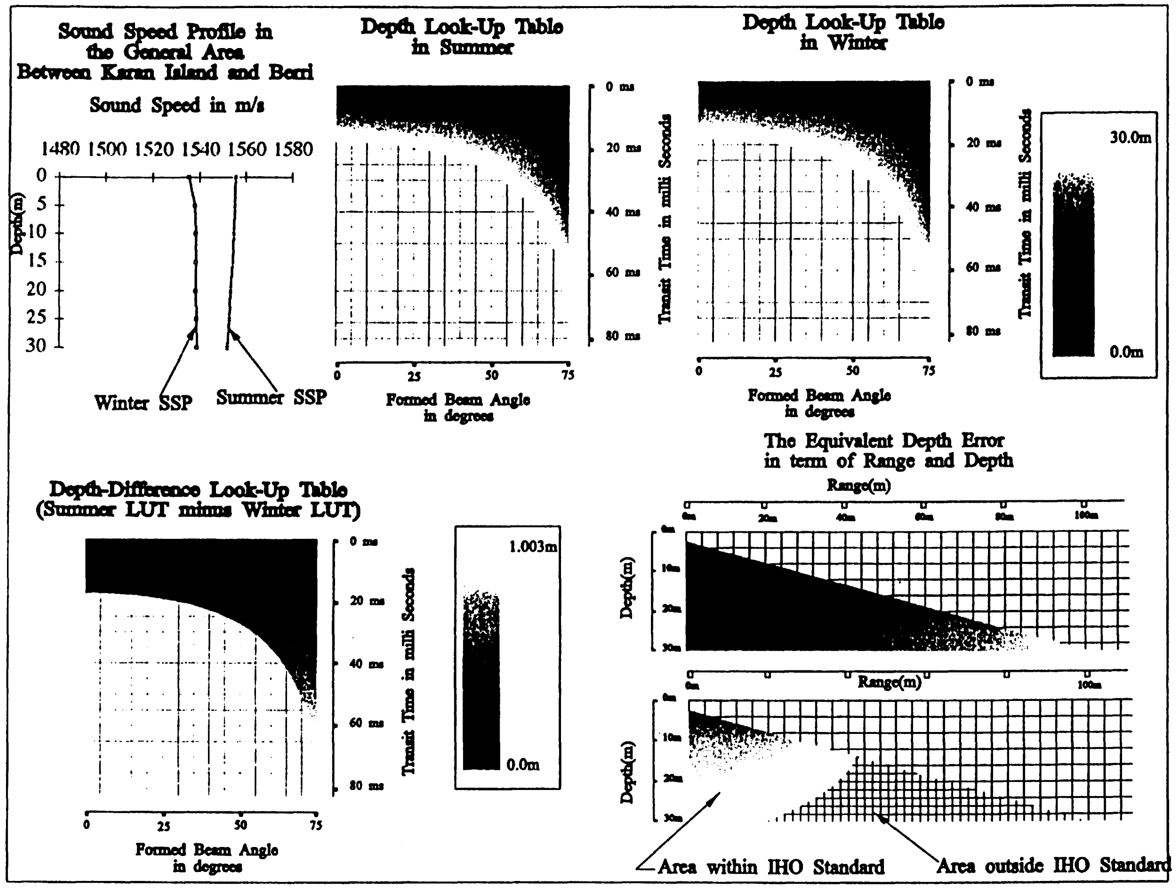

Figure 4-1b

The depth effect of applying one SSP in summer over another in winter, both SSPs of the general area between Karan Island and Berri for 2.5 m draft case.

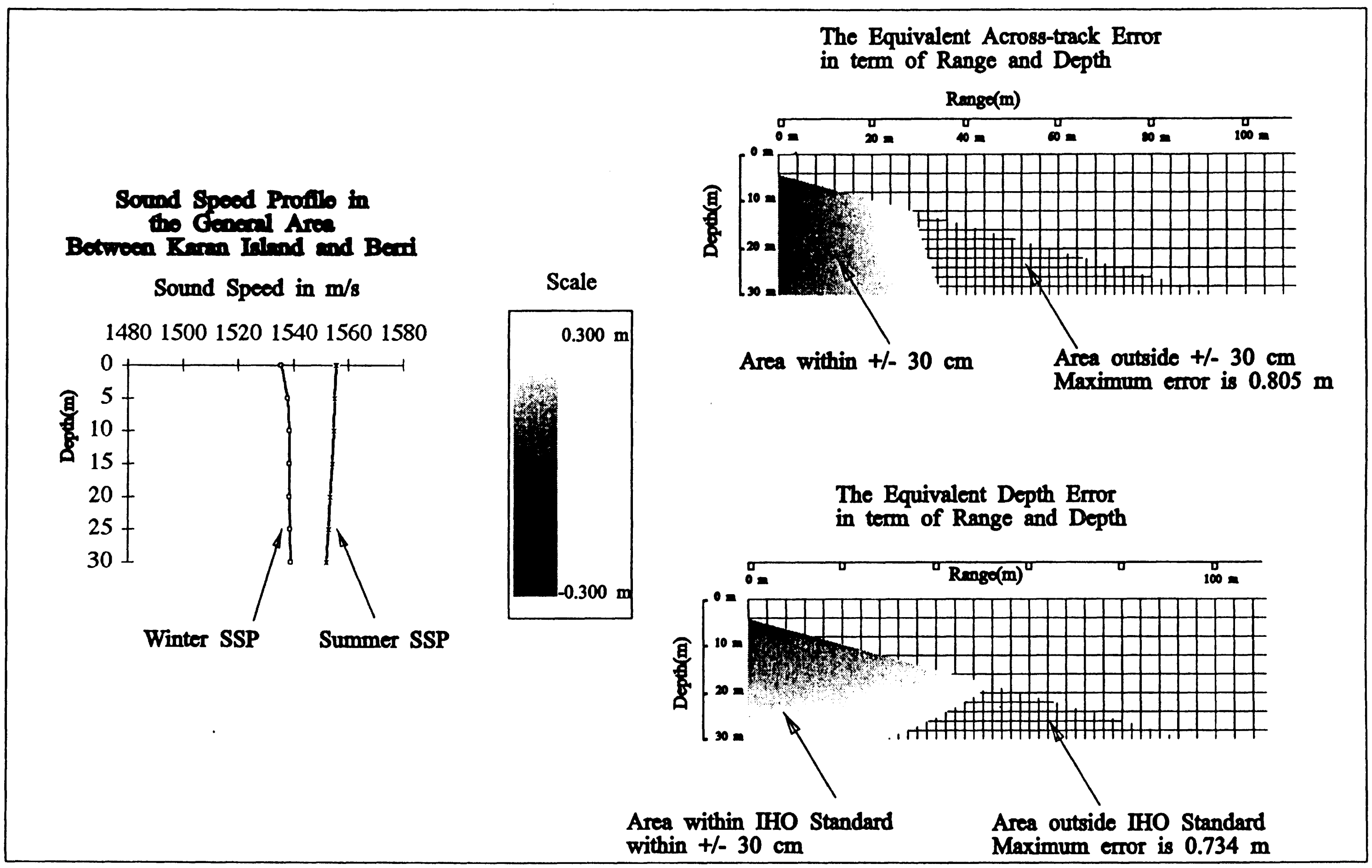

Figure 4-2
The effect of using one SSP in summer over another SSP in winter, both SSPs of the general area between Karan Island and Berri for 4.3 m draft case.

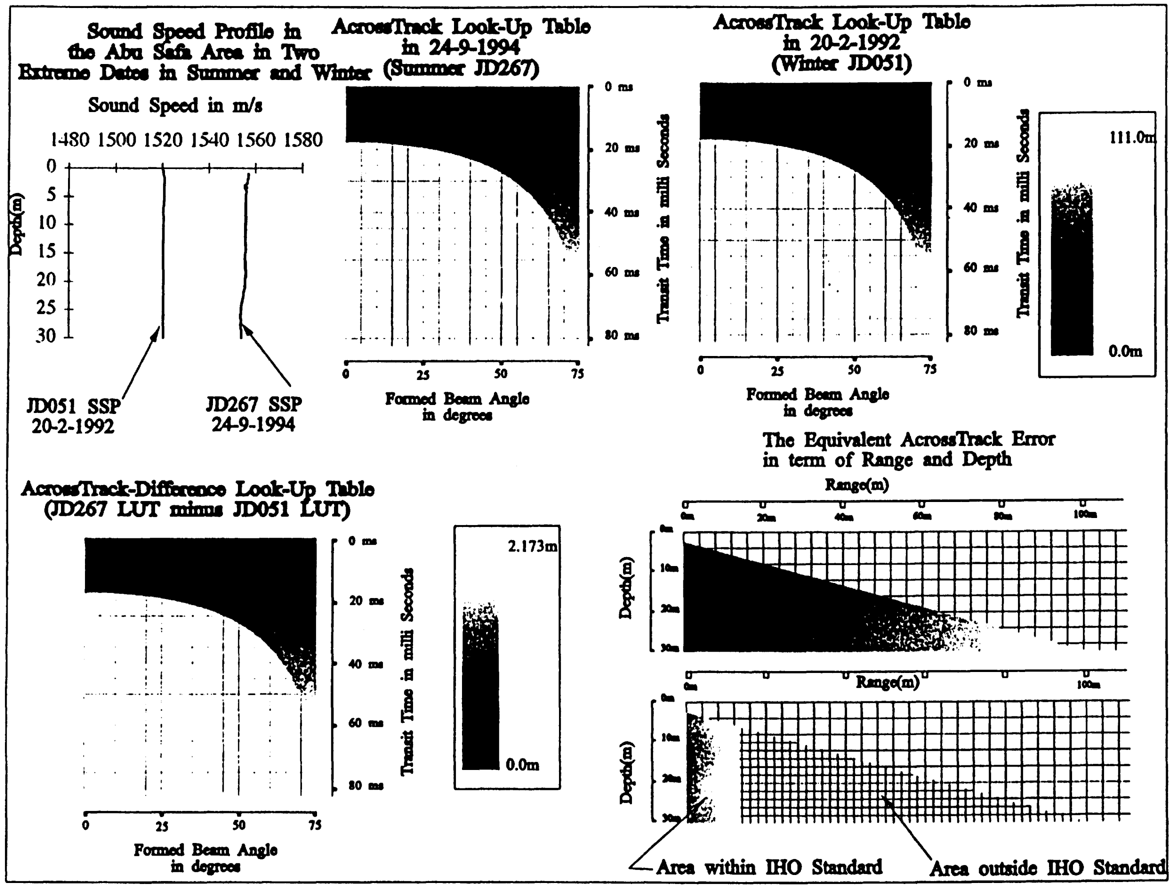

Figure 4-3a

The across-track effect of applying one SSP in summer over another in winter, both SSPs of Abu Safa for 2.5 m draft case.

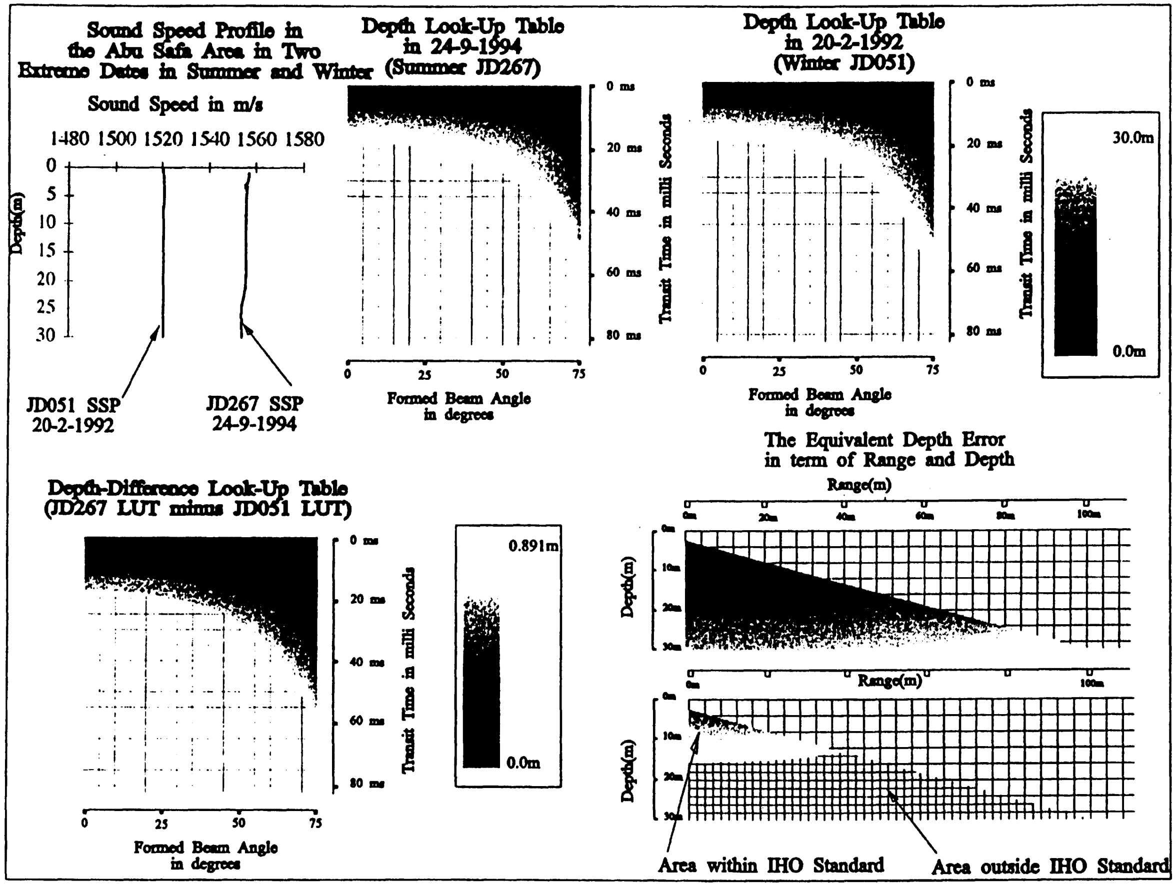

Figure 4-3b

The depth effect of applying one SSP in summer over another in winter, both SSPs of Abu Safa for 2.5 m draft case.

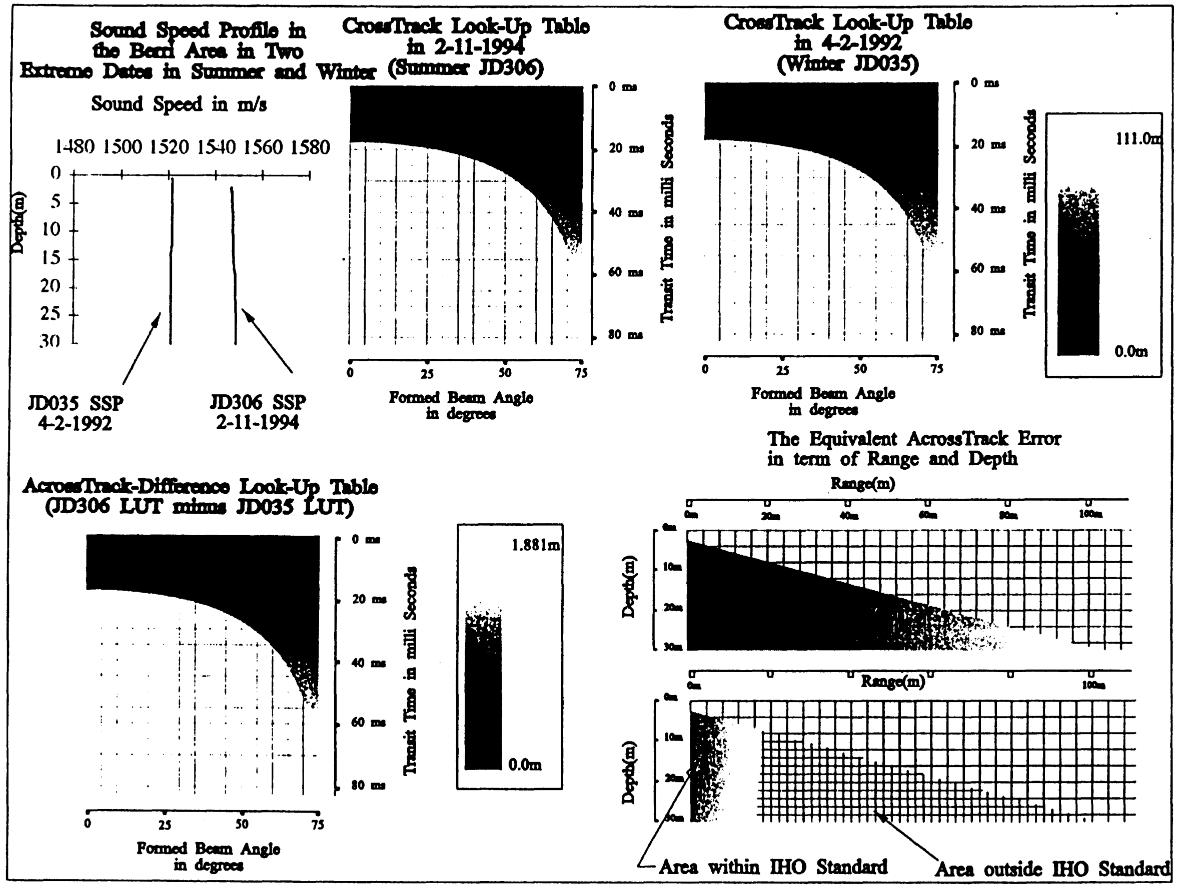

Figure 4-4a

The across-track effect of applying one SSP in summer over another in winter, both SSPs of Berri for 2.5 m draft case.

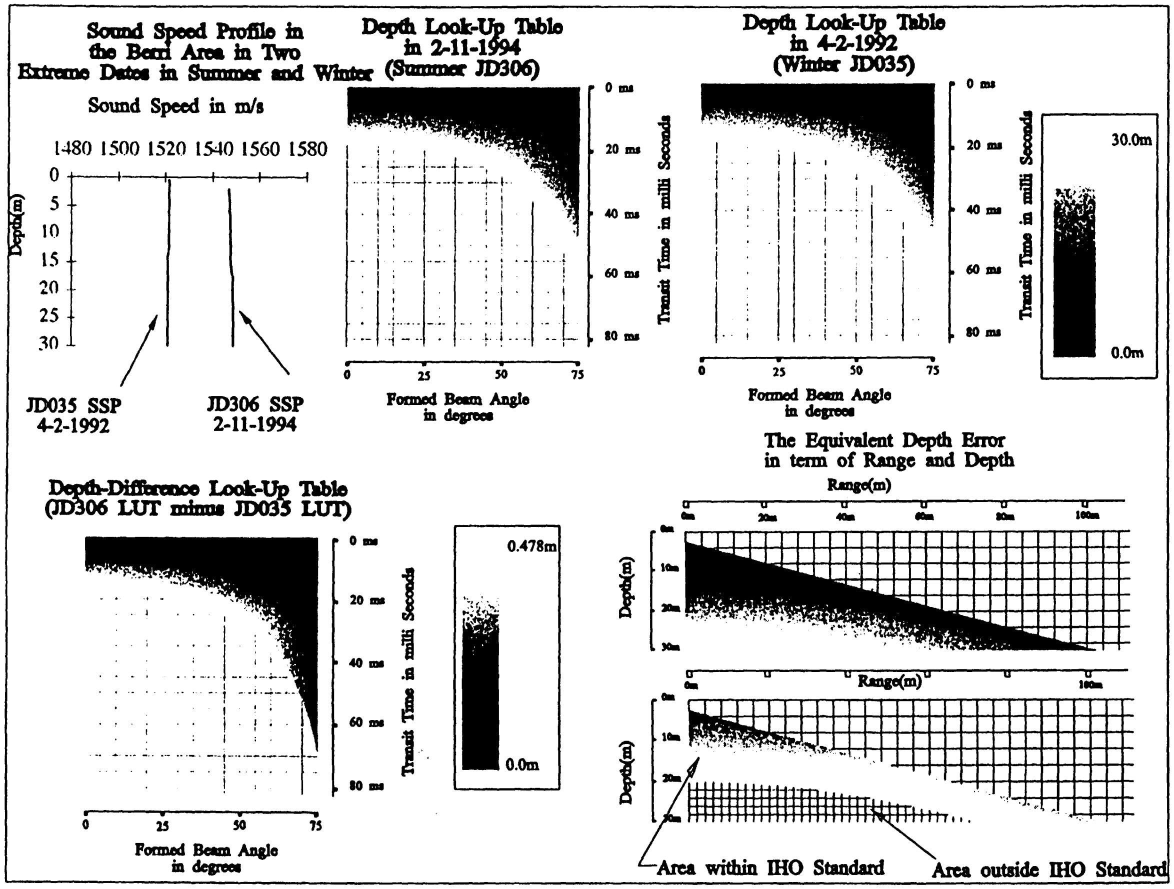

Figure 4-4b

The depth effect of applying one SSP in summer over another in winter, both SSPs of Berri for 2.5 m draft case.

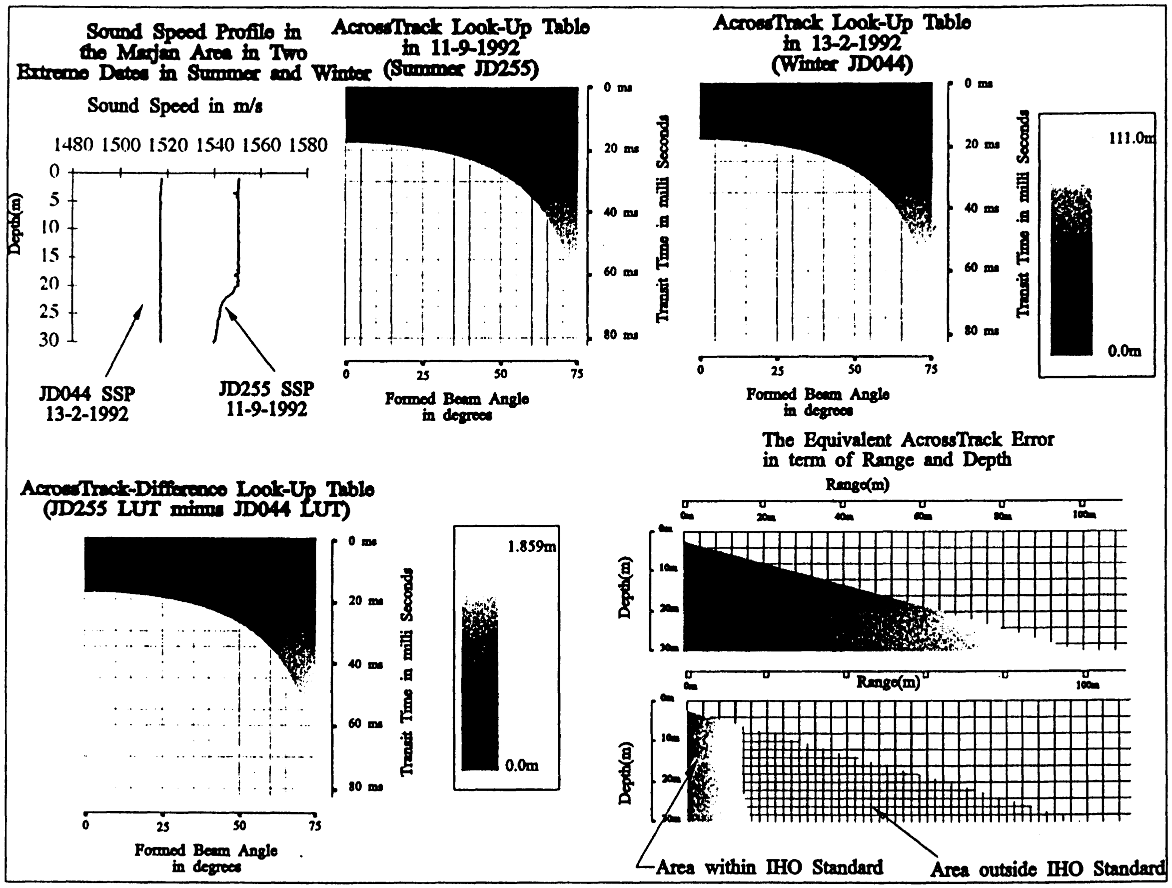

Figure 4-5a

The across-track effect of applying one SSP in summer over another in winter, both SSPs of Marjan for 2.5 m draft case.

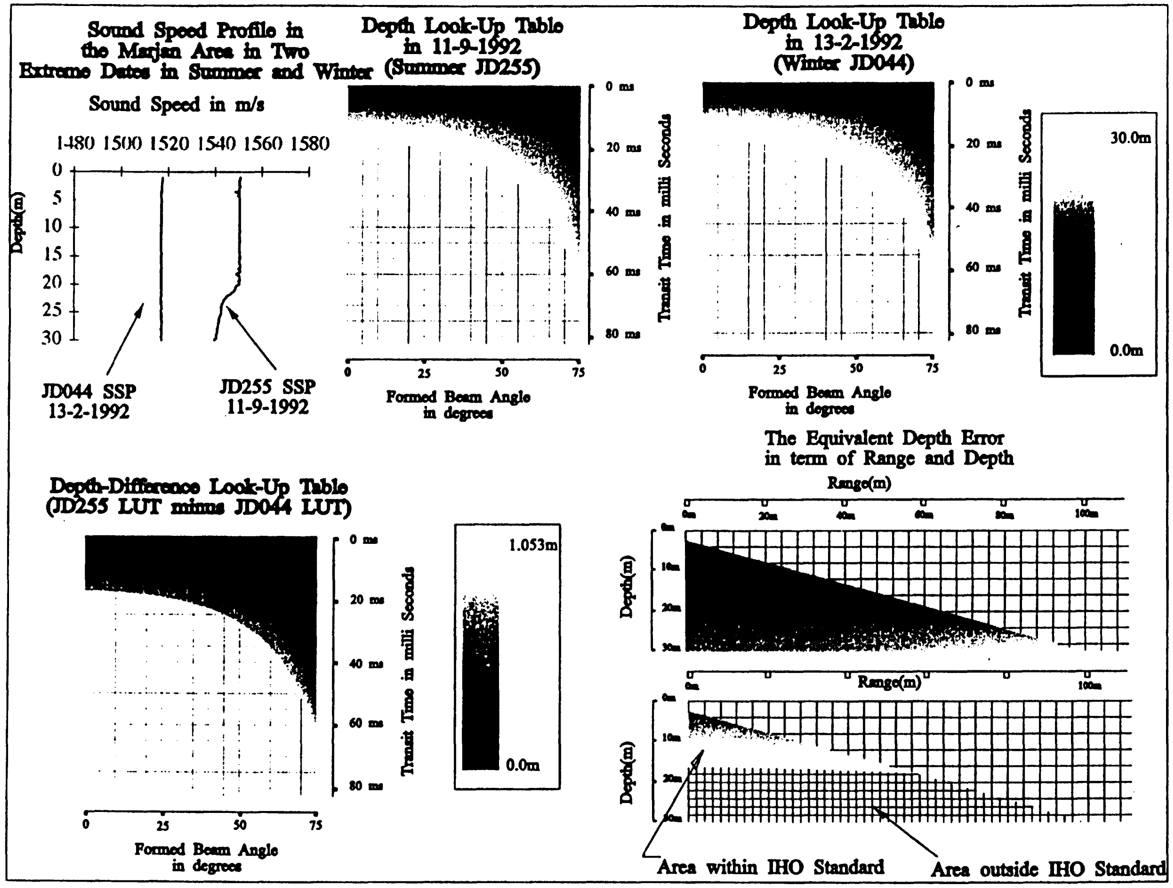

Figure 4-5b

The depth effect of applying one SSP in summer over another in winter, both SSPs of Marjan for 2.5 m draft case.

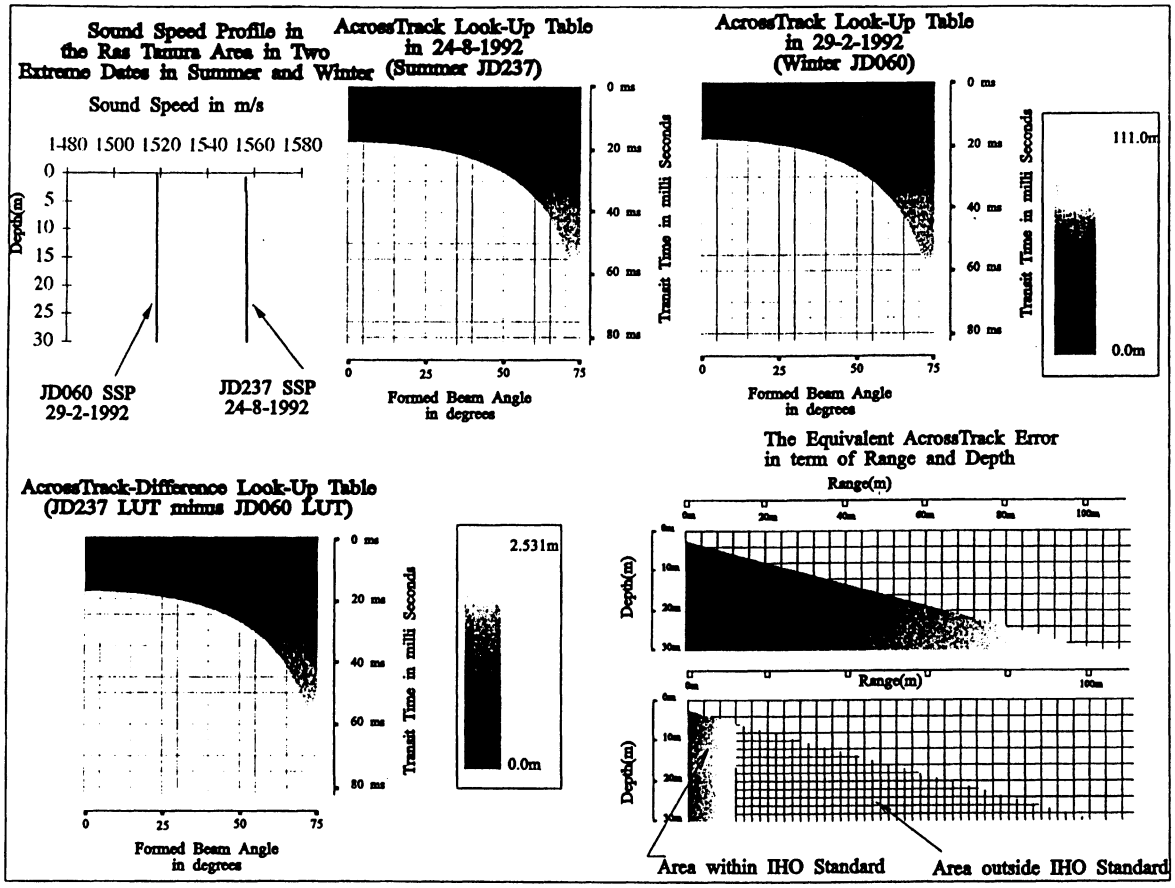

Figure 4-6a

The across-track effect of applying one SSP in summer over another in winter, both SSPs of Ras Tanura for 2.5 m draft case.

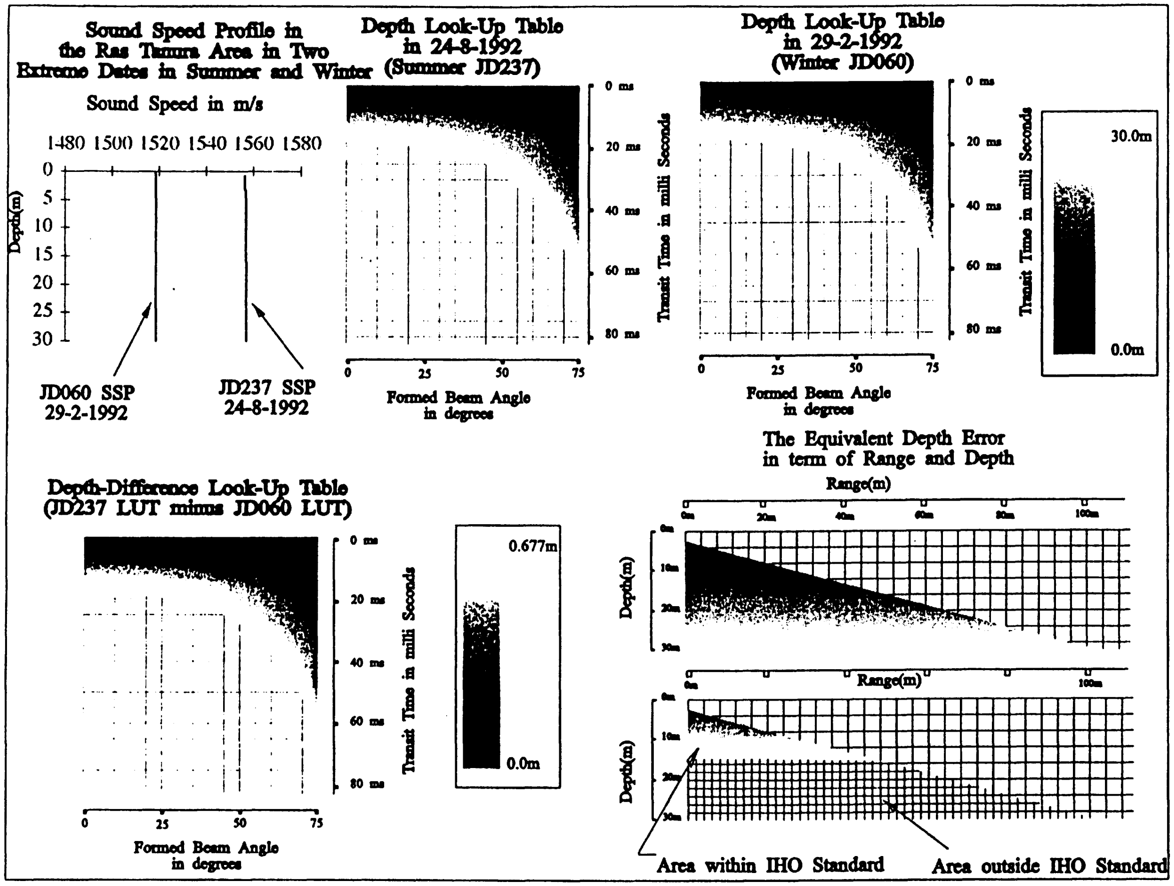

Figure 4-6b

The depth effect of applying one SSP in summer over another in winter, both SSPs of Ras Tanura for 2.5 m draft case.

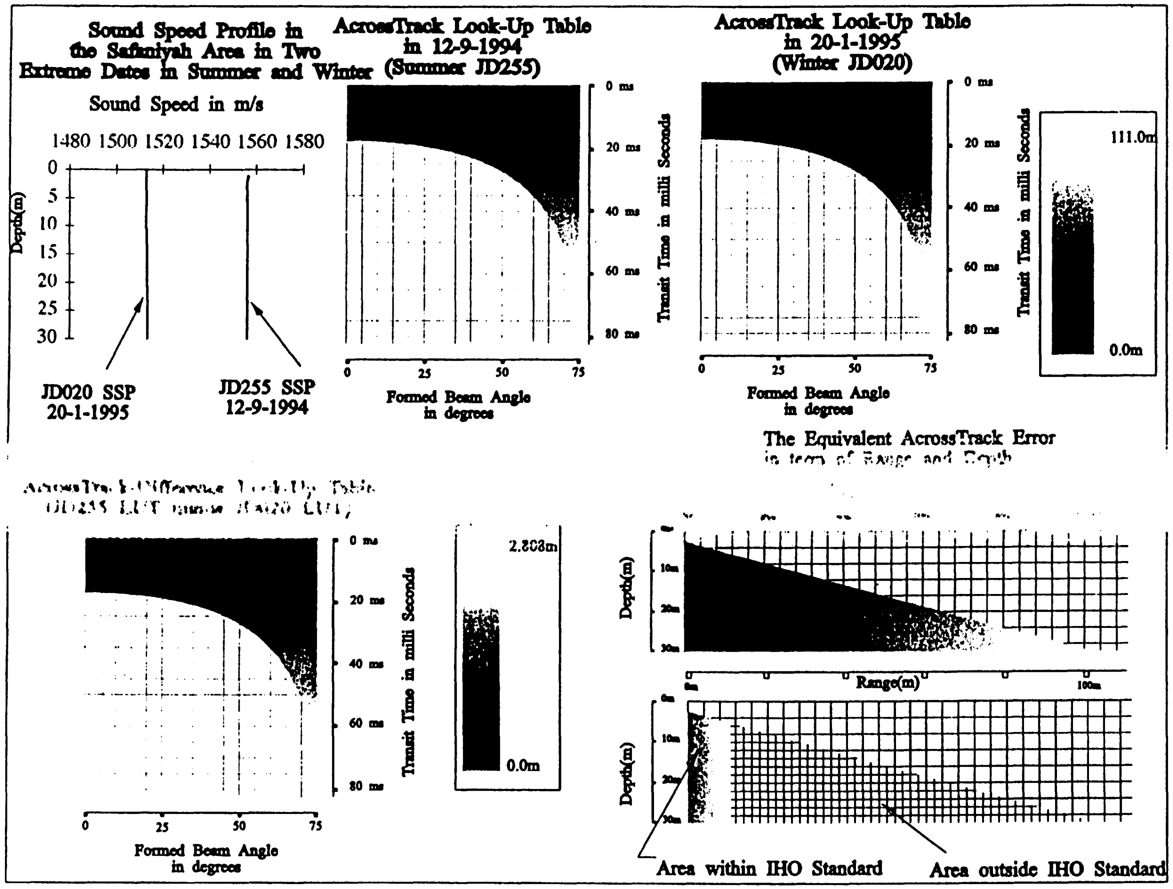

Figure 4-7a

The across-track effect of applying one SSP in summer over another in winter, both SSPs of Safaniyah for 2.5 m draft case.

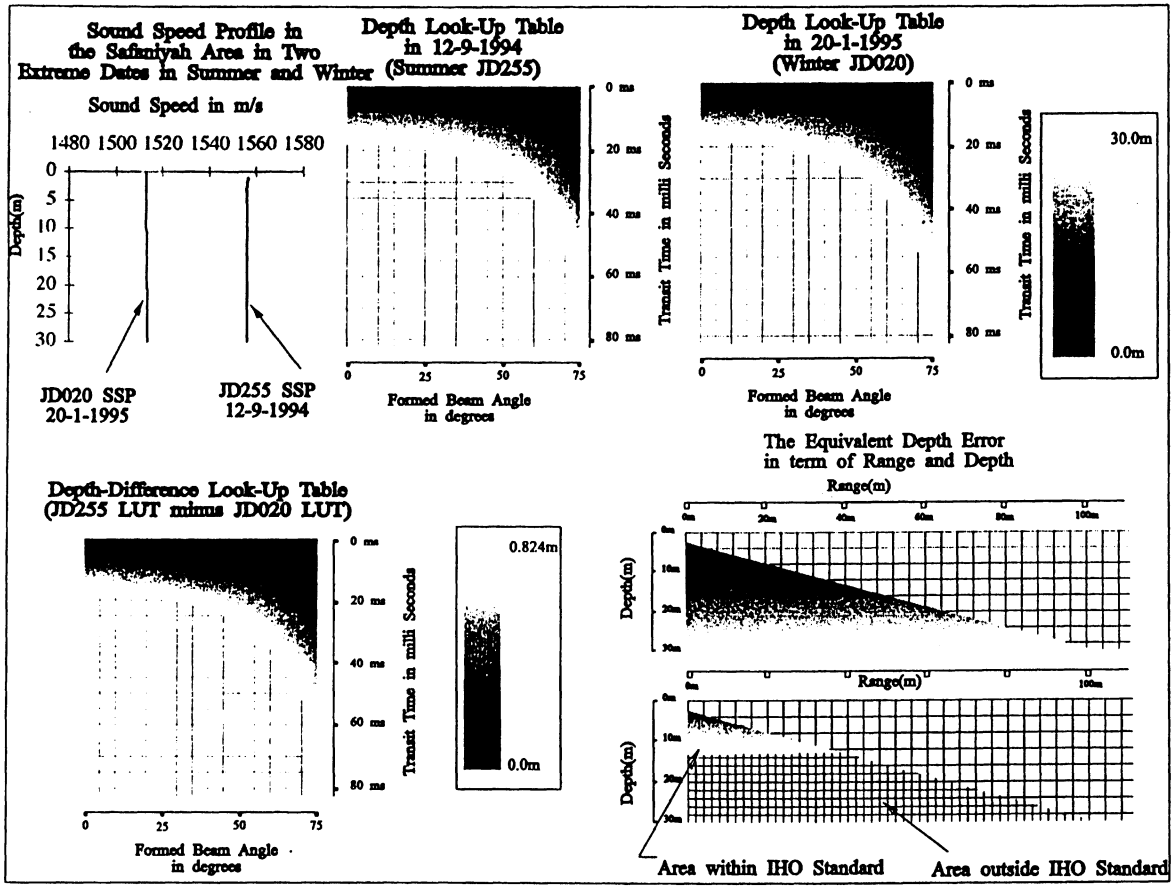

Figure 4-7b

The depth effect of applying one SSP in summer over another in winter, both SSPs of Safaniyah for 2.5 m draft case.

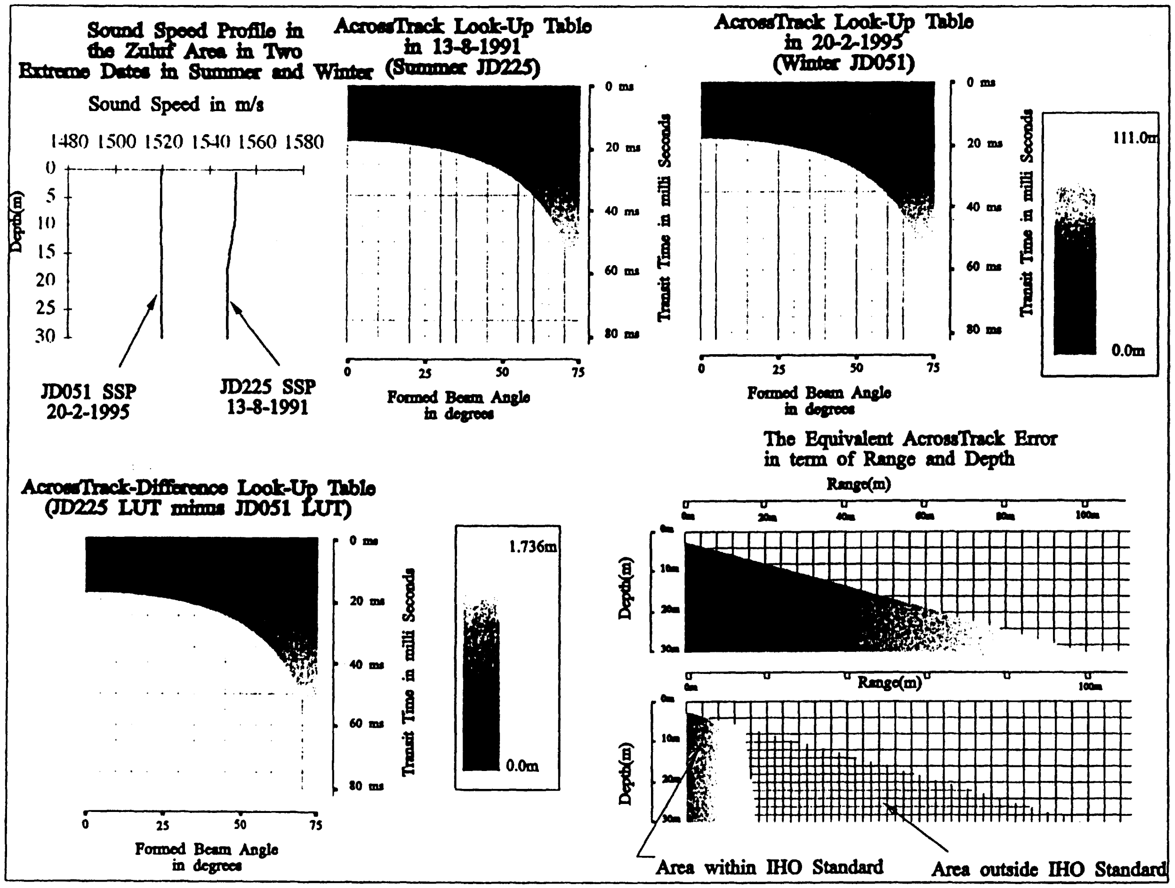

Figure 4-8a

The across-track effect of applying one SSP in summer over another in winter, both SSPs of Zuluf for 2.5 m draft case.

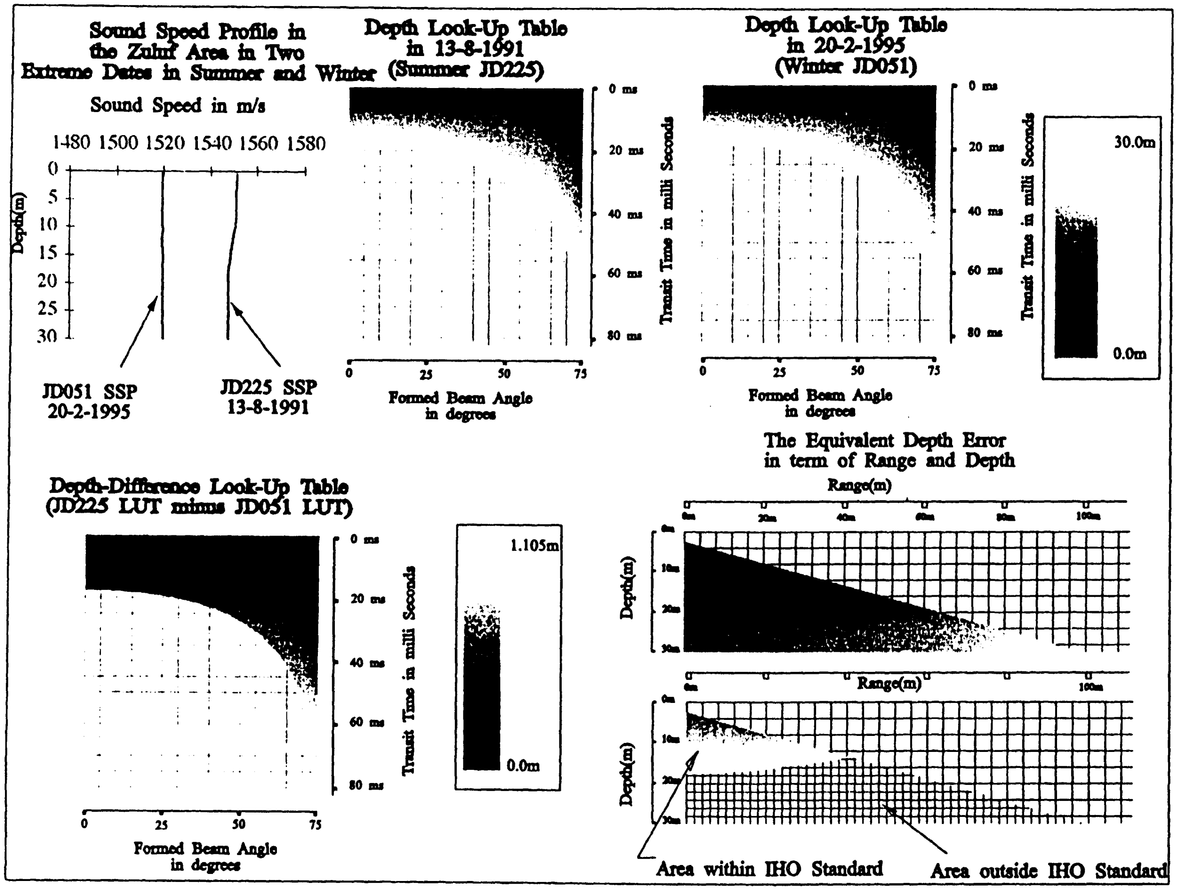

Figure 4-8b

The depth effect of applying one SSP in summer over another in winter, both SSPs of Zuluf for 2.5 m draft case.

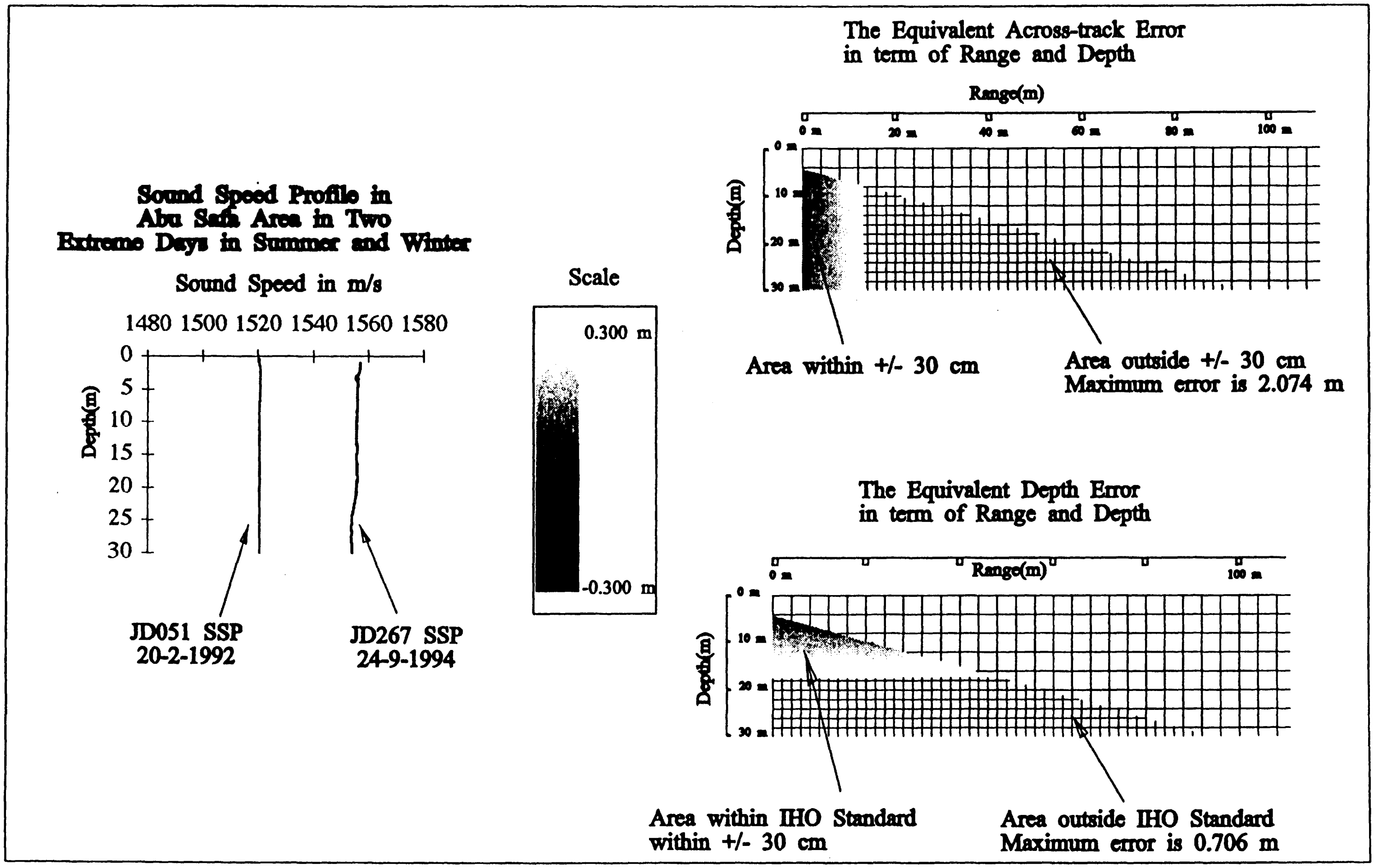

Figure 4-9
The effect of using one SSP in summer over another SSP in winter, both SSPs of Abu Safa for 4.3 m draft case.

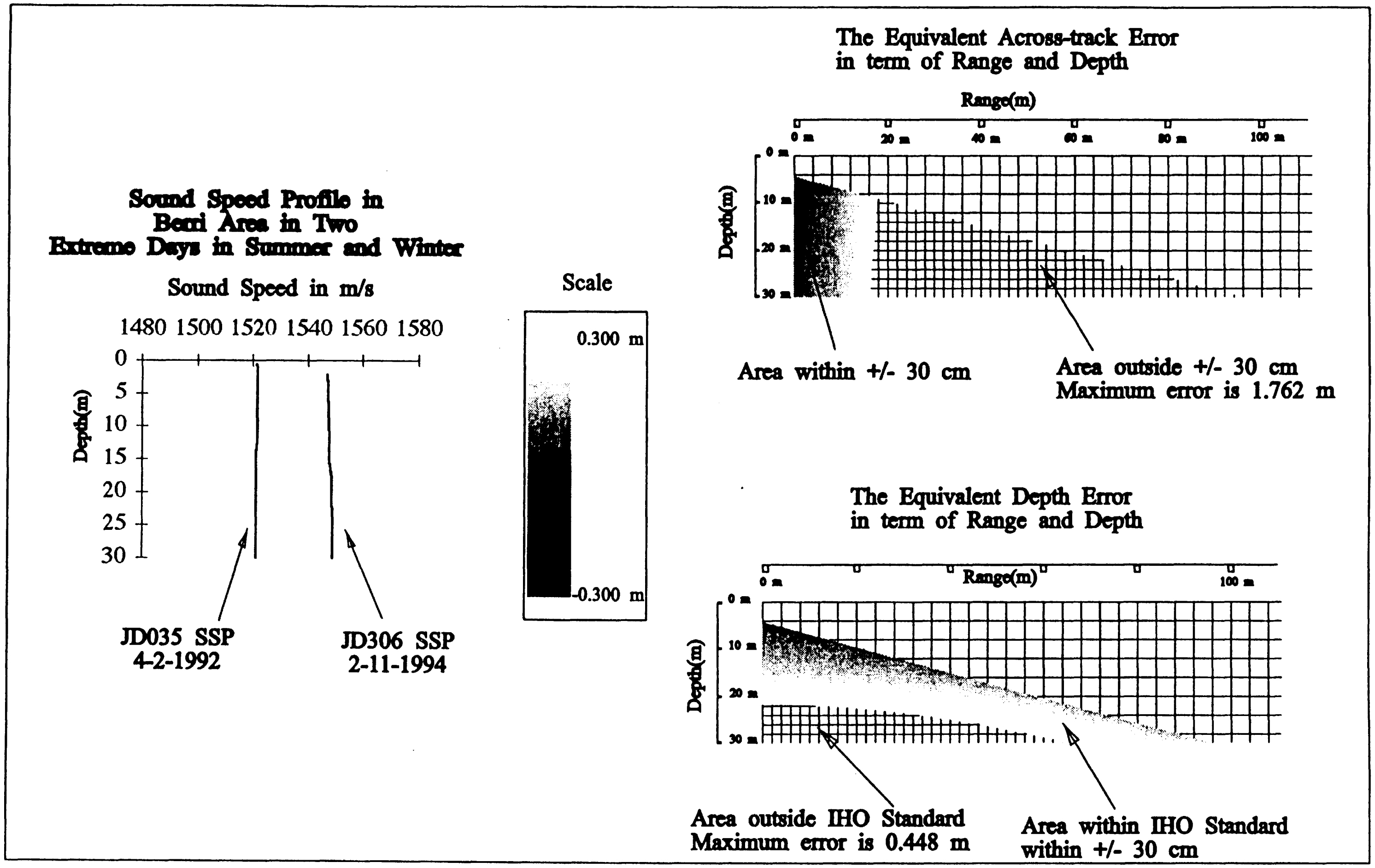

Figure 4-10
The effect of using one SSP in summer over another SSP in winter, both SSPs of Berri for 4.3 m draft case.

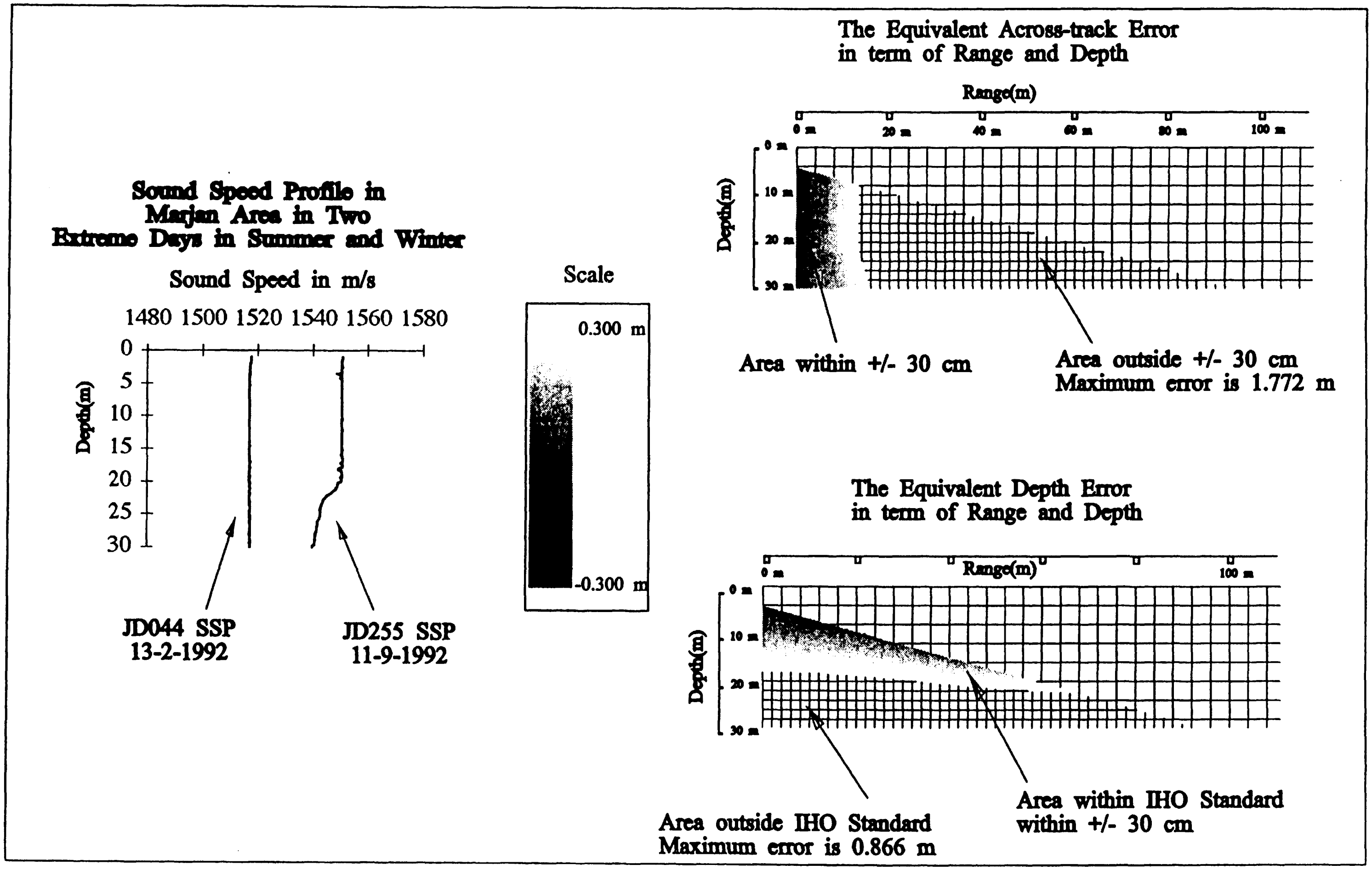

Figure 4-11
The effect of using one SSP in summer over another SSP in winter, both SSPs of Marjan for 4.3 m draft case.

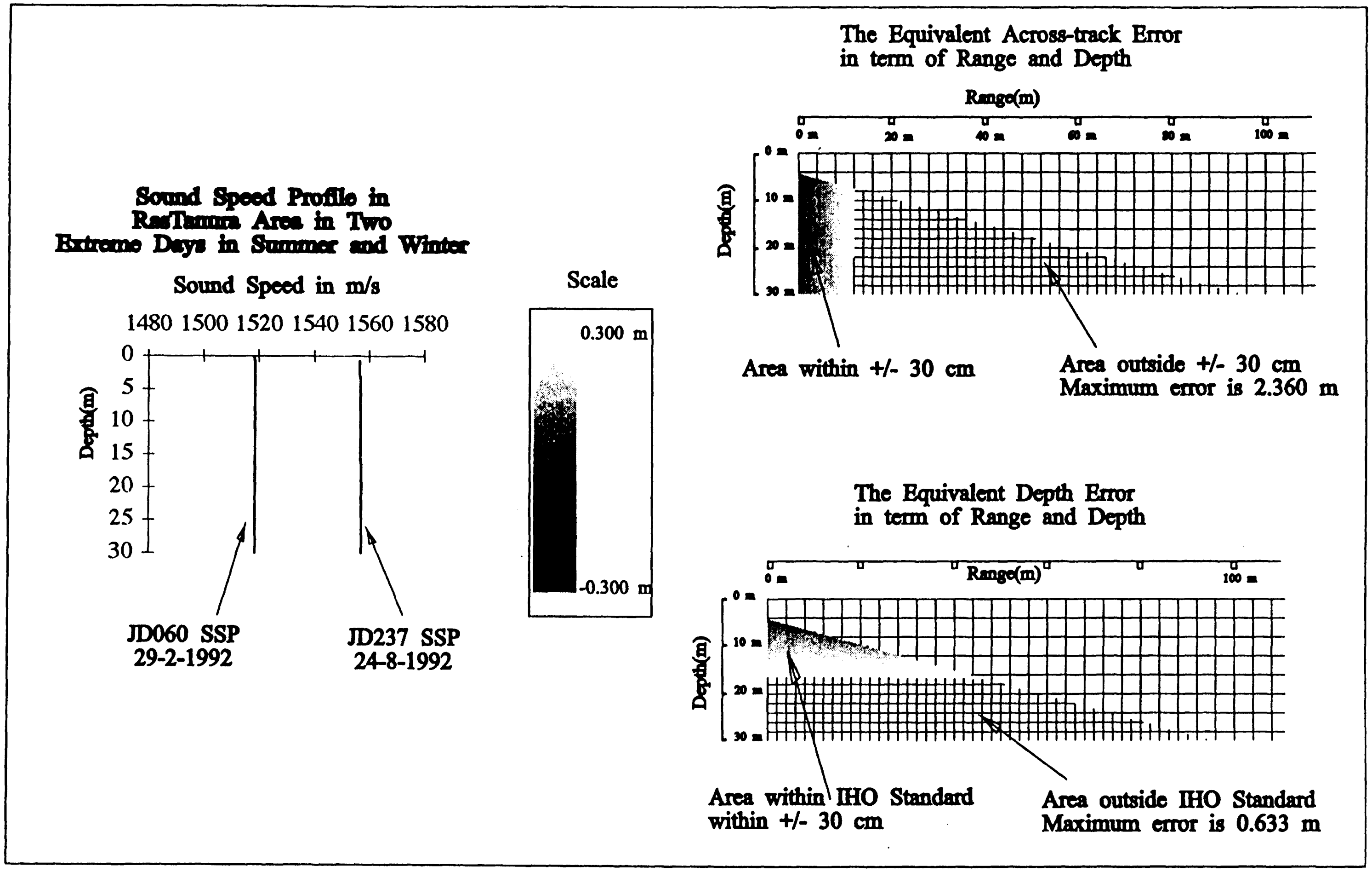

Figure 4-12
The effect of using one SSP in summer over another SSP in winter, both SSPs of Ras Tanura for 4.3 m draft case.

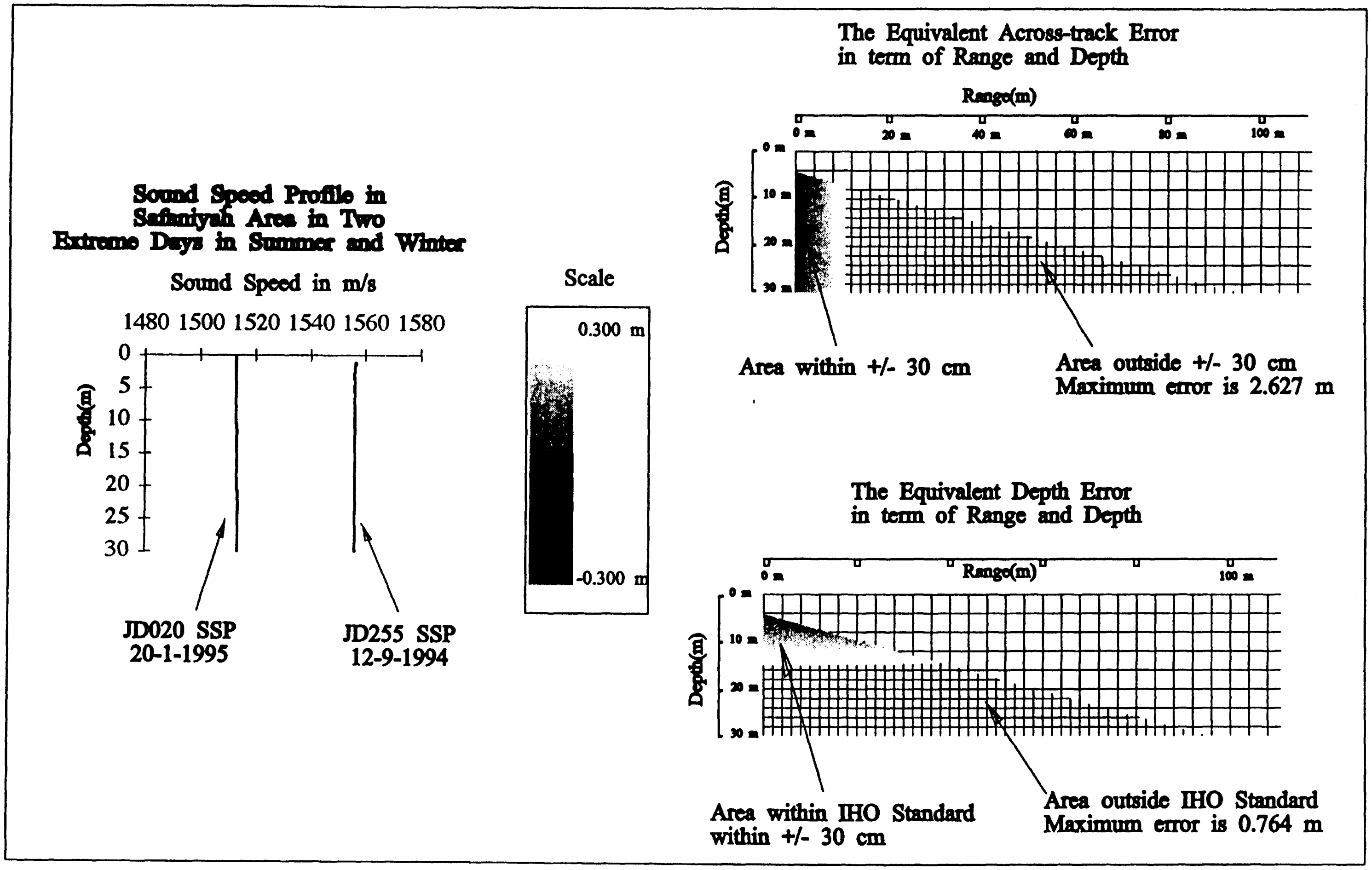

Figure 4-13
The effect of using one SSP in summer over another SSP in winter, both SSPs of Safaniyah for 4.3 m draft case.

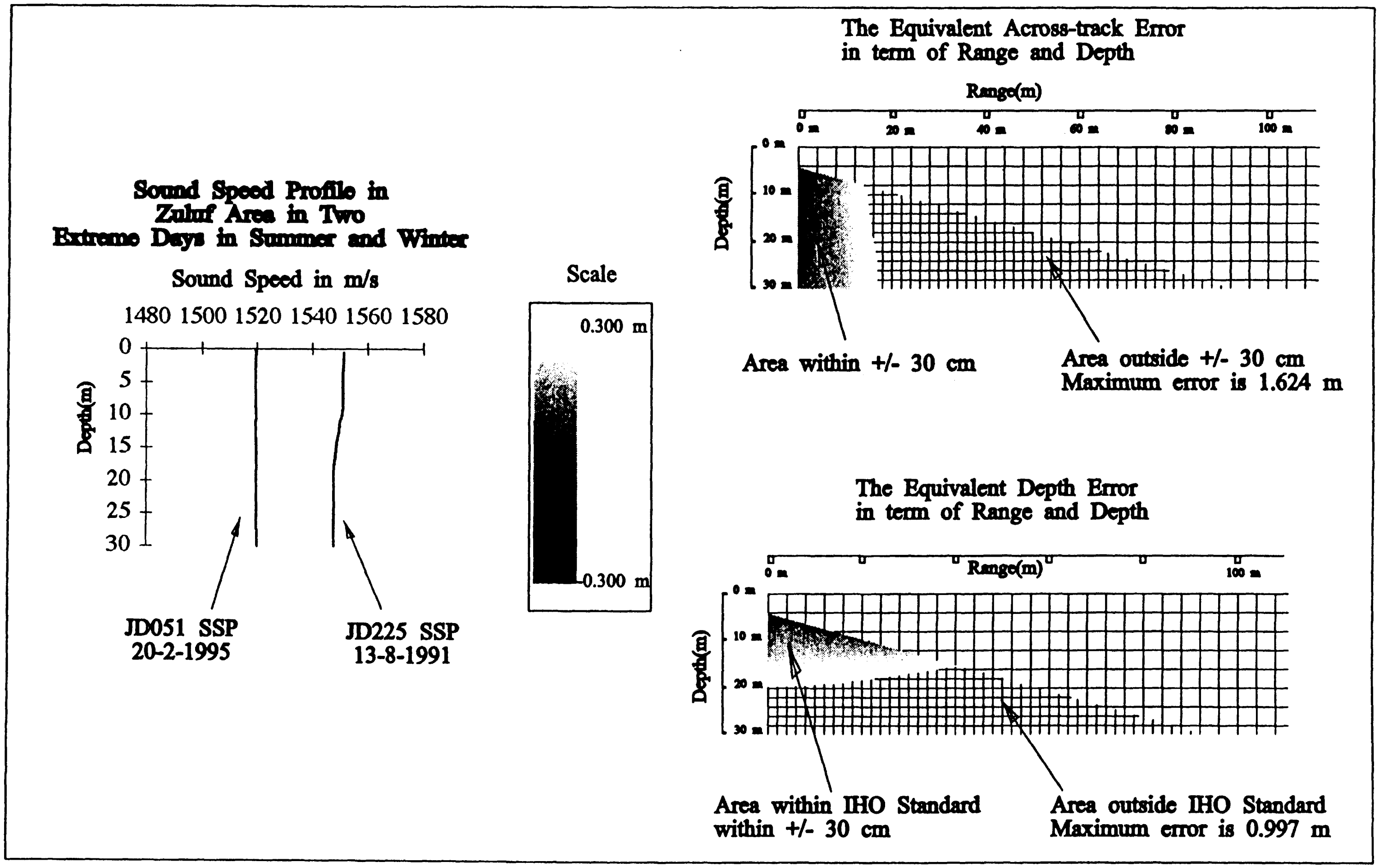

Figure 4-14
The effect of using one SSP in summer over another SSP in winter, both SSPs of Zuluf for 4.3 m draft case.

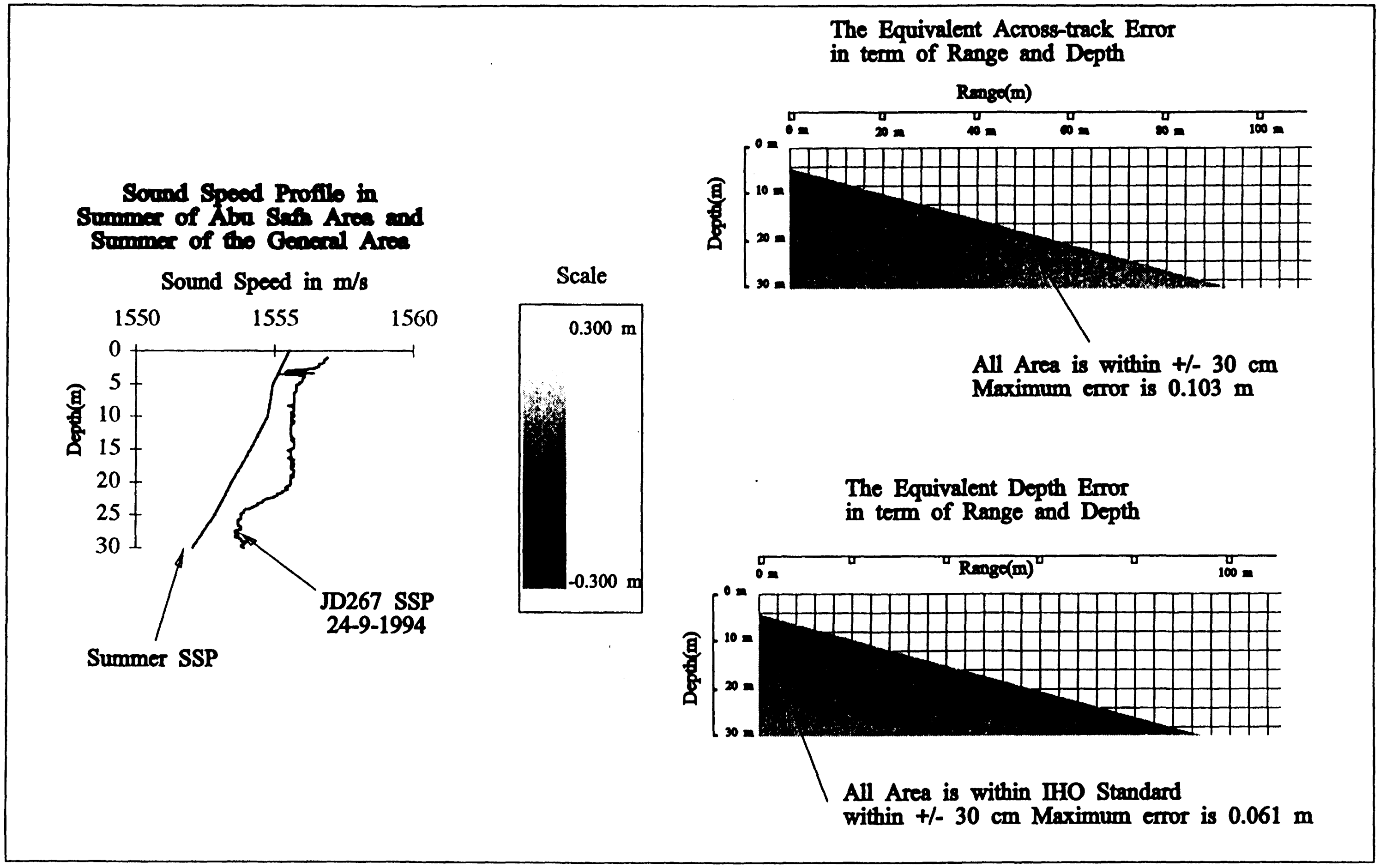

Figure 4-15
The effect of applying one SSP in summer of Abu Safa over SSP in summer of the general area for 4.3 m draft case.

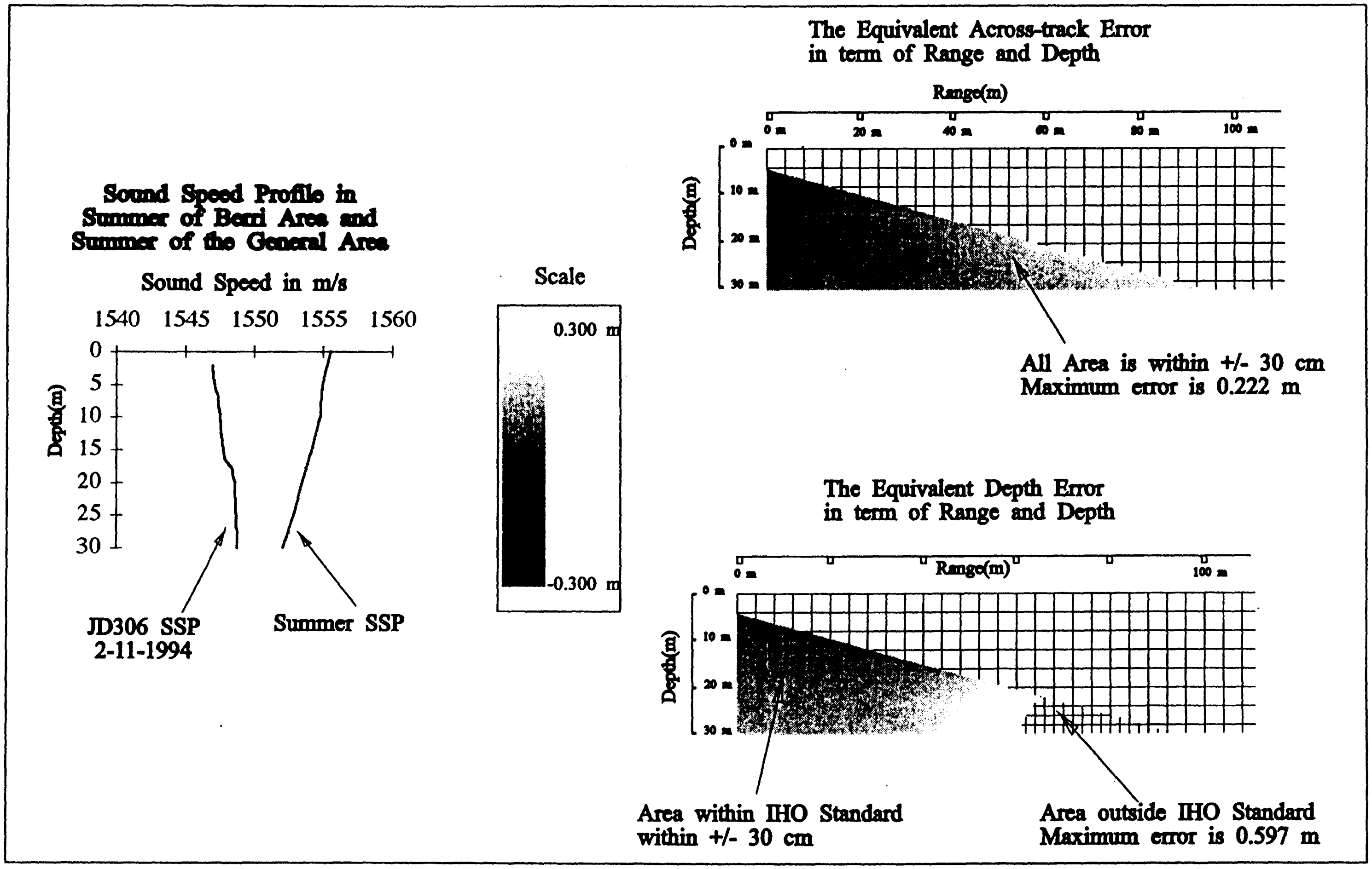

Figure 4-16
The effect of applying one SSP in summer of Berri over SSP in summer of the general area for 4.3 m draft case.

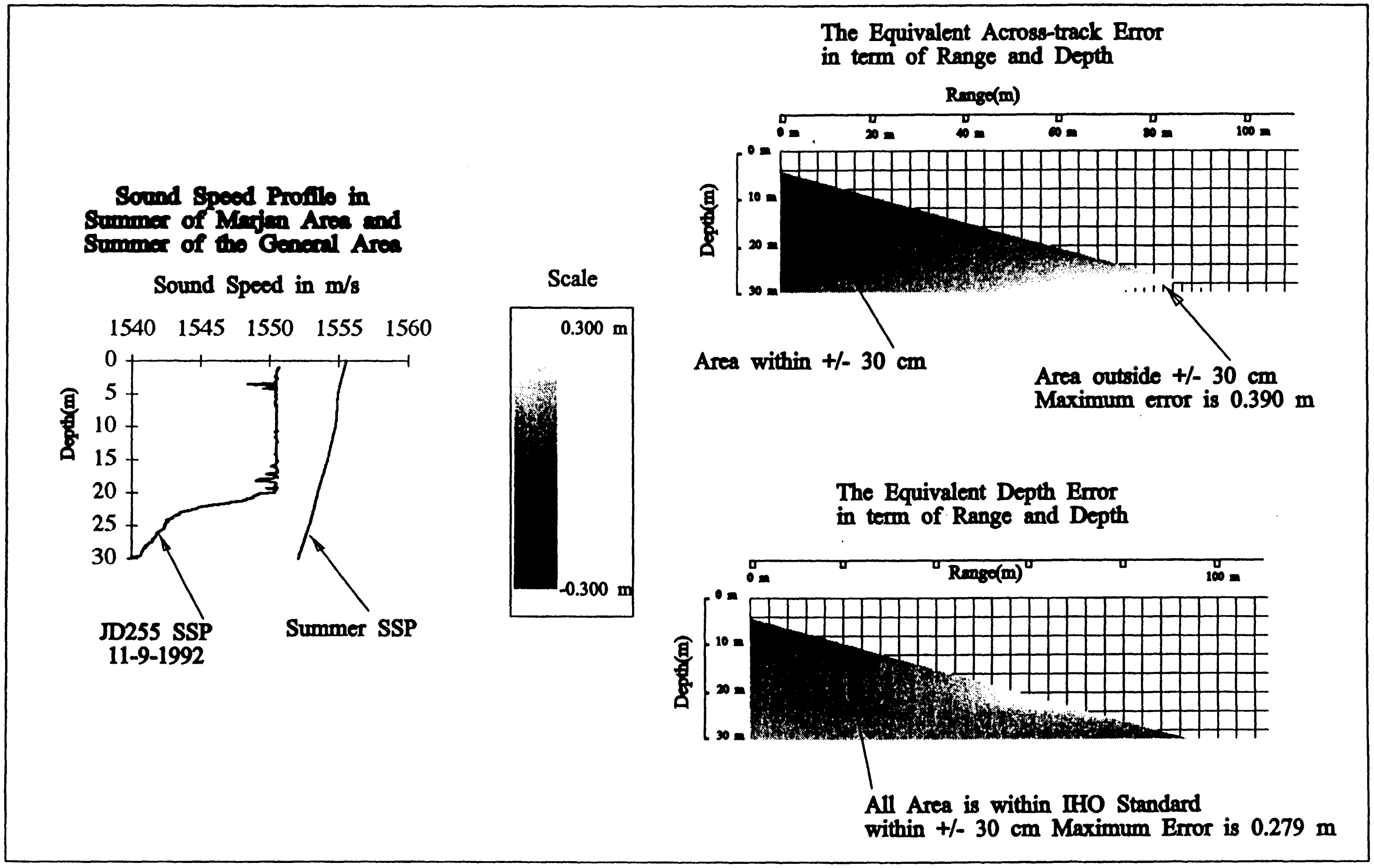

Figure 4-17
The effect of applying one SSP in summer of Marjan over SSP in summer of the general area for 4.3 m draft case.

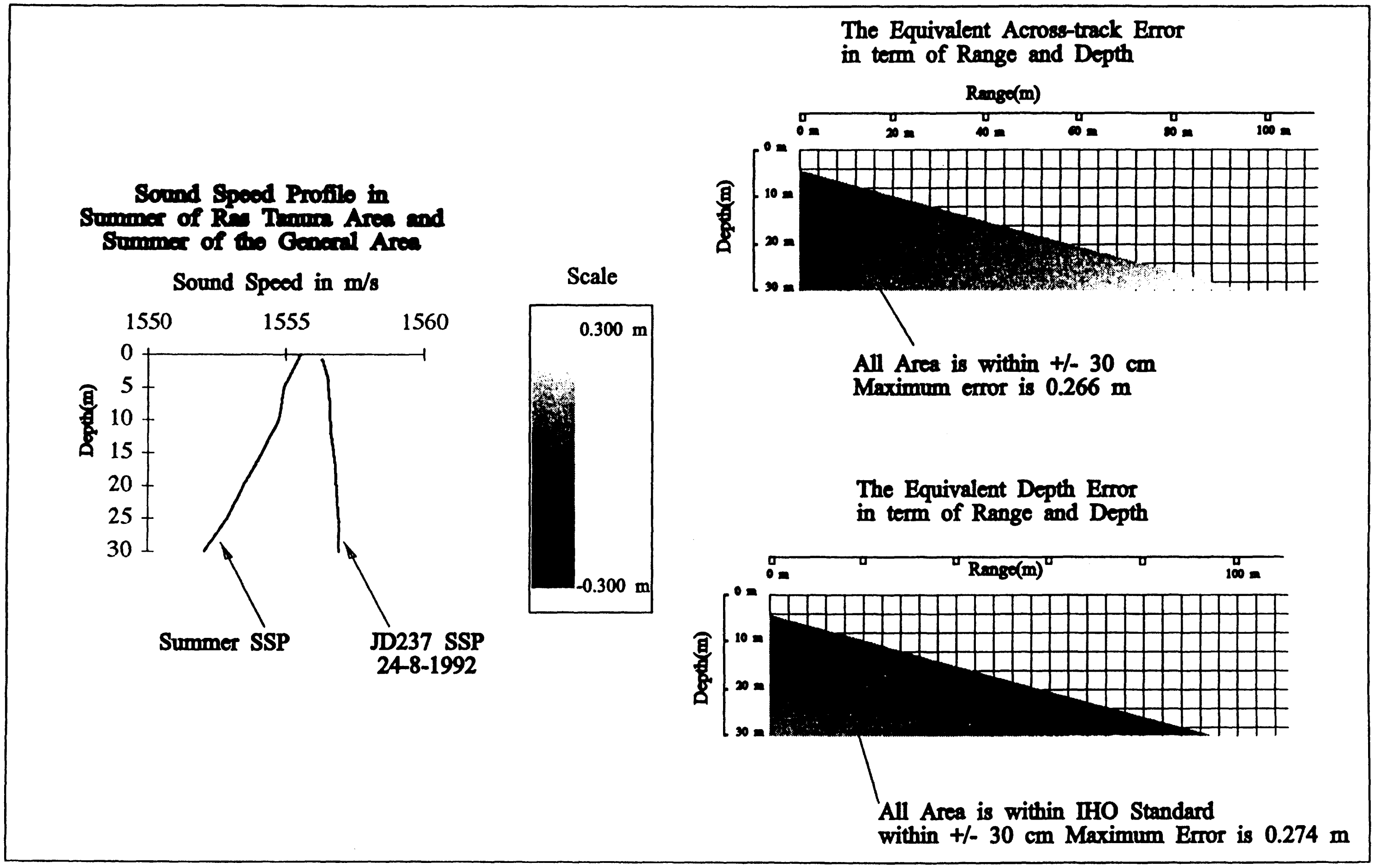

Figure 4-18
The effect of applying one SSP in summer of Ras Tanura over SSP in summer of the general area for 4.3 m draft case.

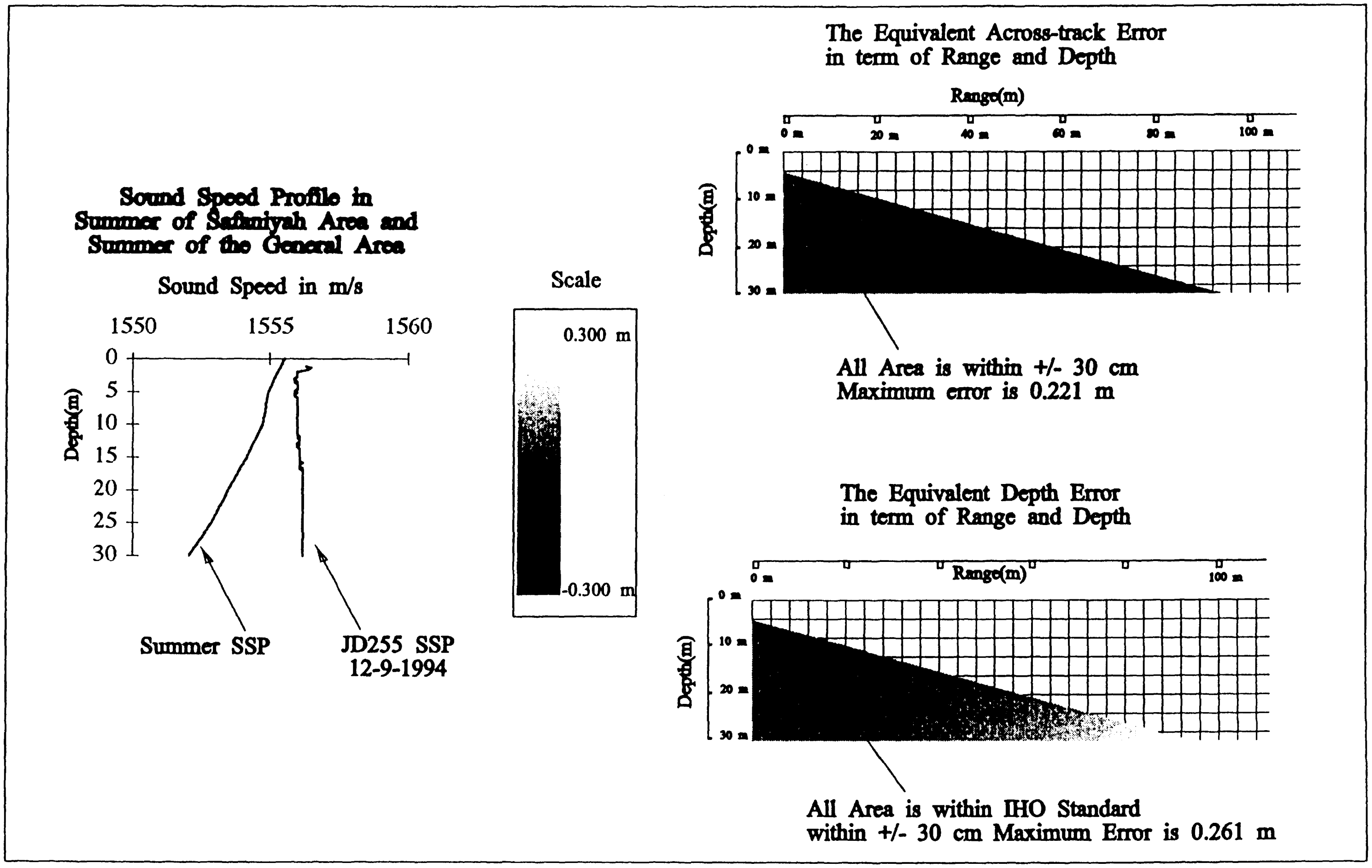

Figure 4-19
The effect of applying one SSP in summer of Safaniyah over SSP in summer of the general area for 4.3 m draft case.

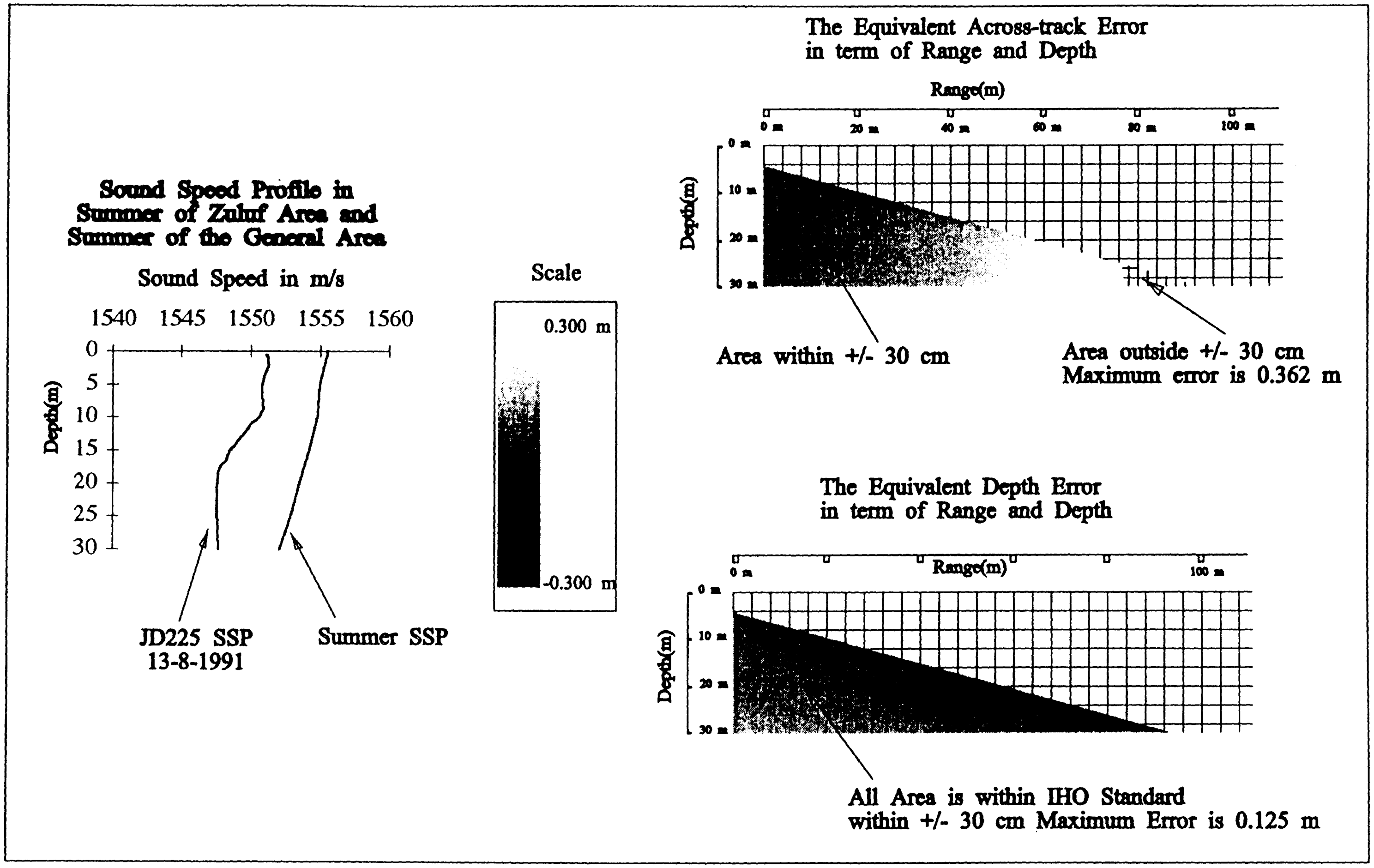

Figure 4-20
The effect of applying one SSP in summer of Zuluf over SSP in summer of the general area for 4.3 m draft case.

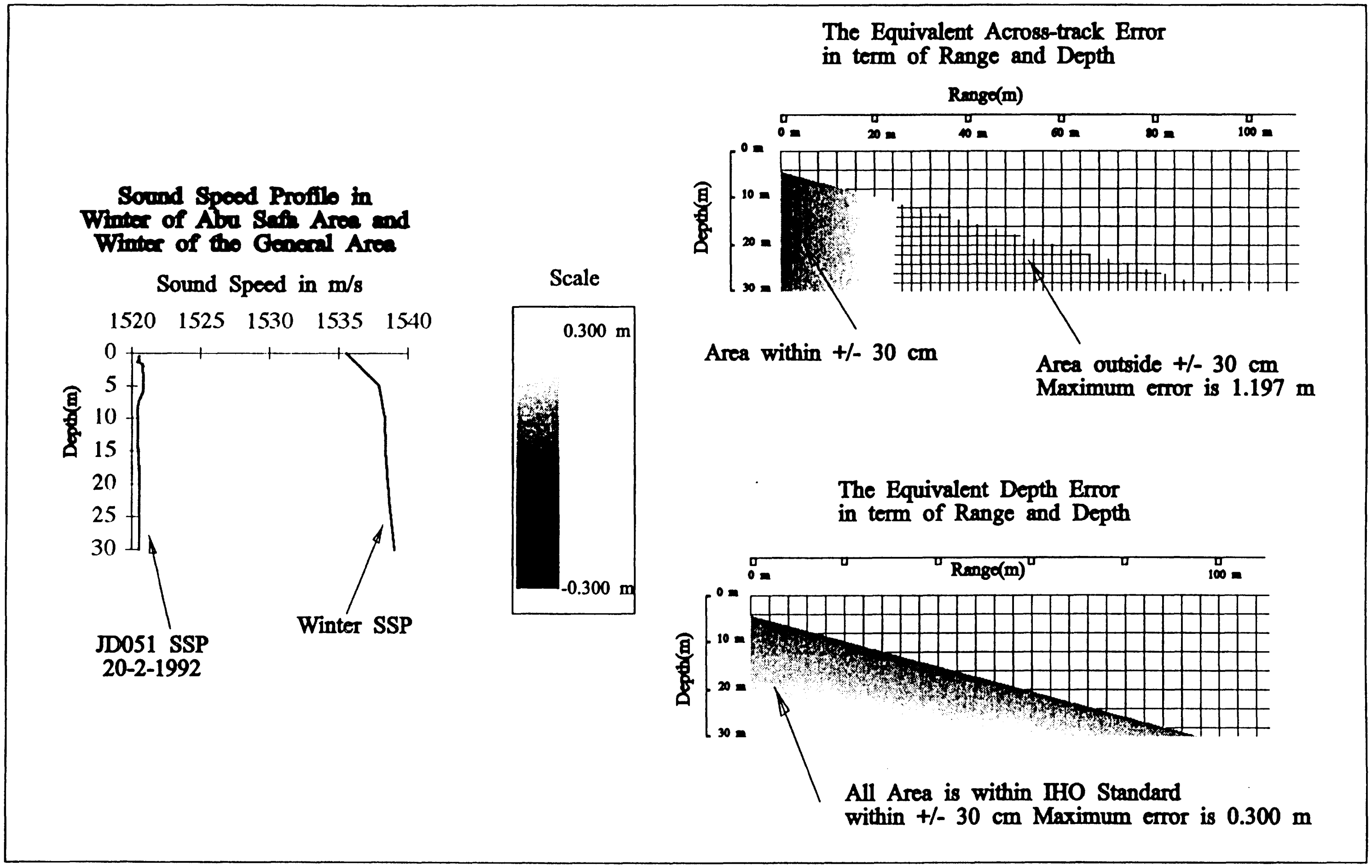

Figure 4-21
The effect of applying one SSP in winter of Abu Safa over SSP in winter of the general area for 4.3 m draft case.

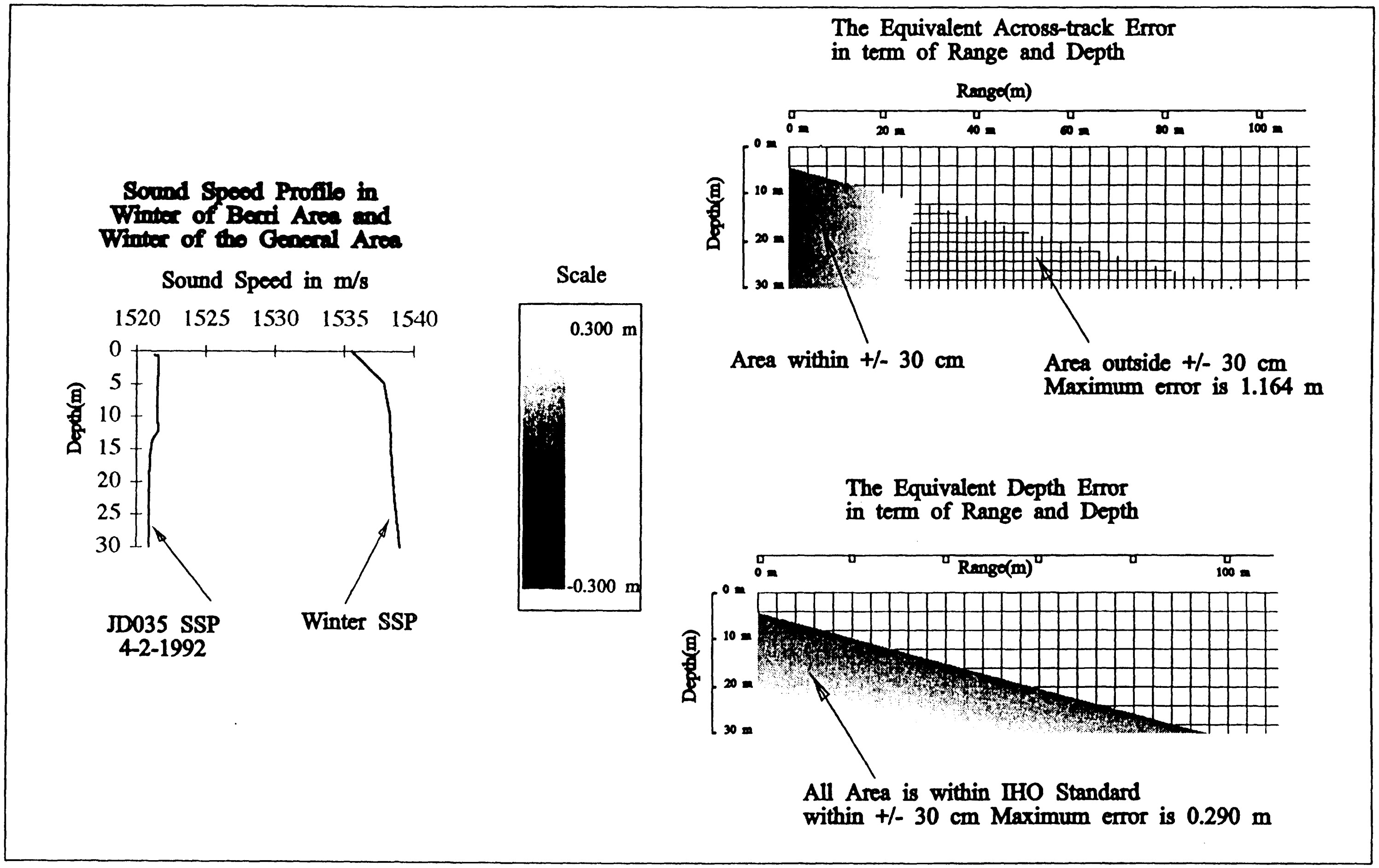

Figure 4-22
The effect of applying one SSP in winter of Berri over SSP in winter of the general area for 4.3 m draft case.

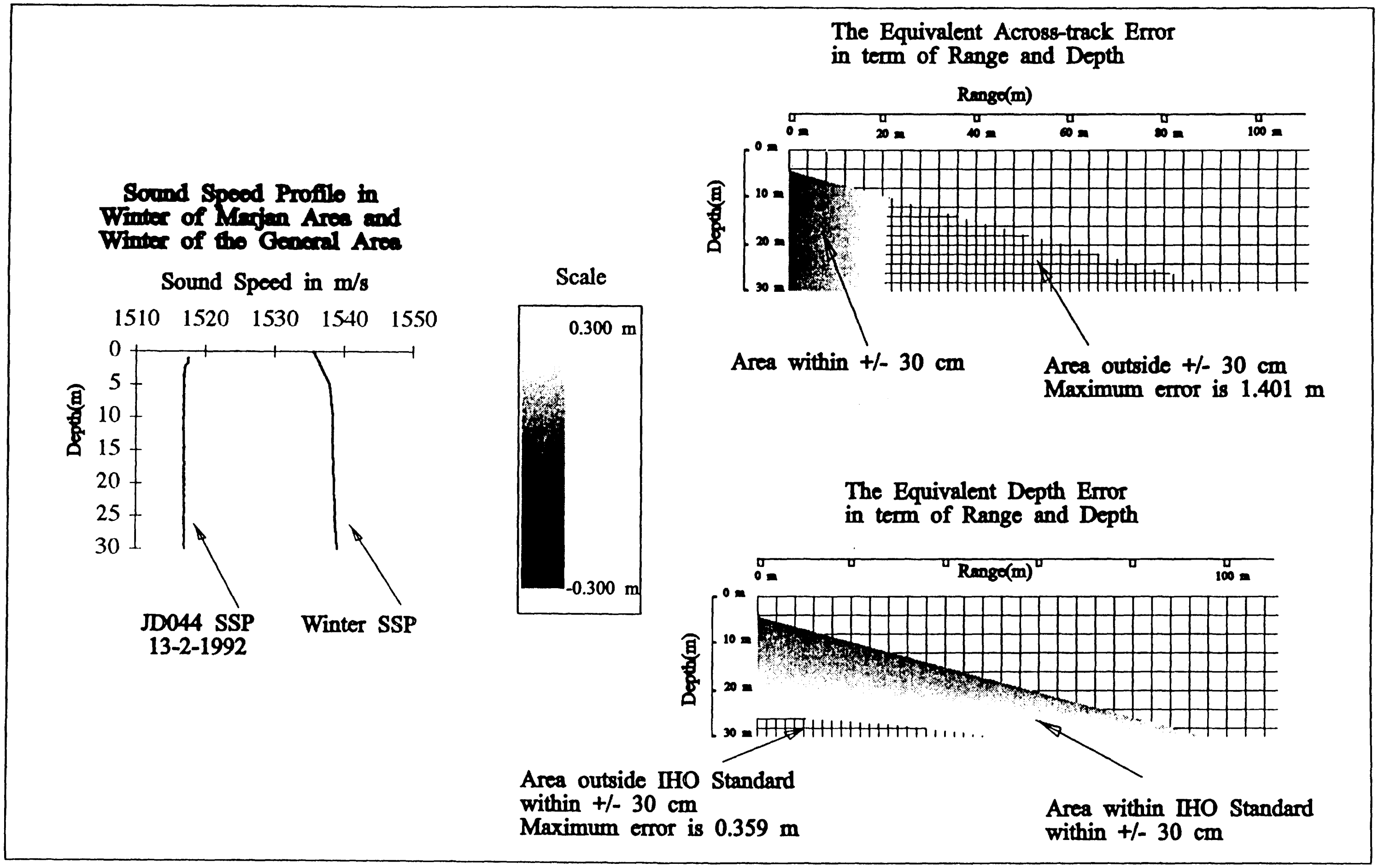

Figure 4-23
The effect of applying one SSP in winter of Marjan over SSP in winter of the general area for 4.3 m draft case.

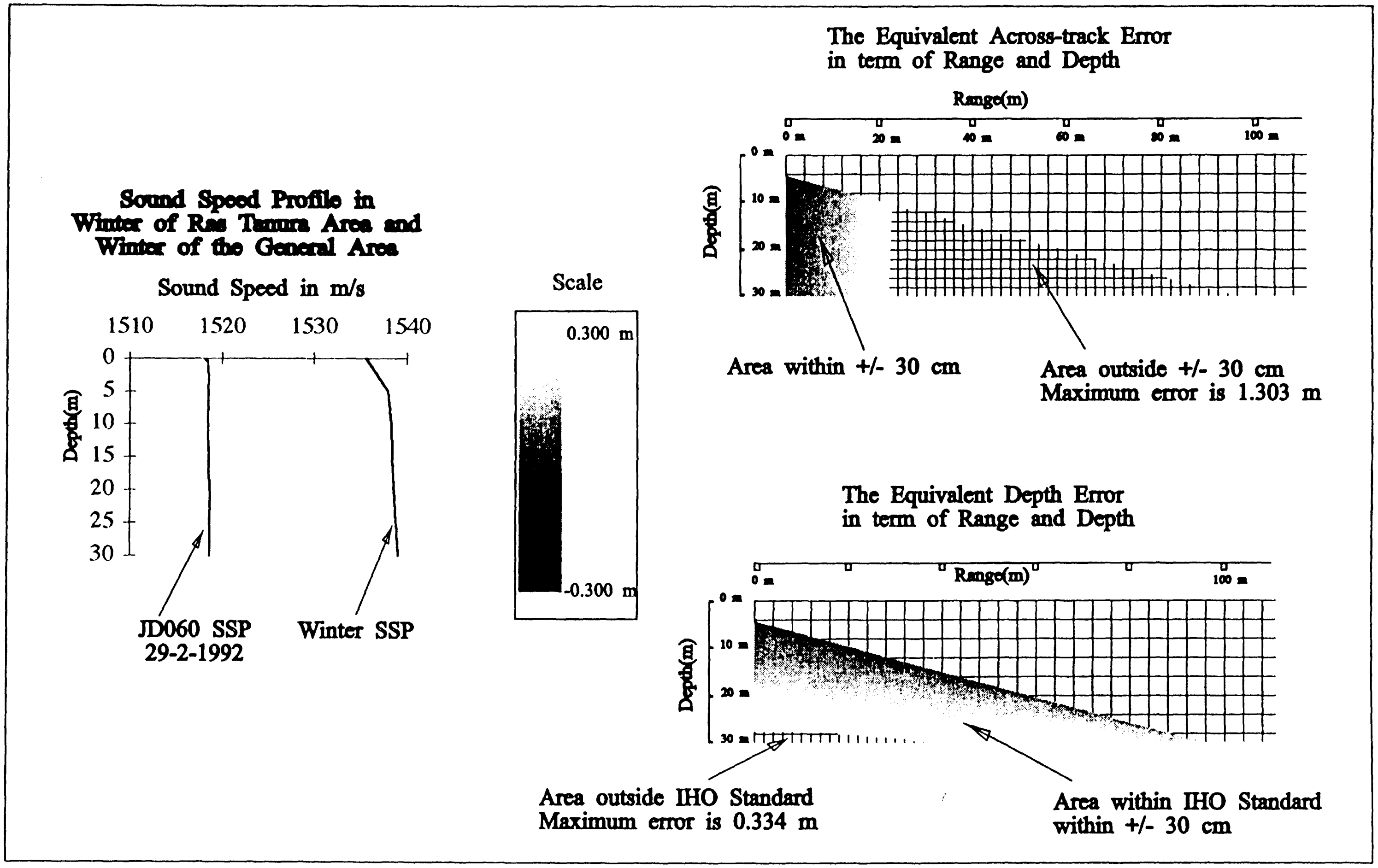

Figure 4-24
The effect of applying one SSP in winter of Ras Tanura over SSP in winter of the general area for 4.3 m draft case.

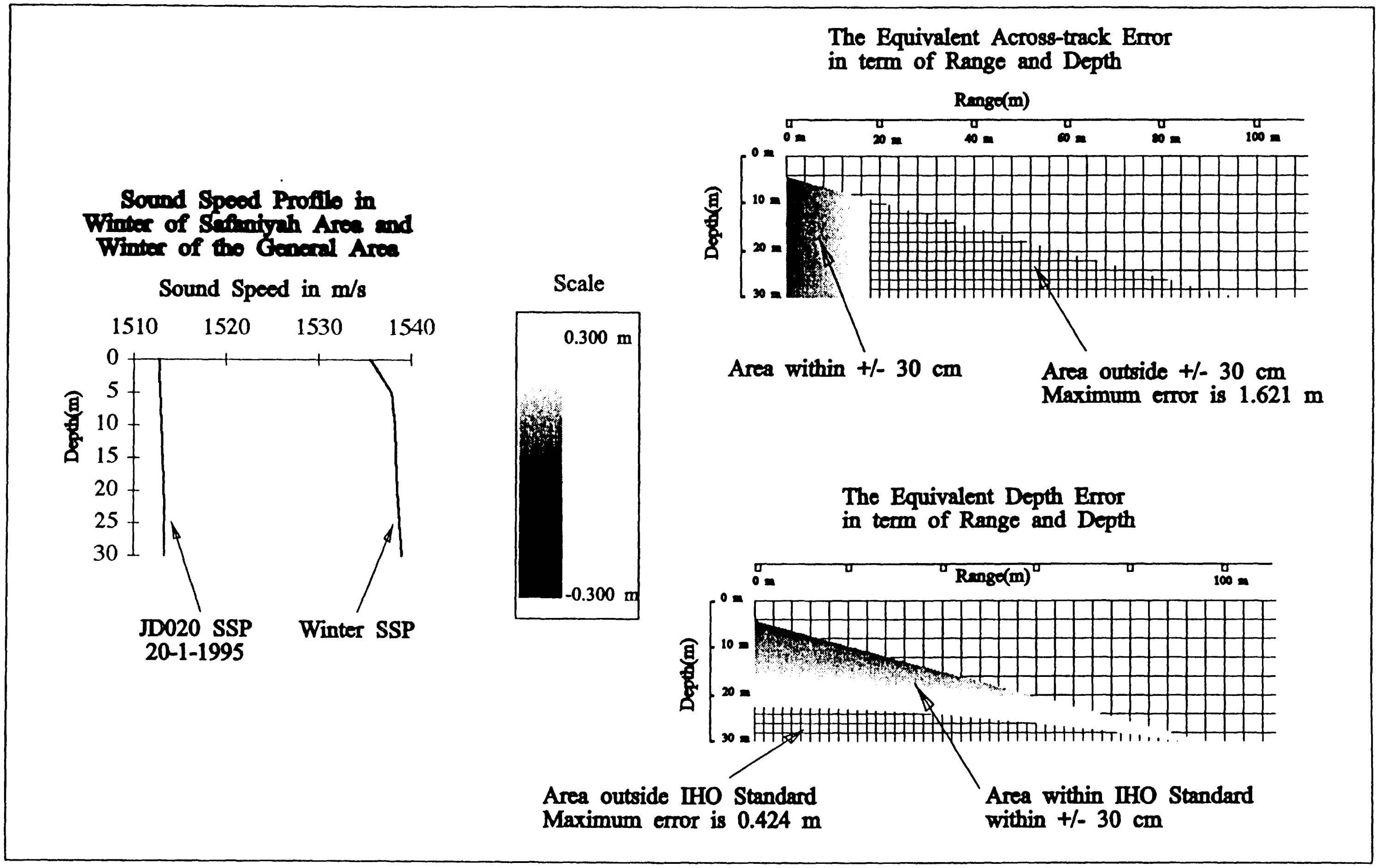

Figure 4-25
The effect of applying one SSP in winter of Safaniyah over SSP in winter of the general area for 4.3 m draft case.

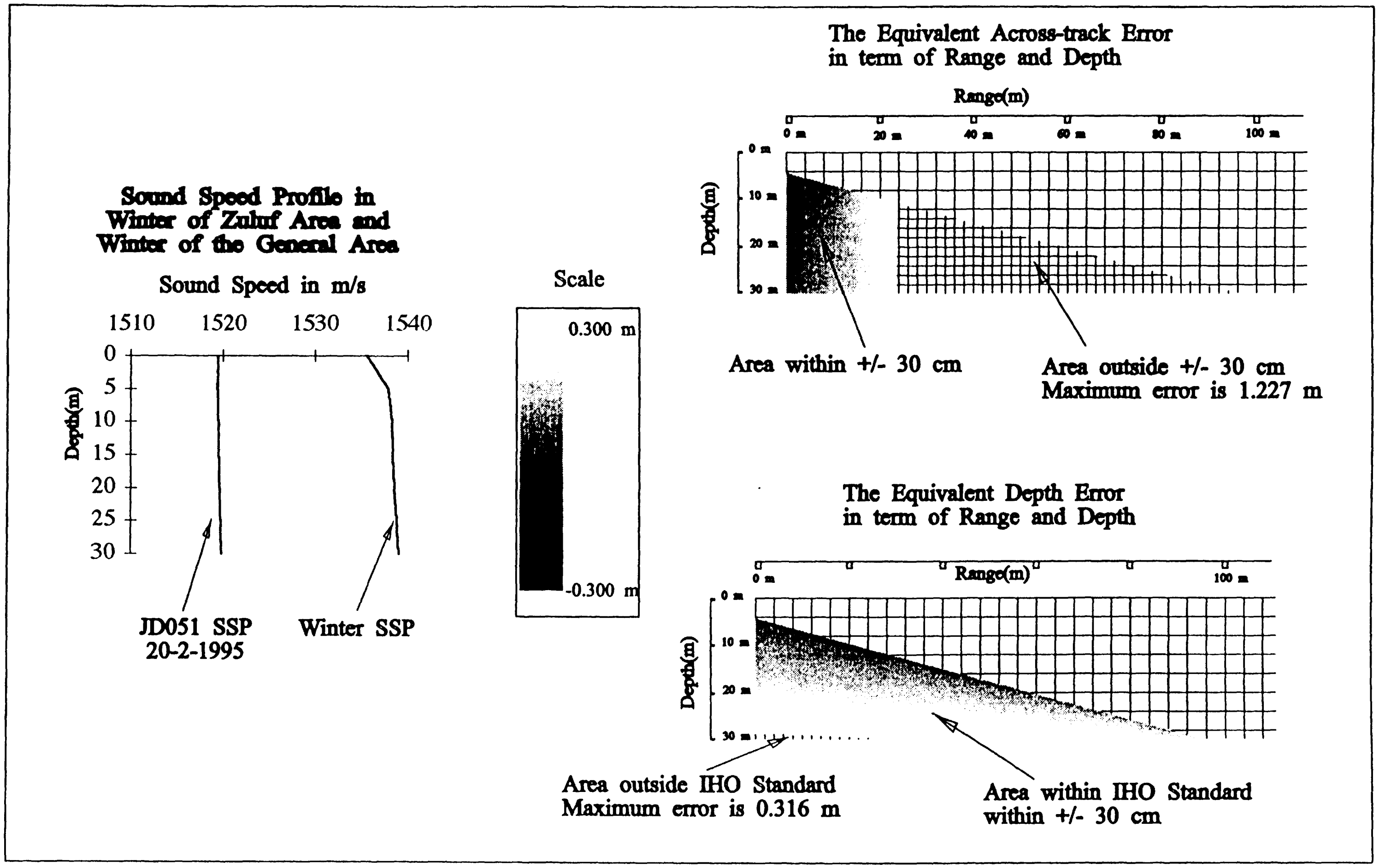

Figure 4-26
The effect of applying one SSP in winter of Zuluf over SSP in winter of the general area for 4.3 m draft case.

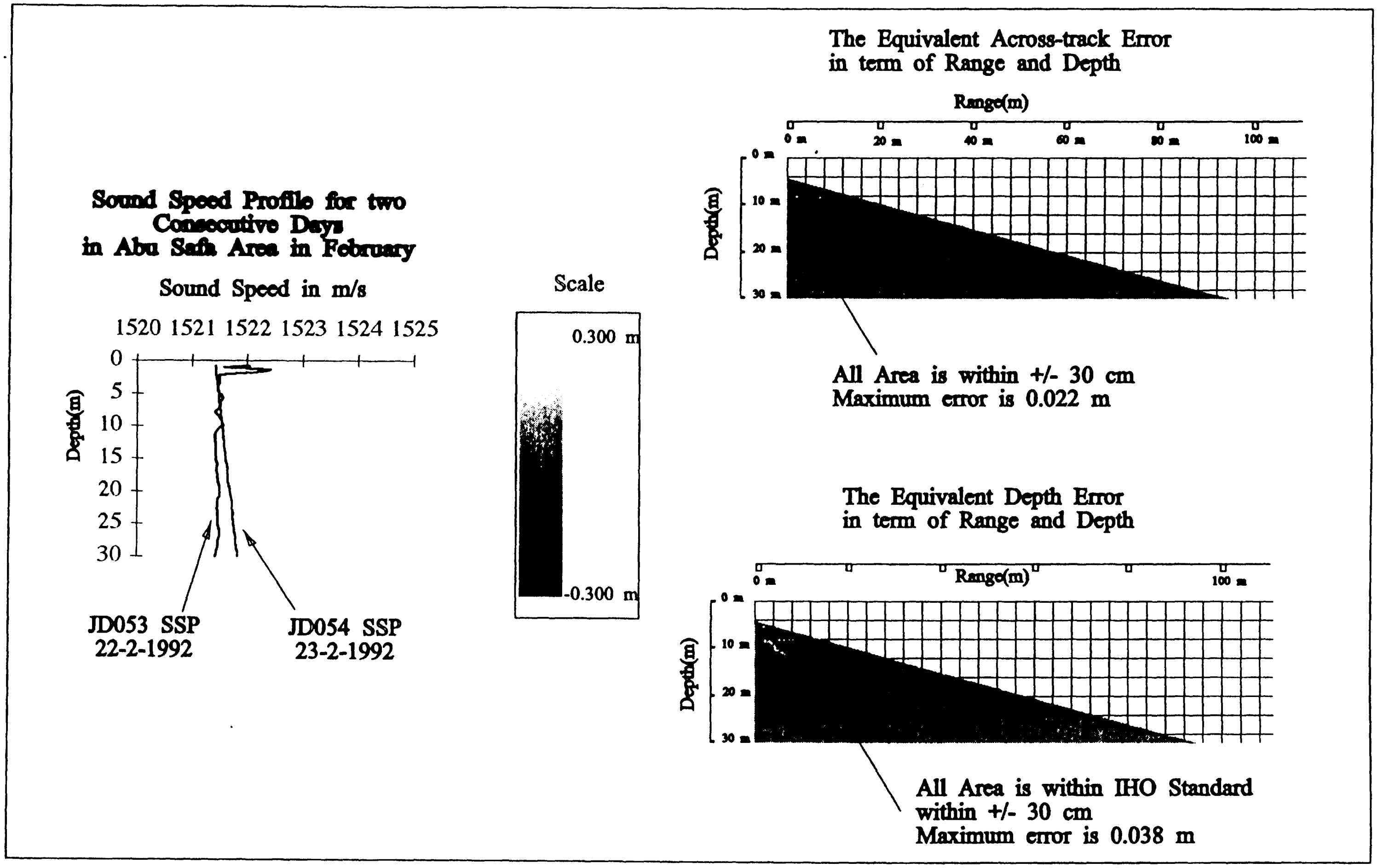

Figure 4-27
The effect of applying one SSP over another SSP for the next day in Abu Safa in February, both SSPs are normal, for 4.3 m draft case.

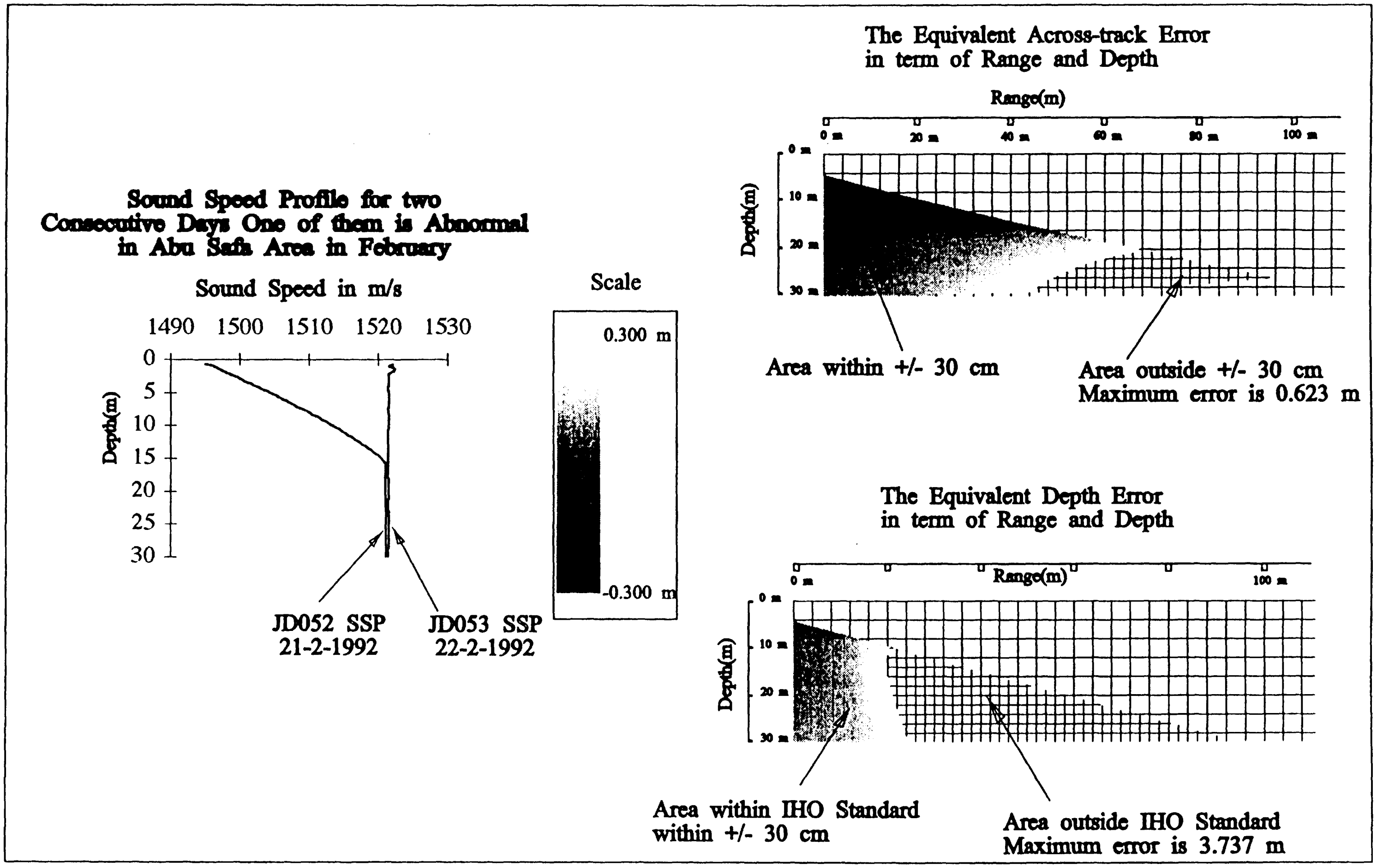

Figure 4-28
The effect of applying one SSP over another SSP for the next day in Abu Safa in February, one SSP is abnormal, for 4.3 m draft case.

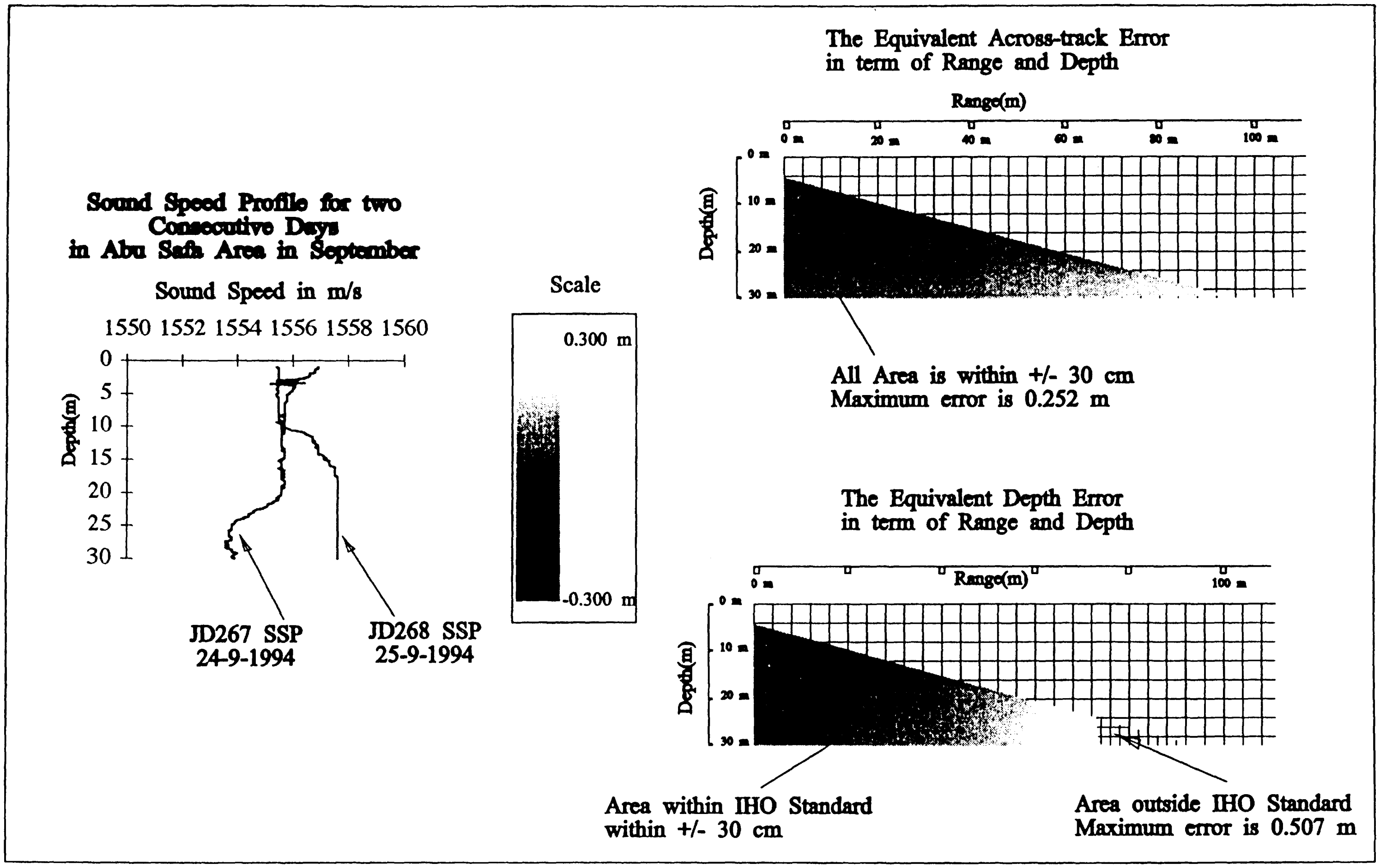

Figure 4-29
The effect of applying one SSP over another SSP for the next day in Abu Safa in September, both SSPs are abnormal, for 4.3 m draft case.

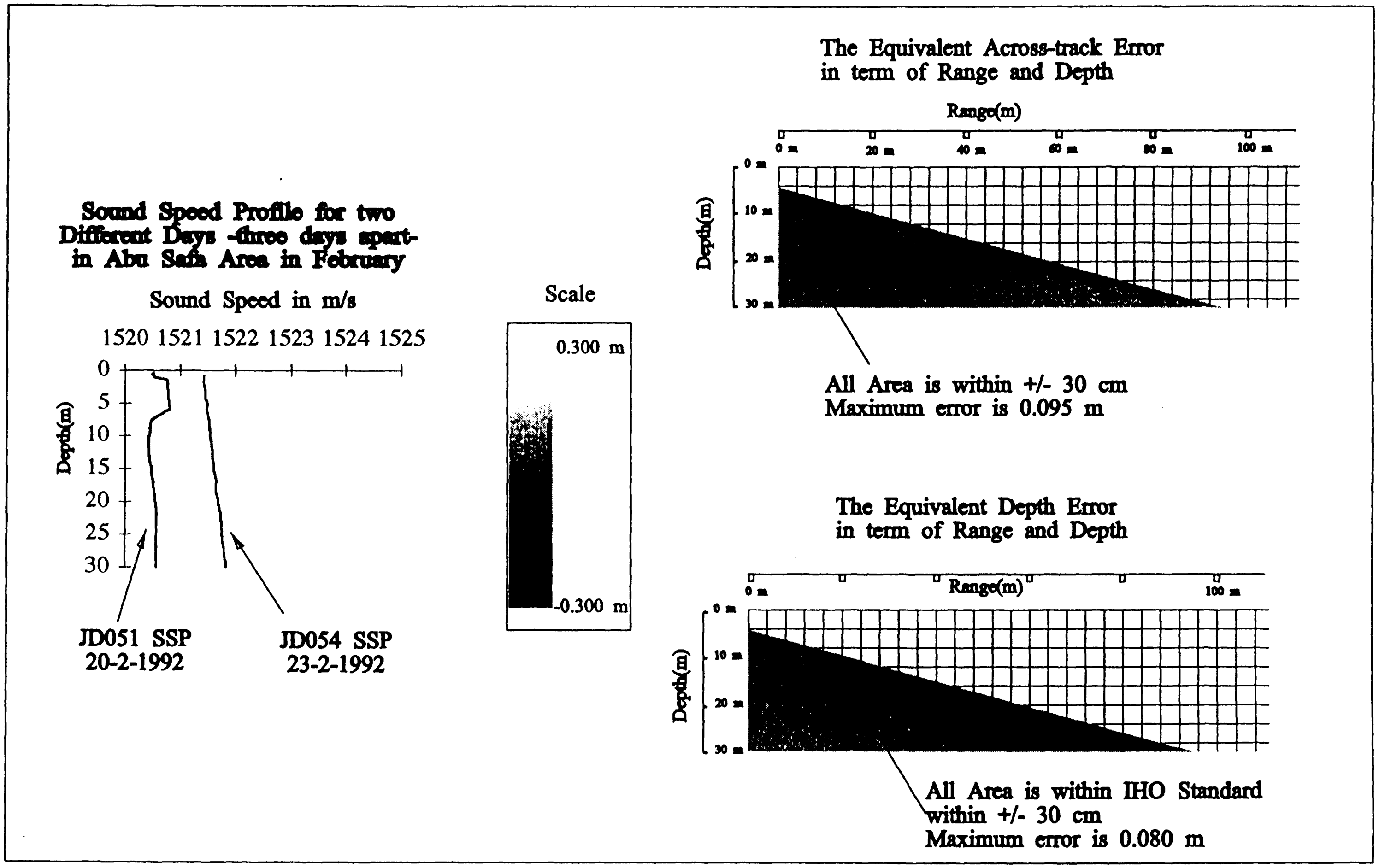

Figure 4-30
The effect of applying one SSP over another SSP three days later in Abu Safa in February, both SSPs are normal, for 4.3 m draft case.

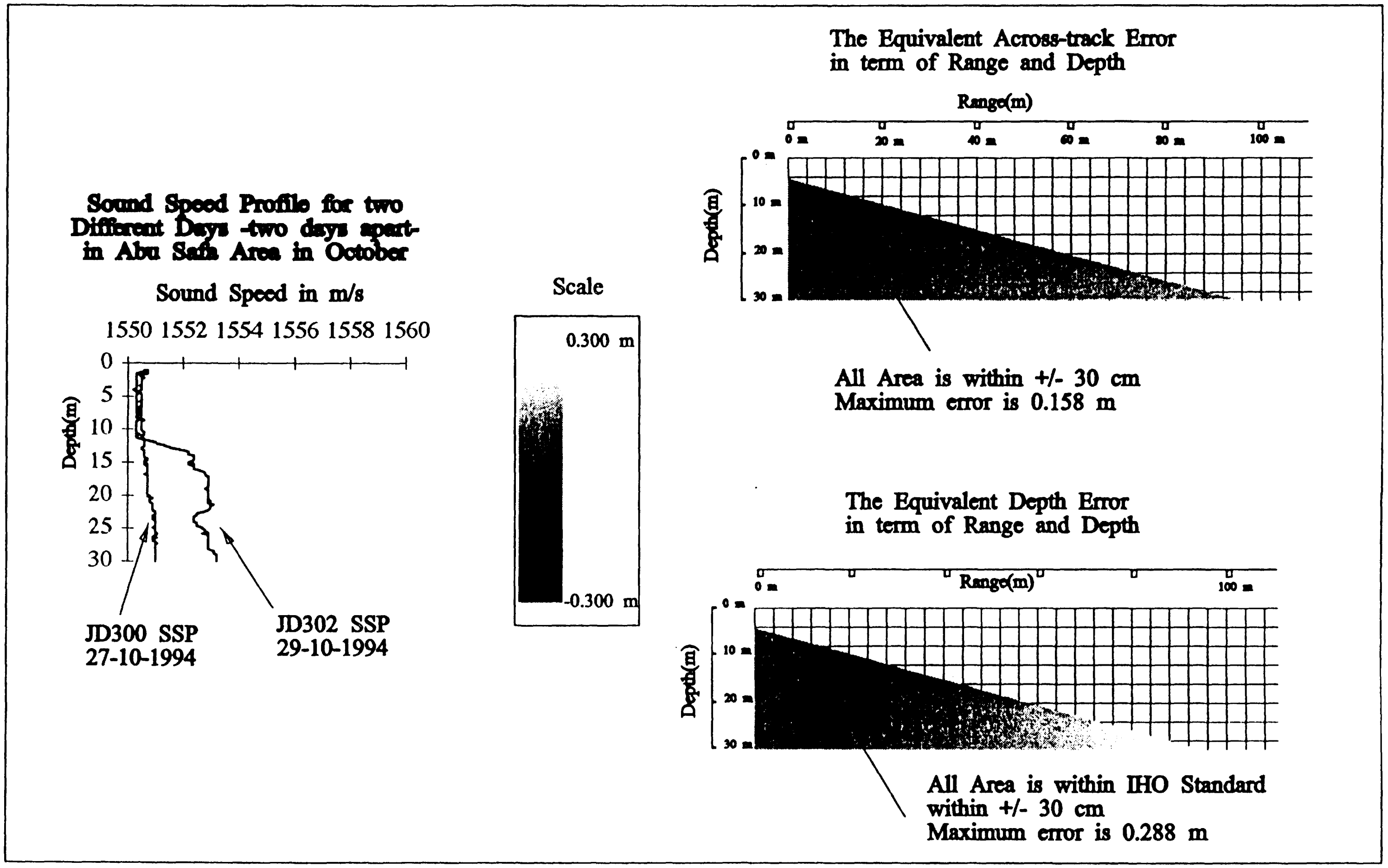

Figure 4-31
The effect of applying one SSP over another SSP two days later in Abu Safa in October, both SSPs are normal, for 4.3 m draft case.

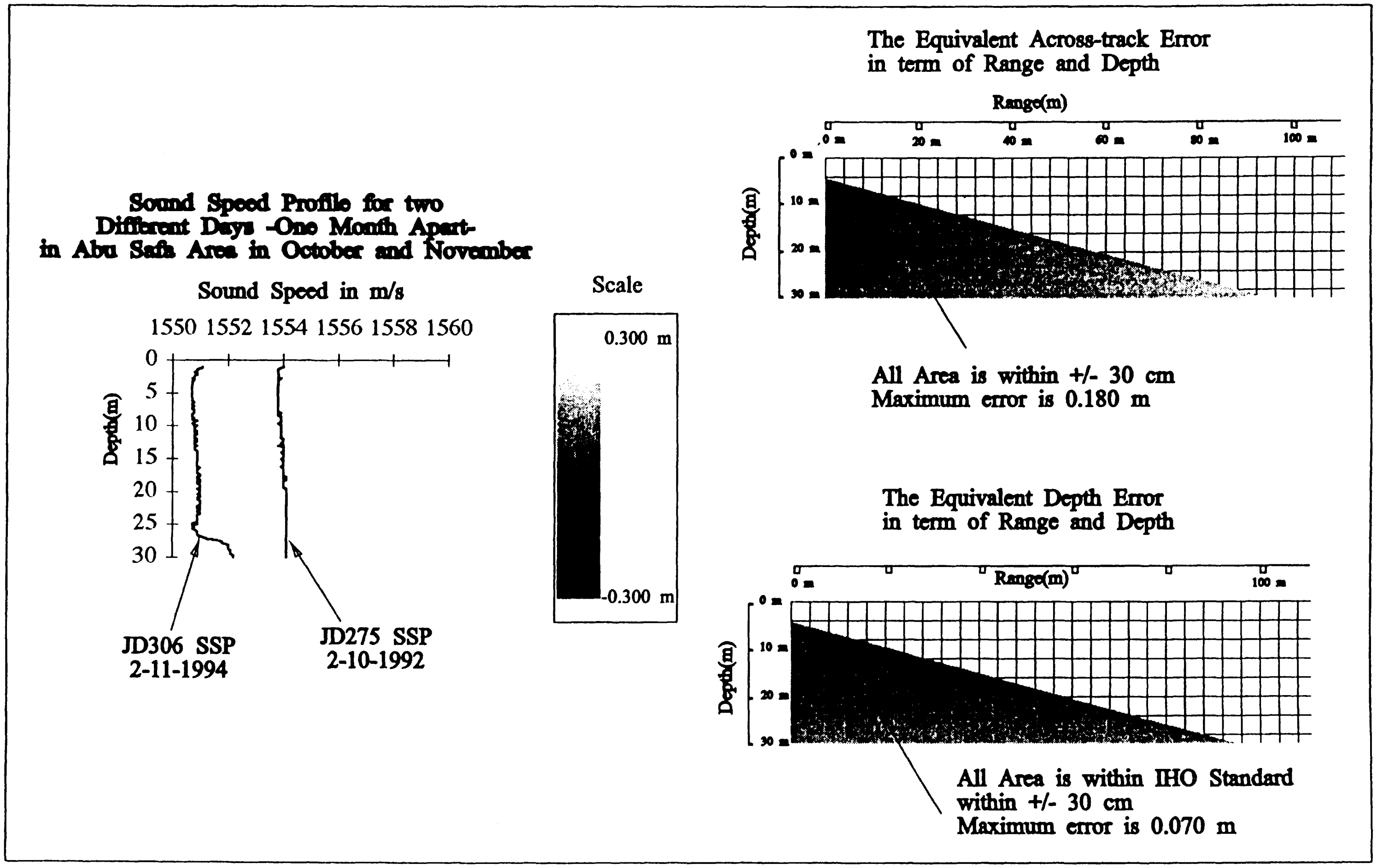

Figure 4-32
The effect of applying one SSP over another SSP a month later in Abu Safa in October and November, both SSPs are normal, for 4.3 m draft case.

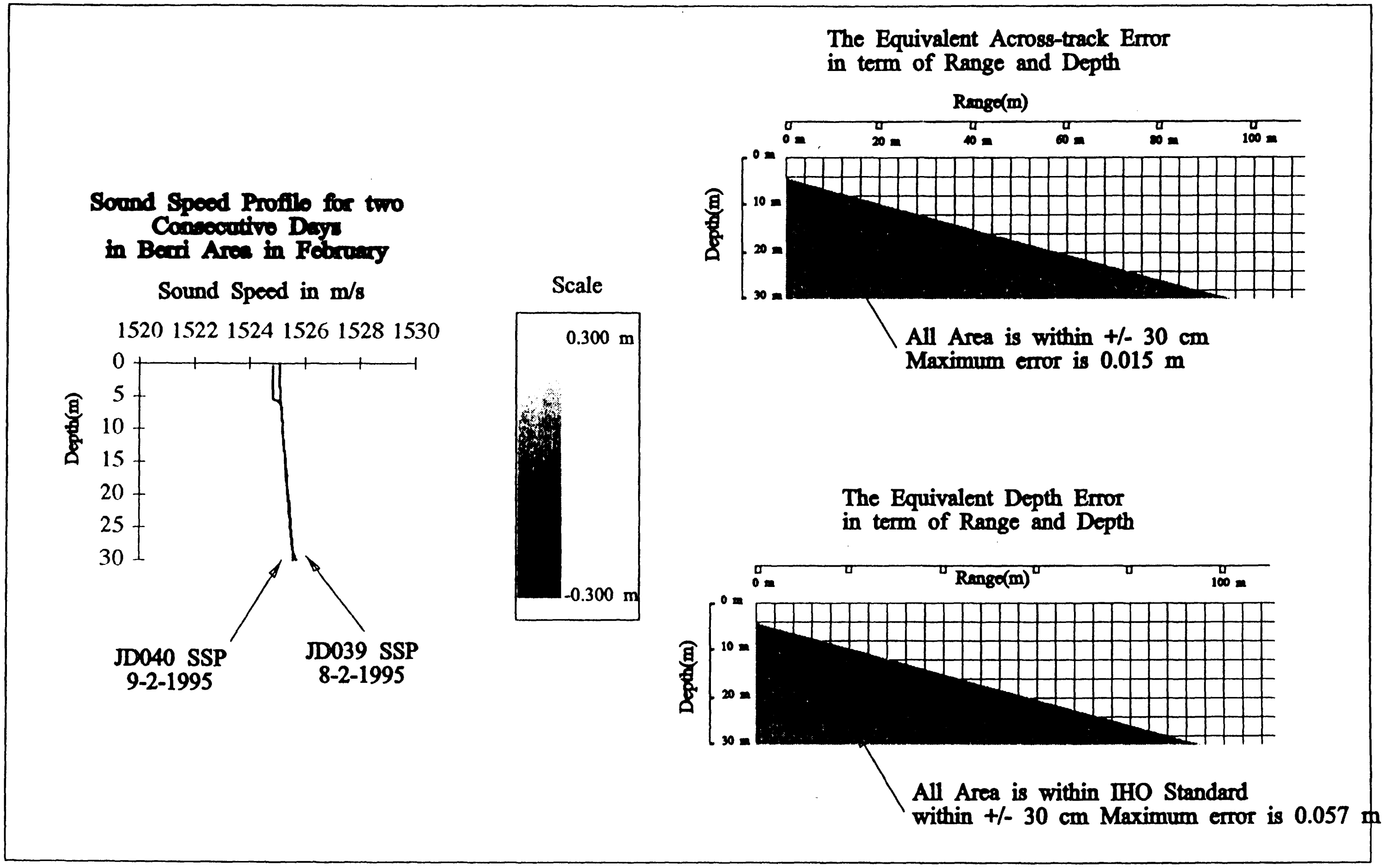

Figure 4-33
The effect of applying one SSP over another SSP for the next day in Berri in February, both SSPs are normal, for 4.3 m draft case.

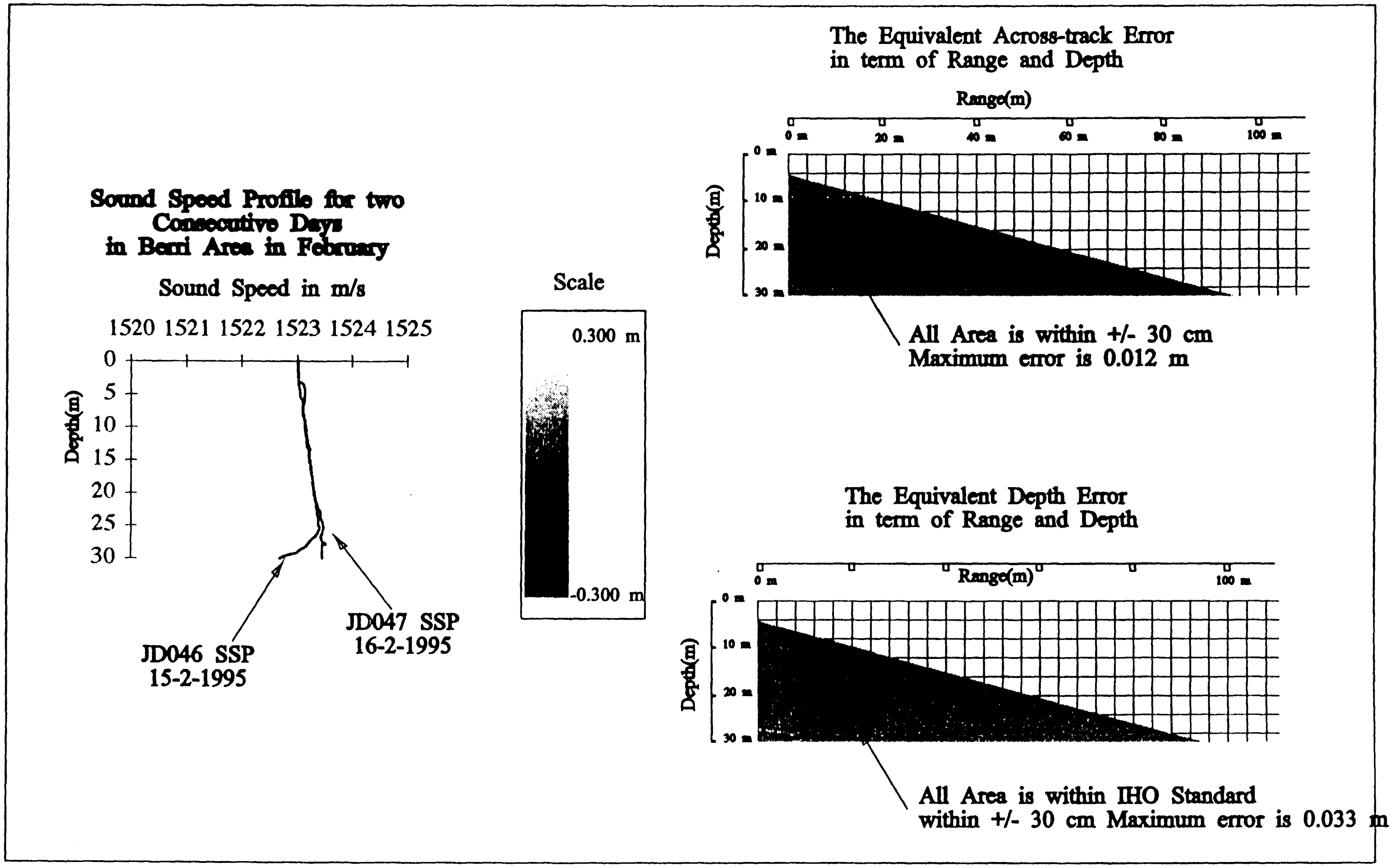

Figure 4-34
The effect of applying one SSP over another SSP for the next day in Berri in February, both SSPs are normal, for 4.3 m draft case.

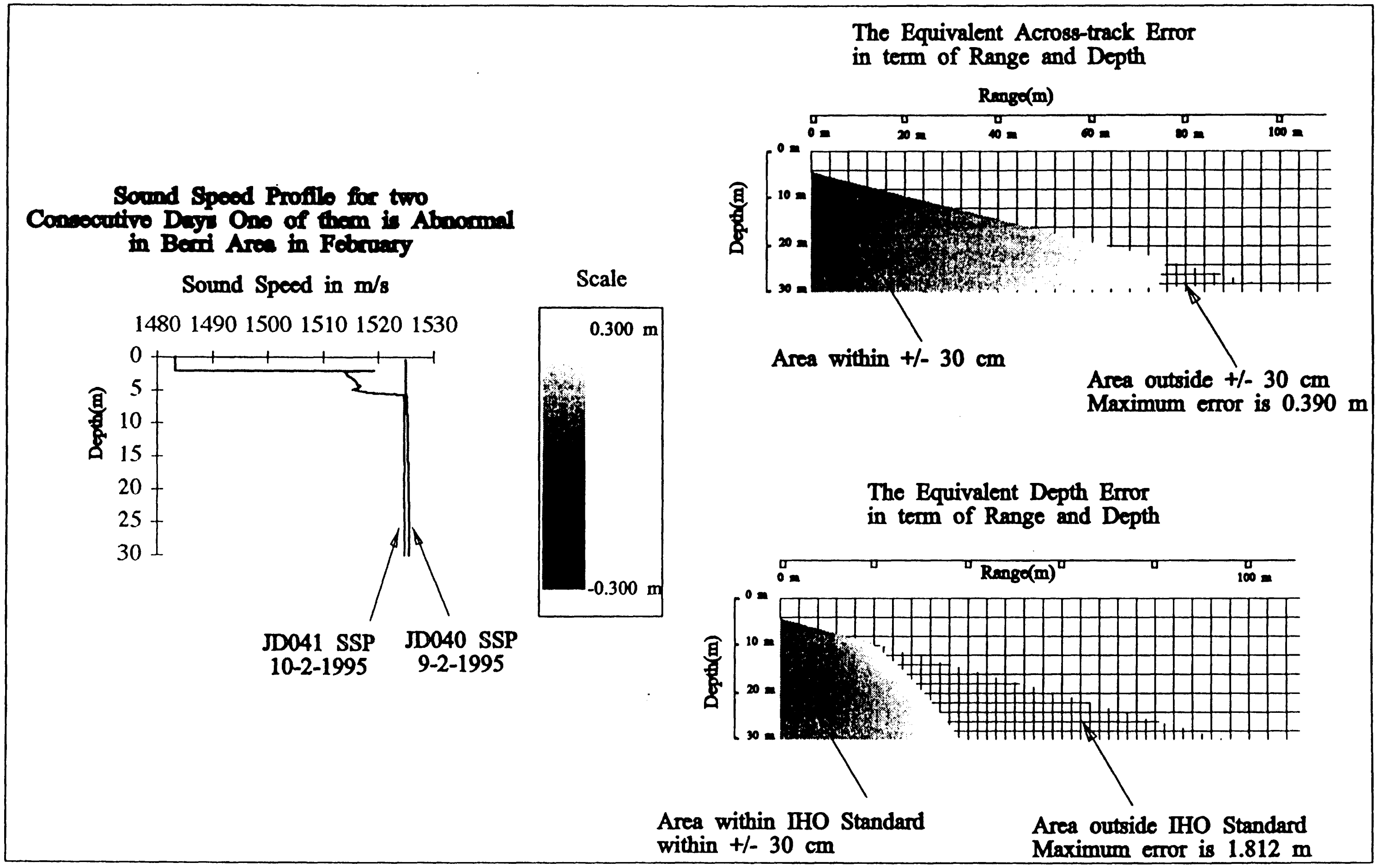

Figure 4-35
The effect of applying one SSP over another SSP for the next day in Berri in February, one SSP is abnormal, for 4.3 m draft case.

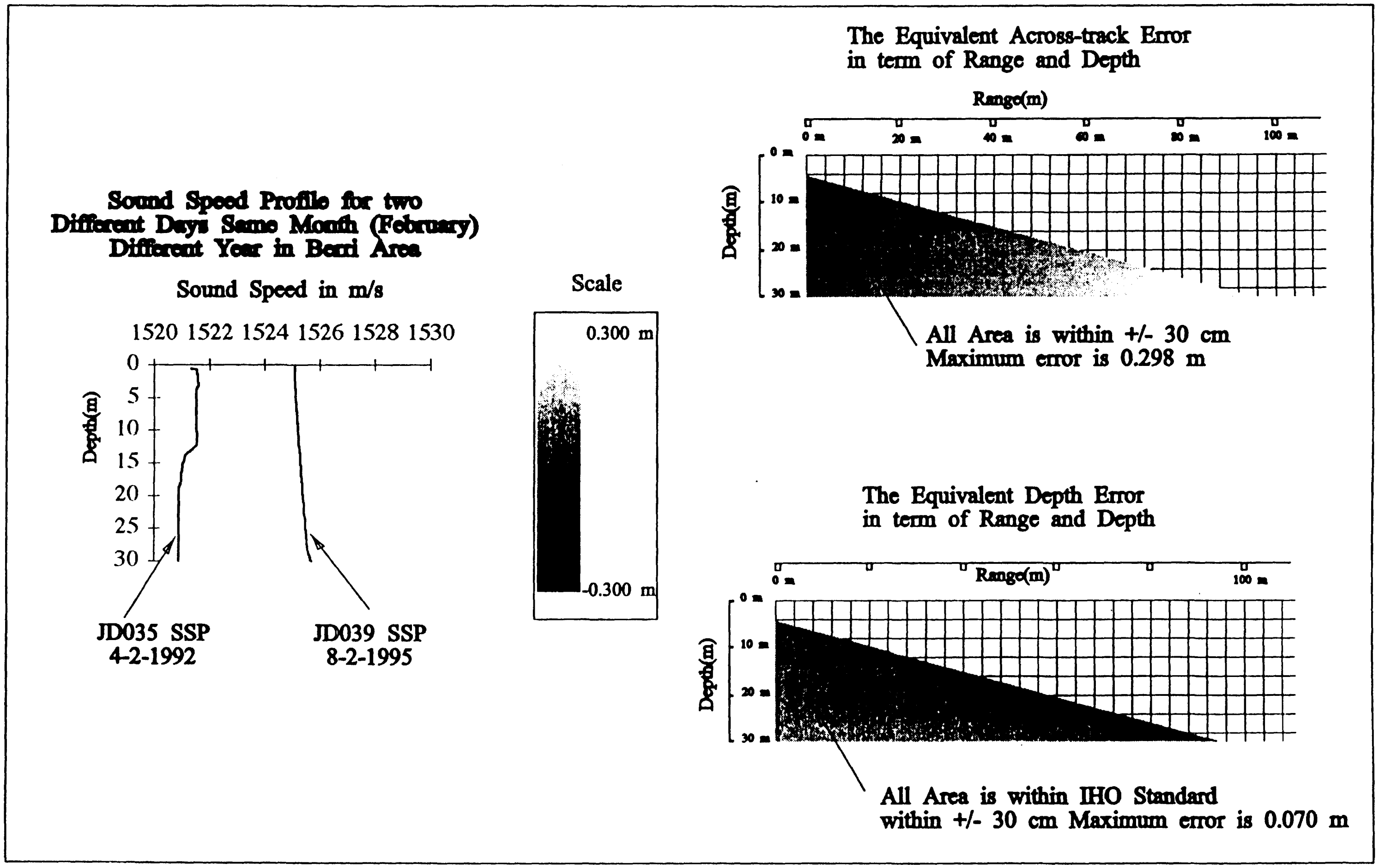

Figure 4-36
The effect of applying one SSP over another SSP three years and four days later in Berri in February, one SSP is abnormal, for 4.3 m draft case.

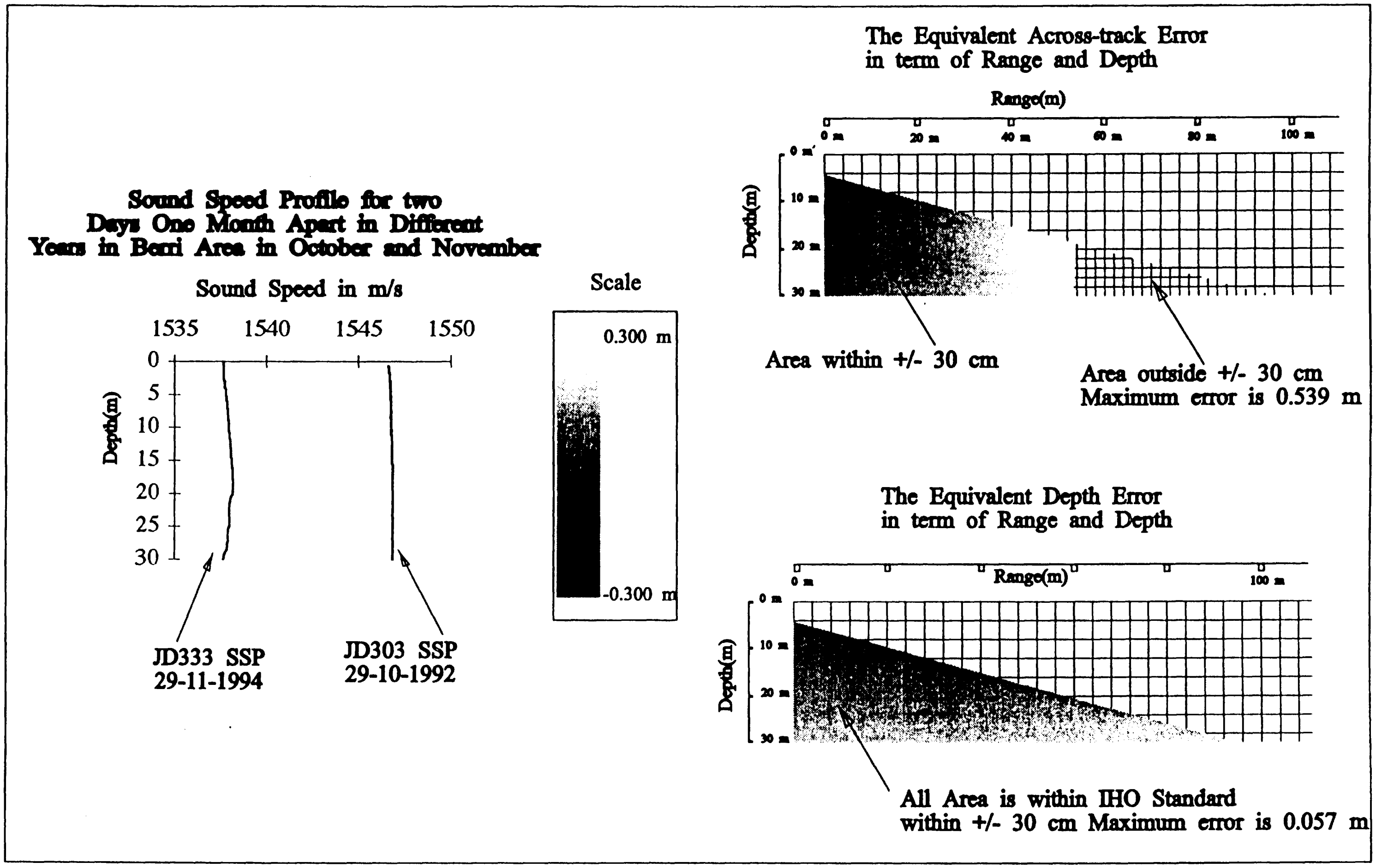

Figure 4-37
The effect of applying one SSP over another SSP one month later in Berri in October and November, both SSPs are normal, for 4.3 m draft case.

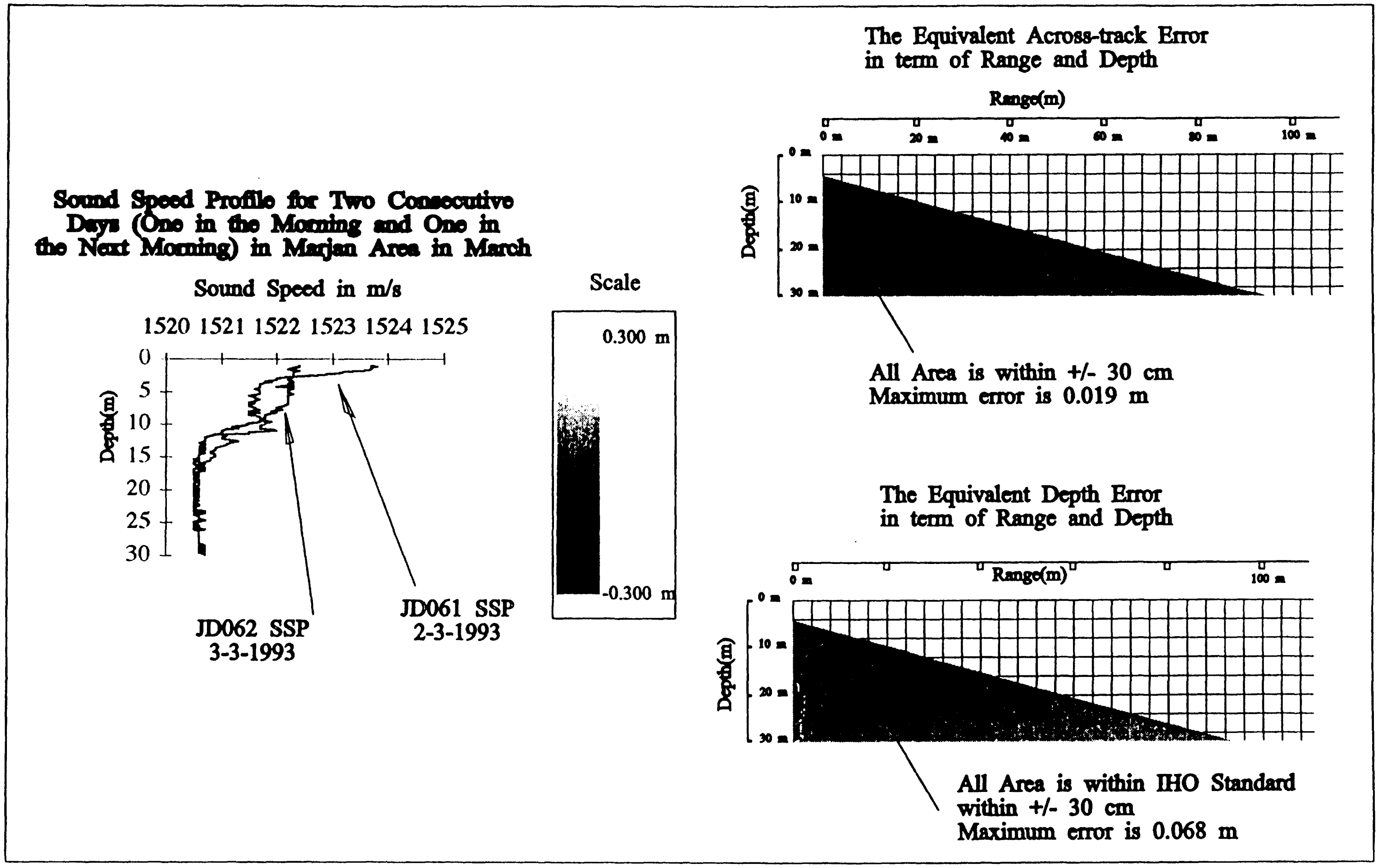

Figure 4-38
The effect of applying one SSP over another SSP for the next day in Marjan in March, both SSPs are normal, for 4.3 m draft case.

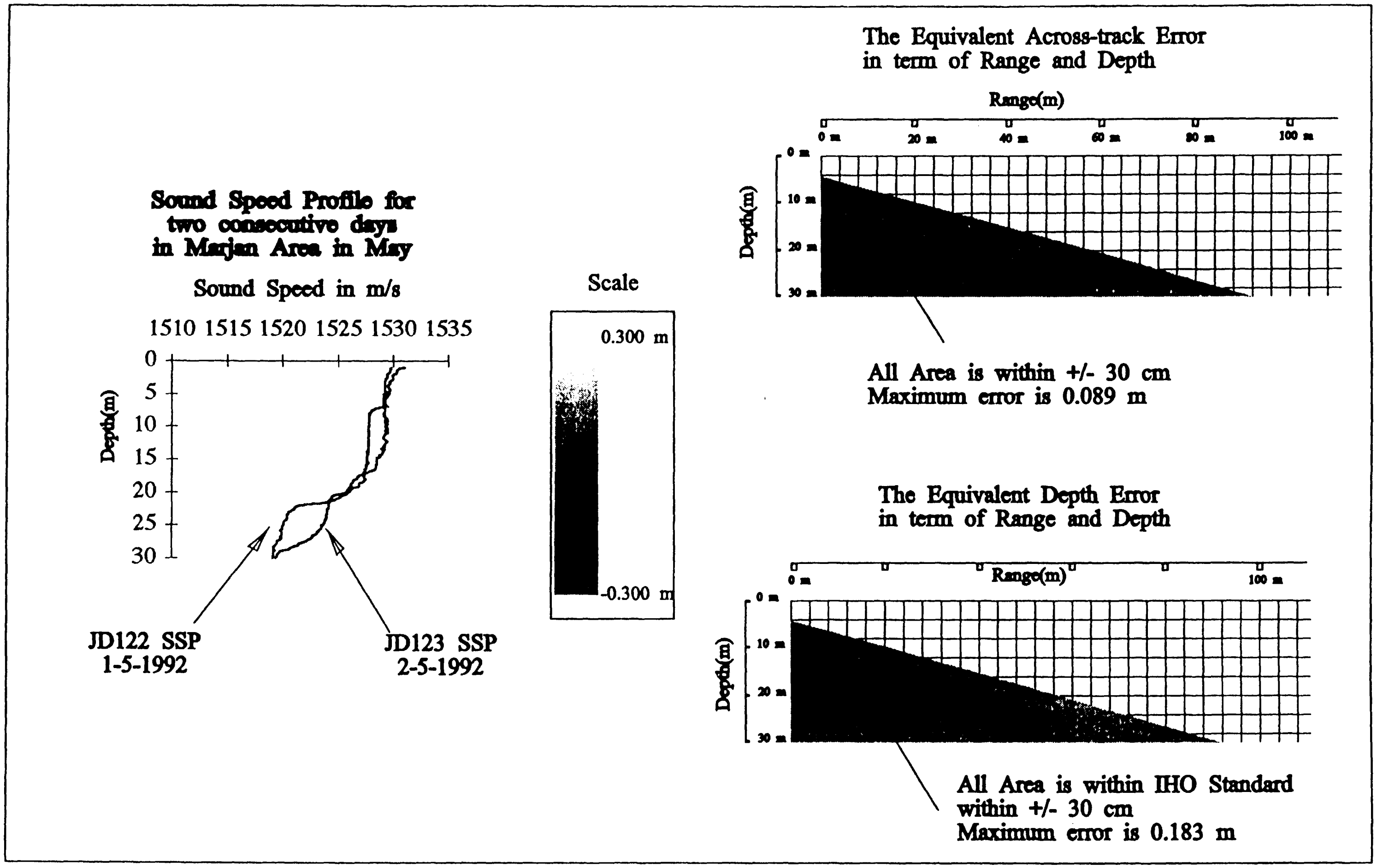

Figure 4-39
The effect of applying one SSP over another SSP for the next day in Marjan in May, both SSPs are abnormal, for 4.3 m draft case.

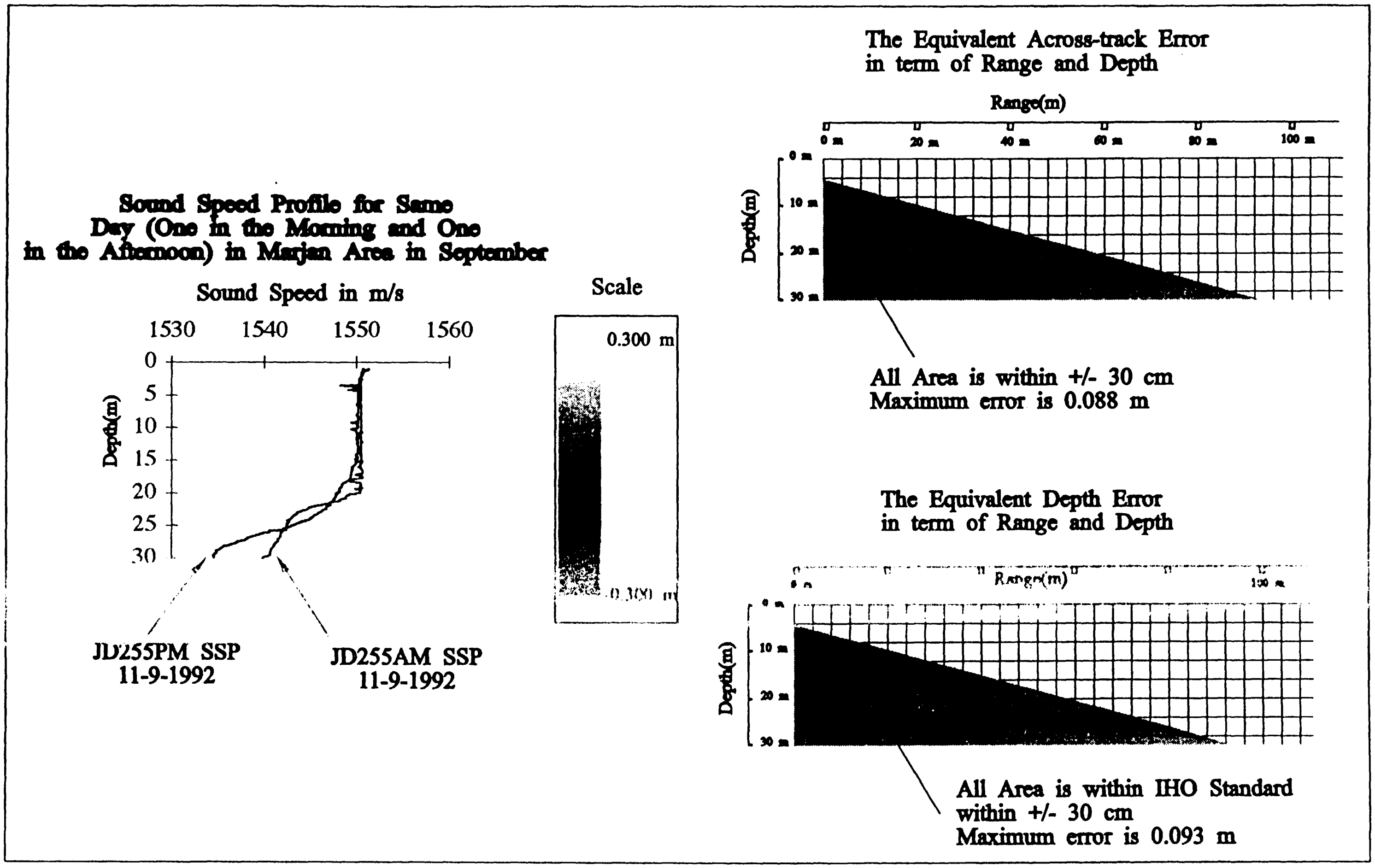

Figure 4-40
The effect of applying one SSP in the morning over another SSP in the afternoon in the same day in Marjan in September, both SSPs are abnormal, for 4.3 m draft case.

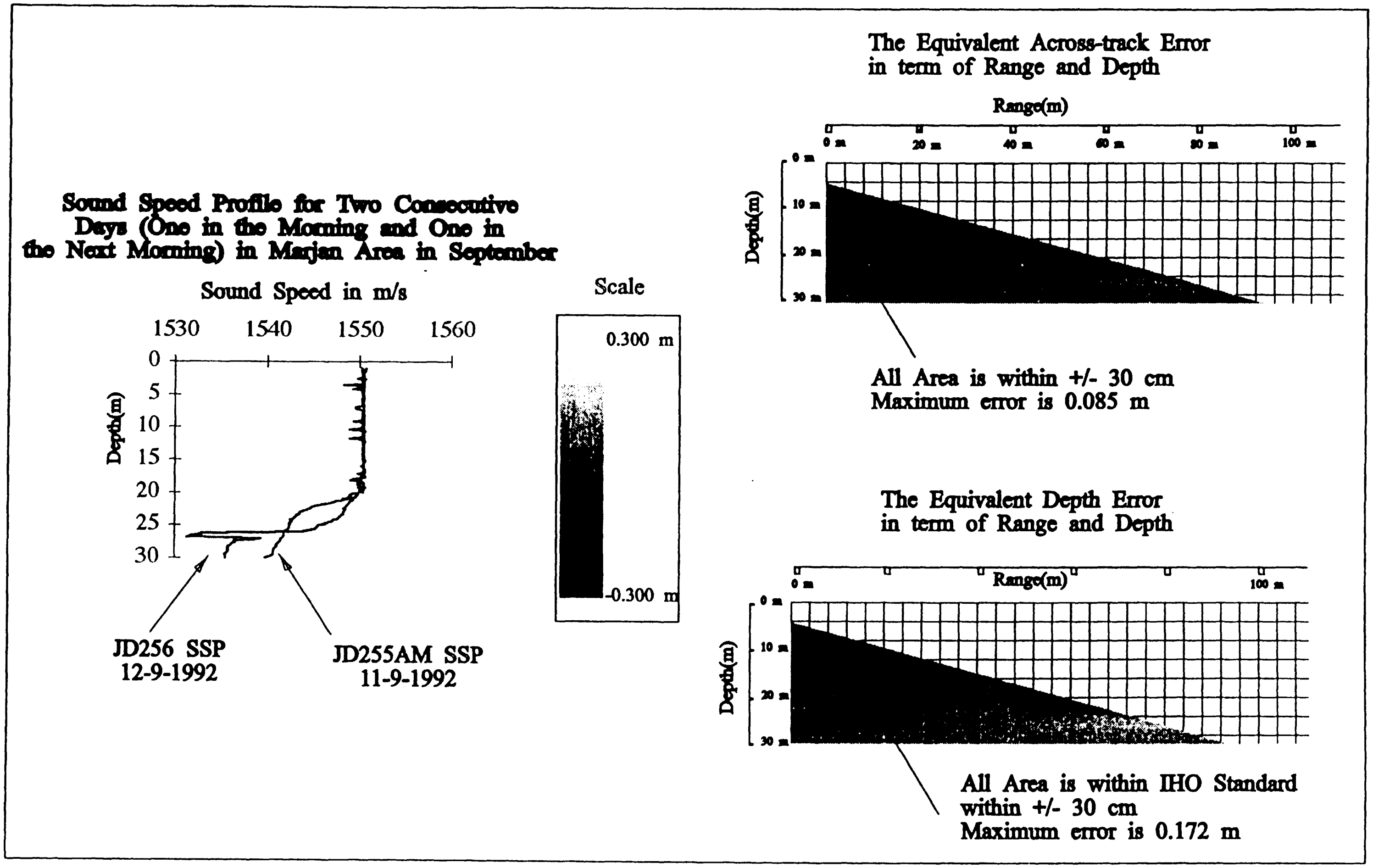

Figure 4-41
The effect of applying one SSP in the morning over another SSP in the morning of the next day in Marjan in September, both SSPs are abnormal, for 4.3 m draft case.

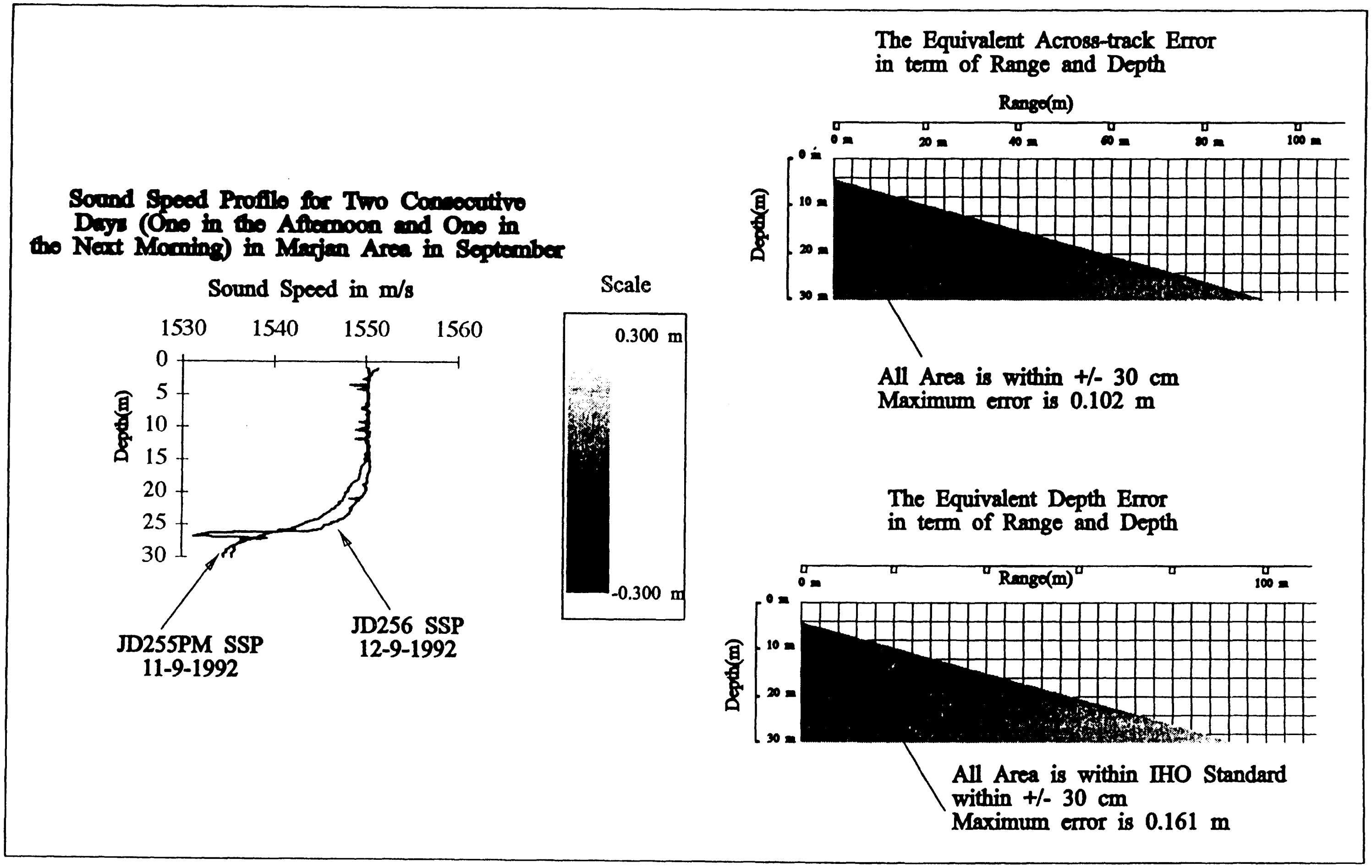

Figure 4-42
The effect of applying one SSP in the afternoon over another SSP in the morning of the next day in Marjan in September, both SSPs are abnormal, for 4.3 m draft case.

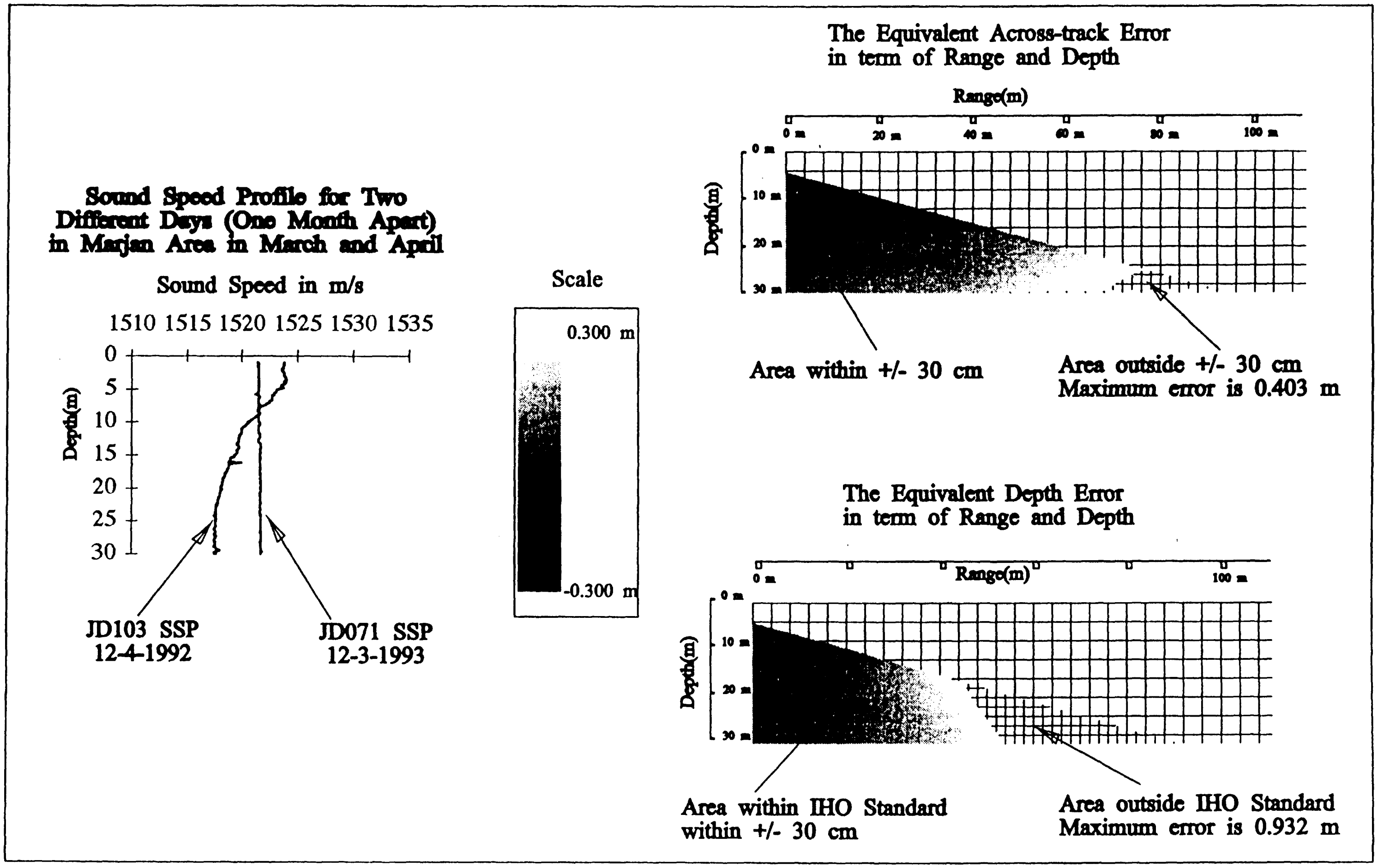

Figure 4-43
The effect of applying one SSP over another SSP one month later in Marjan in March and April, one SSP is abnormal, for 4.3 m draft case.

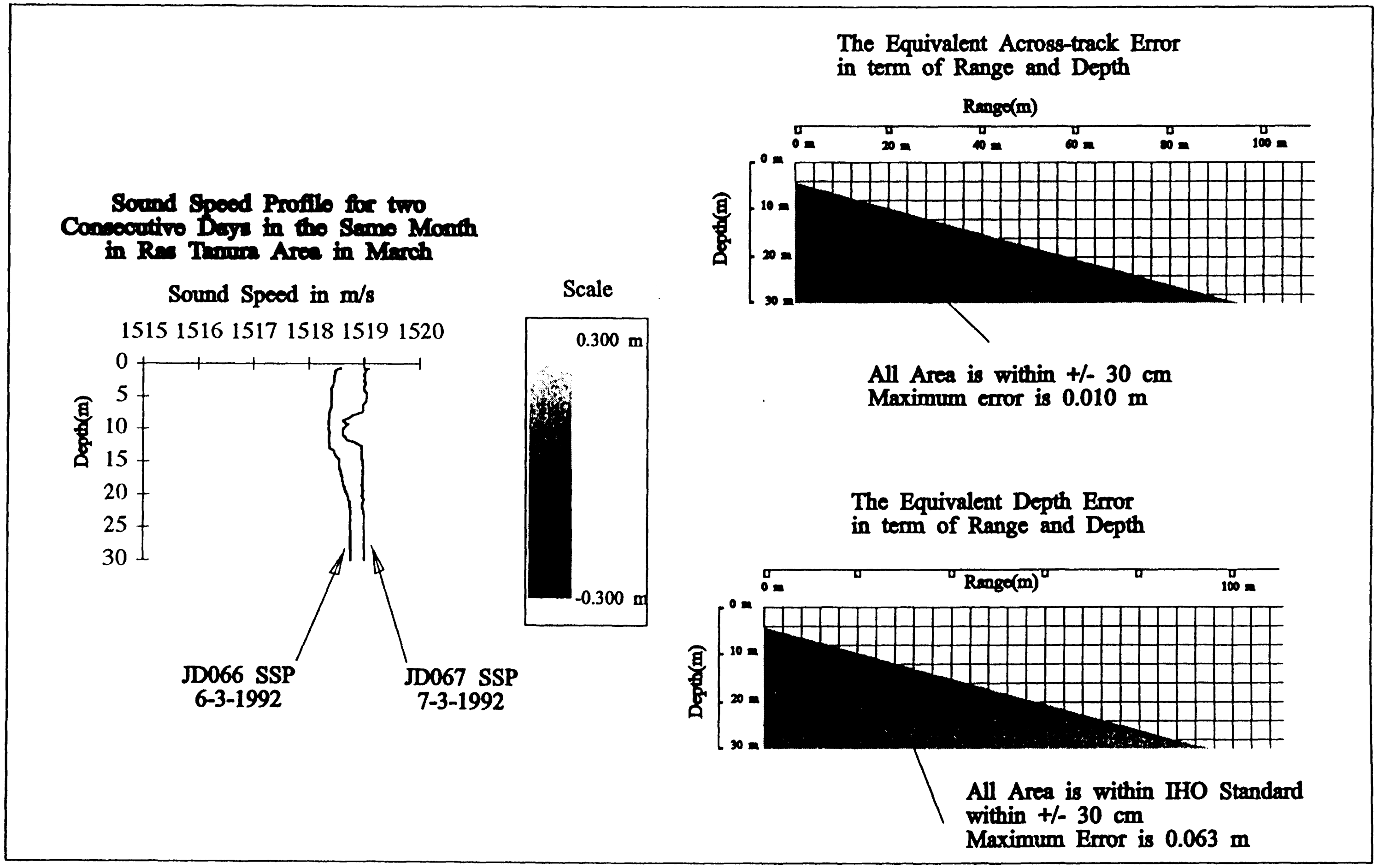

Figure 4-44
The effect of applying one SSP over another SSP for the next day in Ras Tanura in March, both SSPs are normal, for 4.3 m draft case.

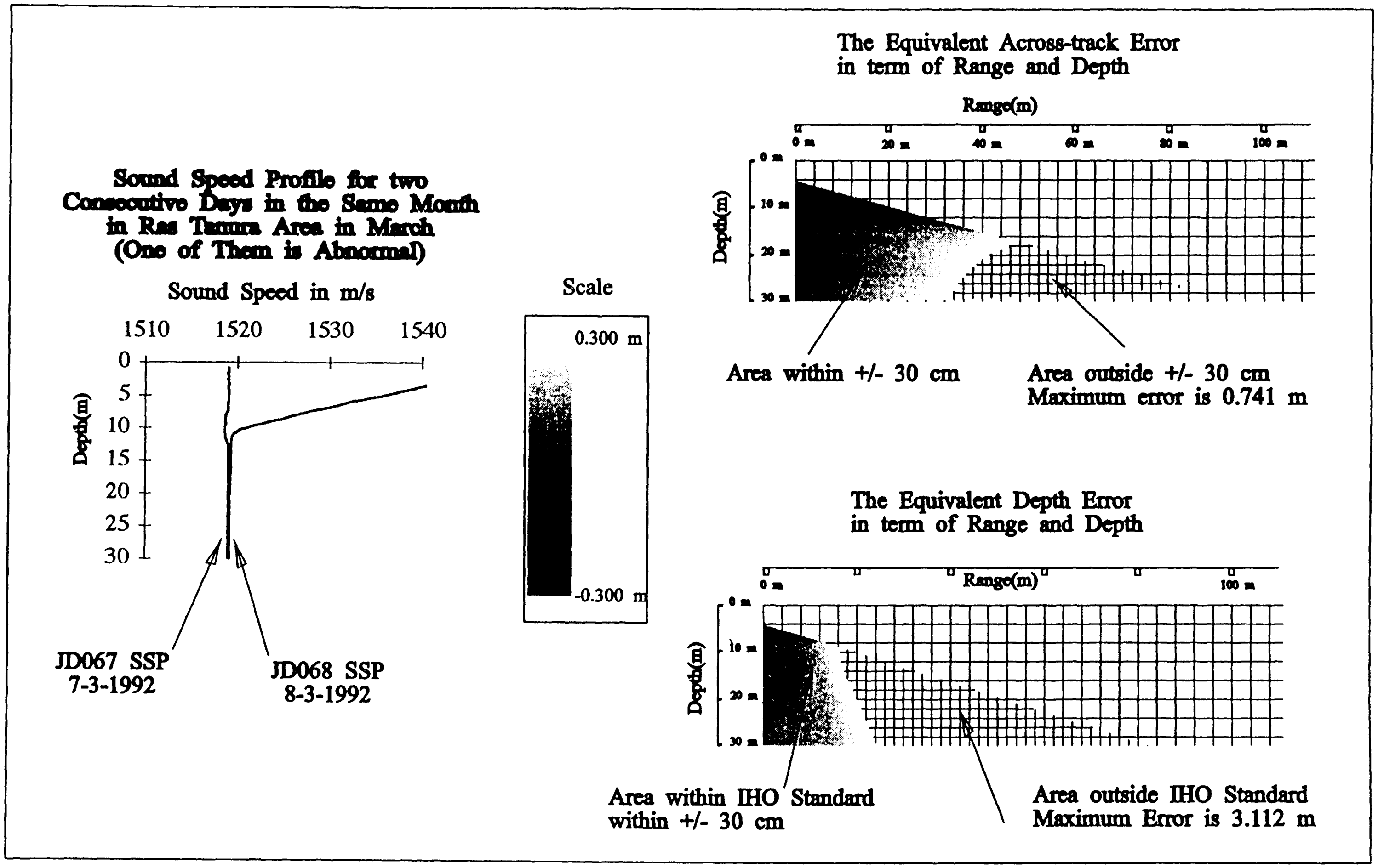

Figure 4-45
The effect of applying one SSP over another SSP for the next day in Ras Tanura in March, one SSP is abnormal, for 4.3 m draft case.

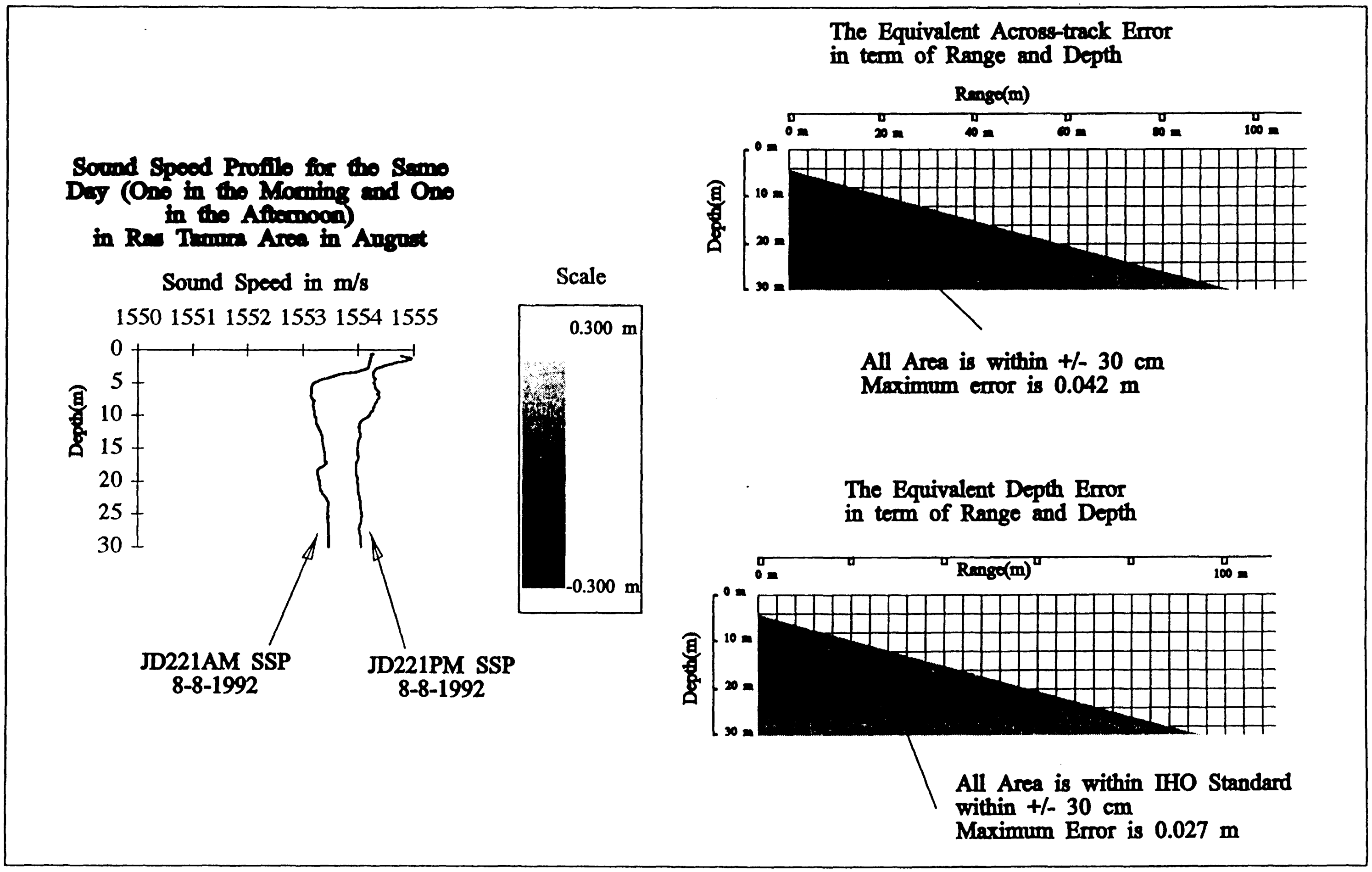

Figure 4-46
The effect of applying one SSP in the morning over another SSP in the afternoon in the same day in Ras Tanura in August, one SSP is abnormal, for 4.3 m draft case.

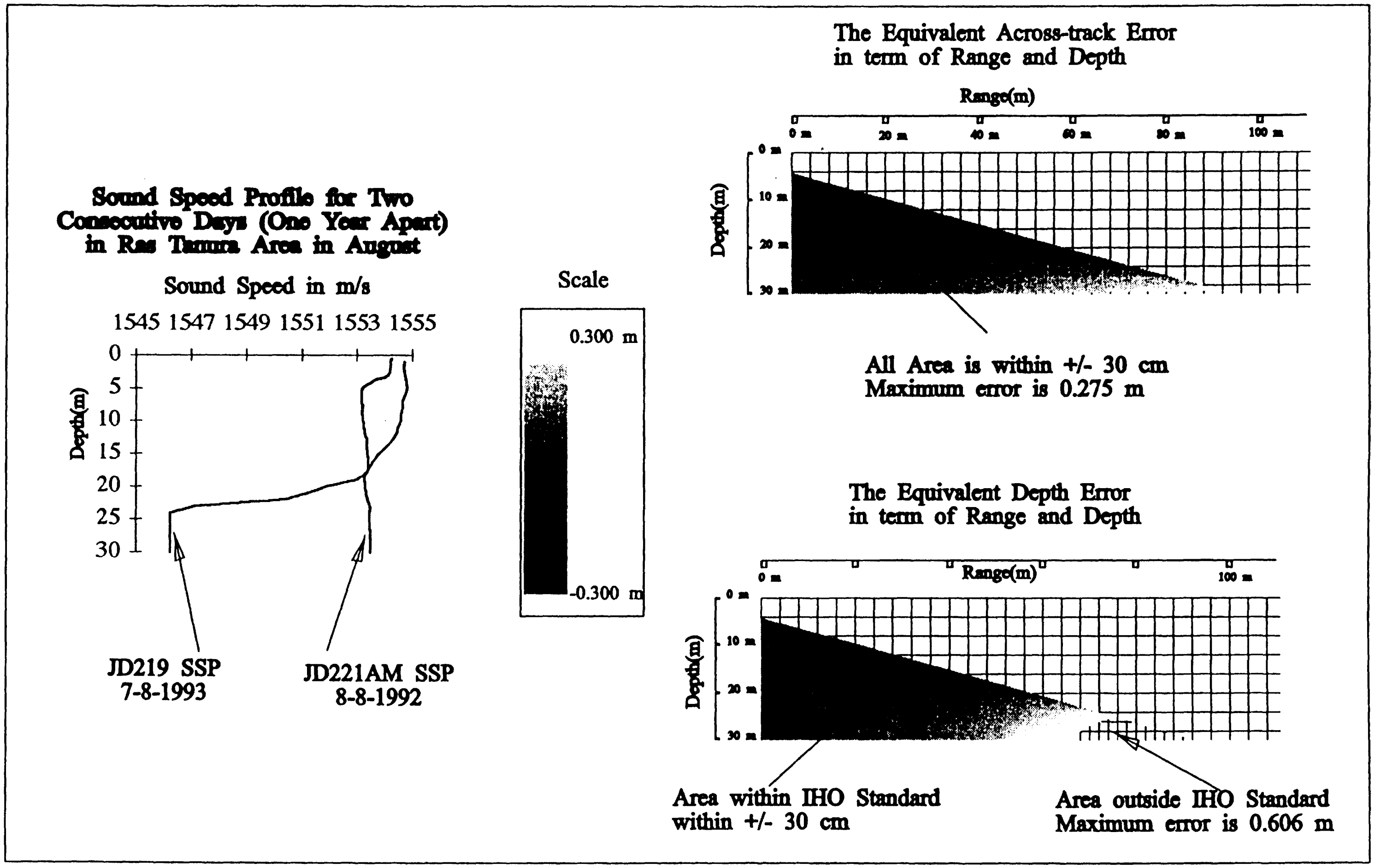

Figure 4-47
The effect of applying one SSP in the morning over another SSP in the morning of the previous day one year later in Ras Tanura in August, one SSP is abnormal, for 4.3 m draft case.

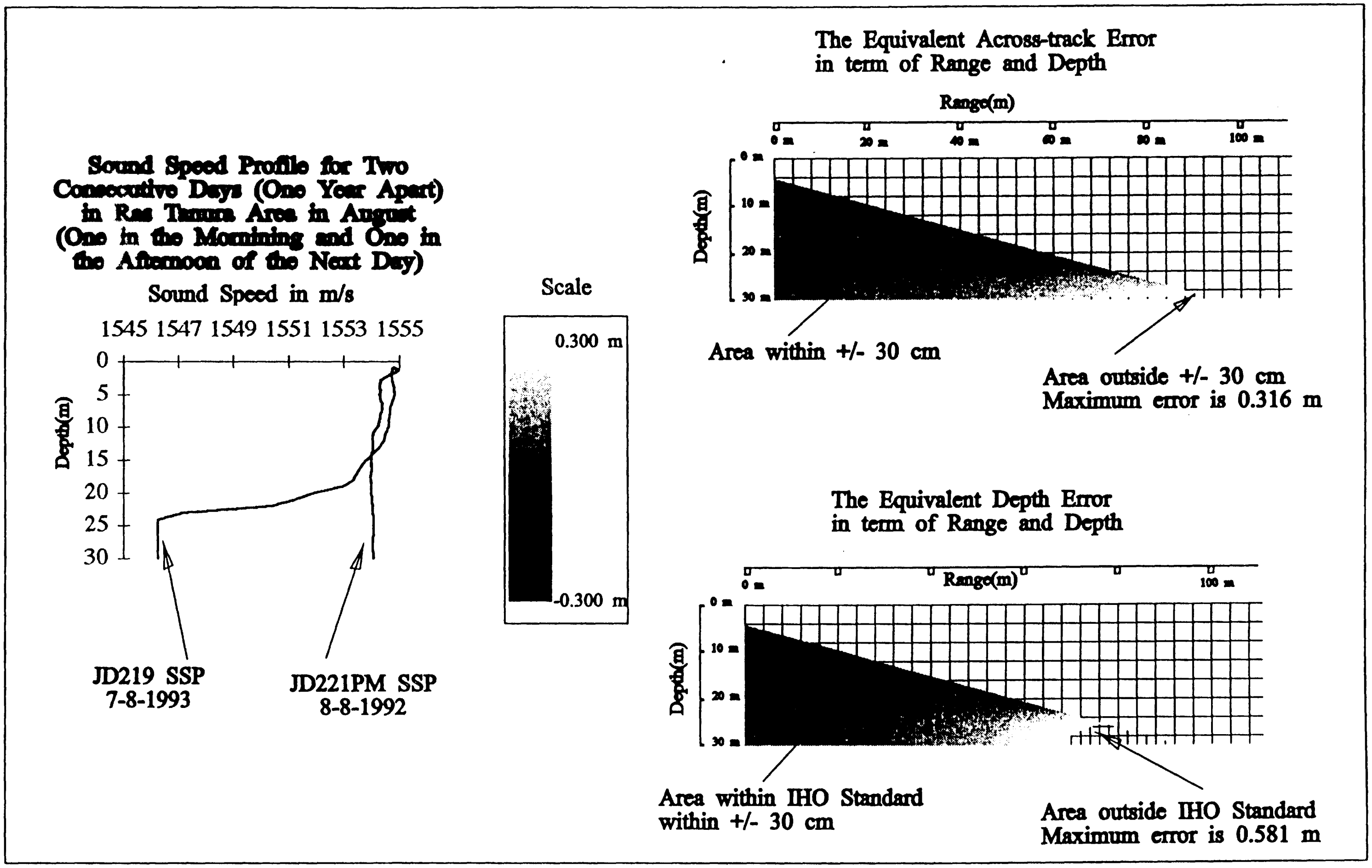

Figure 4-48
The effect of applying one SSP in the morning over another SSP in the morning of the previous day one year later in Ras Tanura in August, one SSP is abnormal, for 4.3 m draft case.

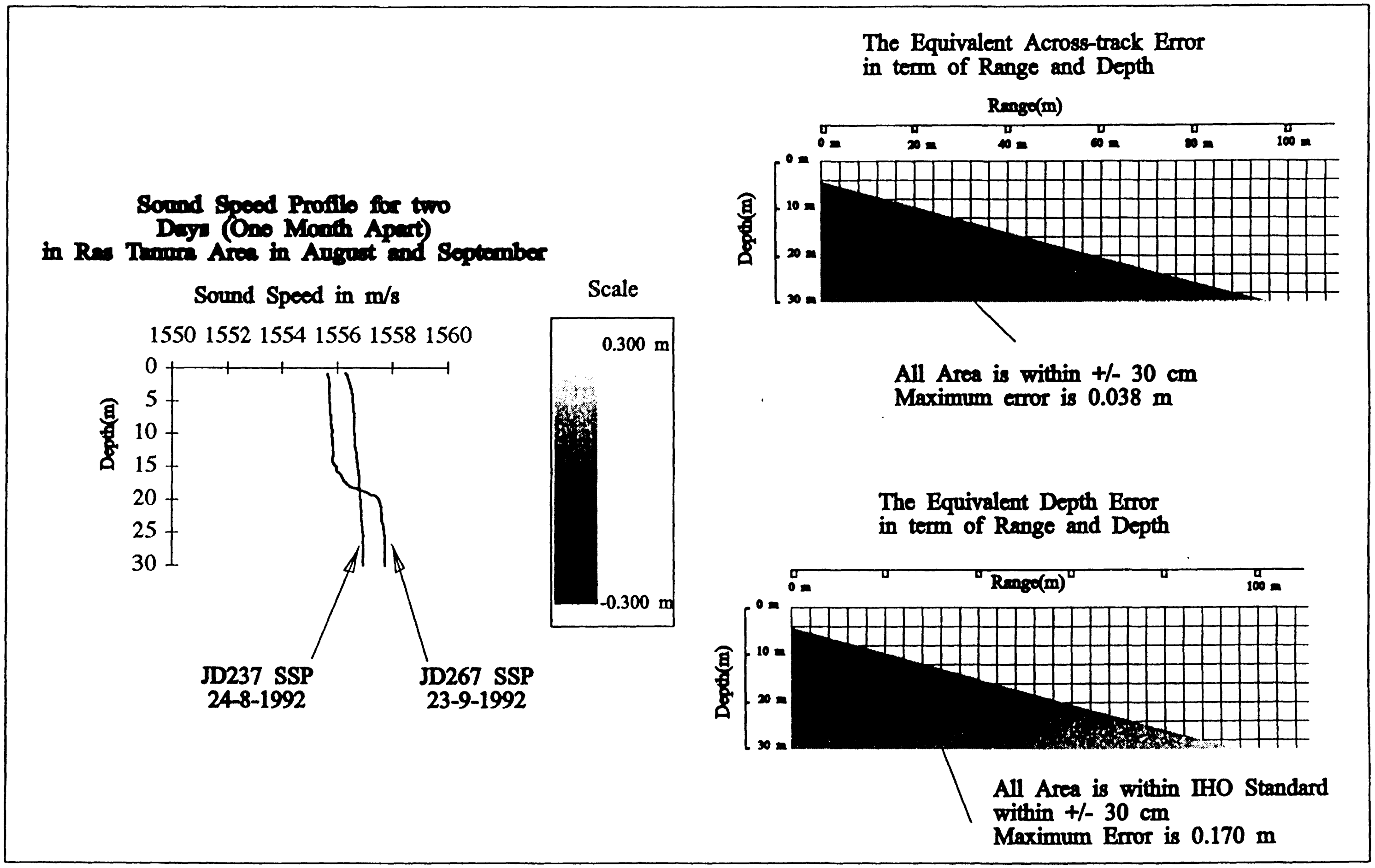

Figure 4-49
The effect of applying one SSP over another SSP a month later in Ras Tanura in August and September, both SSPs are normal, for 4.3 m draft case.

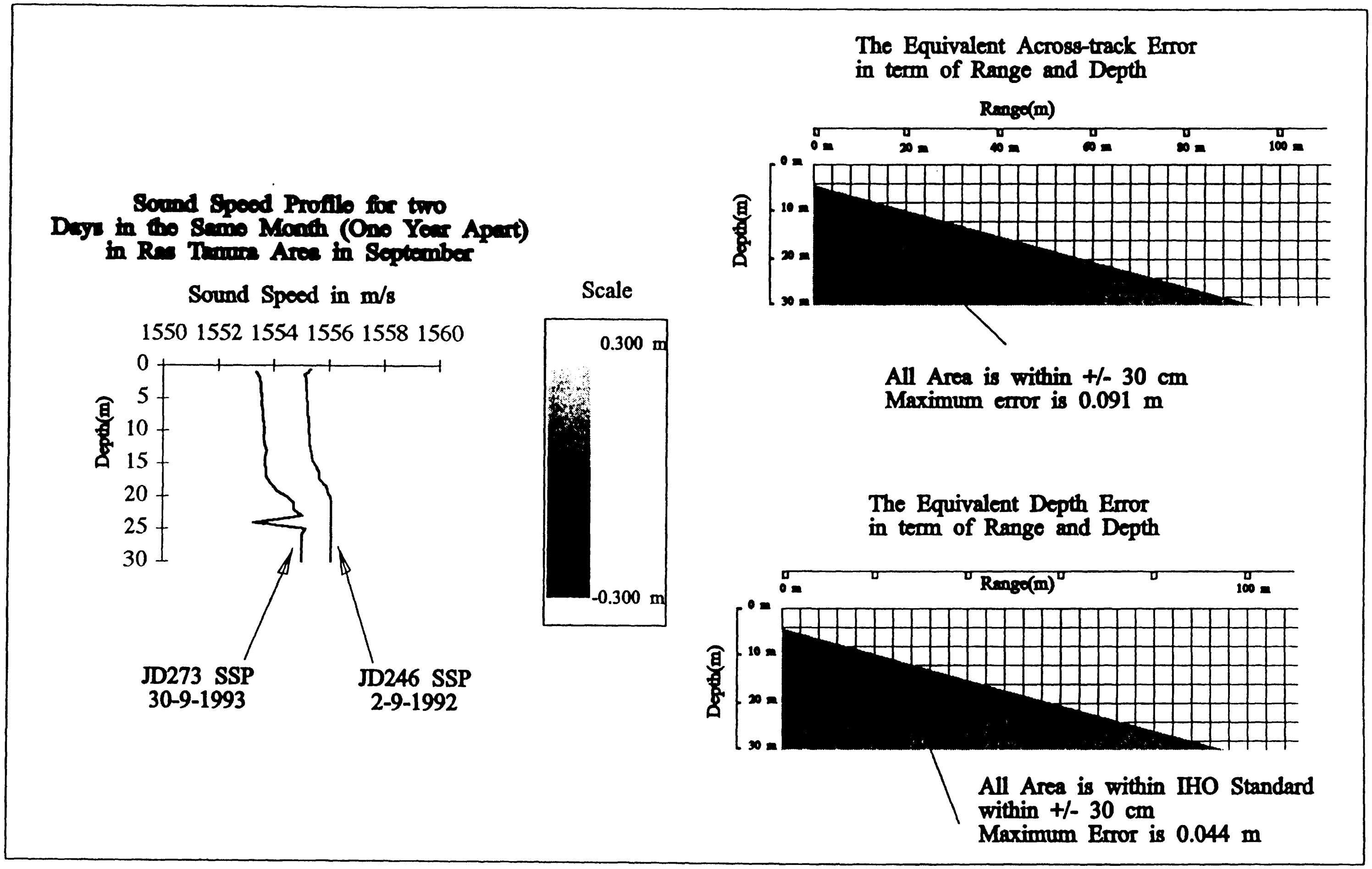

Figure 4-50
The effect of applying one SSP in the beginning of the month over another SSP at the end of the month in Ras Tanura in September, both SSPs are normal, for 4.3 m draft case.

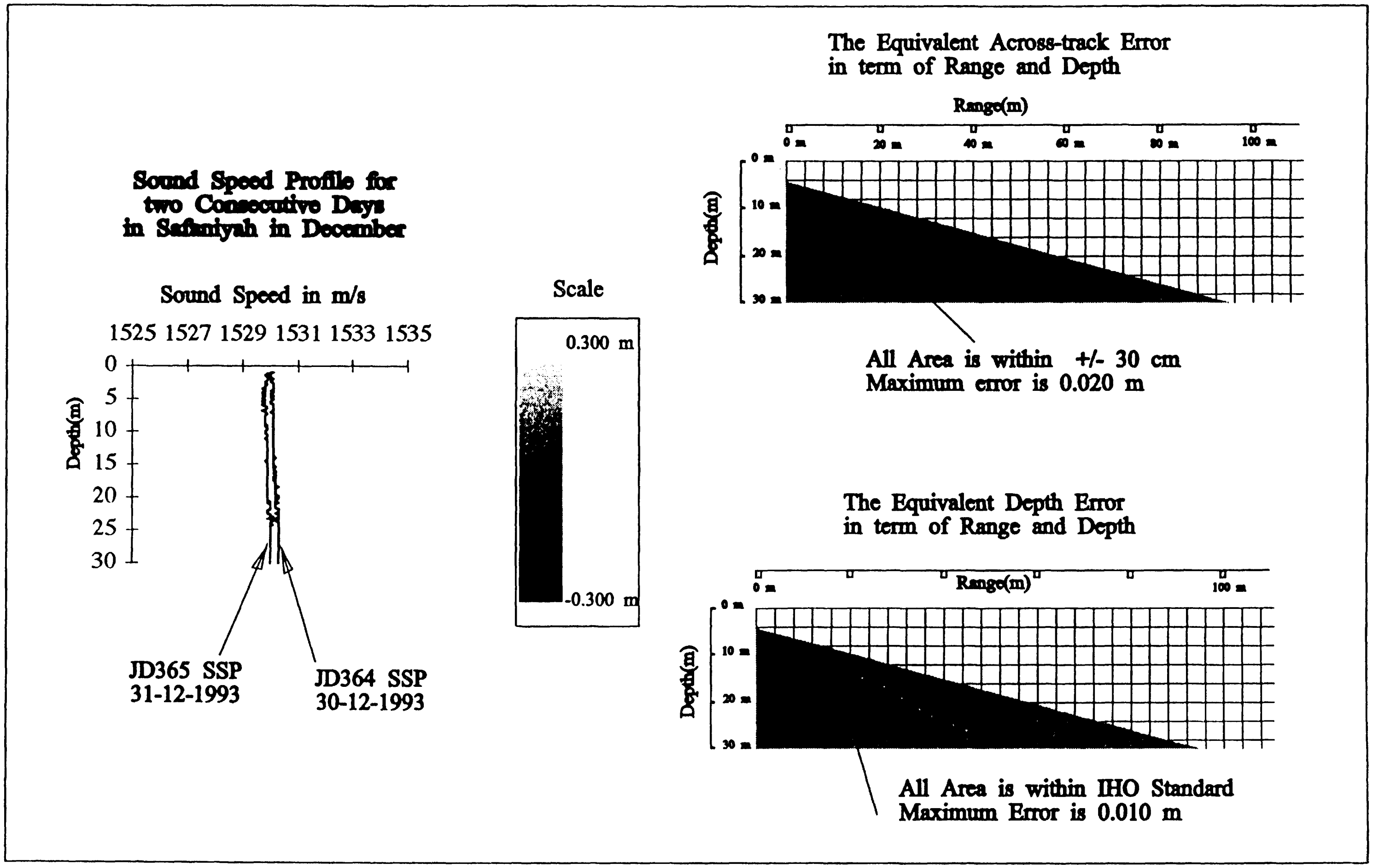

Figure 4-51
The effect of applying one SSP over another SSP for the next day in Safaniyah in December, both SSPs are normal, for 4.3 m draft case.

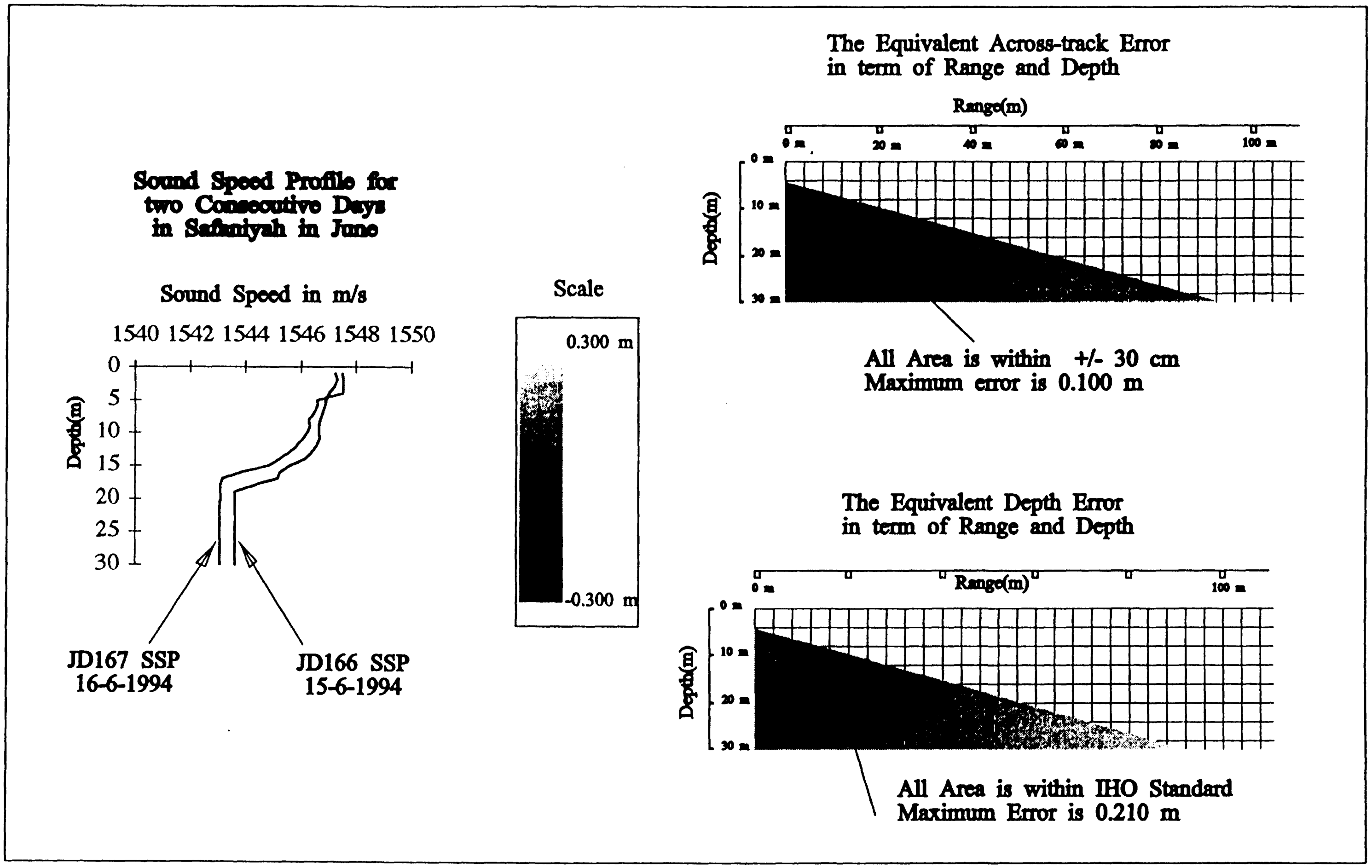

Figure 4-52
The effect of applying one SSP over another SSP for the next day in Safaniyah in June, both SSPs are abnormal, for 4.3 m draft case.

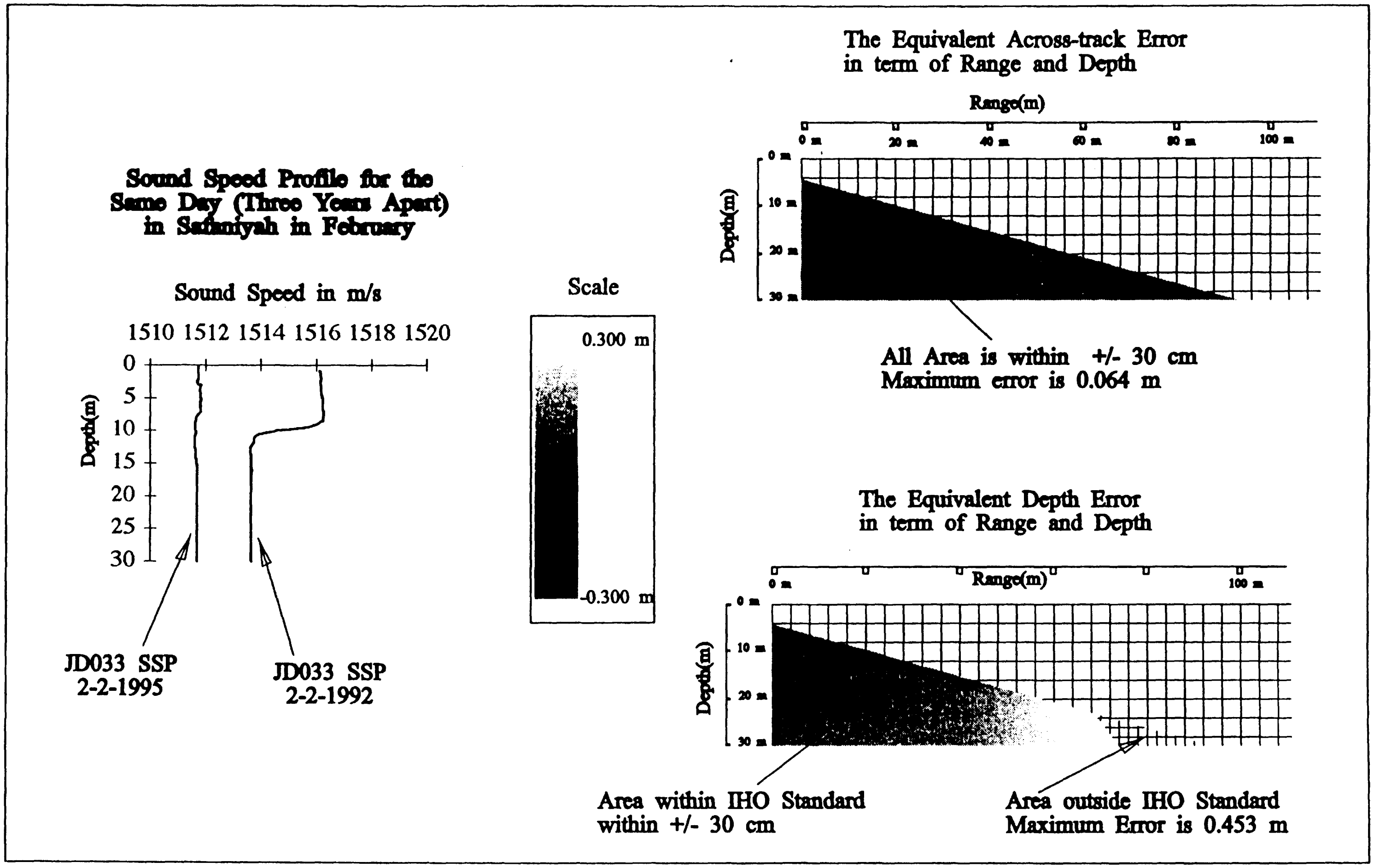

Figure 4-53
The effect of applying one SSP over another SSP for the same day three years later in Safaniyah in February, one SSP is abnormal, for 4.3 m draft case.

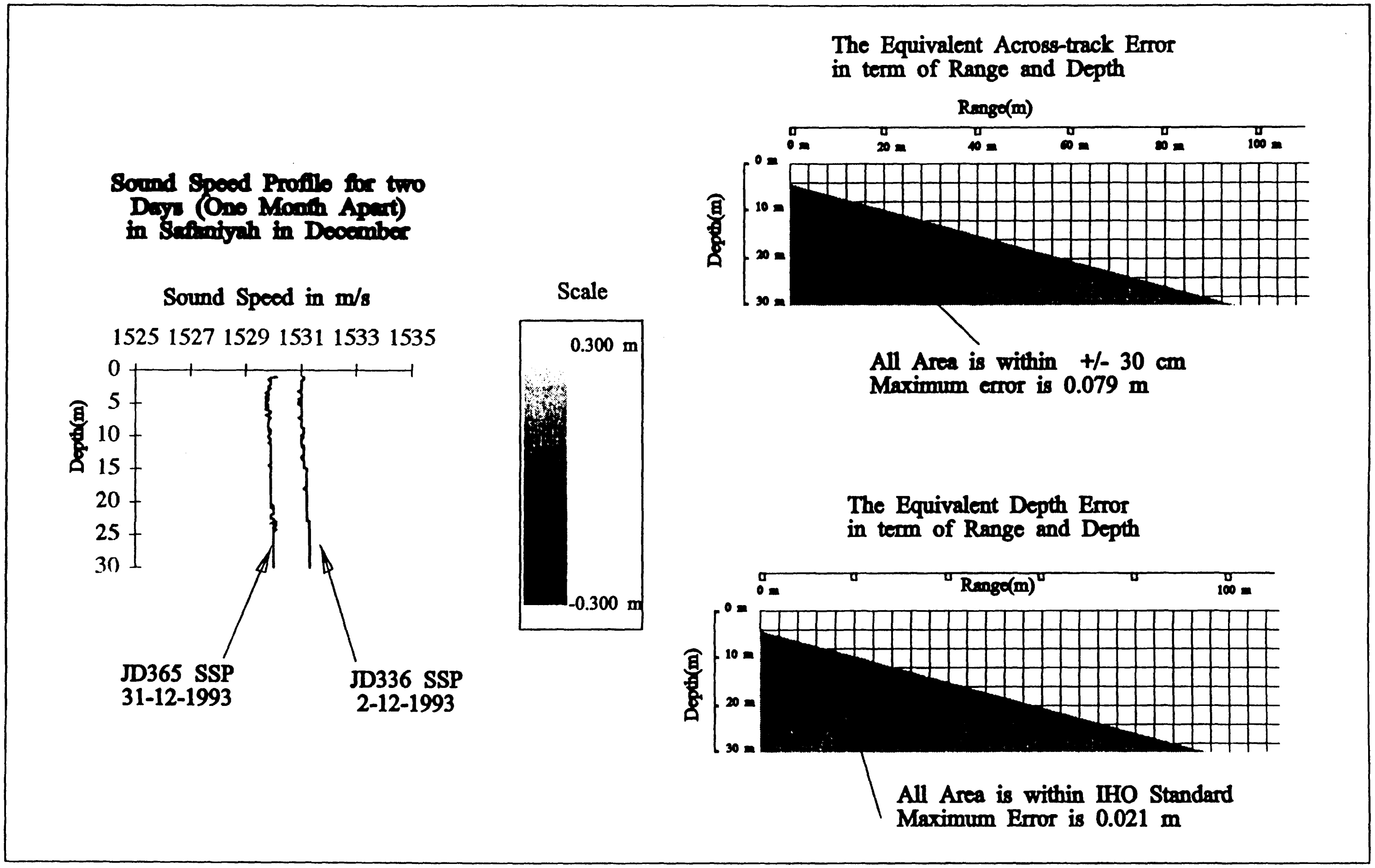

Figure 4-54
The effect of applying one SSP in the beginning of the month over another SSP at the end of the month in Safaniyah in December, both SSPs are normal, for 4.3 m draft case.

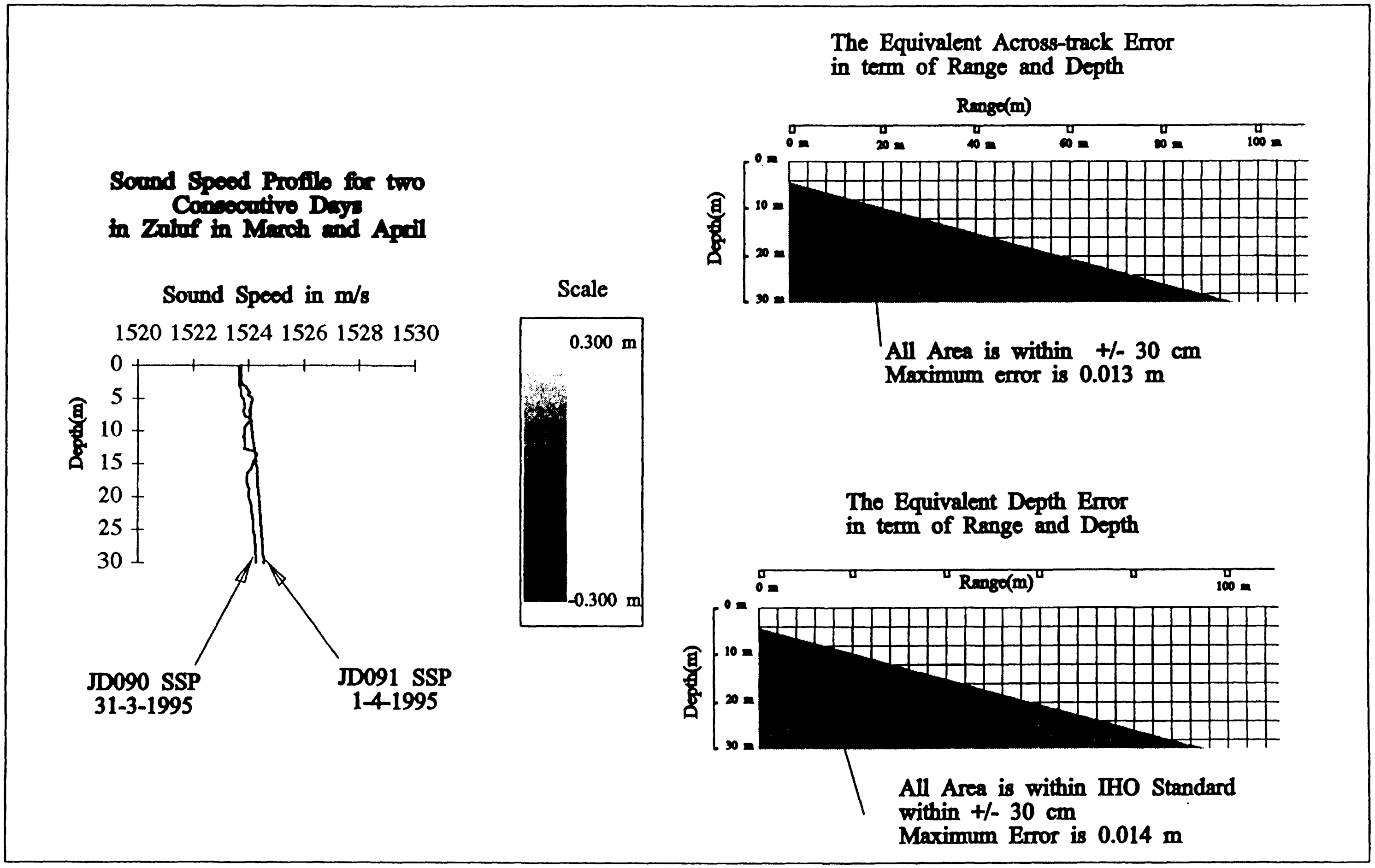

Figure 4-55
The effect of applying one SSP over another SSP for the next day in Zuluf in March and April, both SSPs are normal, for 4.3 m draft case.

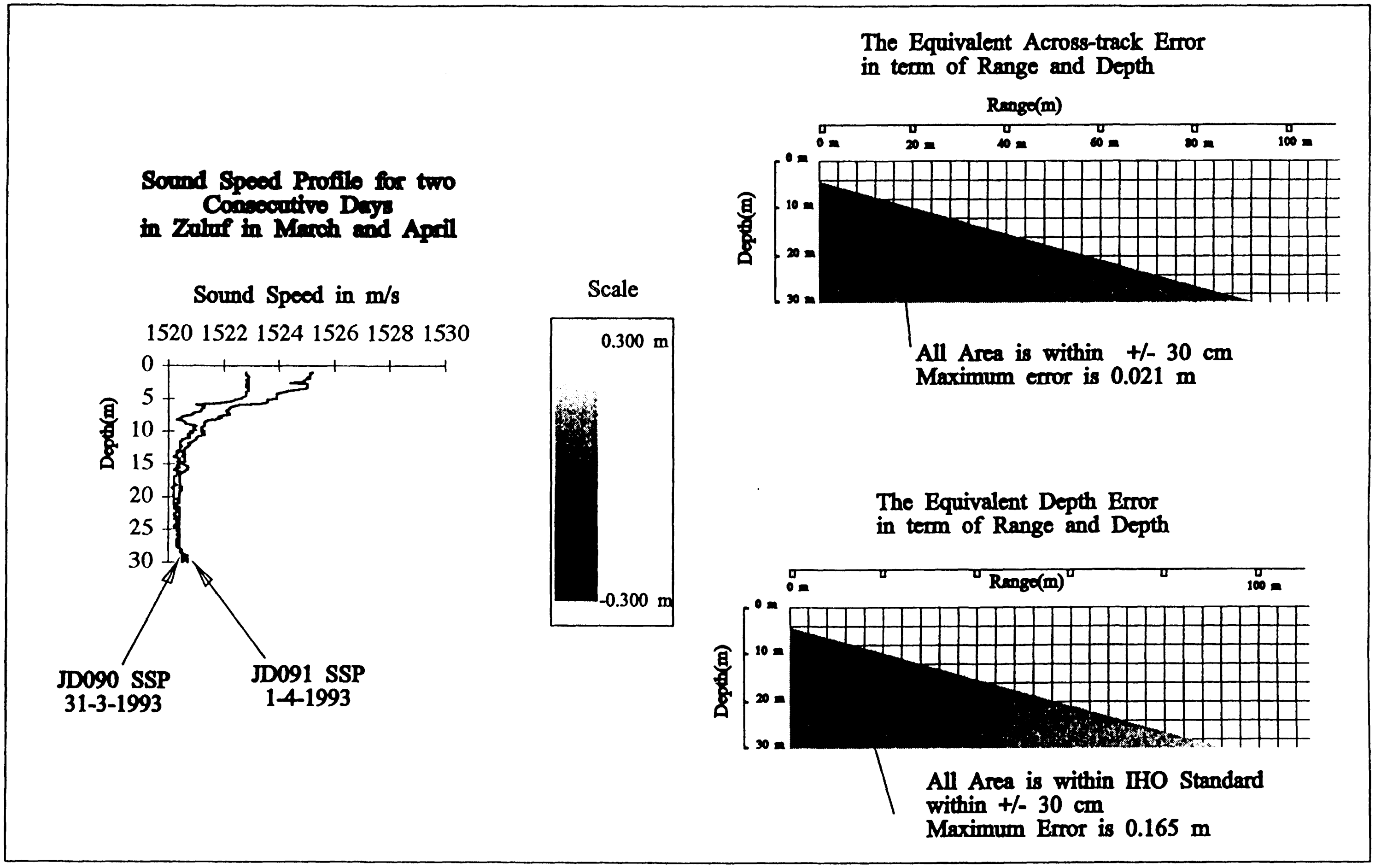

Figure 4-56
The effect of applying one SSP over another SSP for the next day in Zuluf in March and April, both SSPs are abnormal, for 4.3 m draft case.

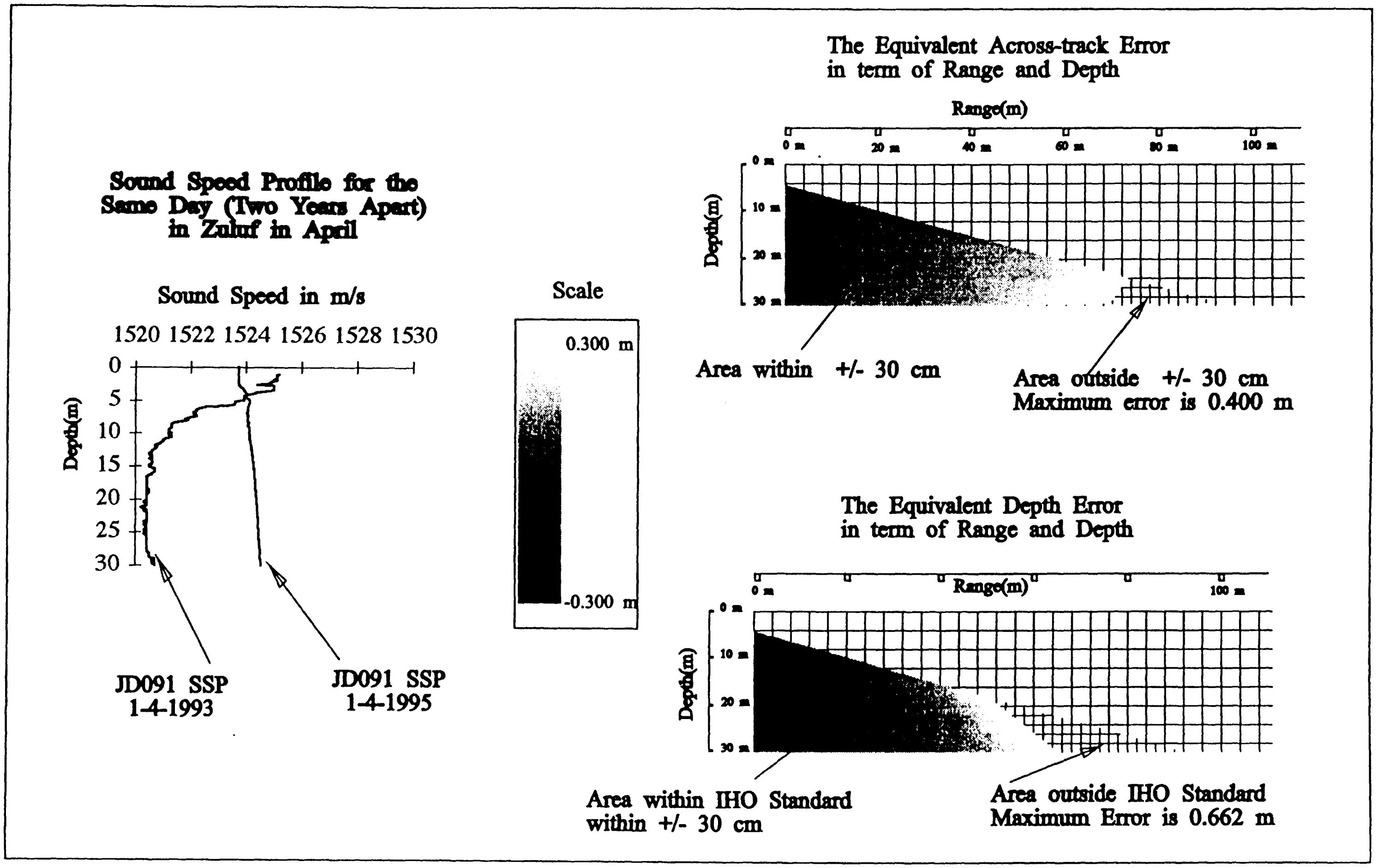

Figure 4-57
The effect of applying one SSP over another SSP for the same day two years later in Zuluf in April, one SSP is abnormal, for 4.3 m draft case.

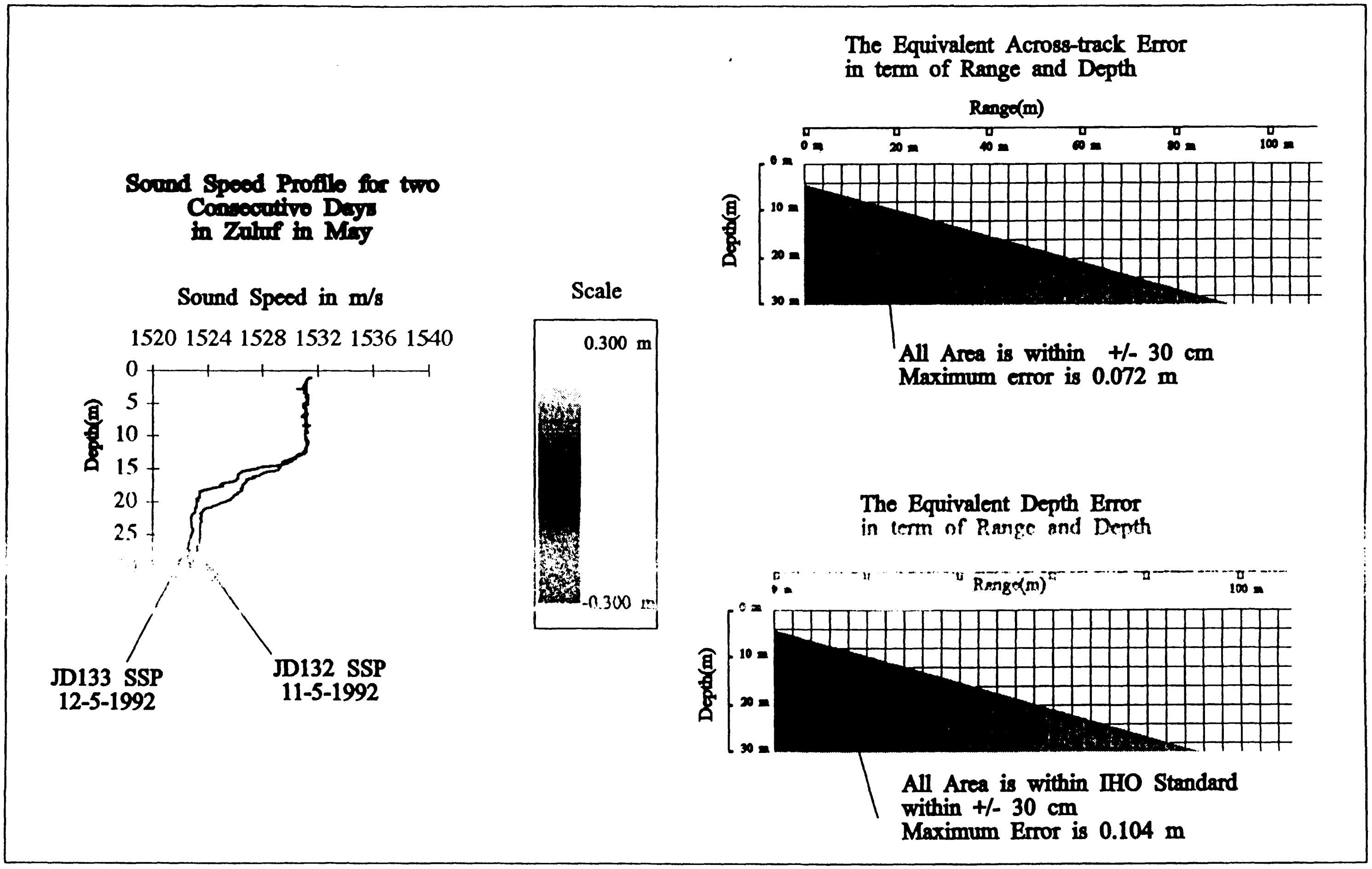

Figure 4-58
The effect of applying one SSP over another SSP for the next day in Zuluf in May, both SSPs are abnormal, for 4.3 m draft case.

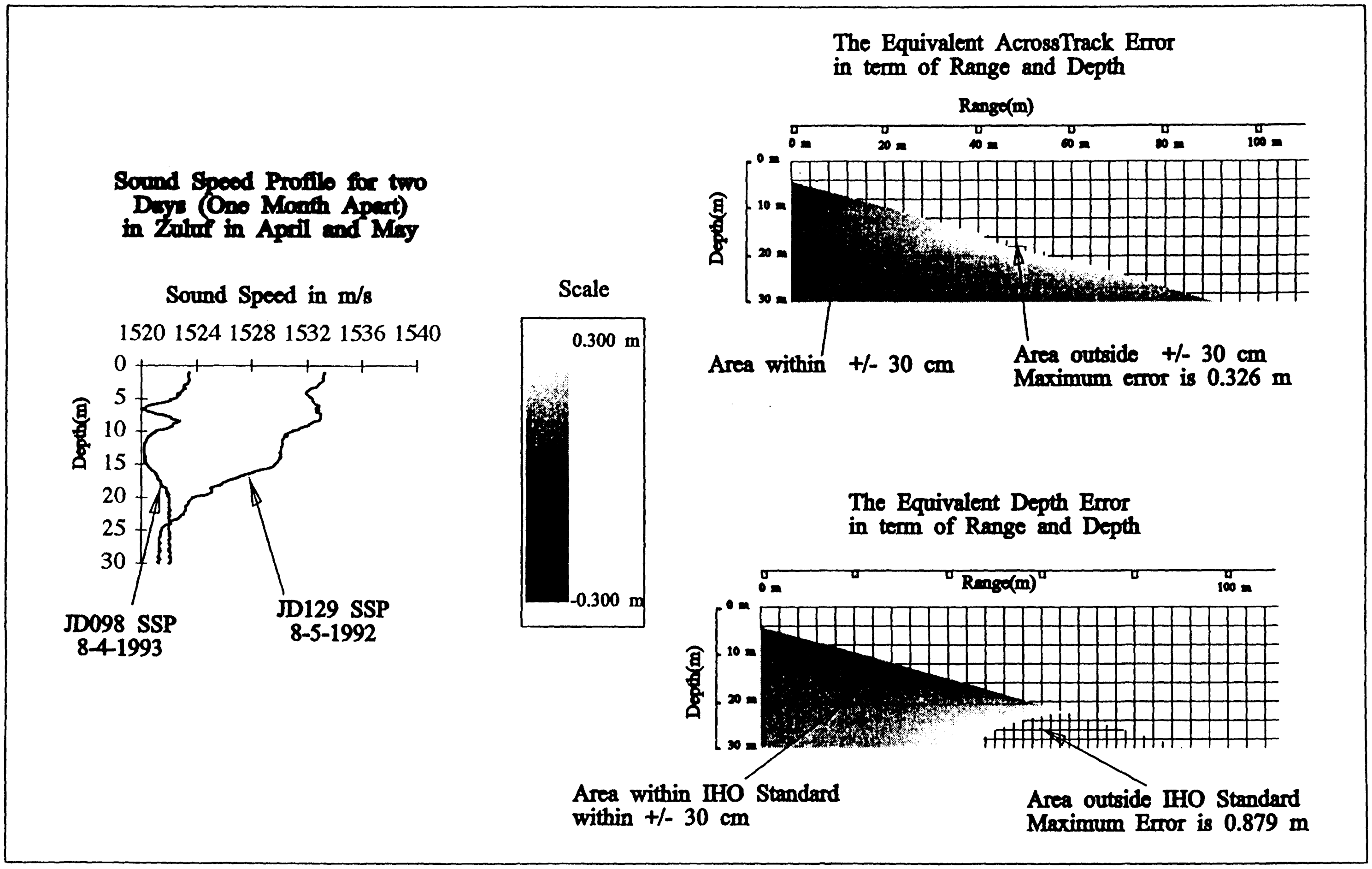

Figure 4-59
The effect of applying one SSP over another SSP one month later in Zuluf in April and May, both SSPs are abnormal, for 4.3 m draft case.

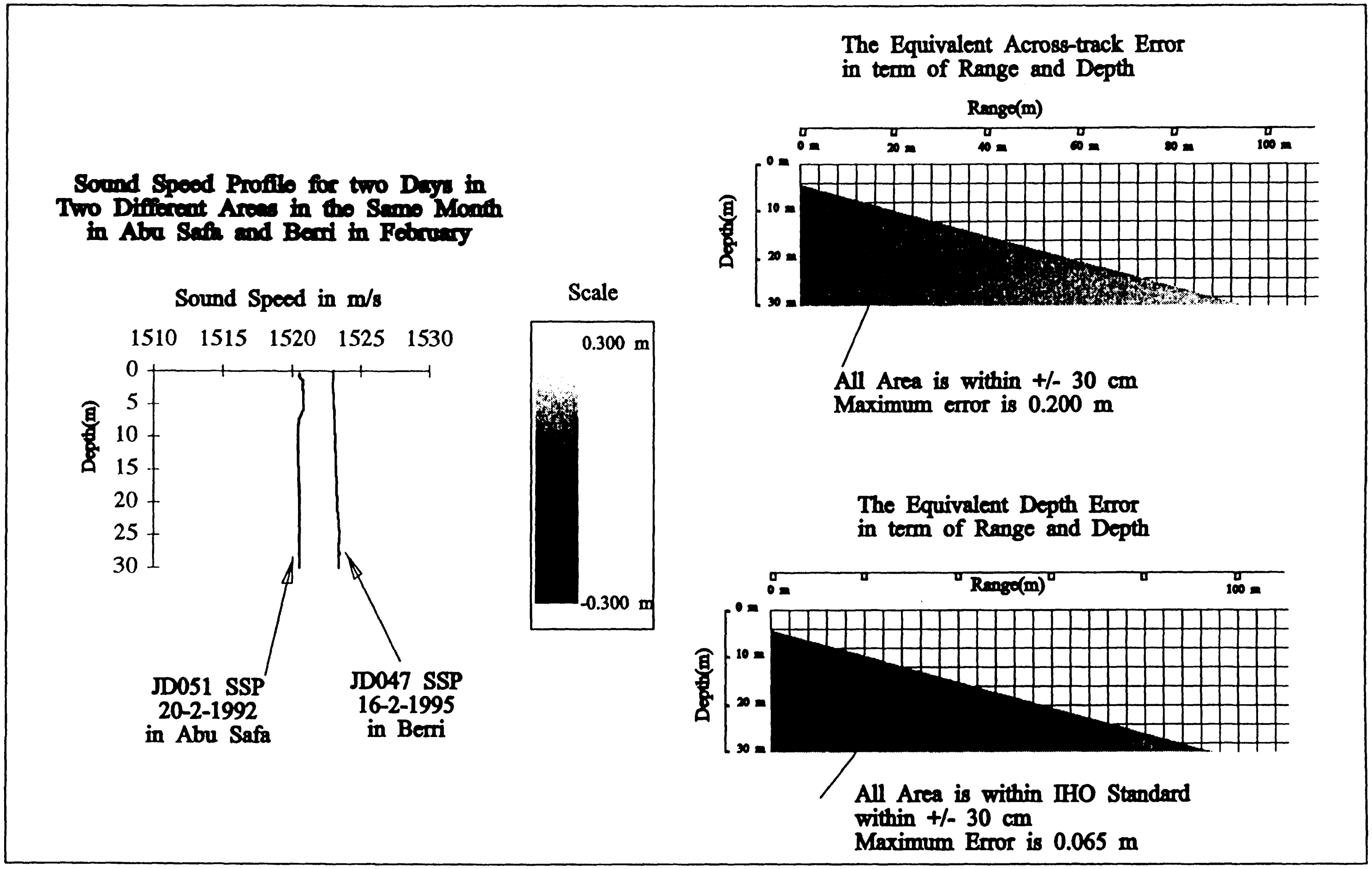

Figure 4-60
The effect of applying one SSP in Abu Safa over another SSP in Berri in February, both SSPs are normal, for 4.3 m draft case.

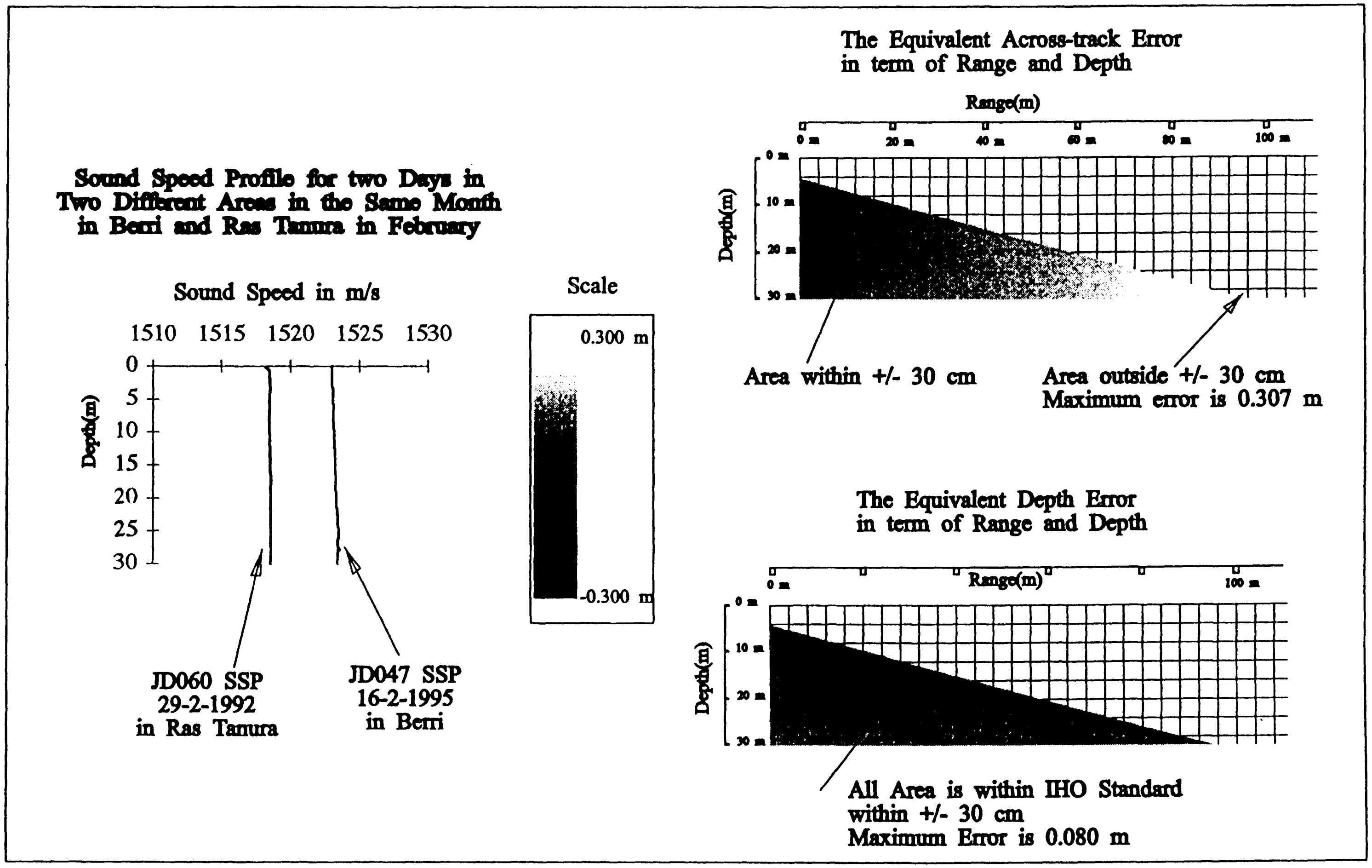

Figure 4-61
The effect of applying one SSP in Berri over another SSP in Ras Tanura in February, both SSPs are normal, for 4.3 m draft case.

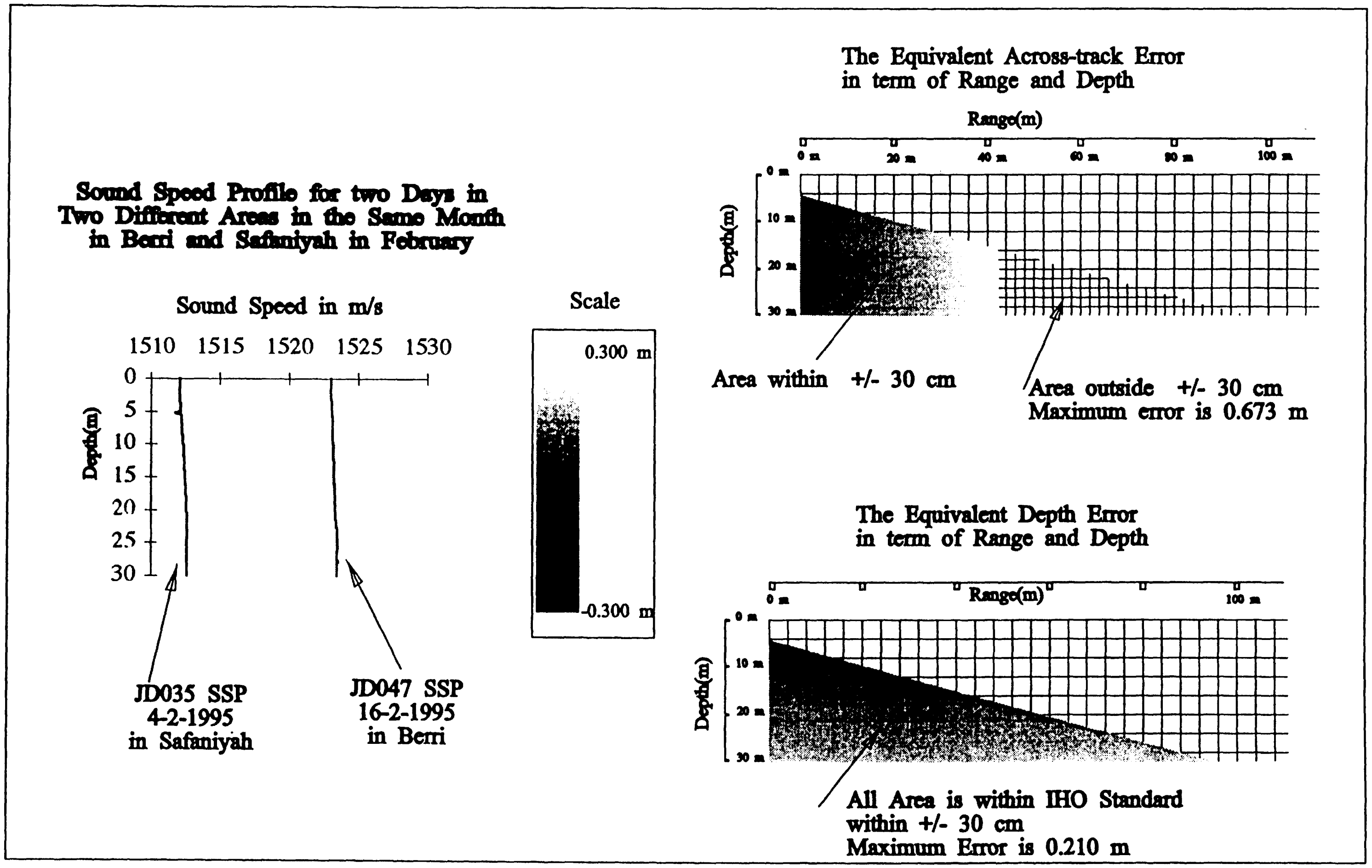

Figure 4-62
The effect of applying one SSP in Berri over another SSP in Safaniyah in February, both SSPs are normal, for 4.3 m draft case.

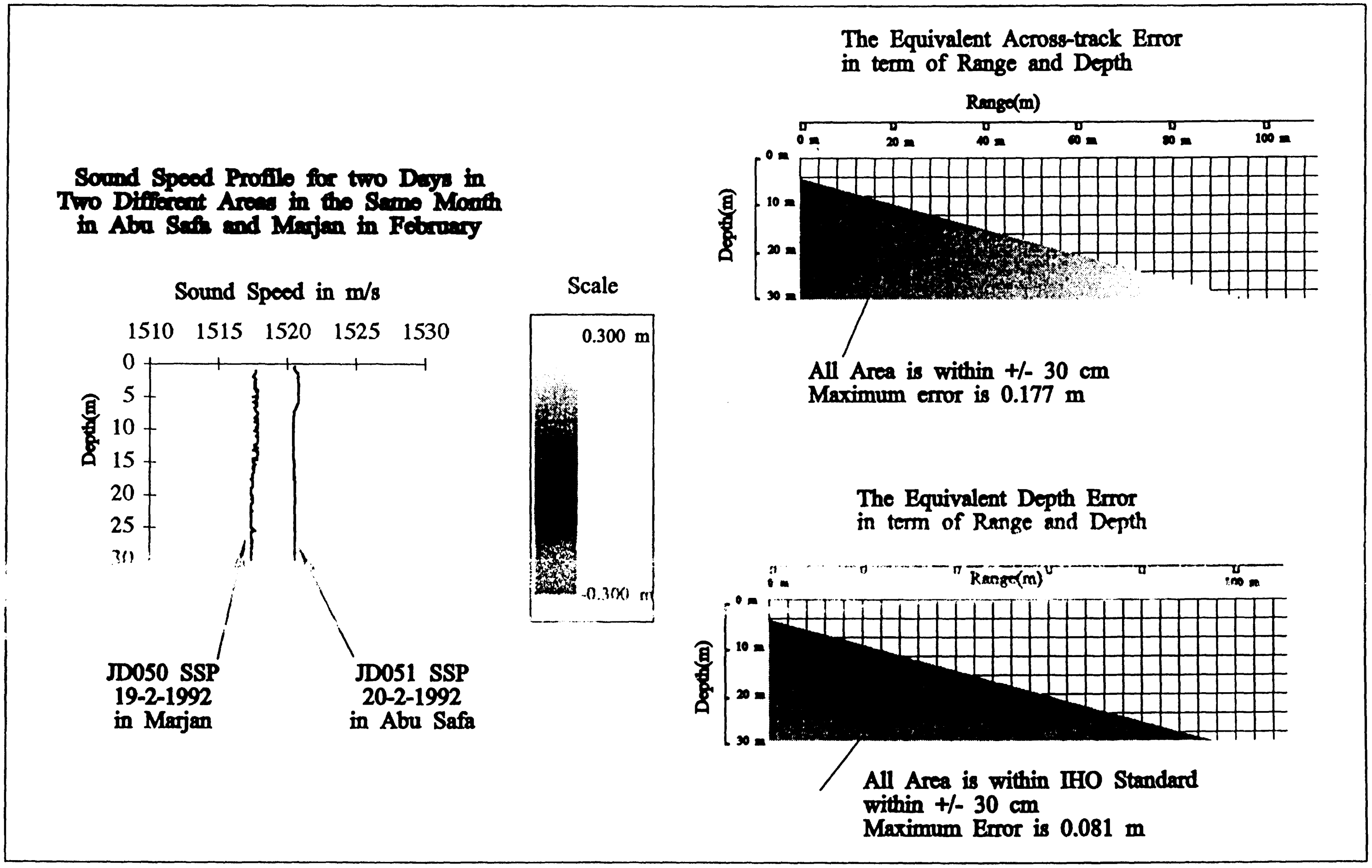

Figure 4-63
The effect of applying one SSP in Abu Safa over another SSP in Marjan in February, both SSPs are normal, for 4.3 m draft case.

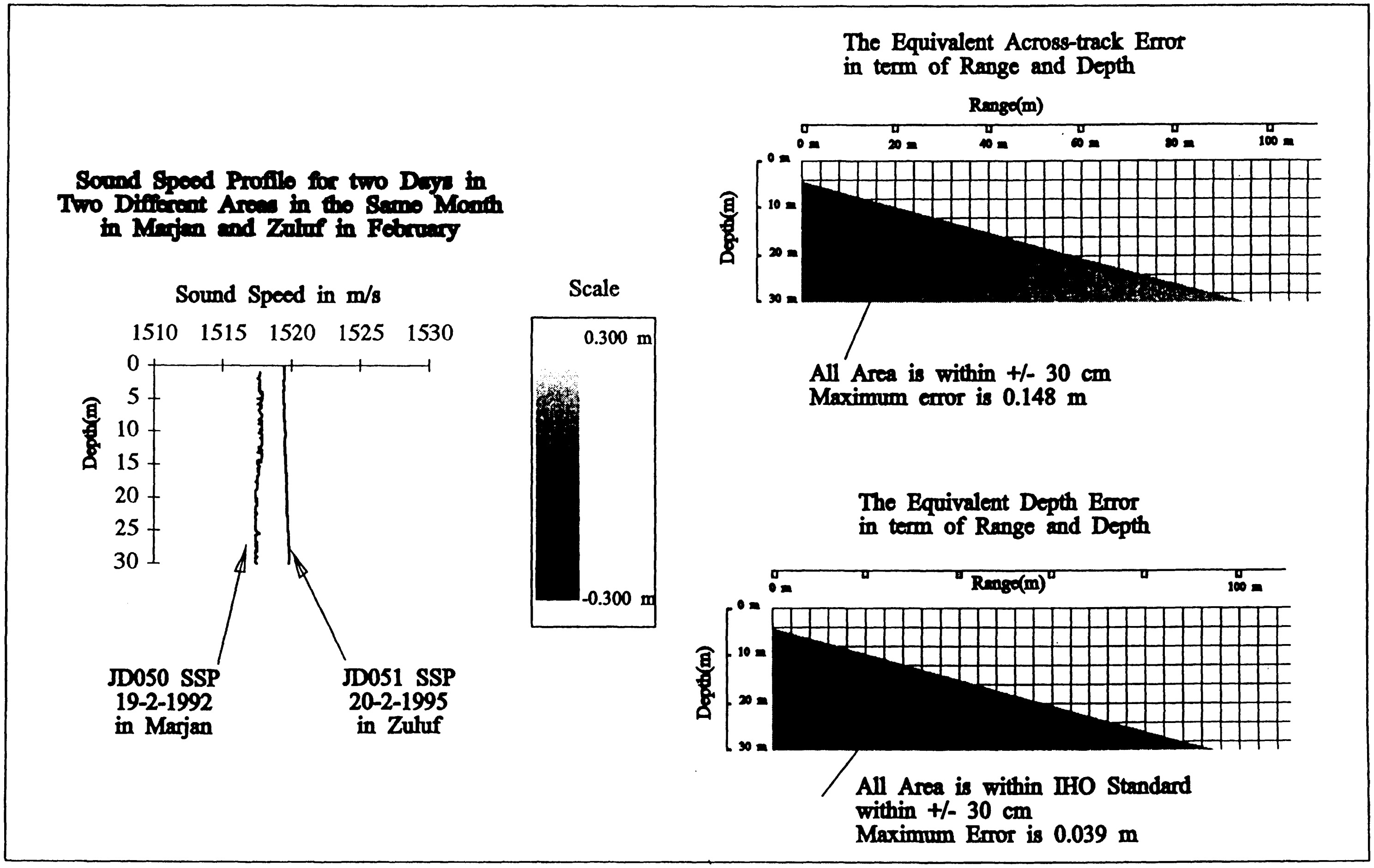

Figure 4-64
The effect of applying one SSP in Marjan over another SSP in Zuluf in February, both SSPs are normal, for 4.3 m draft case.

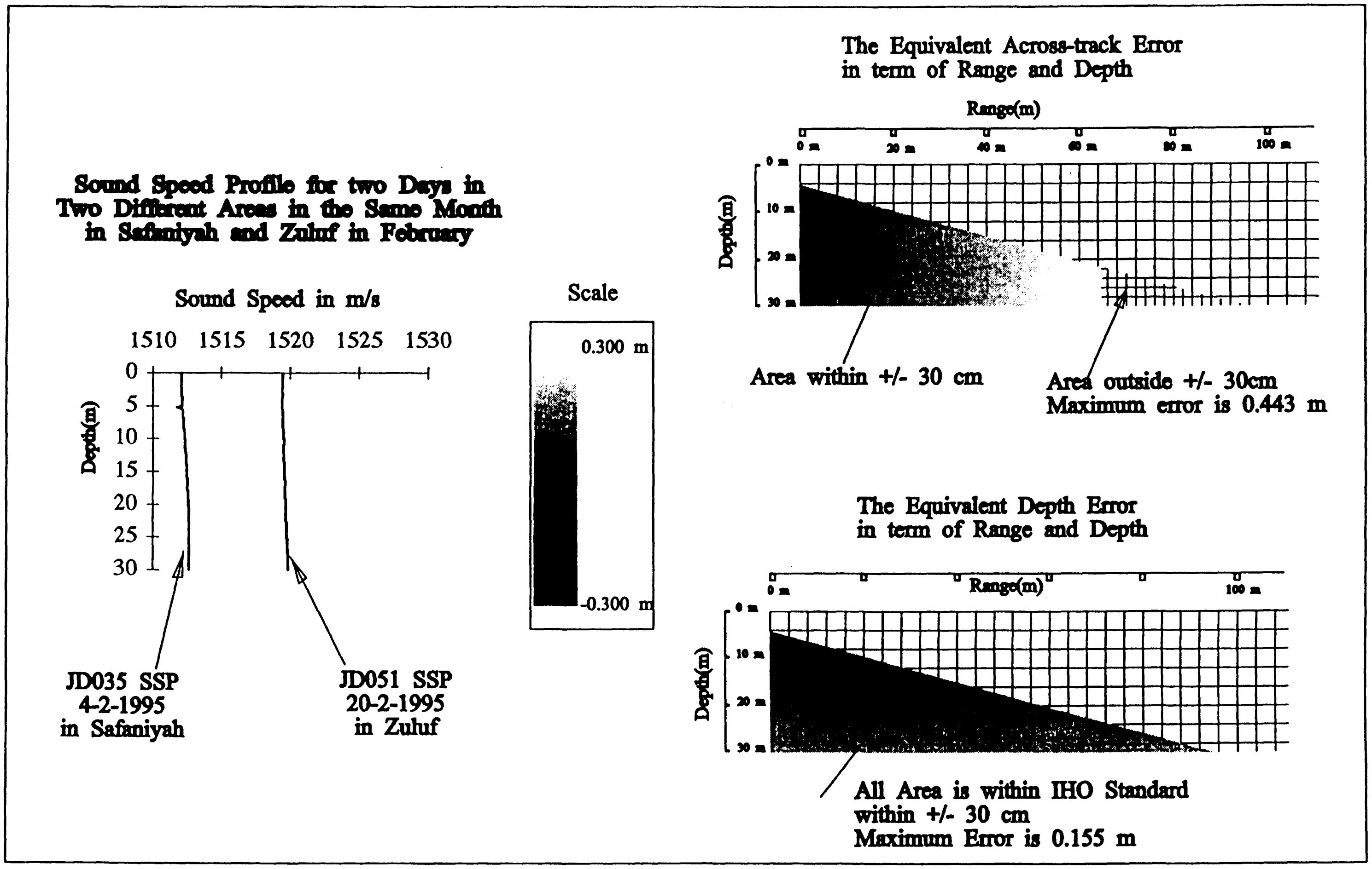

Figure 4-65
The effect of applying one SSP in Safaniyah over another SSP in Zuluf in February, both SSPs are normal, for 4.3 m draft case.

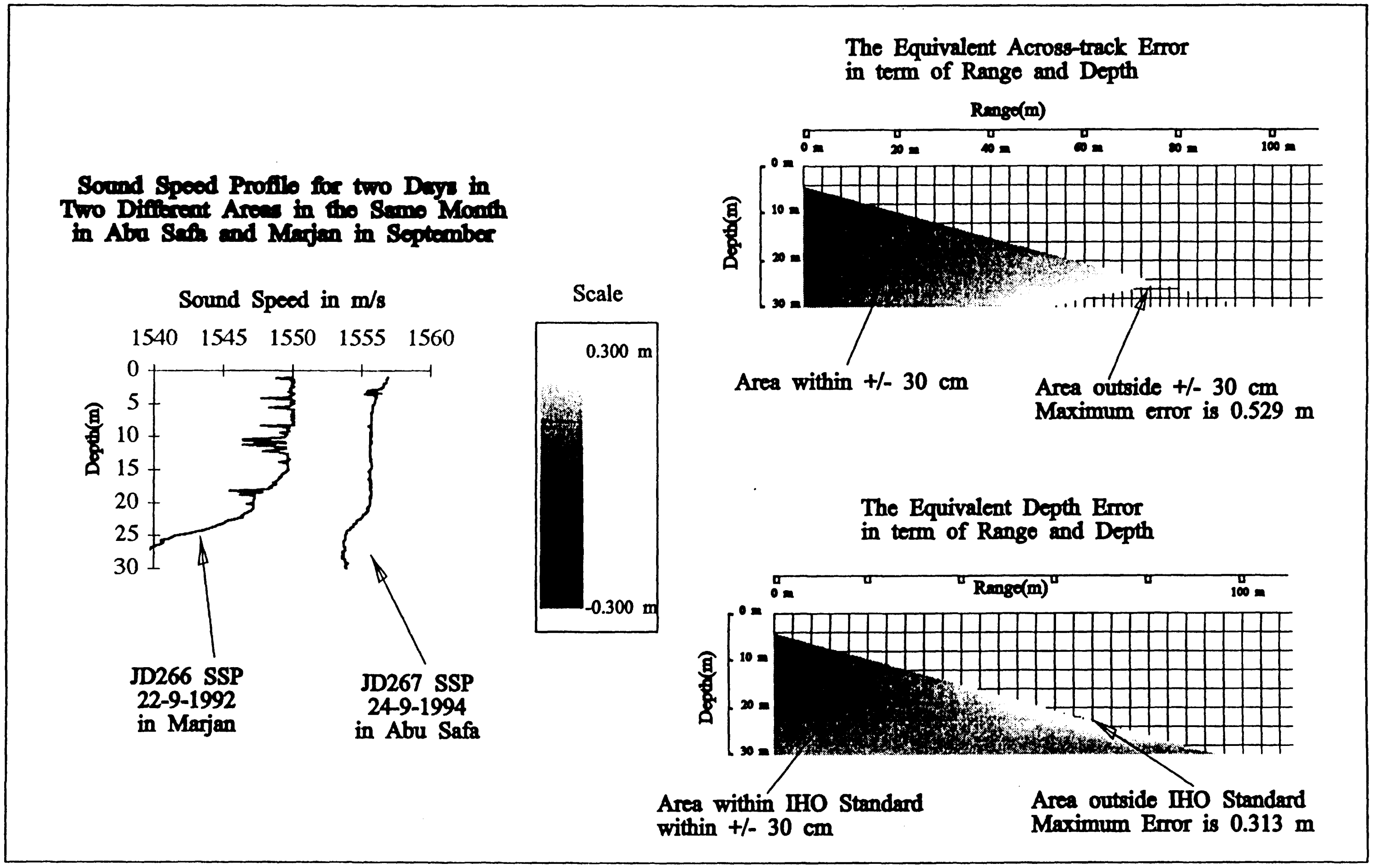

Figure 4-66
The effect of applying one SSP in Abu Safa over another SSP in Marjan in September, one SSP is abnormal, for 4.3 m draft case.

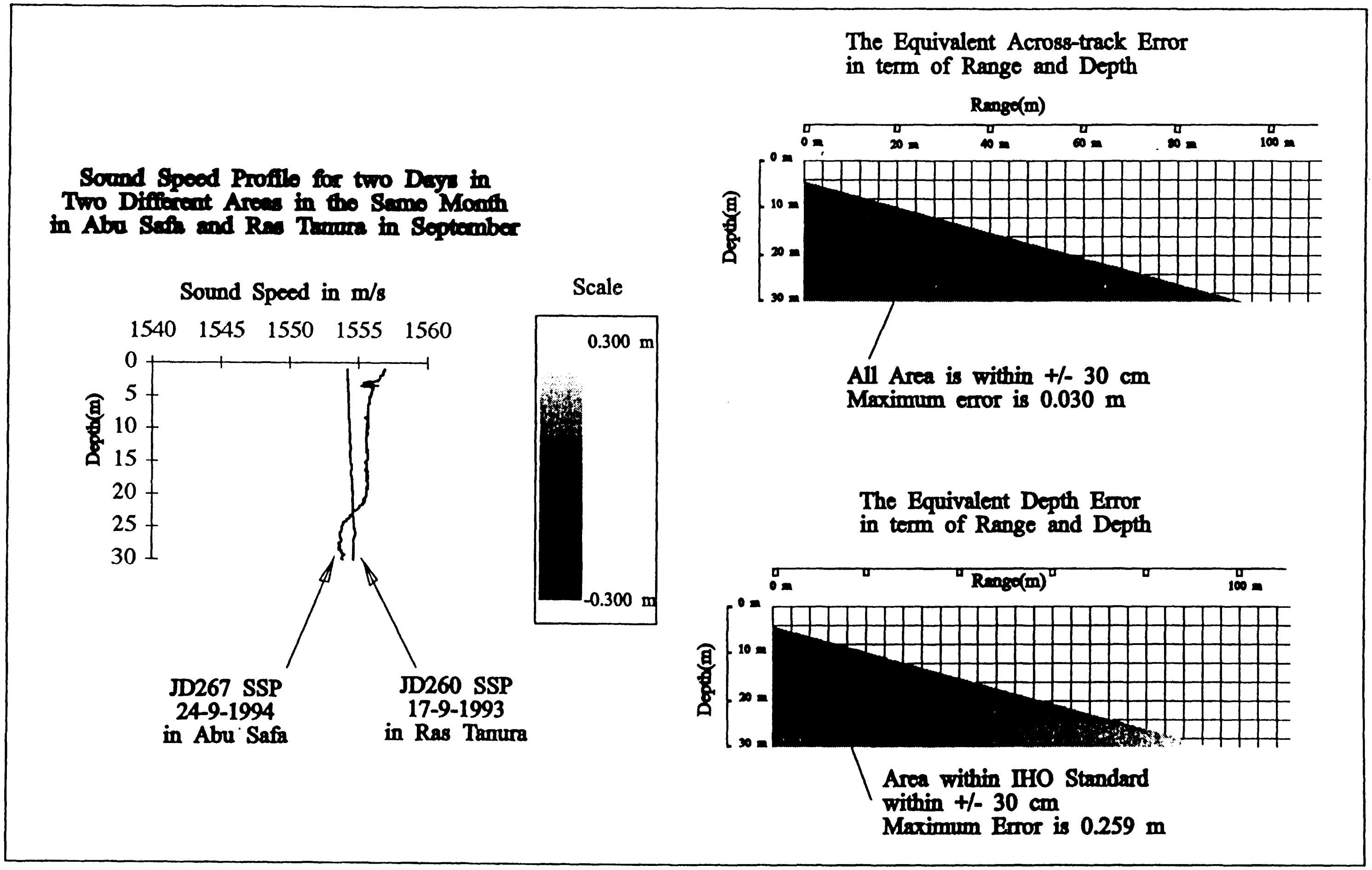

Figure 4-67
The effect of applying one SSP in Abu Safa over another SSP in Ras Tanura in September, both SSPs are normal, for 4.3 m draft case.

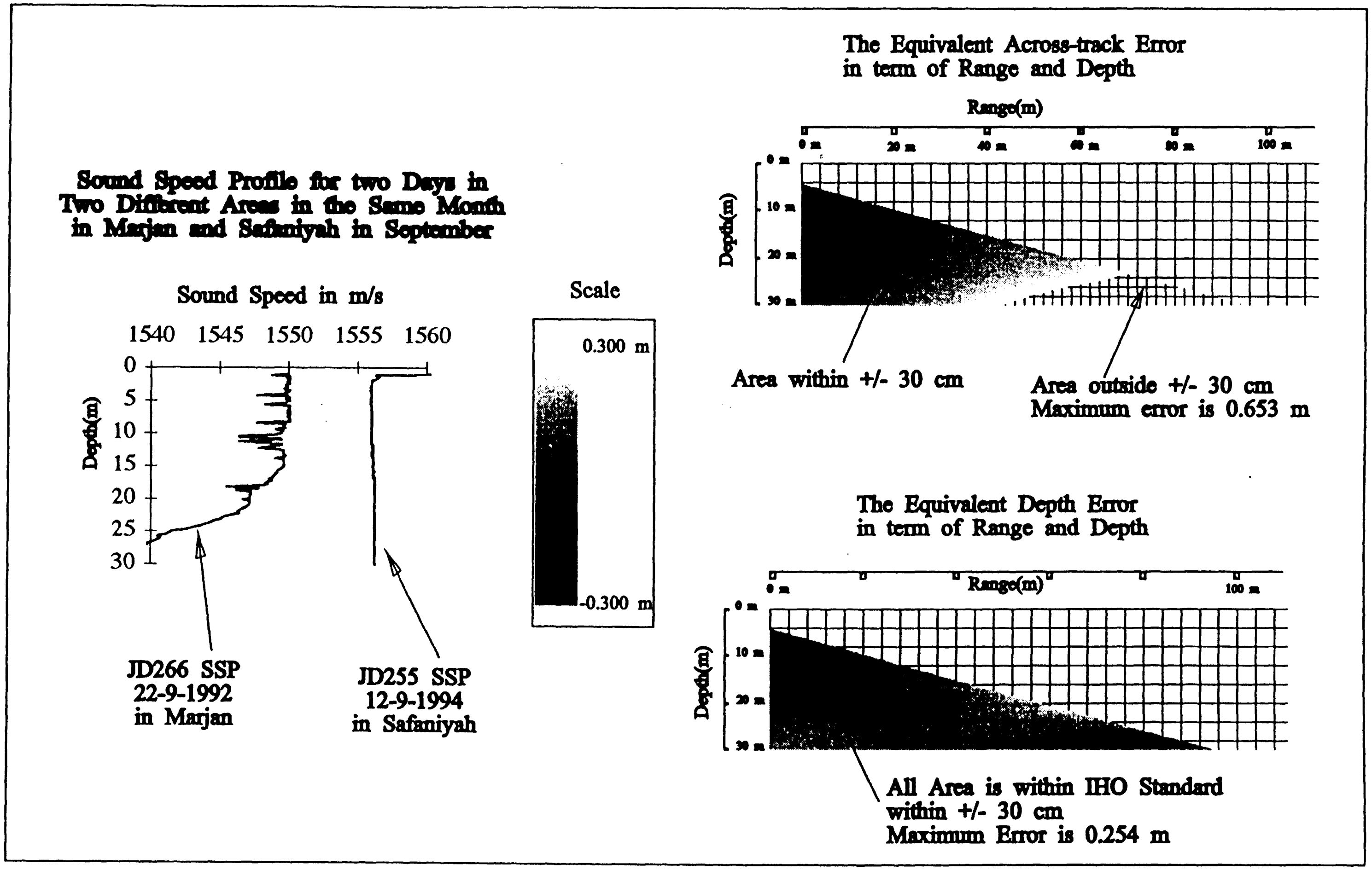

Figure 4-68
The effect of applying one SSP in Marjan over another SSP in Safaniyah in September, one SSP is abnormal, for 4.3 m draft case.

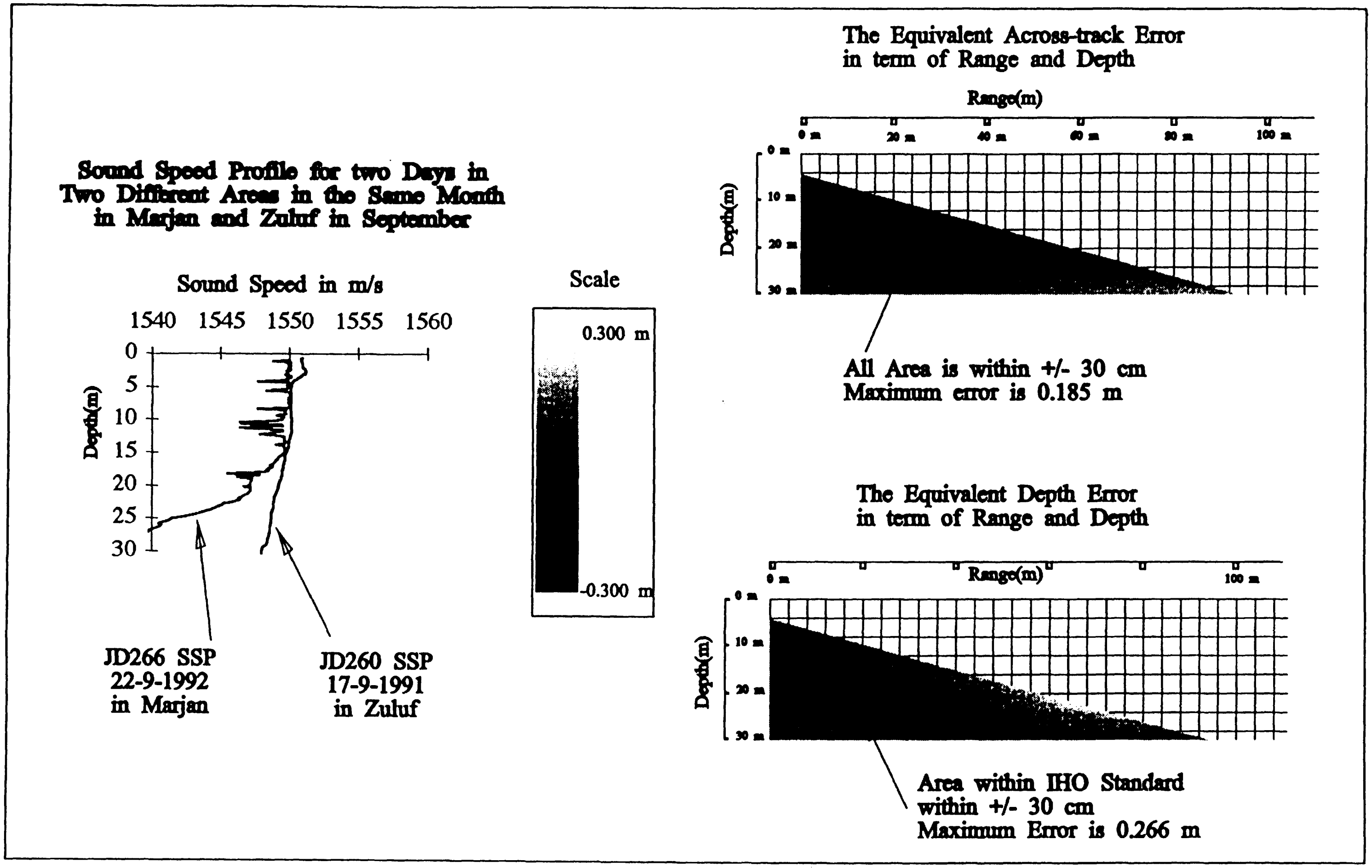

Figure 4-69
The effect of applying one SSP in Marjan over another SSP in Zuluf in September, one SSP is abnormal, for 4.3 m draft case.

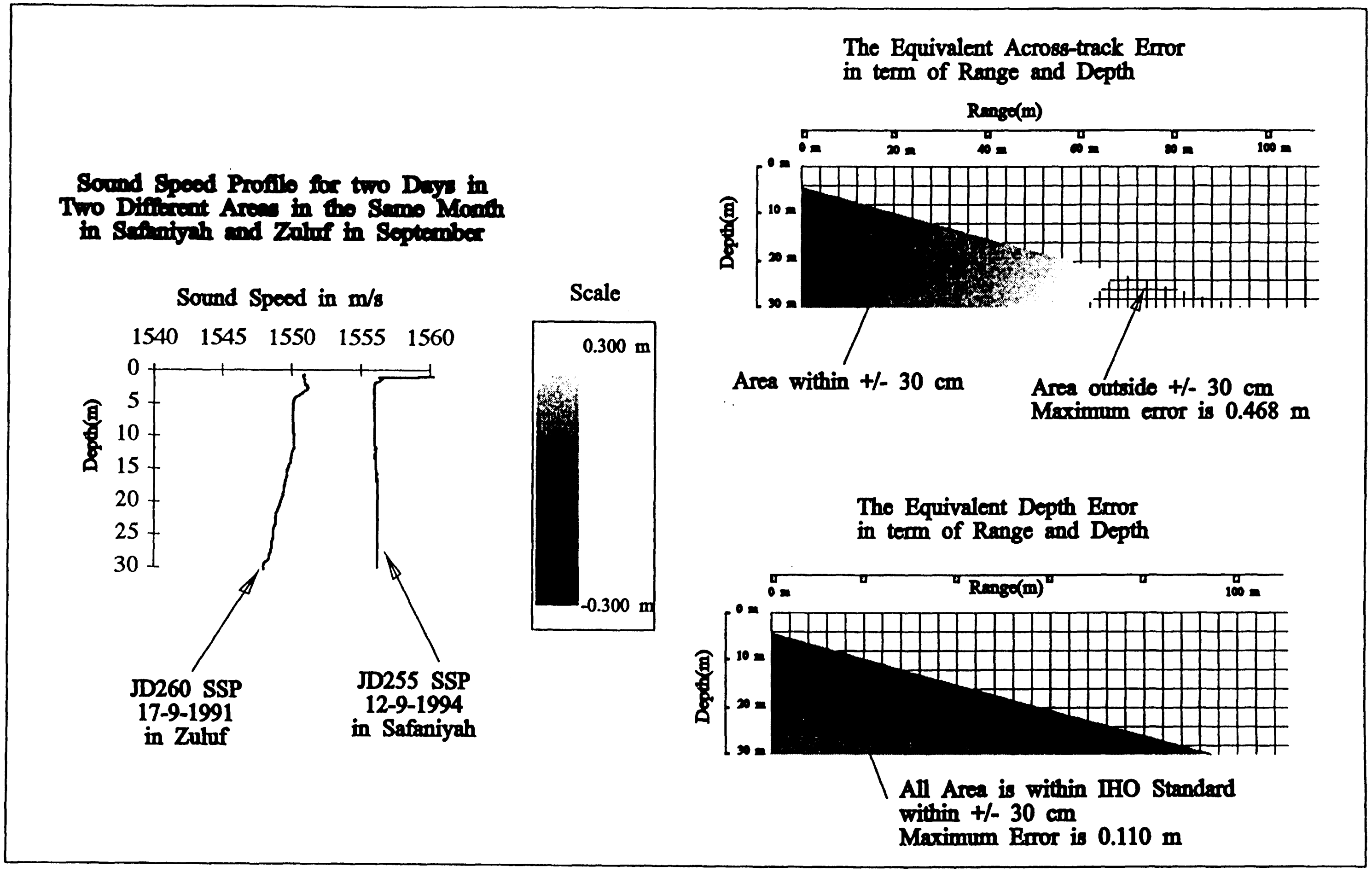

Figure 4-70
The effect of applying one SSP in Safaniyah over another SSP in Zuluf in September, both SSPs are normal, for 4.3 m draft case.

Vita

Author's full name:	Fahad Ateik Alamri
Place and date of birth:	Jeddah, 18 January 1963
Permanent Address:	HSU, Saudi Aramco Ras Tanura, Saudi Arabia 31311
School attended: (with dates)	Abdurahman ibn Auf Elementary School 1971-1977 Alhadeetha Intermediate School 1977-1980 Badr Ashamelah Secondary School 1980-1982
Universities attended: (with dates and degree obtained)	Ferris State University 1984-1988 B.Sc. in Surveying